CLEARINGHOUSE FOR FEDERAL SCIENTIFIC AND TECHNICAL INFORMATION CFSTI
DOCUMENT MANAGEMENT BRANCH 410.11

LIMITATIONS IN REPRODUCTION QUALITY

ACCESSION # AD 606 712

☑ 1. WE REGRET THAT LEGIBILITY OF THIS DOCUMENT IS IN PART UNSATISFACTORY. REPRODUCTION HAS BEEN MADE FROM BEST AVAILABLE COPY.

☐ 2. A PORTION OF THE ORIGINAL DOCUMENT CONTAINS FINE DETAIL WHICH MAY MAKE READING OF PHOTOCOPY DIFFICULT.

☐ 3. THE ORIGINAL DOCUMENT CONTAINS COLOR, BUT DISTRIBUTION COPIES ARE AVAILABLE IN BLACK-AND-WHITE REPRODUCTION ONLY.

☐ 4. THE INITIAL DISTRIBUTION COPIES CONTAIN COLOR WHICH WILL BE SHOWN IN BLACK-AND-WHITE WHEN IT IS NECESSARY TO REPRINT.

☐ 5. LIMITED SUPPLY ON HAND: WHEN EXHAUSTED, DOCUMENT WILL BE AVAILABLE IN MICROFICHE ONLY.

☐ 6. LIMITED SUPPLY ON HAND: WHEN EXHAUSTED DOCUMENT WILL NOT BE AVAILABLE.

☐ 7. DOCUMENT IS AVAILABLE IN MICROFICHE ONLY.

☐ 8. DOCUMENT AVAILABLE ON LOAN FROM CFSTI (TT DOCUMENTS ONLY).

☐ 9.

PROCESSOR:

TSL-107-10/64

DASA 1309

Ninth Quarterly Report

on

PROJECT STAR DUST

by

Herbert W. Feely
Ben Davidson
James P. Friend
Raymond J. Lagcmarsino
Micah W. M. Leo

Prepared for the Defense Atomic Support Agency

September 1, 1963

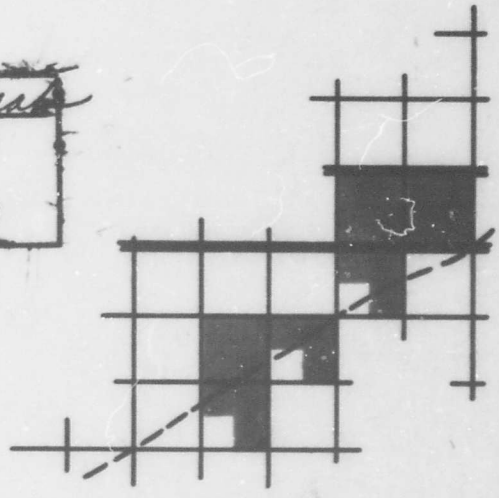

ISOTOPES, INC.

Ninth Quarterly Report

on

PROJECT STAR DUST

by

Herbert W. Feely
Ben Davidson
James P. Friend
Raymond J. Lagomarsino
Micah W. M. Leo

A report on work performed under Contract DA-49-146-XZ-079
prepared for the Defense Atomic Support Agency
Washington, D.C. 20301

September 1, 1963

ISOTOPES, INCORPORATED
123 Woodland Avenue
Westwood, New Jersey

ABSTRACT

Work which has been done on Project Star Dust during the preceding contract year is reviewed. Filter samples of stratospheric radioactivity have been collected using WU-2, RB-57 and RB-52 aircraft. Lower altitude collections included intensive sampling in the vicinity of extrusions of stratospheric air into the troposphere during the spring of 1963. A number of radiochemical and radiometric procedures used during Project Star Dust and developed since the issuance of the final report on Project HASP are described.

Electron microscope measurements of stratospheric particles collected by direct flow impactors have provided data which are consistent with the vertical concentration profile reported by Junge and coworkers and are consistent with the existence of the stratospheric aerosol in thin cloud-like laminae. The average particle size distribution function found approximates a log-normal distribution with a geometric mean radius of 0.275 micron. This disagrees significantly in the size range of ≤ 0.2 micron radius with the size distribution function found by Junge and co-workers. Aitken nuclei with radii < 0.1 micron, not collected by the impactor used, may produce a second peak in the size distribution curves at approximately 0.04 micron radius. Nuclear debris should become attached primarily to the small Aitken nuclei rather than to the larger sulfate particles.

The stratospheric burden of nuclear debris increased to unprecedented values, at least in the Northern Hemisphere, as a result of the 1961 and 1962 Soviet test series. The stratospheric burden of strontium-90 rose from about 0.9 megacurie in the third quarter of 1961 to about 2.0 megacuries in early 1962 and to about 7.4 megacuries in early 1963. Measurements of barium-140 in fresh debris during 1961 to 1963 provided data which suggest the presence of an organized circulation in the vicinity of the tropopause gap. Most debris from the 1961 and 1962 Soviet tests stabilized below 60 thousand feet in the polar stratosphere, but the debris increased in altitude as it moved equatorward. Although the Soviet debris spread laterally quite rapidly within the polar stratosphere, its transport through the tropical stratosphere was rather slow. The stratospheric distribution of antimony-124 was similar to the distributions of manganese-54 and iron-55 during 1962, suggesting a common origin for all of these products of neutron activation in one or more events during the 1961 Soviet test series. During early 1963, however, antimony-124 was found in high concentrations only at altitudes of 55 thousand feet and higher, while manganese-54 and iron-55 were found in fairly high concentrations at all altitudes in the Northern Hemisphere. This difference evidently resulted from new injections of these nuclides by more than one device during the late 1962 Soviet test series.

The stratospheric distribution of the cosmic-ray product beryllium-7 during 1960 and 1961 (before the 1961 Soviet test series) were generally similar to the theoretical distribution in a stagnant atmosphere, with

some differences which probably are attributable to eddy diffusion within the stratosphere and between the stratosphere and troposphere. During 1962 and early 1963, however, the distribution of this nuclide reflected the artificial production of beryllium-7 during the 1961 and 1962 nuclear weapons tests. Stratospheric concentrations of natural lead-210 appear to equal about 0.3 dpm/1000 scf, and lead-210 and polonium-210 appear to be in radioactive equilibrium within the stratosphere.

The Star Dust model of atmospheric mixing and transfer has been further developed into a diffusion-rainout model which includes a tropopause, tropopause gap and a tropospheric sink in the form of a rainout mechanism. Four models with variations in initial conditions are presented showing: (1) a successful reproduction of the observed latitudinal distribution of rainout, (2) the realism of the rainout mechanism used, (3) the sensitive relationship between the vertical exchange coefficients and the rainout mechanism, (4) the inability of the models to achieve as high a time transient rate decrease of central concentration as is observed, and (5) the effect of the rainout mechanism on reproducing the observed poleward decrease in height of the level of maximum concentration. Development of the basic model has proceeded to include the effects of particle terminal velocity and transport by non-zero meridional and vertical velocities.

Carbon-14 concentrations in carbon dioxide in ground level air in northern New Jersey showed a sharp increase beginning in April 1963, and reached values equal to 191 per cent of the natural carbon-14 activity by early August 1963.

Measurements of the vertical distribution of strontium-90 and cesium-137 in 9 Kansas soils, sampled during 1960, showed a close association of the two nuclides at all levels in the upper 12 inches of some soils, but a separation of the nuclides in other soils. The mean values of the total deposition in the 9 soils were 88 $\pm$ 35 mc Sr^{90}/mi^2 and 138 $\pm$ 81 mc Cs^{137}/mi^2.

TABLE OF CONTENTS

TABLE OF CONTENTS (continued)

TABLE OF CONTENTS (continued)

TABLE OF CONTENTS (continued)

Isotopes, Inc.

REPORT PREPARATION

The following persons have contributed to the writing of the various chapters of this report:

Chapters 1 and 2: H. Feely, M. Leo

Chapter 3: J. Friend

Chapter 4: R. Lagomarsino, D. Bogen, R. Schultz, K. Roach, B. Caridi and H. Feely

Chapters 5 and 6: H. Feely

Chapter 7: B. Davidson

Chapter 8: H. Feely

Chapter 9: M. Leo, H. Feely, R. Lagomarsino, D. Bogen

Chapter 10: H. Feely, H. Seitz

The editing of the report has been performed by H. Feely, J. Hardaway and H. Seitz.

BLANK PAGE

CHAPTER 1. INTRODUCTION

This is the ninth quarterly report to be issued during Project Star Dust. Our primary purpose in preparing this report is to review the work which has been done on the project during the past contract year.

Most of the techniques of sample collection and analysis and of data reduction which are presently being used during Project Star Dust are quite similar to those employed during Project HASP, The High Altitude Sampling Program. Nevertheless there have been enough changes in techniques used since the publication of DASA-1300, the final report on Project HASP[1], to warrant a review of some of these sampling changes. Therefore, included in this report are descriptions of the present Star Dust sampling program and of some of the radiochemical and radiometric procedures currently in use.

A review is given of recent progress in the study of the physical characteristics of stratospheric particulate, in the description of the stratospheric distribution of nuclear debris and of some natural activities, in the development of the Star Dust model of atmospheric circulation and exchange, in measurements of carbon-14 concentrations in ground-level air and in the study of the vertical distribution of certain fission products in soil.

Purpose and Method of Project Star Dust

Project Star Dust has been undertaken to prepare a mathematical model of atmospheric mixing and circulation which can be used to predict stratospheric hold-up and ultimate patterns of deposition on the surface of the earth of radioactive debris injected into the stratosphere by nuclear weapons tests, by burn-up on re-entry of nuclear power packs for earth satellites, or by other causes.

Information obtained from several atmospheric "tracers" is being used to guide the selection of values for the various meteorological parameters included in the model. Among these tracers are ozone and several artificial and

natural radionuclides,such as strontium-90, tungsten-185, carbon-14 and beryllium-7. The results of measurements of atmospheric radioactivity made during Project HASP, Project Star Dust and other studies are used to determine the atmospheric distribution of the radioactive tracers and the changes which occur in these distributions as a function of time.

The numerical model of atmospheric mixing and circulation which is being developed provides an objective method of experimentation in the attempt to simulate the actual processes affecting the movement of radioactive contaminants within the stratosphere. It permits evaluation of the effect upon the movement of the contaminant, of the source configuration, of diffusion, of possible general circulation within the stratosphere, of the settling velocity of particles and of possible tropospheric removal mechanisms.

Aside from their contribution to the development of the model, the measurements of the stratospheric distribution of debris from nuclear weapons tests also provide information needed for the estimation of the potential future hazard from the stratospheric burden of radioactivity from past nuclear tests.

Progress During the Contract Year, 1962-1963

During 1963 there has been an extension of the range in latitude covered by regular Star Dust sampling at the higher altitudes, and an increased effort at sampling in the vicinity of the tropopause and in the troposphere. There were limited periods during 1962 when sampling for Star Dust was performed by aircraft based in the Canal Zone and in Australia, but in 1963 such sampling became routine. Throughout early 1963 sampling in Australia was limited to missions flown northward from Laverton, but during September, 1963 missions flown southward from Laverton are also to be made part of the regular schedule. It is planned that orbit missions near Laverton at altitudes of 30 to 45 thousand feet, flown by RB-57 aircraft, will also be added to the

regular flight schedule by early 1964.

During the Spring of 1963 regular sampling at 20, 25, 30 and 35 thousand feet was begun at two latitudes, 65°N and 35°N, to provide data on concentrations of nuclear debris in the troposphere. Intensive sampling of the troposphere and stratosphere in the vicinity of extrusions of stratospheric air into the troposphere was performed as part of Project Springfield during March to May 1963. The Springfield flights were directed by Professor E. Danielsen of Pennsylvania State University. A special Star Dust report, written by Professor Danielsen, is to be issued during early 1964 to give the final results of this study.

Nuclear debris injected into the stratosphere by the 1961 Soviet test series and by the 1962 United States and Soviet test series has contained several products of neutron activation, in addition to the usual fission products, which may be used as tracers of atmospheric motions. Manganese-54, iron-55, antimony-124 and several other nuclides were produced in unusually large quantities by both the 1961 and 1962 Soviet tests. Yttrium-88 was also produced in quantity by one or more devices tested by the Soviet Union in 1962. The rocket shot Starfish Prime, detonated at about 400 kilometers over Johnston Island on 9 July 1962 produced cadmium-109 and cadmium-113m, to be used as a tracer for debris from that source. These potential tracers have been added to the Star Dust analytical procedures during 1962 and 1963, and as a result data are being obtained which should be useful in the testing of the Star Dust model of atmospheric motions.

Fresh debris from the 1962 United States test series was intercepted a number of times by Star Dust missions during May to August 1962, and fresh debris from the 1962 Soviet tests was intercepted repeatedly during September 1962 to March 1963. Calculations of the stratospheric burdens of strontium-90 resulting from these test series have been made as part of the effort during

Star Dust measurements to monitor stratospheric concentrations of nuclear debris.

Beginning with samples collected during May 1963 the cosmic ray products phosphorus-32, phosphorus-33 and sodium-22 were added to the Star Dust analytical program, and analysis of samples for the tracer nuclides rhodium-102, lead-210 and polonium-210 was discontinued. The rhodium-102 tracer measurements were discontinued because it has been reported that rhodium-102 was produced during the 1962 United States tests, so that it is no longer useful as a unique tracer for the 1958 rocket shot Orange[2]. Results of past lead-210 and polomium-210 measurements have not been sufficiently encouraging to justify the continuation of the analysis of these nuclides at this time.

The simple numerical diffusion model of atmospheric mixing and transfer has been further developed into a diffusion-rainout model, which includes a tropopause, tropopause gap and a tropospheric sink in the form of a rainout mechanism. The basic model has been modified to include the effects of particle terminal velocity and transport by non-zero meridional and vertical velocities (general circulation terms).

Studies of the physical and chemical properties of the stratospheric aerosol, of the concentration of carbon-14 in ground-level air in northern New Jersey and of the vertical distribution of certain fission products in soils have continued. Progress in these studies is discussed in later chapters.

Future Plans

During the coming year it is expected that we will continue to monitor the stratospheric concentrations of the fission products strontium-90, cesium-137, cerium-144 and promethium-147. The shorter-lived fission products strontium-89, yttrium-91 and zirconium-95 will also be measured as long as their activities are detectable. We will also monitor the activation products plutonium-239, cadmium-109, cadmium-113m, yttrium-88, manganese-54, iron-55, cobalt-57 and

antimony-124. The analysis of the cosmic ray products beryllium-7, phosphorus-32, phosphorus-33 and sodium-22 in a set of samples collected once each month will also be continued.

The collection of gas samples of stratospheric air for analysis of carbon-14 as part of the Star Dust program was begun in August 1963. The data which result from these analyses should prove valuable in the testing of the Star Dust model.

The sampling of ground-level air for carbon-14 analysis will continue throughout the coming year, but the collection of soil samples has been terminated. Analysis of fission products in the soil samples will be completed during the coming year and the final results will be reported.

Further investigations of the effect of the inclusion of general circulation terms in the Star Dust model will be investigated. The model will be tested using data from polar injections as well as tropical injections. Observations made during Project Star Dust of the movement of debris from the 1961 and 1962 Soviet tests as well as observations made during Project HASP of the movement of tungsten-185 injected by Operation Hardtack will be used in testing the model. Data for other tracers will be used in these tests as needed.

Future reports of Star Dust data and conclusions will be issued on a semi-annual basis. A report which is to be completed by 1 August 1964 will contain final flight and radiochemical data for Star Dust samples collected during 1961 and 1962. The following report, which is to be completed by 1 January 1965, will contain final flight and radiochemical data for Star Dust samples collected during 1963.

CHAPTER 2. THE STAR DUST SAMPLING PROGRAM

The sampling techniques used during Project Star Dust have generally been similar to those used during Project HASP, but there have been a few changes. These have involved especially the types of aircraft used and the flight paths followed by the aircraft. Changes in the probe sampler used to collect stratospheric particles for studies of the physical and chemical nature of the stratospheric aerosol will be discussed in Chapter 3.

Collection of Filter Samples

When Project HASP began the sampling vehicles used were six WU-2 aircraft equipped with nose samplers. During 1959 hatch samplers were added to these aircraft, thereby increasing their collection capability from four samples to ten samples per mission. On occasion these aircraft were temporarily replaced by other WU-2 aircraft which lacked the nose sampler but could collect six samples per mission using the hatch sampler. Also as part of Project HASP three missions were flown to the North Pole by RB-52 aircraft during 1959.

During Project Star Dust approximately equal use has been made of WU-2 aircraft which are equipped with nose samplers and of those which are not so equipped. But beginning in early 1963 there has been a substitution of flights by RB-57A aircraft at altitudes of 39 and 43 thousand feet for the WU-2 flights of 40 and 45 thousand feet. Thus the WU-2 is now used only at the higher altitudes of 50 to approximately 70 thousand feet. A series of orbit missions were flown in the vicinity of Fairbanks, Alaska at 20, 25, 30 and 35 thousand feet by RB-57 aircraft during the first half of 1962. Since early 1963 such flights have again been flown regularly in the vicinity of Fairbanks and also in the vicinity of Amarillo, Texas. On some of these missions C-130 aircraft have been used instead of RB-57 aircraft.

Extensive tropospheric sampling was performed in the Star Dust sampling corridor during the autumn of 1962 utilizing WB-50 and C-130 aircraft,

and intensive sampling in the vicinity of extrusions of stratospheric air into the troposphere was performed during the spring of 1963 as part of "Project Springfield", using WB-50 and RB-57 aircraft. These Springfield missions, directed by Professor Edwin F. Danielsen of Pennsylvania State University, collected samples at a variety of altitudes in several different regions of the western and mid-western United States.

During the first year of Project HASP, when the sampling capability was limited to four samples per flight, all four were usually collected at a single altitude. Occasional vertical samplings were made, especially during mid-1958, with each of the samples being collected at a different altitude over a single location. Not until mid-1959, however, when the installation of hatch samplers increased the sampling capability to ten samples per flight, did it become routine procedure to sample at two altitudes on each flight. Since the beginning of Project Star Dust, however, it has been the practice for each flight to sample at least two altitudes, and vertical soundings which sampled as many as seven altitudes during a single mission have been common.

The Star Dust Sampling Corridor

An attempt was made during the design of the Star Dust sampling program to obtain sampling within a meridional corridor. As in Project HASP, however, the ideal situation could not be attained, and the sampling corridor consists instead of a series of quasi-meridional segments. These segments are more or less contiguous between 70^{o}N and 10^{o}S, but the segments north and south of Australia are far removed in longitude from the others.

The HASP sampling corridor was discussed in the final report on Project HASP[1]. The various configurations of the Star Dust sampling corridor during 1961-1963 are summarized in Tables 1 to 5, and in Figures 1 to 5.

Isotopes, Inc.

During the first seven months of the sampling program, June to December 1961, regular Star Dust sampling was confined to missions flown northward and southward from Laughlin A.F.B., Texas, and to orbit missions in the vicinity of Laughlin[3]. Additional samples were obtained, however, from deployments of aircraft between Eielson A.F.B., Alaska and Laughlin during September 1961, from missions flown south from Hickam A.F.B., Hawaii during June 1961, from deployments of aircraft between Hickam and East Sale, Australia via Nandi, Fiji Islands, during October and December 1961, from orbit missions flown in the vicinity of East Sale, and from missions flown southward from East Sale during October and November 1961. All missions, except one flown north from Laughlin during September 1961, were at altitudes of 50 thousand feet or higher.

The Star Dust sampling program was extended during January 1962 to cover more intensively a greater range of latitude and altitude. Missions were flown northward and southward from Eielson and Laughlin, and orbit missions were flown in the vicinity of each base[4]. Missions were scheduled to cover each five thousand foot level between 40 thousand feet and maximum altitude (but only between 55 thousand feet and maximum altitude on missions southward from Laughlin) once every two weeks. Beginning in March 1962 a mission was flown to the North Pole at about 40 thousand feet by an RB-52 aircraft once each month, and orbit missions were flown at 20, 25, 30 and 35 thousand feet in the vicinity of Eielson by RB-57 aircraft once each week. Samples were received[4] from missions flown northward and southward from Howard A.F.B., Canal Zone, and from orbit missions flown in the vicinity of that base during April, June and July 1962. Some samples were also received from a deployment of aircraft from Laughlin to Guam, via Hickam and Wake Island during June 1962, from a deployment of aircraft from Hickam to East Sale via Nandi, and from a mission flown south from East Sale during March 1962.

Isotopes, Inc.

Regular Star Dust sampling during late August to November 1962 was limited to "vector" missions flown between Eielson and Laughlin by WU-2 aircraft (generally at 55 thousand feet between 64°N and 40°N and at 55, 60 or 65 thousand feet between 40°N and 31°N) and between Eielson and McClellan A.F.B., California by WB-50 and C-130 aircraft (generally at 18 or 30 thousand feet). The low altitude flights continued, actually, into January 1963. Samples were also received from a series of missions flown northward from Heyford, England during August and September 1962, from a deployment of aircraft to Laverton, Australia during September 1962, and from missions flown northward from Laverton beginning in October 1962.

There was an expansion of Star Dust sampling in December 1962, and by January 1963 the regular Star Dust missions included flights northward and southward from Eielson, Laughlin and Albrook A.F.B. in the Canal Zone, and northward from Laverton[5]. The complete set of missions was flown twice per month. One mission was flown eastward from Laughlin in December 1962 to sample variations of activity in the zonal direction. Beginning in March 1963 WU-2 aircraft were replaced by RB-57A aircraft at the lower altitudes, 40 and 45 thousand feet, and the schedule was soon changed to 39 and 43 thousand feet to better accommodate the capabilities of these aircraft. Also beginning in March a series of missions at 20, 25, 30 and 35 thousand feet were flown in the vicinity of Eielson and of Amarillo, Texas once every two days. By June 1963 the frequency of these flights had been decreased to once per week at both Amarillo and Eielson. Also during early 1963 there was a resumption of monthly flights to the North Pole by RB-52 aircraft.

The home base of the 4080th Strategic Wing, S.A.C., which performs the Star Dust WU-2 missions, was changed from Laughlin to Davis-Monthan A.F.B., Arizona during early July 1963. While this move was being made several missions

were flown along the WU-2 flight tracks at altitudes between 50 and about 63 thousand feet by RB-57D aircraft equipped with U-1 samplers. By the second half of July 1963 regular missions flown northward and southward from Davis-Monthan had replaced the missions formerly flown from Laughlin. During September 1963 the frequency of orbit missions at 20 to 35 thousand feet is to be reduced from once per week to once per month near Amarillo and twice per month near Eielson. Missions flown southward from Laverton are scheduled to become part of the regular Star Dust flight schedule during September 1963. These missions will extend the Star Dust sampling corridor to about 50^{o}S. Otherwise the pattern of Star Dust sampling during late 1963 will remain the same as that maintained during early 1963.

At times during 1961 to 1963 aliquots of samples collected for other programs have been used to supplement Star Dust sampling. Such samples have included filters collected during orbit missions flown in the vicinity of Eielson, Laughlin, Laverton and other bases in both the Northern and Southern Hemispheres at altitudes ranging from 15 to nearly 70 thousand feet.

Table 1. Flight Tracks of Star Dust Missions During 1961

	Northern Limit	Southern Limit	Altitudes(Kft.)
Deployments between Eielson A.F.B., Alaska and Laughlin A.F.B., Texas:			
	63°40'N, 145°25'W	30°27'N, 101°25'W	~70
Missions Northward from Laughlin A.F.B., Texas:			
	48°00'N, 97°25'W	27°44'N, 98°00'W	(40,45),50,55,60,65,~70
Orbit Missions near Laughlin A.F.B., Texas:			
	30°00'N, 100°00'W	-----	55,60,65,~70
Missions Southward from Laughlin A.F.B., Texas:			
	27°40'N, 99°07'W	14°55'N, 92°15'W	(60,65),~70
Missions Southward from Hickam A.F.B., Hawaii:			
	19°41'N, 158°00'W	7°00'N, 162°15'W	50,60,65,~70
Deployments between Hickam A.F.B., Hawaii and East Sale R.A.A.F.B., Australia via Nandi:			
	20°00'N, 158°00'W	35°18'S, 149°11'E	~70
Orbit Mission near East Sale R.A.A.F.B., Australia:			
	38°00'S, 147°00'E	-----	55,60,65,~70
Missions Southward from East Sale R.A.A.F.B., Australia:			
	40°00'S, 147°30'E	60°00'S, 147°30'E	~70

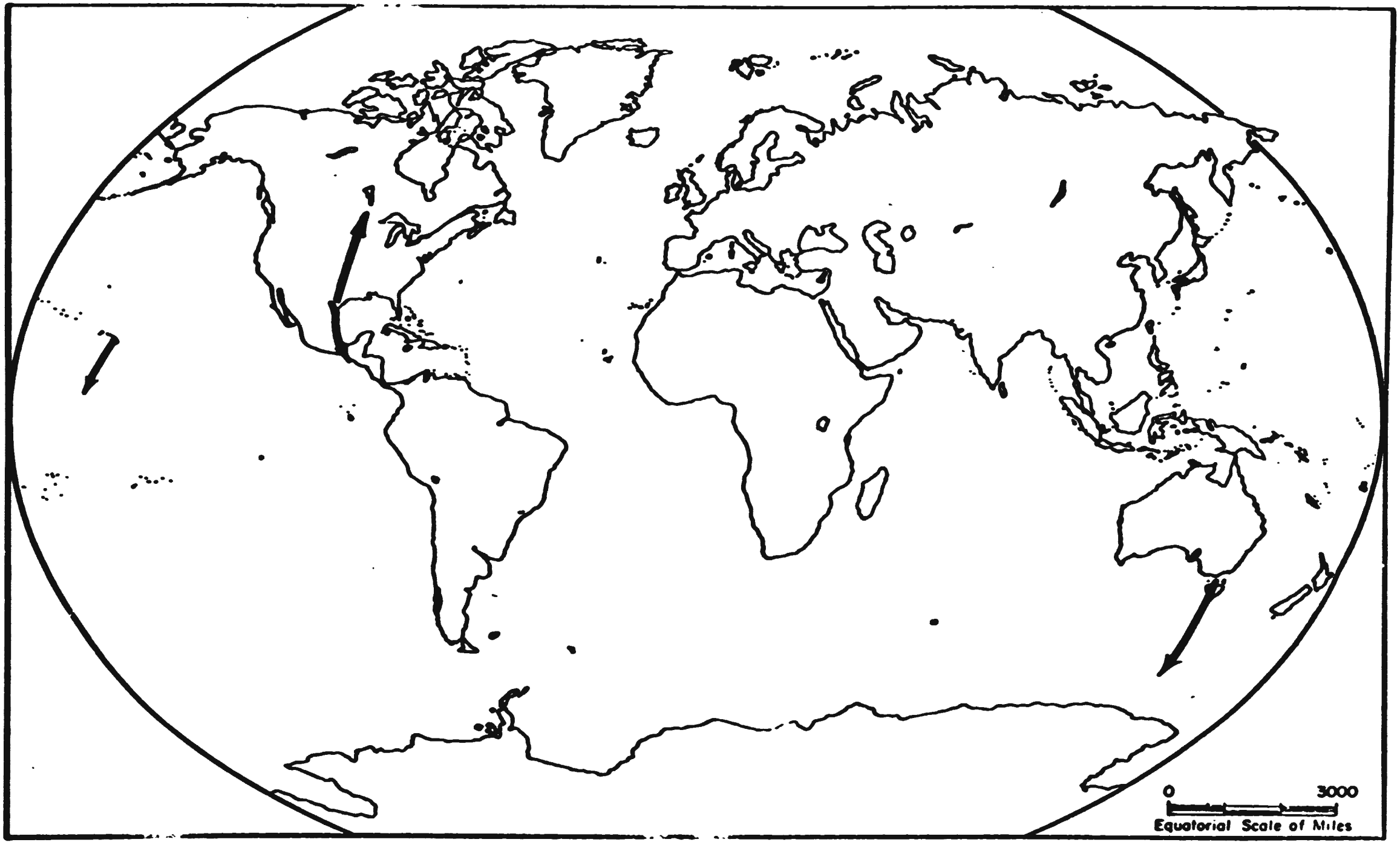

FIGURE 1 · FLIGHT TRACKS OF STAR DUST MISSIONS DURING 1961

Table 2. Flight Tracks of Star Dust Missions During Early 1962

	Northern Limit	Southern Limit	Altitudes(Kft.)
Missions to the North Pole by RB-52 Aircraft:			
	90°00'N, 120°00'W	60°00'N, 120°00'W	~40
Missions Northward from Eielson A.F.B., Alaska:			
	70°11'N, 146°53'W	64°49'N, 147°30'W	40,45,50,55,60, 65,~70
Orbit Missions near Eielson A.F.B., Alaska:			
	64°04'N, 147°47'W	--------	20,25,30,35,40,45, 50,55,60,65,~70
Missions Southward from Eielson A.F.B., Alaska:			
	64°02'N, 145°42'W	48°57'N, 122°35'W	40,45,50,55,60, 65,~70
Missions Northward from Laughlin A.F.B., Texas:			
	48°40'N, 112°20'W	31°50'N, 100°40'W	40,45,50,55,60, 65,~70
Orbit Missions near Laughlin A.F.B., Texas:			
	30°00'N, 100°00'W	-------	40,45,50,55,60, 65,~70
Missions Southward from Laughlin A.F.B., Texas:			
	29°37'N, 98°21'W	15°00'N, 92°25'W	55,60,65,~70
Deployment from Laughlin A.F.B., Texas to Andersen A.F.B., Guam, via Hickam A.F.B. and Wake Island:			
	31°15'N, 104°00'W	14°06'N, 146°25'E	~70
Missions Northward from Howard A.F.B., Canal Zone:			
	15°00'N, 82°30'W	08°46'N, 79°33'W	40,45,50,55,60, 65,~70
Orbit Missions near Howard A.F.B., Canal Zone:			
	08°00'N, 79°33'W	--------	40,45,50,55,60, 65,~70

Table 2. Flight Tracks of Star Dust Missions During Early 1962 (Continued)

	Northern Limit	Southern Limit	Altitudes(Kft.)
Missions Southward from Howard A.F.B., Canal Zone:			
	08°46'N, 79°33'W	10°00'S, 78°40'W	40,45,50,55,60, 65,~70
Deployments between Hickam A.F.B., Hawaii and East Sale R.A.A.F.B., Australia via Nandi:			
	20°00'N, 158°00'W	38°05'S, 147°10'E	~70
Missions Southward from East Sale R.A.A.F.B., Australia:			
	40°00'S, 148°00'E	61°00'S, 147°30'E	65

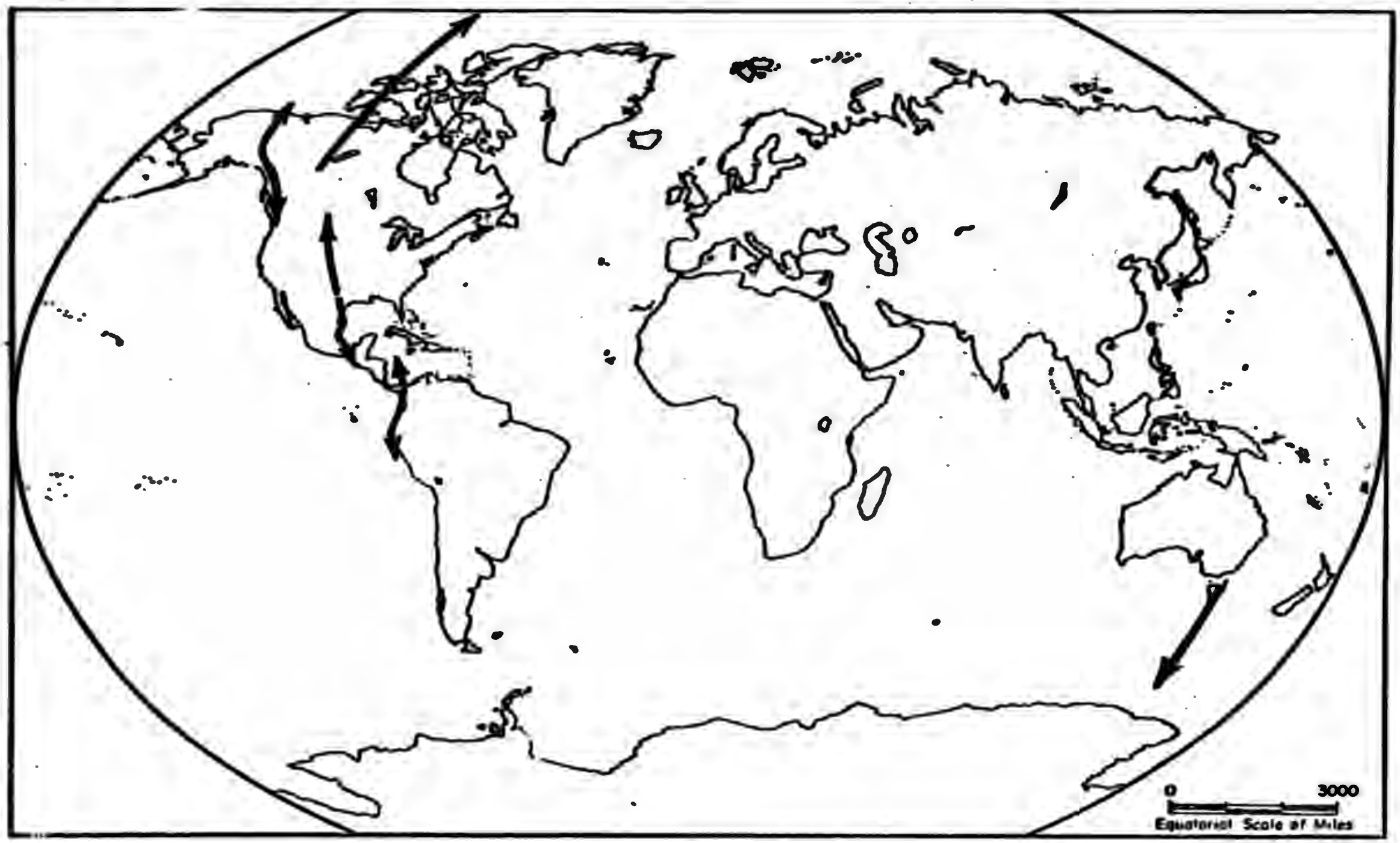

FIGURE 2· FLIGHT TRACKS OF STAR DUST MISSIONS DURING EARLY 1962

Table 3. Flight Tracks of Star Dust Missions During August to November 1962

	Northern Limit	Southern Limit	Altitudes (Kft.)
Missions Northward from Heyford, England:			
	73°40'N, 17°45'E	54°00'N, 02°14'W	60,~70
Vector Missions between Eielson A.F.B., Alaska and Laughlin A.F.B., Texas:			
	64°00'N, 146°00'W	31°00'N, 103°00'W	55,60,~65
Vector Missions between Eielson A.F.B., Alaska and McClellan A.F.B., California:			
	65°00'N, 147°00'W	38°00'N, 121°00'W	usually 18 or 30
Deployment from Hickam A.F.B., Hawaii to Laverton, Australia via Nandi:			
	18°25'N, 158°25'W	37°20'S, 145°10'E	65
Missions Northward from Laverton, Australia:			
	15°00'S, 145°00'E	37°00'S, 145°00'E	55,60,65,~70

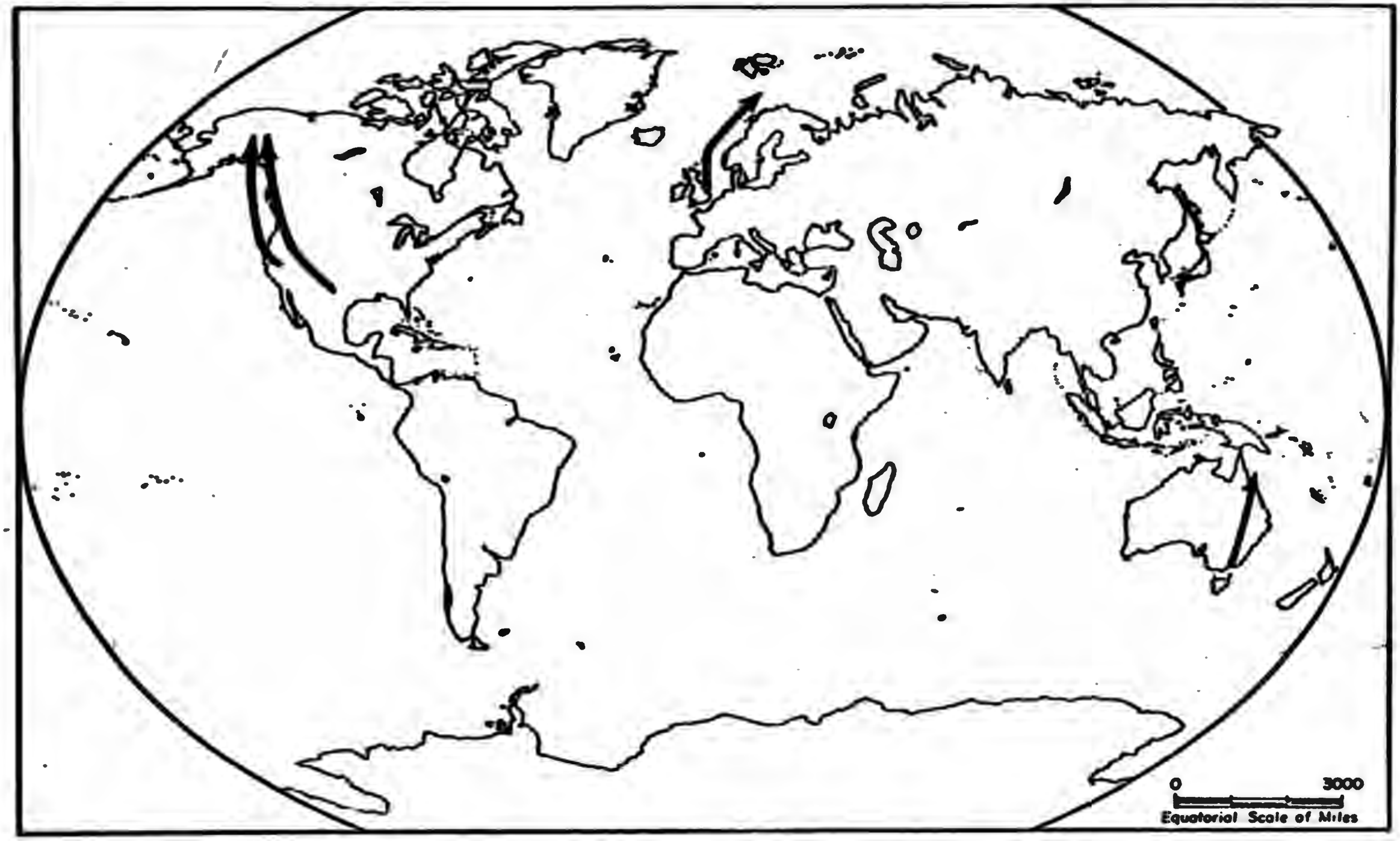

FIGURE 3· FLIGHT TRACKS OF STAR DUST MISSIONS DURING AUGUST TO NOVEMBER 1962

Table 4. Flight Tracks of Star Dust Missions During Early 1963

	Northern Limit	Southern Limit	Altitudes (Kft.)
Missions to the North Pole by RB-52 Aircraft:			
	90°00'N, 120°00'W	60°00'N, 120°00'W	~40
Missions Northward from Eielson A.F.B., Alaska:			
	70°07'N, 143°25'W	64°35'N, 147°00'W	40,45,50,55,60, 65,~70
Orbit Missions near Eielson A.F.B., Alaska:			
	65°00'N, 147°30'W	----------	20,25,30,35
Missions Southward from Eielson A.F.B., Alaska:			
	64°43'N, 147°00'W	48°55'N, 122°35'W	40,45,50,55,60, 65,~70
Missions Northward from Laughlin A.F.B., Texas:			
	48°40'N, 112°20'W	31°20'N, 100°30'W	40,45,50,55,60, 65,~70
A Mission Eastward from Laughlin A.F.B., Texas:			
	37°51'N, 100°00'W	30°25'N, 81°33'W	55,65
Orbit Missions near Amarillo, Texas:			
	36°00'N, 102°20'W	----------	20,25,30,35
Missions Southward from Laughlin A.F.B., Texas:			
	31°20'N, 100°25'W	19°00'N, 95°11'W	55,60,65,~70
Missions Northward from Albrook A.F.B., Canal Zone:			
	20°00'N, 86°25'W	09°00'N, 79°20'W	55,60,65,~70
Missions Southward from Albrook A.F.B., Canal Zone:			
	09°10'N, 79°30'W	10°00'S, 79°00'W	55,60,65,~70
Missions Northward from Laverton, Australia:			
	15°13'S, 145°00'E	37°00'S, 145°00'E	55,60,65,~70

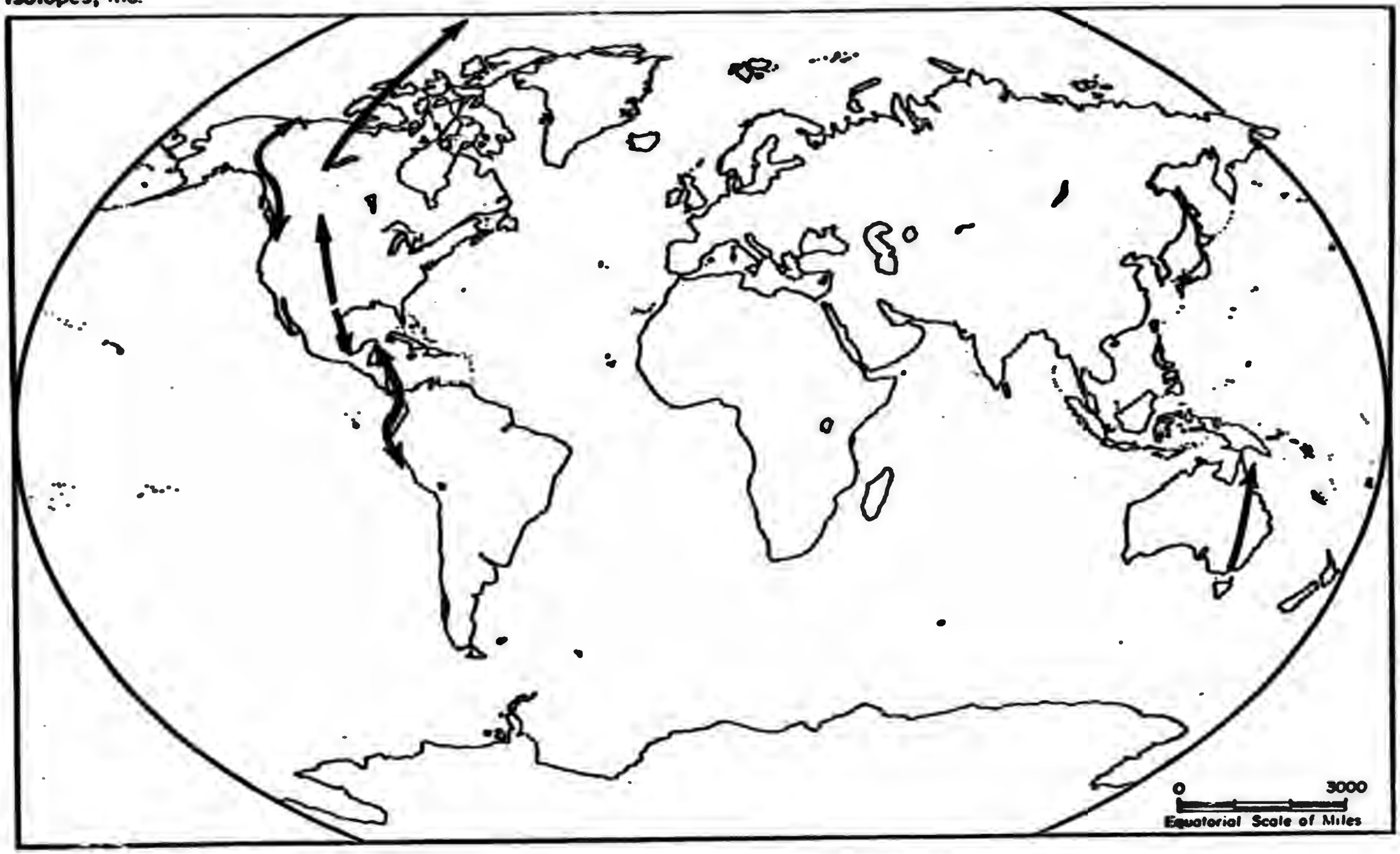

FIGURE 4 · FLIGHT TRACKS OF STAR DUST MISSIONS DURING EARLY 1963

Table 5. Flight Tracks of Star Dust Missions During Late 1963

	Northern Limit	Southern Limit	Altitudes(Kft.)
Missions to the North Pole by RB-52 Aircraft:			
	90°00'N, 120°00'W	60°00'N, 120°00'W	~40
Missions Northward from Eielson A.F.B., Alaska:			
	70°10'N, 143°40'W	64°35'N, 147°00'W	39,43,50,55, 60,65,~70
Orbit Missions near Eielson A.F.B., Alaska:			
	65°00'N, 147°30'W	----------	20,25,30,35
Missions Southward from Eielson A.F.B., Alaska:			
	64°43'N, 147°00'W	48°55'N, 122°35'W	39,43,50,55 60,65,~70
Missions Northward from Davis-Monthan A.F.B., Arizona:			
	48°17'N, 122°37'W	32°07'N, 110°50'W	39,43,50,55, 60,65,~70
Orbit Missions near Amarillo, Texas:			
	36°00'N, 102°20'W	----------	20,25,30,35
Missions Southward from Davis-Monthan A.F.B., Arizona:			
	31°22'N, 100°27'W	20°00'N, 96°05'W	55,60,65,~70
Missions Northward from Albrook A.F.B., Canal Zone:			
	20°00'N, 86°25'W	09°00'N, 79°20'W	55,60,65,~70
Missions Southward from Albrook A.F.B., Canal Zone:			
	09°10'N, 79°30'W	10°00'S, 79°00'W	55,60,65,~70
Missions Northward from Laverton, Australia:			
	15°00'S, 145°00'E	37°00'S, 145°00'E	55,60,65,~70
Missions Southward from Laverton, Australia:			
	37°50'S, 144°45'E	50°00'S, 147°30'E	55,60,65,~70

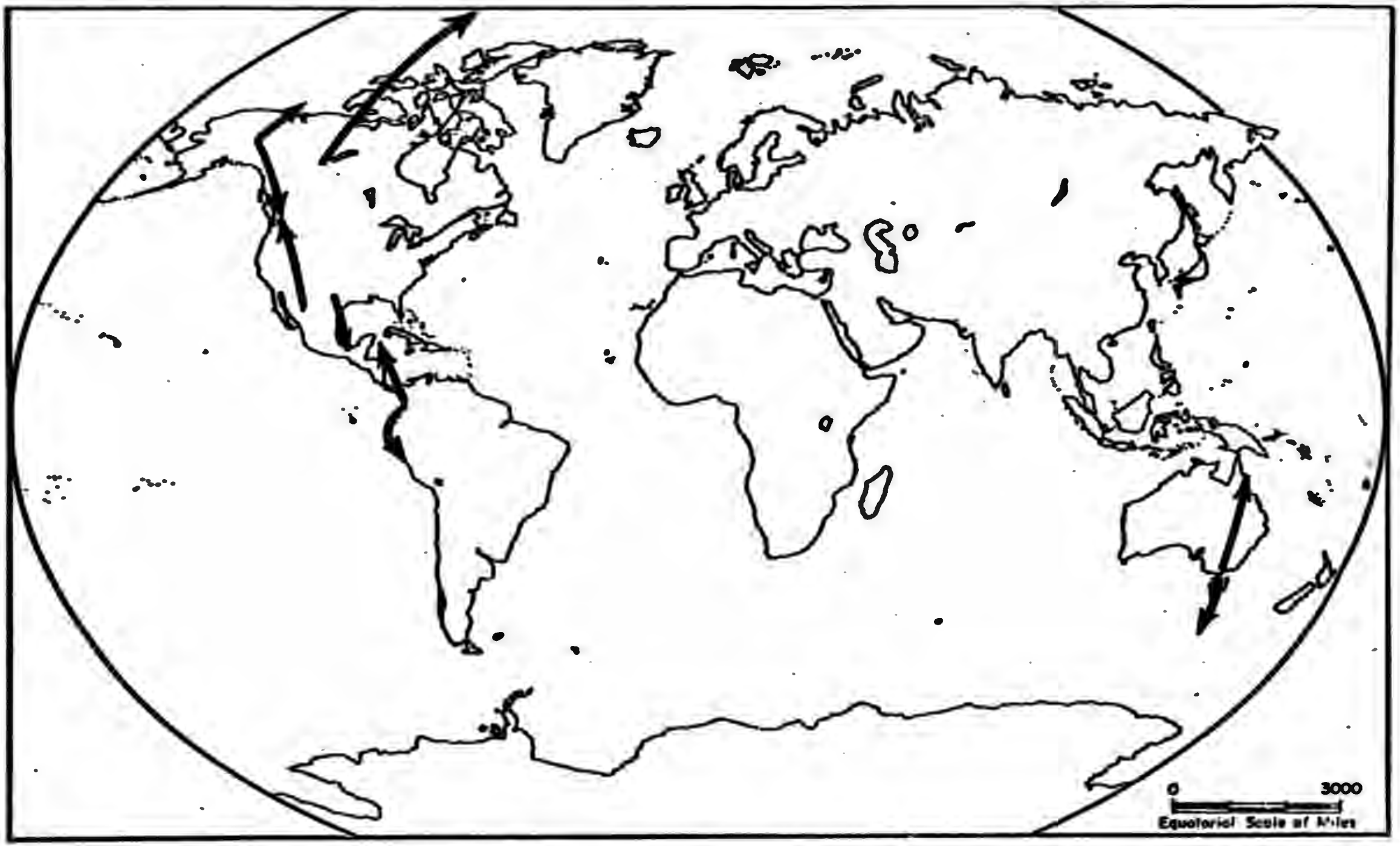

FIGURE 5· FLIGHT TRACKS OF STAR DUST MISSIONS DURING LATE 1963

CHAPTER 3. THE STRATOSPHERIC AEROSOL

The study of stratospheric particles was undertaken initially in Project HASP in order to shed some light upon the physical and chemical natures of the material with which world-wide fallout was associated. These studies have been continued in Project Star Dust with the same general goals. It was considered that continued sampling would provide more reliable estimates of the temporal and spatial distributions of the particulate matter. In late 1961 an improved aircraft-mounted sampling probe became available, and with it the opportunity to obtain more detailed information on the particle size-frequency spectrum.

This chapter is concerned with:

(a) a description of the new probe, its operation, and its collection characteristics;

(b) a description of the method of analysis of the particle sizes;

(c) the presentation of the results of particle sampling in Star Dust;

(d) a discussion of the results and their significance with respect to world-wide fallout.

Particle Sampling and Analysis

The basic methods of particle sampling and analysis used during Project Star Dust have been the same as those used during Project HASP; the particles were collected by aircraft-mounted direct flow impactors, and the main analytical tool was electron microscopy.

Until October 1961 only the "window" type of sampler was available for use on the WU-2 aircraft. At that time two "tip" probes (see Figure 2.1 of Volume 5, Part II, DASA 1300) and three newly designed "Mark III" probes were made available. These probes, shown schematically in

Figure 6, were designed by Mr. James E. Manson of Air Force Cambridge Research Laboratory. In mid-1962 all Star Dust aircraft were modified to carry the Mark III probes, and a total of six were available for use. In all, 70 samples were collected between 5 January 1961 and 12 December 1963. There were 18 "window", 10 "tip" and 42 Mark III samples. For reasons which are discussed later, only the "tip" and Mark III samples will be considered in this report. Of the total of 52 samples, only 12 were of suitable condition to be subjected to thorough particle size analysis. The reasons for this low yield of usable samples will be evident below.

The basic design features of the Mark III impaction probe are shown in Figure 6. The impaction area has two different widths. This design permits collection of larger particles on the portion with larger width without the interference of particles smaller than the "cut-off" radius. The narrow portion has, of course, a "cut-off" at much smaller radius. In this work, only the deposit on the small width portion was studied. As will be seen later, because of their small size, the major fraction of the particles of the stratospheric sulfate aerosol are deposited upon the narrow portion of the probe.

Experience with the "window" impactor was used in the development of the improved design of the Marx III probe. Below are listed the primary new design features and the reasons for adopting them. (See also Figure 6.)

(a) Air-tight housing: This feature, along with the fins, is incorporated in the probe to eliminate the condensation of moisture from tropospheric air on the hygroscopic particles collected from the stratosphere. The main seal is provided by the "o"-ring in the end cap of the sample plunger.

Isotopes, Inc.

(b) Fins: Basically these provide a large surface so that the probe may quickly come into thermal equilibrium with the environment. This prevents water from condensing on the cooler probe when the aircraft descends from the stratosphere into the warmer and moister troposphere. Additionally, but not less importantly, a coating of silicone oil is applied to the outer surface of the probe to prevent icing.

(c) Sampling surface extending beyond the probe body: This eliminates the "dead air" space which caused peculiar "banding" of the deposit in the "window" probe. The resulting surface then approximates a ribbon type of impactor rather than a cylinder type.

(d) Small (1/8 inch)transverse dimension (width) of the impaction surface: This permits collection of particles down to 0.14 micron radius with efficiencies greater than about 40% at 60 thousand feet altitude. This compares with < 1% for particles of 0.14 micron radius for the "window" probe.

It is to be noted that features (c) and (d) are present in the "tip" probe, although there are basic differences in the overall shape and size of the extensible portions of the two devices.

The field operational aspects of the Mark III probe have been essentially the same as those of the "window" probe, although there have been changes in packaging for shipment.

The preparation of the probes for sampling, the unloading of the probes after exposure, and the electron microscopic and electron diffraction analyses have been performed by Ernest F. Fullam, Inc., Schenectady, N.Y.

The collection surface for all samples consists of a thin carbon film supported by a thick (0.003 to 0.005 inch) film of nitrocellulose. Three specimen grids from each sample are prepared for electron microscopic analysis by placing copper grids beneath the original thick film and dissolving the film of nitrocellulose in vapors of amyl acetate. The thin carbon film with the sample particles are left supported by the copper grid. Although there is still a "banding" or "pile-up" effect at the

inboard end of the Mark III probe samples it is not as pronounced as in samples from the "window" probe. The micrographs used for determining the particle size-frequency distribution are chosen so that proper weighting for the "pile-up" is attained in each sample. Normally, about 5 to 10 micrographs, each representing 1440 square microns of sample, are counted. Electron diffraction patterns have been obtained for many of the samples.

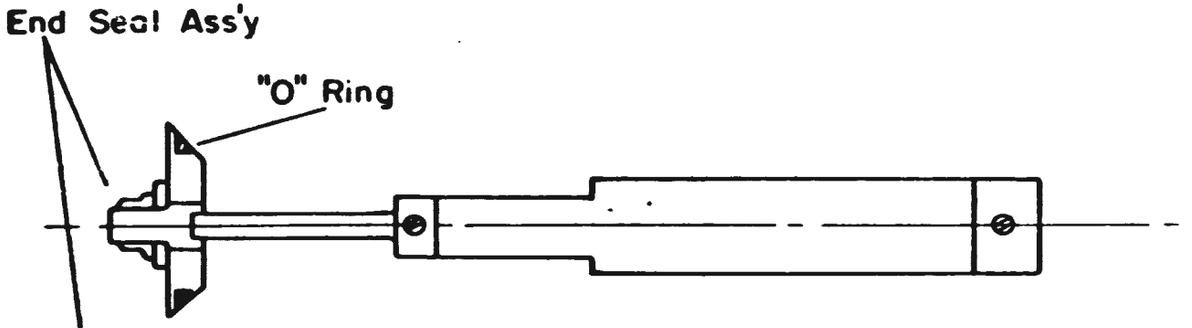

Figure 6a · IMPACTION SURFACE OF MARK III PROBE

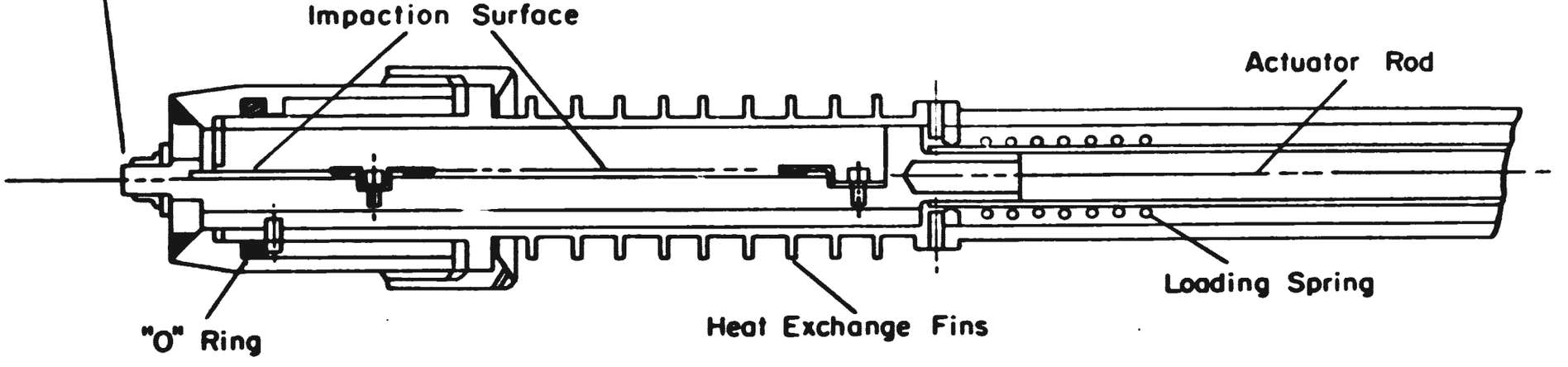

Figure 6b · MARK III IMPACTOR PROBE ASSEMBLY

Isotopes, Inc.

Results of Particle Measurements

One of the most prominent physical properties of the collected particles is their hygroscopicity. In many of the samples the effects of reaction with moisture were quite pronounced, causing flattening of the particles. Since the probes were air tight, it is believed that the particles exist to some extent in association with water in the stratosphere. The particles may exist as moist solids or even as droplets in extreme cases. The method of correction for the effects of flattening of the particles was explained in detail in DASA-1300.

As in the case of the HASP samples, it was necessary to apply theoretical impaction efficiencies[6] to the observed distributions of particle sizes. The impaction parameter, ψ, was calculated for a given particle size according to the definition:

$$\psi = \frac{C \rho_p V_o D_p^2}{18\mu D_c}$$

where: C = Cunningham correction factor for gas resistance experienced by small particles,

D_p = diameter of the particles,

D_c = width of the collector,

ρ_p = density of the particulate material,

μ = coefficient of viscosity of the air,

V_o = velocity of the free aerosal stream relative to the collector.

The theoretical relationship between $\sqrt{\psi}$ and the impaction efficiency η for a hypothetical, infinitesimally thin ribbon, after Ranz and Wong[6], is shown in Figure 7. The values of ψ were computed for particular values of the particle diameter, D_p, utilizing flight data to

obtain C (a function of altitude and D_p), V_o and μ (a function of temperature only), and using D_c = 0.32 cm and ρ_p = 2 g/cm^3. (The actual density of ammonium sulfate is 1.78 g/cm^3 while that of ammonium persulfate is 1.98 g/cm^3.)

In this work the value of μ is 1.422×10^{-4} poise, corresponding to a temperature of 216.66°K which is the ARDC Model Atmosphere value for the stratosphere. A 10°K temperature difference would result in less than 10% change in the calculated number concentration. The percentage changes are smaller for the larger particles which are collected with higher efficiencies.

All of the data pertinent to the computation of the concentrations in air of various particle size fractions are shown for each sample in Table 6. Also shown are flight data and dates of collection. The listed values of radius are the mean radii of the class intervals for which the count data were determined. The column headed $1/\eta$ is the reciprocal of the efficiency. The listed observed frequencies of particles of the various classes are multiplied by $1/\eta$ and divided by the volume of air sampled to give the values of $\bar{n}_i$, the concentrations of particles in the various classes. The total number concentration for a sample is found by summing the values of $\bar{n}_i$. The volume concentration, $\bar{V}$, is computed by:

$$\bar{V} = \frac{4}{3}\pi \sum \bar{n}_i \; r_i^3 = \sum \bar{V}_i$$

Table 7 lists the chemical compositions of various samples as determined by selected area electron diffraction. The data showing the locations and collection dates of the samples are given here since some of these for which composition was determined were not analyzed for particle size distribution.

Table 8 is a summary of the particle number and volume concentrations. The table contains location and sampling date information, and the samples are grouped according to altitude.

Since the variations in the number concentrations appear to be quite large, it is desirable to reduce the particle size-frequency distributions to a form which is independent of number concentration. Accordingly, the quantity

$$f(r) = \frac{1}{n} \frac{dn}{d(\log r)}$$

was computed for each size class in each sample. This is simply accomplished by dividing each $\bar{n}_i$ by the center difference $\delta (\log r_i)$ and by $\bar{n}$. The results of this calculation are shown in Table 9. The values of the distribution functions, f(r), are listed for each r_i in each sample and the average and median values of f(r) are listed for each r_i. The distribution functions for the individual samples are shown plotted in Figure 8a - 1. The average distribution function is plotted in Figure 9.

The nearly parabolic shape of the average distribution function suggests a log-normal distribution. In Figure 10 is shown a log-probability plot of the average distribution function. The straight line drawn among the points is a log-normal distribution with (geometric) mean radius 0.275 micron and a geometric standard deviation of 1.37.

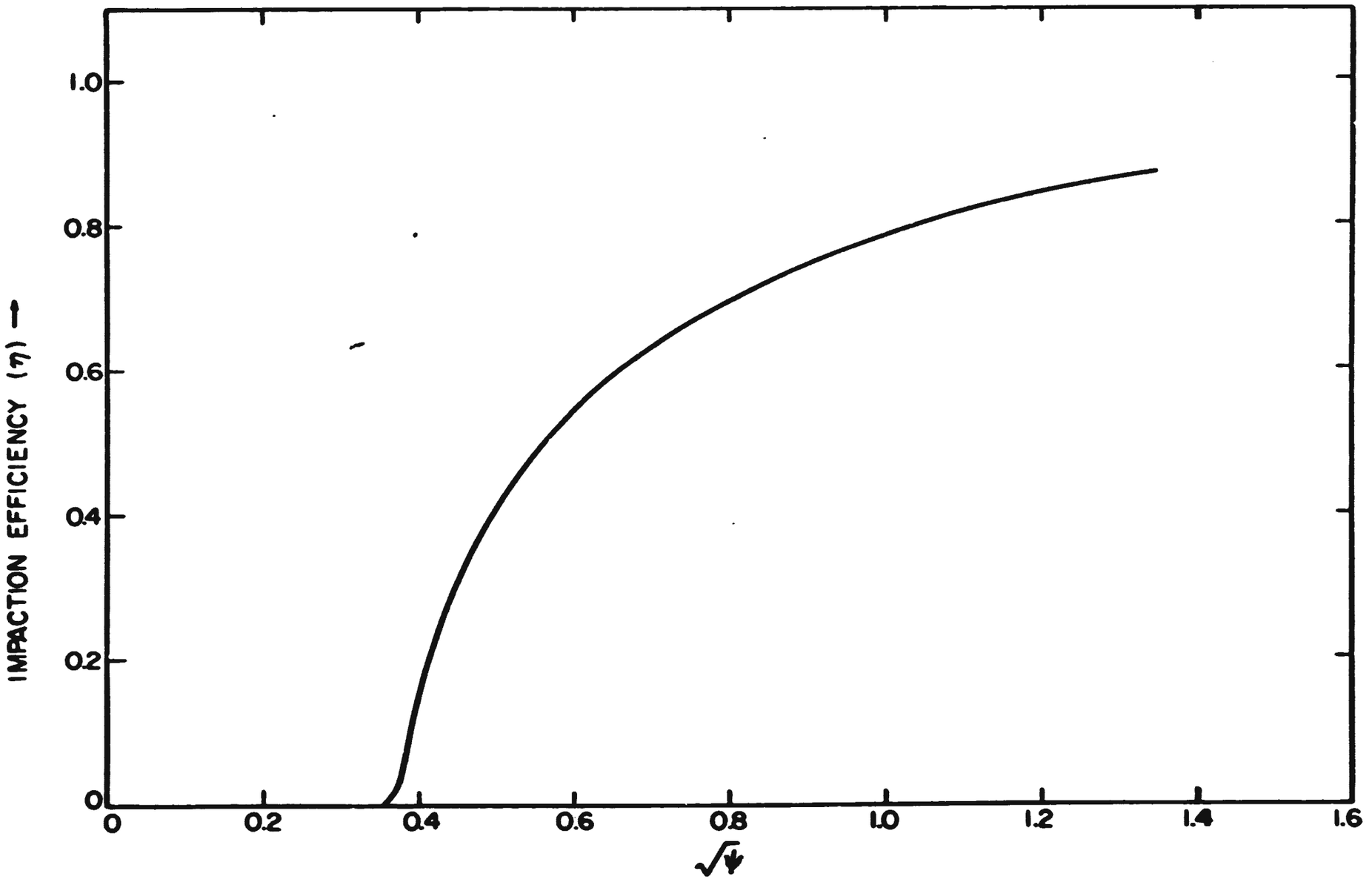

FIGURE 7 THEORETICAL IMPACTION EFFICIENCIES OF A RIBBON (after RANZ and WONG)

Isotopes, Inc.

Table 6. Flight Data and Particle Size Measurements for Star Dust Impactor Samples

Sample No. 243 Date of Collection: 13 Feb 1962

Latitude	Longitude	Altitude (feet)	TAS (knots)	Time (min)
32:00N/49:00N	100:00W/112:00W	60,000	410	169

Normalized Volume: 2.140×10^{8} cm^3

Radius (μ)	$\frac{1}{\eta}$	Obs. Frequency $\times 10^{-4}$ (cm^{-2})	$\bar{n} \times 10^{5}$ (cm^{-3})	$\bar{V} \times 10^{5}$ (μ^3/cm^3)
.138	2.43	11.88	135	1.48
.160	2.07	37.44	362	6.15
.182	1.81	51.77	438	11.0
.199	1.76	44.15	363	12.0
.224	1.66	73.06	567	26.6
.244	1.60	108.36	810	49.4
.264	1.57	98.20	720	55.4
.282	1.53	101.18	723	68.0
.300	1.46	42.18	288	32.5
.318	1.43	39.67	265	35.5
.336	1.40	16.83	110	17.4
.352	1.38	15.59	100	18.2
.370	1.36	11.98	76.2	16.2
.386	1.34	4.92	30.8	7.39
.402	1.33	5.32	33.0	8.98
.418	1.31	1.95	11.9	3.63
.432	1.30	4.73	28.7	9.67
.448	1.28	.36	2.18	0.82
.462	1.27	.45	2.67	1.10
.478	1.26	.22	1.26	0.57
.492	1.25	.14	0.81	0.40

Number Concentration: 5.07×10^{-2} cm^{-3} Volume Concentration: 3.82×10^{-3} μ^3/cm^3

Table 6. (continued)

Sample No. 244 Date of Collection: 13 Feb 1962

Latitude	Longitude	Altitude (feet)	TAS (knots)	Time (min)
32:00N/49:00N	100:00W/112:00W	50,000	380	191

Normalized Volume: $2.24 \times 10^{8} cm^{3}$

Radius (μ)	$\frac{1}{\eta}$	Obs. Frequency $\times 10^{-4}$ (cm^{-2})	$\bar{n} \times 10^{5}$ (cm^{-3})	$\bar{V} \times 10^{5}$ (μ^{3}/cm^{3})
.138	9.09	1.47	59.5	0.654
.160	4.59	4.96	102	1.73
.182	3.22	4.26	60.8	1.52
.199	2.82	6.11	76.7	2.53
.224	2.30	6.58	67.2	3.16
.244	2.08	13.90	129	7.87
.264	1.92	18.76	161	12.4
.282	1.83	23.51	192	18.0
.300	1.75	23.51	184	20.8
.318	1.69	25.08	189	25.3
.336	1.65	17.00	125	19.8
.352	1.61	14.52	105	19.1
.370	1.58	7.06	49.6	10.5
.386	1.54	6.74	46.2	11.1
.402	1.52	.16	1.09	0.296
.418	1.49	.31	2.06	0.628
.432	1.47	.31	2.03	0.684
.448	1.45	-	-	-
.462	1.42	-	-	-
.478	1.40	-	-	-
.492	1.38	.16	0.994	0.495
.614	1.27	.16	0.914	0.885

Number Concentration: 1.55×10^{-2} cm^{-3} Volume Concentration: 1.57×10^{-3} μ^{3}/cm^{3}

Table 6. (continued)

Sample No. 245 Date of Collection: 13 Mar 1962

Latitude	Longitude	Altitude (feet)	TAS (knots)	Time (min)
48:40N/31:20N	112:20W/100:40W	40,000	324	209

Normalized Volume: $2.09 \times 10^{8}\ cm^{3}$

Radius (μ)	$\frac{1}{\eta}$	Obs. Frequency $\times 10^{-4}$ (cm^{-2})	$\bar{n} \times 10^{5}$ (cm^{-3})	$\bar{V} \times 10^{5}$ (μ^{3}/cm^{3})
.138	-	-	-	-
.160	-	3.87	-	-
.182	-	6.58	-	-
.199	32.26	4.00	616	20.3
.224	6.90	3.23	106	4.98
.244	4.40	12.21	257	15.7
.264	3.41	11.95	194	14.9
.282	2.98	24.81	353	33.2
.300	2.67	28.89	368	41.6
.318	2.43	21.06	245	32.8
.336	2.26	24.49	264	41.7
.352	2.11	13.66	138	25.1
.370	1.98	4.00	37.8	8.01
.386	1.89	1.42	12.8	3.07
.402	1.84	1.81	16.0	4.35
.418	1.77	.52	4.42	1.35
.432	1.73	.13	1.21	0.41
.448	1.69	.26	2.20	0.83
.462	1.65	.13	1.16	0.48
.478	1.62	.39	3.08	1.40
.492	1.59	-	-	-
.506	1.56	.13	1.09	0.59
.520	1.54	.13	1.08	0.64

Number Concentration: $2.62 \times 10^{-2}\ cm^{-3}$ Volume Concentration: $2.51 \times 10^{-3}\ \mu^{3}/cm^{3}$

Table 6. (continued)

Sample No. 252 Date of Collection: 19 Jun 1962

Latitude	Longitude	Altitude (feet)	TAS (knots)	Time (min)
31:15N/48:35N	101:27W/112:21W	50,000	384	194

Normalized Volume: 2.30×10^{8} cm^{3}

Radius (μ)	$\frac{1}{\eta}$	Obs. Frequency $\times 10^{-4}$ (cm^{-2})	$\bar{n} \times 10^{5}$ (cm^{-3})	$\bar{V} \times 10^{5}$ (μ^{3}/cm^{3})
.138	9.09	8.93	353	3.88
.160	4.59	11.77	235	4.00
.182	3.22	13.98	196	4.90
.199	2.82	17.57	215	7.10
.224	2.30	13.73	138	6.49
.244	2.08	0.87	7.90	0.48
.264	1.92	3.86	32.2	2.48
.282	1.83	15.64	124	11.6
.300	1.75	14.38	109	12.3
.318	1.69	12.28	90.2	12.1
.336	1.65	9.72	69.6	11.0
.352	1.61	5.10	35.7	6.5
.370	1.58	0.19	1.26	0.27
.386	1.54	2.89	19.4	4.66
.402	1.52	4.91	32.4	8.81
.418	1.49	2.50	16.2	4.94
.432	1.47	0.29	1.91	0.64
.448	1.45	2.70	17.0	6.39
.462	1.42	0.29	1.85	0.76
.478	1.40	7.03	42.8	19.5
.492	1.38	0.19	1.10	0.55
.506	1.37	2.50	14.9	8.08
.520	1.36	2.31	13.6	8.00
.534	1.35	0.19	1.08	0.69
.548	1.33	2.31	13.3	9.15
.560	1.32	0.10	0.53	0.39
.574	1.30	-	-	-
.588	1.29	-	-	-
.600	1.28	-	-	-
.614	1.27	0.10	0.51	0.49

Number Concentration: 1.78×10^{-2} cm^{-3} Volume Concentration: 1.56×10^{-3} μ^{3}/cm^{3}

Table 6. (continued)

Sample No. 254 Date of Collection: 12 Jun 1962

Latitude	Longitude	Altitude (feet)	TAS (knots)	Time (min)
31:09N/48:35N	101:25W/112:22W	55,000	403	175

Normalized Volume: $2.18 \times 10^{8} cm^{3}$

Radius (μ)	$\frac{1}{\eta}$	Obs. Frequency $\times 10^{-4}$ (cm^{-2})	$\bar{n} \times 10^{5}$ (cm^{-3})	$\bar{V} \times 10^{5}$ (μ^3/cm^3)
.138	3.34	4.68	71.8	0.79
.160	2.63	9.24	112	1.90
.182	2.26	11.74	122	3.05
.199	2.05	5.19	48.8	1.61
.224	1.87	6.71	57.6	2.71
.244	1.76	16.72	135	8.24
.264	1.69	24.25	188	14.5
.282	1.63	31.51	236	22.2
.300	1.58	50.24	364	41.1
.318	1.54	51.80	366	49.0
.336	1.51	39.68	275	43.4
.352	1.48	21.95	149	27.1
.370	1.45	26.66	177	37.5
.386	1.42	12.88	83.9	20.1
.402	1.40	11.61	74.6	20.3
.418	1.38	2.91	18.5	5.64
.432	1.37	5.56	34.9	11.8
.448	1.35	2.78	17.3	6.50
.462	1.34	-	-	-
.478	1.32	.13	0.79	.36
.492	1.31	-	-	-
.506	1.30	1.39	8.32	4.51

Number Concentration: $2.54 \times 10^{-2} cm^{-3}$ Volume Concentration: $3.22 \times 10^{-3} \mu^3/cm^3$

Isotopes, Inc.

Table 6. (continued)

Sample No. 257 Date of Collection: 26 Jun 1962

Latitude	Longitude	Altitude (feet)	TAS (knots)	Time (min)
31:09N/48:17N	101:25W/112:07W	55,000	389	180

Normalized Volume: 2.162×10^{8} cm^3

Radius (μ)	$\frac{1}{\eta}$	Obs. Frequency $\times 10^{-4}$ (cm^{-2})	$\bar{n} \times 10^{5}$ (cm^{-3})	$\bar{V} \times 10^{5}$ (μ^3/cm^3)
.138	3.57	0.87	14.3	0.16
.160	2.77	4.93	63.2	1.07
.182	2.36	10.92	119	2.98
.199	2.12	9.95	97.5	3.22
.224	1.91	8.01	70.7	3.32
.244	1.79	14.88	123	7.50
.264	1.72	39.24	312	24.0
.282	1.65	59.43	454	42.7
.300	1.61	52.37	390	44.1
.318	1.56	26.52	191	25.6
.336	1.53	18.62	132	20.8
.352	1.50	19.65	136	24.8
.370	1.46	12.84	86.7	18.4
.386	1.44	9.47	63.1	15.1
.402	1.41	4.93	32.1	8.73
.418	1.39	3.38	21.7	6.62
.432	1.38	3.38	21.5	7.24
.448	1.36	1.26	7.89	2.97
.462	1.35	1.06	6.62	2.73
.478	1.33	0.87	5.32	2.42
.492	1.32	1.06	6.47	3.22
.506	1.30	2.13	12.7	6.88

Number Concentration: 2.37×10^{-2} cm^{-3} Volume Concentration: 2.74×10^{-3} μ^3/cm^3

Isotopes, Inc.

Table 6. (continued)

Sample No: 258 Date of Collection: 14 Feb 1963

Latitude	Longitude	Altitude (feet)	TAS (knots)	Time (min)
39:00 N/45:00N	104:00W/109:00 W	60,000	411	60

Normalized Volume: $0.762 \times 10^{8} cm^{3}$

Radius (μ)	$\frac{1}{\eta}$	Obs. Frequency $\times 10^{-4}$ (cm^{-2})	$\bar{n} \times 10^{5}$ (cm^{-3})	$\bar{V} \times 10^{5}$ (μ^{3}/cm^{3})
.138	2.43	.77	24.5	0.270
.160	2.07	4.90	133	2.26
.182	1.81	5.13	122	3.05
.199	1.76	6.10	141	4.65
.224	1.66	16.80	365	17.2
.244	1.60	24.80	522	31.8
.264	1.57	66.60	1,370	105
.282	1.53	62.90	1,260	118
.300	1.46	47.25	907	102
.318	1.43	43.32	812	109
.336	1.40	27.12	498	78.7
.352	1.38	21.90	397	72.2
.370	1.36	14.35	256	54.3
.386	1.34	17.90	315	75.6
.402	1.33	5.93	103	28.0
.418	1.31	10.35	178	54.3
.432	1.30	5.54	94.5	31.8
.448	1.28	1.77	29.7	11.2
.462	1.2,	3.74	63.1	26.0
.478	1.26	.97	16.0	7.30
.492	1.25	2.16	35.4	17.6
.506	1.24	.77	12.5	6.78
.520	1.23	.39	6.27	3.69
.534	1.22	.39	6.22	3.96

Number Concentration: $7.67 \times 10^{-2}\ cm^{-3}$ Volume Concentration: $9.65 \times 10^{-3} \mu^{3}/cm^{3}$

Isotopes, Inc.

Table 6. (continued)

Sample No. 259 Date of Collection: 19 Feb 1963

Latitude	Longitude	Altitude (feet)	TAS (knots)	Time (min)
31:22N/19:30N	100:29W/95:32W	60,000	406	120

Normalized Volume: 1.50×10^{8} cm^3

Radius (μ)	$\frac{1}{\eta}$	Obs. Frequency $\times 10^{-4}$ (cm^{-2})	$\bar{n} \times 10^{5}$ (cm^{-3})	$\bar{V} \times 10^{5}$ (μ^3/cm^3)
.138	2.43	16.3	262	2.88
.160	2.07	40.4	555	9.44
.182	1.81	27.9	335	8.38
.199	1.76	22.3	260	8.58
.224	1.66	86.0	948	44.6
.244	1.60	106.5	1,130	68.9
.264	1.57	83.3	865	66.6
.282	1.53	87.4	887	83.4
.300	1.46	31.9	310	35.0
.318	1.43	40.9	389	52.1
.336	1.40	18.3	171	27.0
.352	1.38	15.1	138	25.1
.370	1.36	8.6	77.5	16.4
.386	1.34	11.8	106	25.4
.402	1.33	8.6	75.8	20.6
.418	1.31	6.4	56.3	17.2
.432	1.30	5.9	50.7	17.1
.448	1.28	.9	7.68	2.89
.462	1.27	.9	7.62	3.14
.478	1.26	.7	5.04	2.30
.492	1.25	.5	3.75	1.87
.506	1.24	.3	2.48	1.34
.520	1.23	.6	4.92	2.89
.534	1.22	.2	1.22	0.776
.548	1.21	.5	3.63	2.50
.560	1.20	.2	1.20	0.881
.574	1.19	.2	1.19	0.940
.588	1.19	.1	1.19	1.01
.600	1.18	.1	1.18	1.06
.614	1.18	.3	2.36	2.28
.626	1.17	.1	1.17	1.19
.640	1.16	.1	1.16	1.28
.652	1.16	.0	-	-

Number Concentration: 6.62×10^{-2} cm^{-3} Volume Concentration: $5.55 \times 10^{-3} \mu^3/cm^3$

Table 6. (continued)

Sample No. 265 Date of Collection: 2 Apr 1963

Latitude	Longitude	Altitude (feet)	TAS (knots)	Time (min)
31:05N/32:30N	99:20W/99:50W	60,000	407	60

Normalized Volume: 0.7542×10^{8} cm^3

Radius (μ)	$\frac{1}{\eta}$	Obs. Frequency $\times 10^{-4}$ (cm^{-2})	$\bar{n} \times 10^{5}$ (cm^{-3})	$\bar{V} \times 10^{5}$ (μ^3/cm^3)
.138	2.43	-	0	0
.160	2.07	-	0	0
.182	1.81	-	0	0
.199	1.76	3.73	86.9	2.87
.224	1.66	1.34	29.5	1.39
.244	1.60	4.87	103	6.28
.264	1.57	8.68	181	13.9
.282	1.53	23.55	478	44.9
.300	1.46	26.87	520	58.8
.318	1.43	13.94	264	35.4
.336	1.40	30.95	574	90.7
.352	1.38	24.46	448	81.5
.370	1.36	19.77	356	75.5
.386	1.34	18.07	321	77.0
.402	1.33	13.41	236	64.2
.418	1.31	3.08	53.4	16.3
.432	1.30	1.67	28.7	9.67
.448	1.28	.36	6.14	2.31
.462	1.27	.80	13.4	5.52
.478	1.26	.27	4.54	2.07
.492	1.25	.88	14.6	7.27
.506	1.24	.44	7.19	3.90
.520	1.23	.62	10.1	5.94
.534	1.22	1.15	18.5	11.8
.548	1.21	.09	1.45	1.00
.560	1.20	.09	1.44	1.06
.574	1.19	.36	5.71	4.51
.588	1.19	.9	14.2	12.1
.600	1.18	.9	14.0	12.6

Number Concentration: 3.79×10^{-2} cm^{-3} Volume Concentration: 6.48×10^{-3} μ^3/cm^3

Isotopes, Inc.

Table 6. (continued)

Sample No. 266 Date of Collection: 7 May 1963

Latitude	Longitude	Altitude (feet)	TAS (knots)	Time (min)
30:40N/33:26N	99:45W/99:30W	60,000	~415	60

Normalized Volume: $0.7691 \times 10^{8} cm^{3}$

Radius (μ)	$\frac{1}{\eta}$	Obs. Frequency $\times 10^{-4}$ (cm^{-2})	$\bar{n} \times 10^{5}$ (cm^{-3})	$\bar{V} \times 10^{5}$ (μ^{3}/cm^{3})
.138	2.43	0	0	0
.160	2.07	0	0	0
.182	1.81	0	0	0
.199	1.76	1.27	29.0	0.96
.224	1.66	10.16	219	10.3
.244	1.60	21.59	449	27.4
.264	1.57	40.64	830	63.9
.282	1.53	92.71	1,840	173
.300	1.46	140.97	2,680	303
.318	1.43	130.81	2,430	326
.336	1.40	139.70	2,540	401
.352	1.38	97.79	1,750	318
.370	1.36	96.52	1,710	362
.386	1.34	77.47	1,350	324
.402	1.33	93.98	1,620	441
.418	1.31	68.58	1,170	357
.432	1.30	60.96	1,030	347
.448	1.28	40.64	676	254
.462	1.27	40.64	671	276
.478	1.26	45.72	749	342
.492	1.25	20.32	330	164
.506	1.24	19.05	307	166
.520	1.23	17.78	284	167
.534	1.22	12.70	201	128
.548	1.21	13.97	220	151
.560	1.20	3.81	59.4	43.6
.574	1.19	13.97	216	171
.588	1.19	5.08	78.5	66.7
.600	1.18	0	0	0
.614	1.18	1.27	19.5	18.9
.626	1.17	5.08	77.2	78.7
.640	1.16	1.27	19.1	21.0
.652	1.16	0	0	0
.664	1.15	1.27	19.0	23.2
-	-	-	-	-
.732	1.14	1.27	18.8	30.8

Number Concentration: 2.36×10^{-1} cm^{-3} Volume Concentration: 5.56×10^{-2} μ^{3}/cm^{3}

Isotopes, Inc.

Table 6. (continued)

Sample No. 268 Date of Collection: 30 Jul 1963

Latitude	Longitude	Altitude (feet)	TAS (knots)	Time (min)
32:00N/33:00N	111:00W/111:00W	60,000	~415	60

Normalized Volume: $0.769 \times 10^{8} cm^{3}$

Radius (μ)	$\frac{1}{\eta}$	Obs. Frequency $\times 10^{-4}$ (cm^{-2})	$\bar{n} \times 10^{5}$ (cm^{-3})	$\bar{V}_3 \times 10^{5}$ (μ^3/cm^3)
.138	2.43	0	0	0
.160	2.07	12.70	342	5.81
.182	1.81	125.73	2,960	74.0
.199	1.76	247.65	5,670	187
.224	1.66	167.64	3,620	170
.244	1.60	123.19	2,560	156
.264	1.57	72.39	1,480	114
.282	1.53	58.42	1,160	109
.300	1.46	58.42	1,110	125
.318	1.43	64.77	1,200	161
.336	1.40	43.18	786	124
.352	1.38	55.88	1,000	182
.370	1.36	48.26	853	181
.386	1.34	35.56	620	149
.402	1.33	34.29	593	161
.418	1.31	20.32	346	106
.432	1.30	19.05	322	108
.448	1.28	13.97	232	87.2
.462	1.27	8.89	147	60.6
.478	1.26	6.35	104	47.4
.492	1.25	11.43	186	92.6
.506	1.24	6.35	102	55.3
.520	1.23	2.54	40.6	23.9
.534	1.22	2.54	40.3	25.6
.548	1.21	0	0	0
.560	1.20	1.27	19.8	14.5
.574	1.19	5.08	78.5	62.0
.588	1.19	5.08	78.5	66.7
.600	1.18	1.27	19.5	17.6
.614	1.18	1.27	19.5	18.9
.626	1.17	1.27	19.3	19.7
.640	1.16	0	0	0
.652	1.16	1.27	19.1	22.2
.664	1.15	1.27	19.0	23.2
.676	1.15	0	0	0

Number Concentration: 2.57×10^{-1} cm^{-3} Volume Concentration: 2.75×10^{-2} μ^3/cm^3

Isotopes, Inc.

Table 6. (continued)

Sample No. 271 Date of Collection: 13 Aug 1963

Latitude	Longitude	Altitude (feet)	TAS (knots)	Time (min)
32:00N/32:00N	111:00W/111:00W	60,000	415	60

Normalized Volume: $0.769 \times 10^{8} cm^{3}$

Radius (μ)	$\frac{1}{\eta}$	Obs. Frequency $\times 10^{-4}$ (cm^{-2})	$\bar{n} \times 10^{5}$ (cm^{-3})	$\bar{V} \times 10^{5}$ (μ^{3}/cm^{3})
.138	2.43	-	0	0
.160	2.07	1.59	42.8	0.73
.182	1.81	12.70	299	7.48
.199	1.76	6.38	146	4.82
.224	1.66	22.30	481	22.6
.244	1.60	17.50	364	22.2
.264	1.57	31.80	649	50.0
.282	1.53	27.00	537	50.5
.300	1.46	27.00	512	57.8
.318	1.43	33.40	621	83.2
.336	1.40	33.40	608	96.1
.352	1.38	19.10	343	62.4
.370	1.36	20.70	366	77.6
.386	1.34	9.55	166	39.8
.402	1.33	3.17	54.8	14.9
.418	1.31	3.17	54.9	16.7
.432	1.30	9.55	161	54.2
.448	1.28	9.55	159	59.8
.462	1.27	1.59	26.3	10.8
.478	1.26	1.59	26.1	11.9
.492	1.25	-	0	0

Number Concentration: 5.62×10^{-2} cm^{-3} Volume Concentration: 7.43×10^{-3} μ^{3}/cm^{3}

Table 7. Composition of Stratospheric Particles in Impaction Samples

Sample Number	Sampling Date	Altitude (Kft)	Latitude	Composition*
241	25 Jan 62	69	30°N	S
242	30 Jan 62	60	31°- 48°N	S
243	13 Feb 62	60	31°- 48°N	S
244	13 Feb 62	50	31°- 48°N	P
245	13 Mar 62	40	31°- 48°N	P
251	5 Jun 62	60	31°- 48°N	P
252	19 Jun 62	50	31°- 48°N	S
254	12 Jun 62	55	31°- 48°N	S
257	26 Jun 62	55	31°- 48°N	M
258	14 Feb 63	60	39°- 45°N	S
259	19 Feb 63	60	31°- 19 1/2°N	S
260	6 Feb 63	65	32°- 56°N	P
262	21 Feb 63	65	49°- 64°N	S

*S = Ammonium Sulfate

P = Ammonium Per Sulfate

M = Mixture of S and P

Table 8. Summary of Particle Number and Volume Concentrations

Sample Number	Collection Date	Altitude (Kft)	Latitude	Longitude	$\bar{n} \times 10^2$ (cm^{-3})	$\bar{V} \times 10^3$ (μ^3/cm^3)
243	13 Feb 62	60	32:49°N	100°-112°W	5.07	3.82
258	14 Feb 63	60	39-45°N	104°-109°W	7.67	9.65
259	19 Feb 63	60	31:22-19:30N	100:29-95:32W	6.66	5.55
265	2 Apr 63	60	31:05-32:30N	99:20-99:50W	3.79	6.48
266	7 May 63	60	30:40-33:26N	99:45-99:30W	23.6	55.6
268	30 Jul 63	60	32°-33°N	111°W	25.7	27.5
271	13 Aug 63	60	32°N	111°W	5.62	7.44
254	12 Jun 62	55	31:09-48:35N	101:25-112:22W	2.54	3.22
257	26 Jun 62	55	31:09-48:17N	101:25-112:07W	2.37	2.74
244	13 Feb 62	50	32°-49°N	100°-112°W	1.55	1.57
252	19 Jun 62	50	31:15-48:35N	101:27-112:21W	1.78	1.56
245	13 Mar 62	40	48:40-31:20N	112:20-100:40W	2.62	2.51

Table 9. Experimental and Average Values of the Size Distribution Function

$\frac{1}{\bar{n}} \frac{d\bar{n}}{d(\log r)}$

Sample	Date	Alt.(kft) \ Radius(μ)	.138	.160	.182	.199	.224	.244	.264	.282	.300	.318	.336
243	13 Feb 62	60.0	0.414	1.19	1.82	1.59	2.53	4.48	4.52	5.14	2.18	2.12	0.983
258	14 Feb 63	60.0	0.049	0.288	0.335	0.407	1.08	1.91	5.68	5.92	4.53	4.30	2.94
259	19 Feb 63	60.0	0.612	1.39	1.06	0.865	3.21	4.76	4.13	4.80	1.78	2.37	1.16
265	2 Apr 63	60.0	0	0	0	0.508	0.175	0.762	1.52	4.54	5.26	2.83	6.86
266	7 May 63	60.0	0	0	0	0.027	0.209	0.533	1.12	2.81	4.35	4.18	4.88
268	30 Jul 63	60.0	0	0.220	2.43	4.88	3.18	2.79	1.83	1.62	1.65	1.89	1.38
271	13 Aug 63	60.0	0	0.126	1.12	0.576	1.93	1.82	3.68	3.44	3.49	4.49	4.91
254	12 Jun 62	55.0	0.440	0.733	1.01	0.425	0.512	1.49	2.36	3.35	5.49	5.85	4.91
257	26 Jun 62	55.0	0.094	0.444	1.06	0.913	0.674	1.46	4.20	6.91	6.32	3.28	2.53
244	13 Feb 62	50.0	0.596	1.09	0.826	1.09	0.976	2.33	3.30	4.45	4.54	4.94	3.65
252	19 Jun 62	50.0	3.08	2.19	2.32	2.67	1.75	0.124	0.574	2.50	2.34	2.06	1.77
245	13 Mar 62	40.0	0	0	0	5.21	0.913	2.75	2.35	4.85	5.38	3.80	4.58
Median Value			0.072	0.366	1.04	0.889	1.03	1.87	2.83	4.50	4.44	3.54	3.29
Average $\left(\frac{1}{\bar{n}} \frac{d\bar{n}}{d(\log r)}\right)$			0.440	0.639	1.00	2.03	1.43	2.10	2.94	4.19	3.94	3.51	3.38

Table 9. Experimental and Average Values of the Size Distribution Function (continued)

$\frac{1}{\bar{n}} \quad \frac{d\bar{n}}{d(\log r)}$

Sample	Date	Alt.(kft) \ Radius(μ)	.352	.370	.386	.402	.418	.432	.448	.462	.478	.492	.506
243	13 Feb 62	60.0	0.942	0.750	0.337	0.376	0.150	0.376	0.029	0.037	0.018	0.012	-
258	14 Feb 63	60.0	2.48	1.67	2.28	0.776	1.49	0.818	0.265	0.584	0.152	0.373	0.135
259	19 Feb 63	60.0	0.989	0.581	0.882	0.657	0.540	0.505	0.079	0.081	0.055	0.045	0.030
265	2 Apr 63	60.0	5.65	4.69	4.70	3.60	0.902	0.503	0.111	0.251	0.087	0.311	0.157
266	7 May 63	60.0	3.54	3.62	3.18	3.97	3.17	2.90	1.96	2.02	2.32	1.13	1.08
268	30 Jul 63	60.0	1.86	1.65	1.34	1.33	0.860	0.831	0.617	0.405	0.295	0.584	0.329
271	13 Aug 63	60.0	2.92	3.25	1.64	0.564	0.625	1.90	1.94	0.332	0.340	0	-
254	12 Jun 62	55.0	2.80	3.48	1.83	1.70	0.466	0.912	0.466	0	0.022	0	0.272
257	26 Jun 62	55.0	2.75	1.83	1.48	0.784	0.587	0.603	0.228	0.198	0.164	0.221	0.446
244	13 Feb 62	50.0	3.23	1.59	1.65	0.040	0.084	0.086	-	-	-	0.051	-
252	19 Jun 62	50.0	0.956	0.035	0.603	1.05	0.581	0.071	0.653	0.073	1.76	0.049	0.695
245	13 Mar 62	40.0	2.52	0.720	0.271	0.352	0.107	0.030	0.057	0.031	0.086	0	0.034
Median Value			2.64	1.66	1.56	0.917	0.584	0.554	0.265	0.198	0.152	0.049	0.146
Average $\left(\frac{1}{\bar{n}} \frac{d\bar{n}}{d(\log r)}\right)$			2.55	1.99	1.68	1.27	0.797	0.795	0.582	0.365	0.481	0.248	0.289

Table 9. Experimental and Average Values of the Size Distribution Function (continued)

Sample	Date	Alt.(kft) \ Radius(μ)	.520	.534	.548	.560	.574	.588	.600	.614	.626	.640	.652	.664
			$\frac{1}{\bar{n}}$ $\frac{d\bar{n}}{d(\log r)}$											
243	13 Feb 62	60.0	-	-	-	-	-	-	-	-	-	-	-	-
258	14 Feb 63	60.0	0.069	0.071	-	-	-	-	-	-	-	-	-	-
259	19 Feb 63	60.0	0.063	0.016	0.052	0.017	0.016	0.018	0.018	0.038	0.019	0.019	-	-
265	2 Apr 63	60.0	0.227	0.428	0.037	0.037	0.142	0.389	0.392	-	-	-	-	-
266	7 May 63	60.0	1.03	0.748	0.903	0.250	0.863	0.345	0	0.089	0.363	0.091	0	0.102
268	30 Jul 63	60.0	0.134	0.137	0	0.076	0.287	0.316	0.080	0.082	0.083	0	0.092	0.093
271	13 Aug 63	60.0	-	-	-	-	-	-	-	-	-	-	-	-
254	12 Jun 62	55.0	-	-	-	-	-	-	-	-	-	-	-	-
257	26 Jun 62	55.0	-	-	-	-	-	-	-	-	-	-	-	-
244	13 Feb 62	50.0	-	-	-	-	-	-	-	0.063	-	-	-	-
252	19 Jun 62	50.0	0.651	0.053	0.722	0.029	0	0	0	0.031	-	-	-	-
245	13 Mar 62	40.0	0.035	-	-	-	-	-	-	-	-	-	-	-
Median Value			0.066	-	-	-	-	-	-	-	-	-	-	-
Average ($\frac{1}{\bar{n}}$ $\frac{d\bar{n}}{d(\log r)}$)			0.201	0.132	0.156	0.0372	0.119	0.0971	0.0445	0.0275	0.0423	0.010		

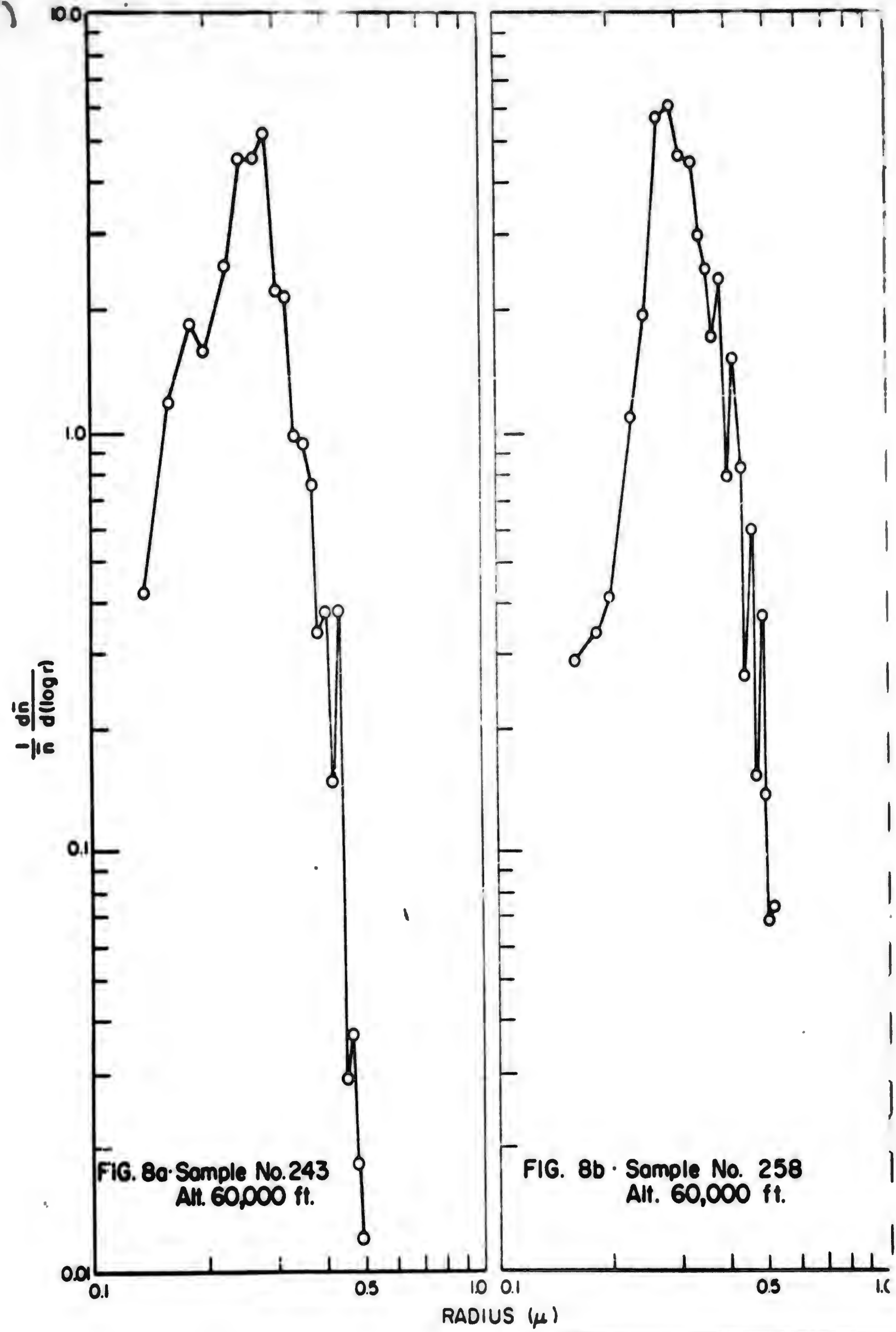

FIG. 8a · Sample No. 243
Alt. 60,000 ft.

FIG. 8b · Sample No. 258
Alt. 60,000 ft.

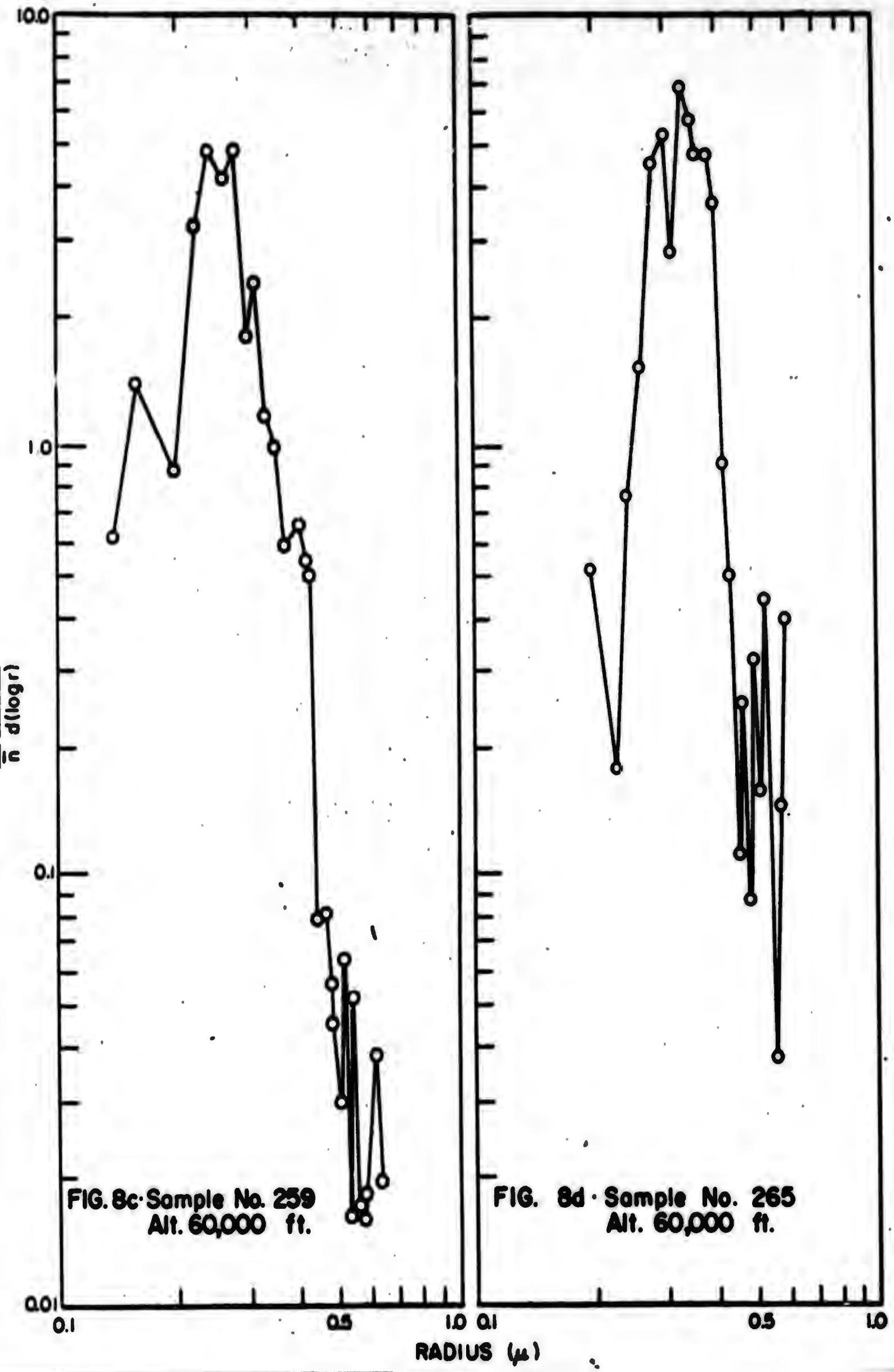

FIG. 8c · Sample No. 259
Alt. 60,000 ft.

FIG. 8d · Sample No. 265
Alt. 60,000 ft.

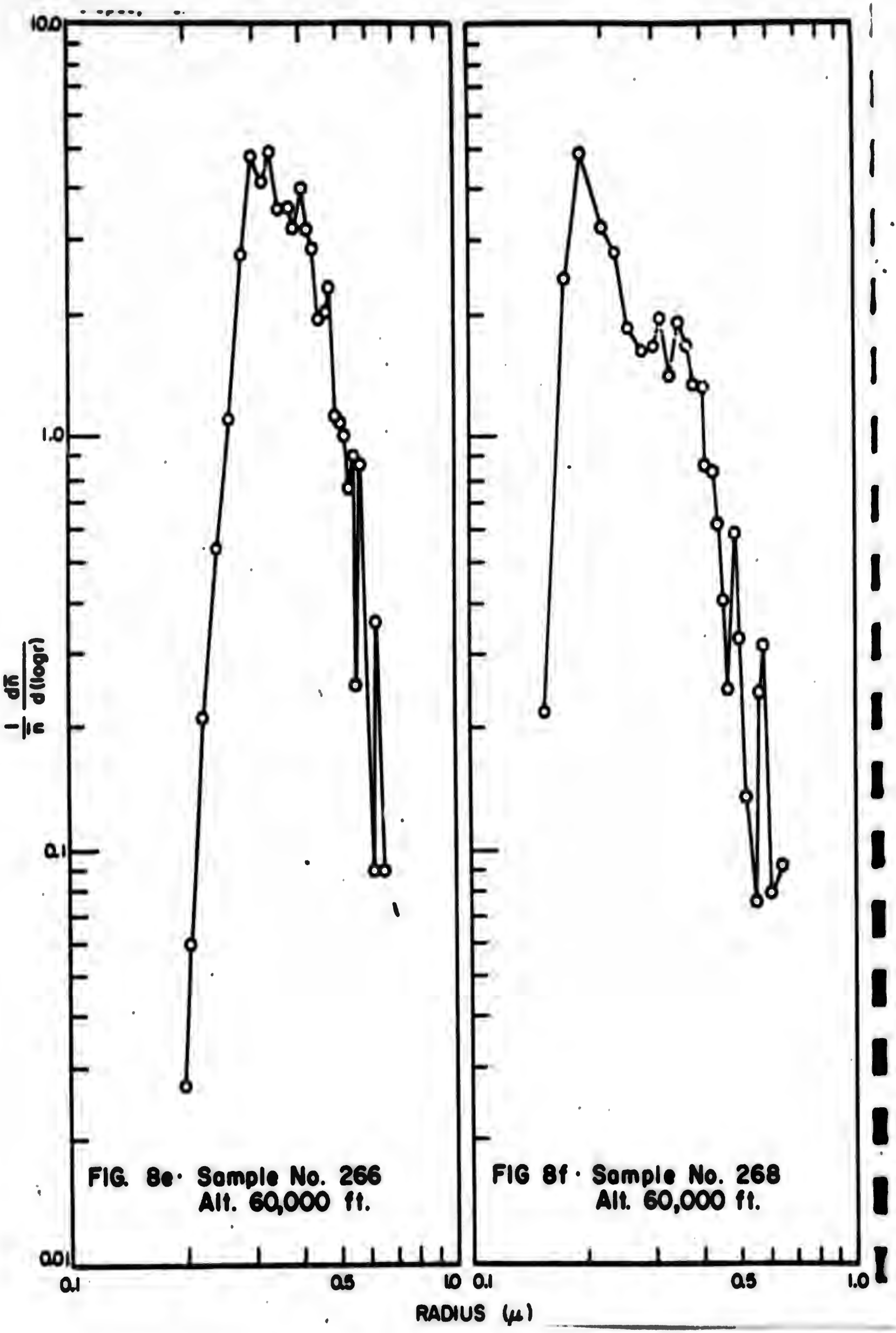

FIG. 8e · Sample No. 266
Alt. 60,000 ft.

FIG 8f · Sample No. 268
Alt. 60,000 ft.

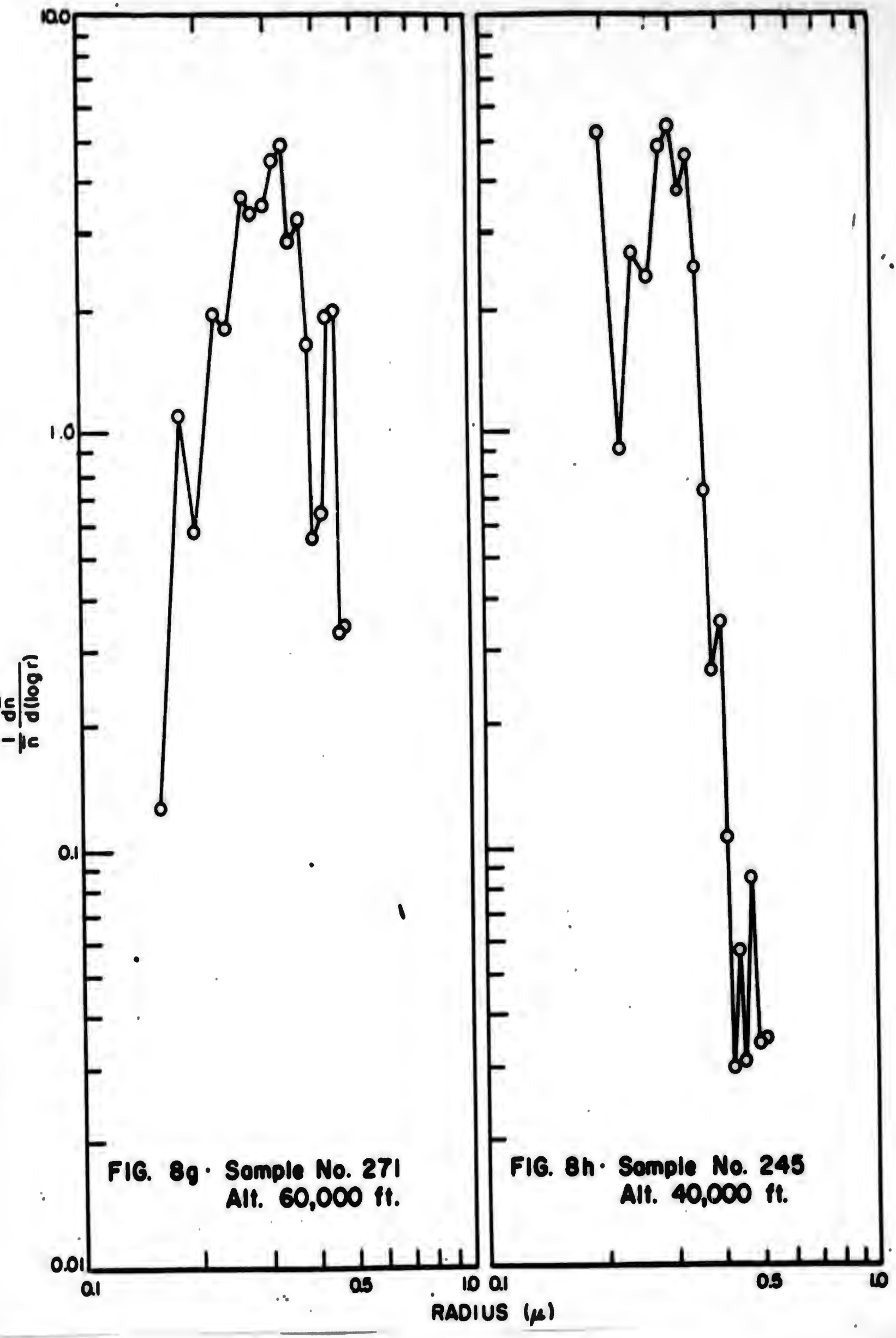

FIG. 8g · Sample No. 271
Alt. 60,000 ft.

FIG. 8h · Sample No. 245
Alt. 40,000 ft.

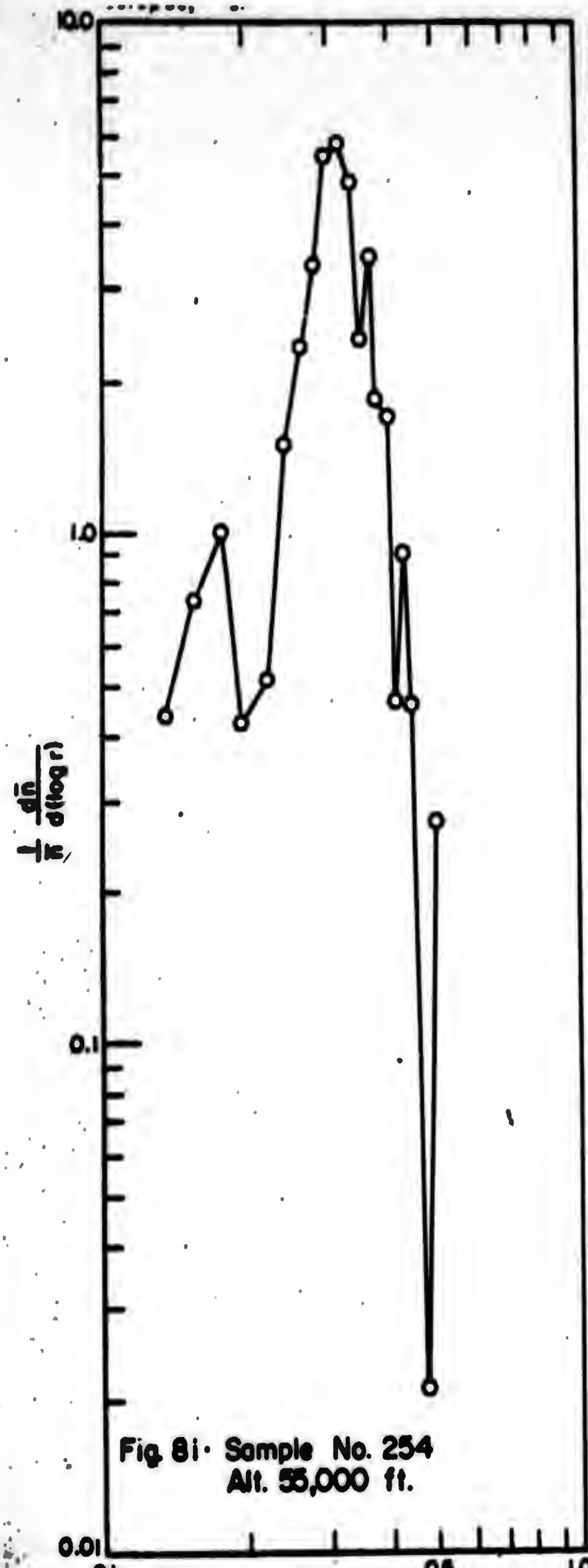

Fig. 8i · Sample No. 254
Alt. 55,000 ft.

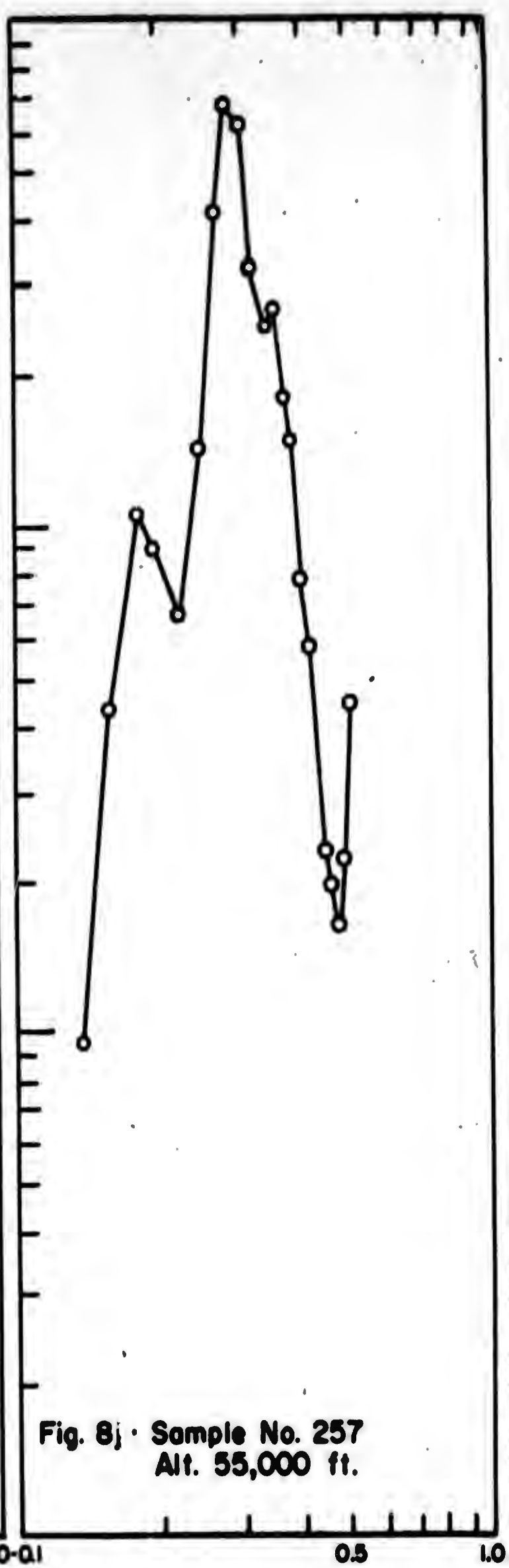

Fig. 8j · Sample No. 257
Alt. 55,000 ft.

RADIUS (μ)

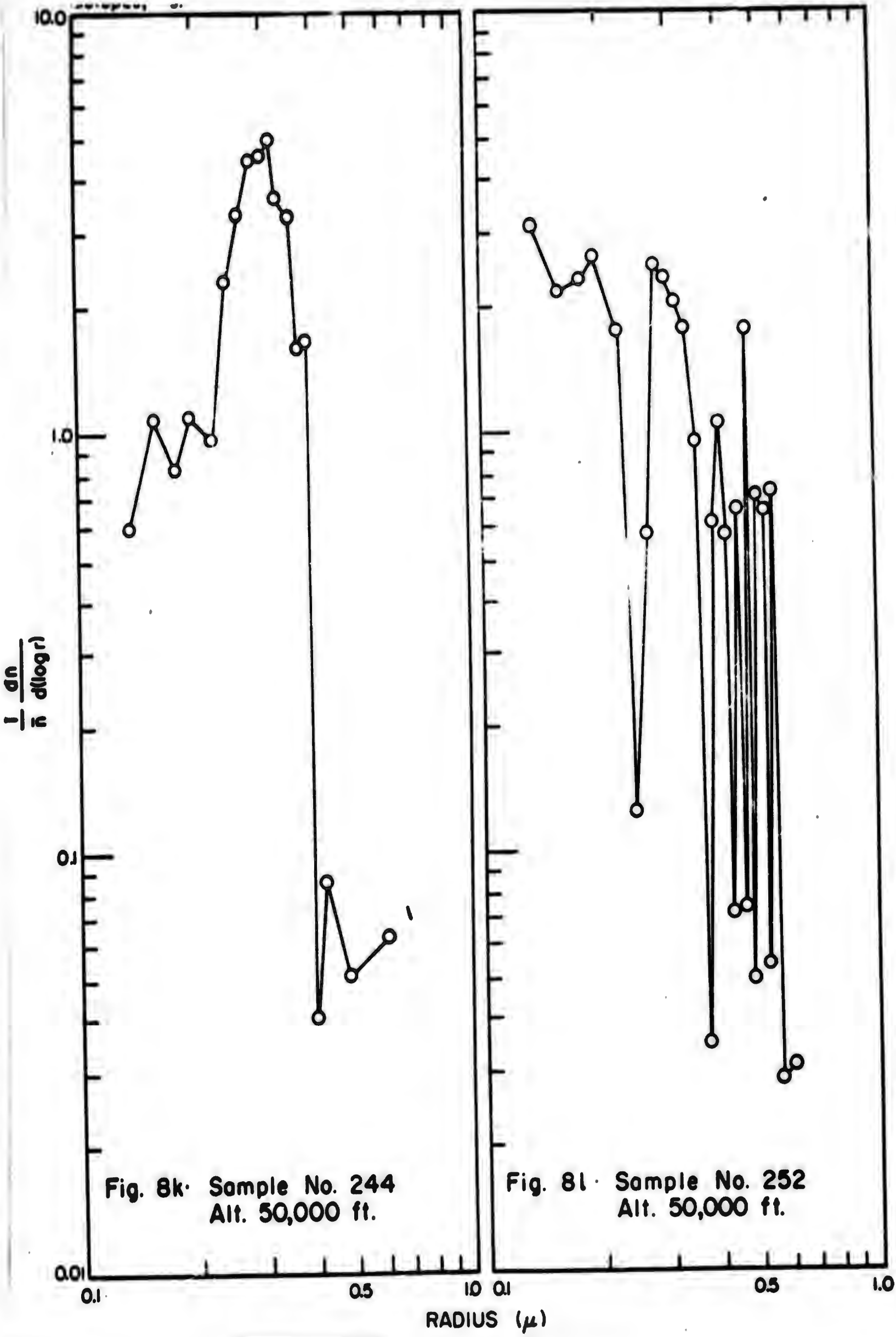

Fig. 8k· Sample No. 244
Alt. 50,000 ft.

Fig. 8l · Sample No. 252
Alt. 50,000 ft.

FIG. 9 · AVERAGE SIZE DISTRIBUTION FUNCTION FOR STRATOSPHERIC PARTICLES

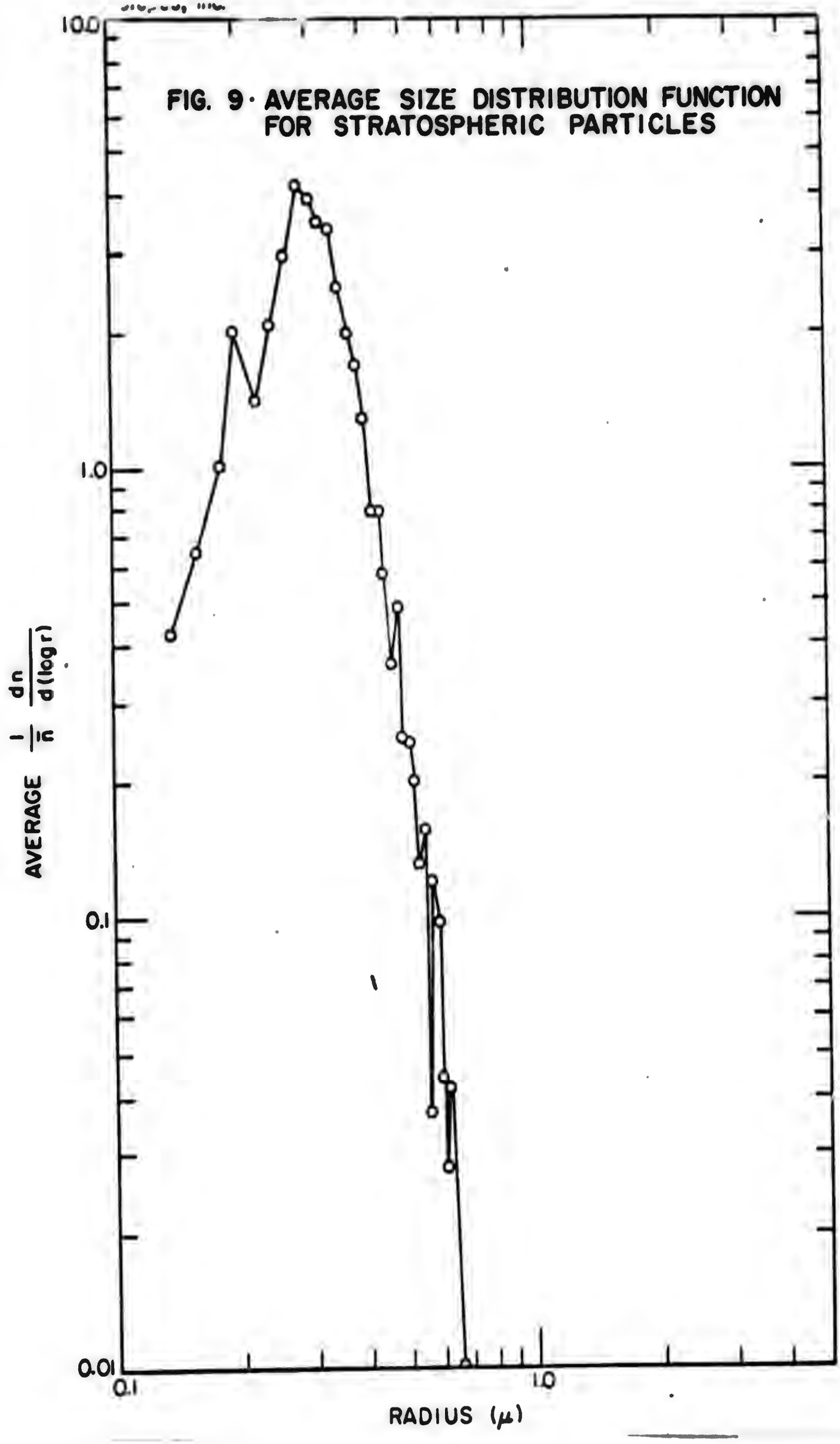

Isotopes, Inc.

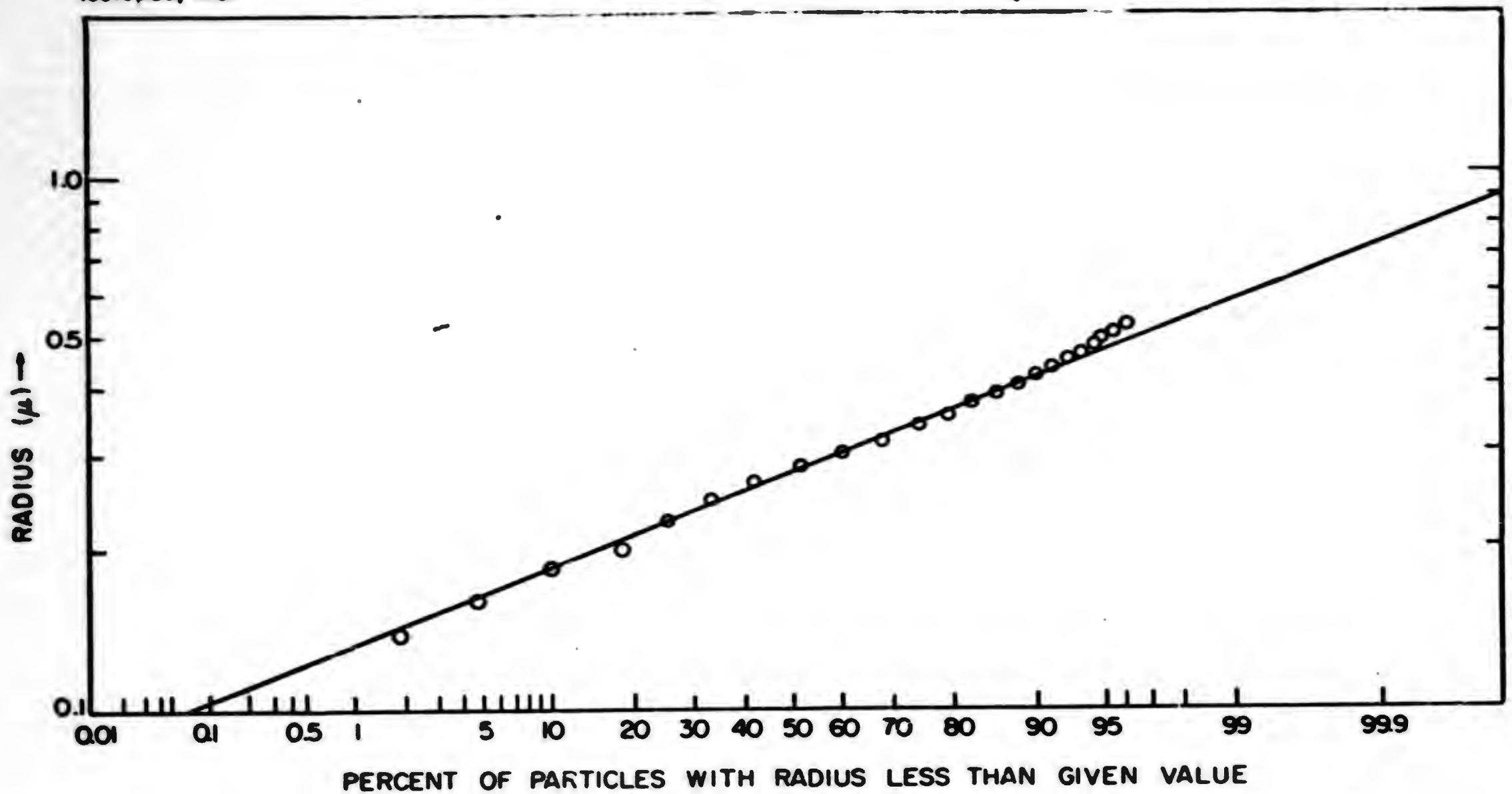

FIGURE 10 · AVERAGE DISTRIBUTION FUNCTION OF STAR DUST SAMPLES

Evaluation of the Measurements

Before we undertake the interpretation of the results let us attempt to evaluate the data in terms of:

(a) uncertainties introduced by the methods of sampling, measurement and computation,

(b) the comparison of the present results with some results obtained by other workers.

Uncertainties in the Calculations

The principal sources of uncertainty in the particle size-concentration data are:

(1) the selection of possible non-representative areas of the samples for electron-microscopic studies,

(2) the improper correction for the effects of moisture on the samples,

(3) the application of the Ranz and Wong semi-empirical theory of impaction of fine particles on an ideal ribbon surface,

(4) possible statistical fluctuations from sample to sample because of the small number of particles contained within particular class intervals.

Of the four sources of uncertainty listed, only item 4 can be said to produce non-systematic errors. There errors are greatest in the concentrations and distribution functions for the largest and the smallest particles observed on our samples, since these are the least numerous in population. The total number concentrations are not greatly affected by these statistical errors since the intermediate sizes, which occur with greatest frequency in the samples, contribute most to the integral under the size-concentration curves.

The use of non-representative areas of the samples would cause relatively greater errors in the number concentrations than in the size distribution functions. The errors from over-correction or under-correction for the effects of moisture (flattening of the particles) would tend to affect the estimates of the relative numbers of small particles most. This would cause errors in both the size distribution function and the number concentrations.

Uncertainties exist in the numbers of small particles due also to the application of the Ranz and Wong theory of impaction. Consistent over-correction or under-correction for moisture effects would lead to systematic bias of the results, as would errors in the Ranz and Wong impaction theory.

The net uncertainty due to the four sources listed above is difficult to assess quantitatively. It can be seen, however, that items 1, 2 and 3 cause the distribution functions and number concentrations to be more uncertain for the smaller particles. To some degree these uncertainties are reflected in the variations of the experimental values of $\frac{1}{n}\frac{dn}{d\log r}$ in a single column in Table 9. Thus, the values near the peak of the distribution function of the radii 0.282 to 0.318 micron show considerably less variation than those for the much smaller or much larger radii. However, it must be pointed out that some (undetermi[illegible] portion of the variations shown in Table 9 may be due to natural variations in production and removal rates of the particles.

The Comparison of Star Dust Results with Previous Findings

Perhaps more perspective regarding these variations can be gained by comparing the present results with some previous findings by other workers. In 1961, Junge et al[7] carried out a variety of measurements of the stratospheric aerosol using balloon-borne equipment. Their measurements of the vertical profiles of number concentrations of large particles ($0.1 < r < 1.0$ micron) gave a broad maximum at about 20 km. altitude. Since the highest altitude samples during our study was 18.3 km. (60 thousand feet) we were not able to demonstrate the occurrence of peak concentrations in the vicinity of 20 km. However, the drop-off of concentrations with decreasing altitude from 18.3 km (see Table 8) is in general agreement with the profile of Junge et al. More recent work by Newkirk and Eddy[8], using light scattering measurements by a balloon-borne coronagraph, showed quite clearly that the stratospheric aerosol exists in thin cloud-like laminae. (Similar conclusions on the existence of layers of aerosols in the stratosphere were drawn by several other workers. These are reviewed by Newkirk and Eddy.) Again, our work was not intensive enough in time or altitude coverage to demonstrate the existence of the aerosol clouds. However, the variations by nearly an order of magnitude in number concentrations of the samples from 60 thousand feet altitude, as shown in Table 8 are consistent with the concept of the clouds of aerosols. It would be very difficult to attribute all of our observed variations to measurement errors. Since our sampling was not sufficiently intensive, the number concentrations in Table 8 cannot be used to give reliable time averaged values.

In one important aspect the present work is not in agreement with previous work. This is in the form of the size distribution function of the stratospheric sulfate particles ($0.1 < r < 1.0$ micron). The details of this distribution function constitute, perhaps, the most significant finding of this investigation. Junge et al[7], from examination of particles collected by balloon-borne impactors, concluded that the radii were distributed approximately according to:

$$dn/d(\log r) \propto r^{-2},$$

or equivalently:

$$dn/dr \propto r^{-3}$$

for the range $0.1 < r < 1.0$ micron. Figure 11 shows their distribution and the distribution found in the present work. The latter is nearly log-normal. In Figure 11 the ordinate $\frac{dn}{d(\log r)}$ has units of cm^{-3} and a particular point on a curve represents the number of particles per cubic centimeter per unit of logr. The curve labeled "Star Dust" corresponds to the average distribution function of Figure 9, and the median value of $\bar{n}$ at 60 thousand feet altitude, namely 0.066 cm^{-3}. Also shown in Figure 11 are limits of uncertainty estimated by Junge et al for their curve, and estimated for the present work based on variations as illustrated in Table 9 and discussed above. It can be readily seen from Figure 11 that the main region of discrepancy is for $r \leq 0.2$ micron.

It is also to be noted that there is a real discrepancy in the shapes of the two distributions shown in Figure 11. The regions of uncertainty for the Star Dust distribution are based primarily on the variations in the absolute values of $\frac{1}{\bar{n}} \frac{dn}{d(\log r)}$ about the mean value and do not completely indicate the reliability of the shape of the

distribution. Our confidence in the general shape of the size distribution function obtained in the present work is based on the occurrence of the peak in the distribution curves of all samples within one class interval of the location of the peak in the mean distribution function.

It is apparent that the discrepancy between the two distributions in Figure 11 is due to one or more systematic errors of the types previously enumerated. The most probable cause is the correction (or lack thereof) for the effects of moisture in flattening the particles. In fact Junge et al[7] point out that they made no effort to apply any correction for this effect, and the sizes were recorded as they appeared on the samples. In many samples where the effects of moisture were prominent the typical patterns seen were of "large" flat particles surrounded by "halos" of smaller particles. (See DASA 1300, Volume 5, Part 11 for illustrations of such patterns.) In the present work, the smaller satellite particles were not included in the counting. If, as would appear to be true, Junge et al included these smaller particles (usually in the range of radius 0.1 to 0.2 micron) in their count, then the discrepancy in the size distribution functions is qualitatively explained.

In their recent work, Newkirk and Eddy[8] assumed in the manner of Junge et al, the functional form of the size-concentration distribution to be:

$$\bar{n} = \bar{n}_o \quad (r/r_2)^{-\delta}$$

with $\delta = 0$ for $r \leq r_2$

$\delta > 0$ for $r > r_2$

where r_2 is some fixed radius. Their experimental results were then used to find values of $\bar{n}_o$ and δ , which later were found to be in substantial agreement with the values found by Junge et al[7]. In light of the present results of the size distribution function, Newkirk and Eddy's results cannot be taken as verification of the distribution of Junge et al.

To clarify the issue here it must be stated that sufficient uncertainties currently exist so that the present results, as well as previously obtained results, should not be made the basis for extensive computations of effects of the stratospheric aerosol. It should also be pointed out that the size distribution function is a basic ingredient in the studies of the aerosol. Without a reasonable estimate of this function no firm conclusions concerning the details of the origin, physical behavior and removal of the particles can be reached.

Junge and his coworkers[7,9], in experiments with balloon-borne Aitken nuclei counters, found that the total particle concentration decreases quite rapidly with height above the tropopause for the first few kilometers and then remains on the order of about 1 cm^{-3} at least up to about 100 thousand feet altitude. The Aitken nuclei are smaller than 0.1 micron radius and would thus not have been collected with appreciable efficiency by the impactors used in the Star Dust program. If the distribution function and number concentrations found in the present work are correct, then in the region of radius less then 0.1 micron the frequency (or number concentration expressed, e.g., as dn/d(logr) must increase again so that the total number concentration will agree with the Aitken nuclei concentration. There is no direct evidence available concerning the average size of the Aitken nuclei. However, Junge et al[7]

estimated that a radius of 0.04 micron would be consistent with some theoretical considerations of mixing by turbulent diffusion from a tropospheric source. Thus it may be that the actual distribution of particle sizes in the stratosphere is bimodal with peaks at 0.3 micron and in the vicinity of 0.04 micron radius.

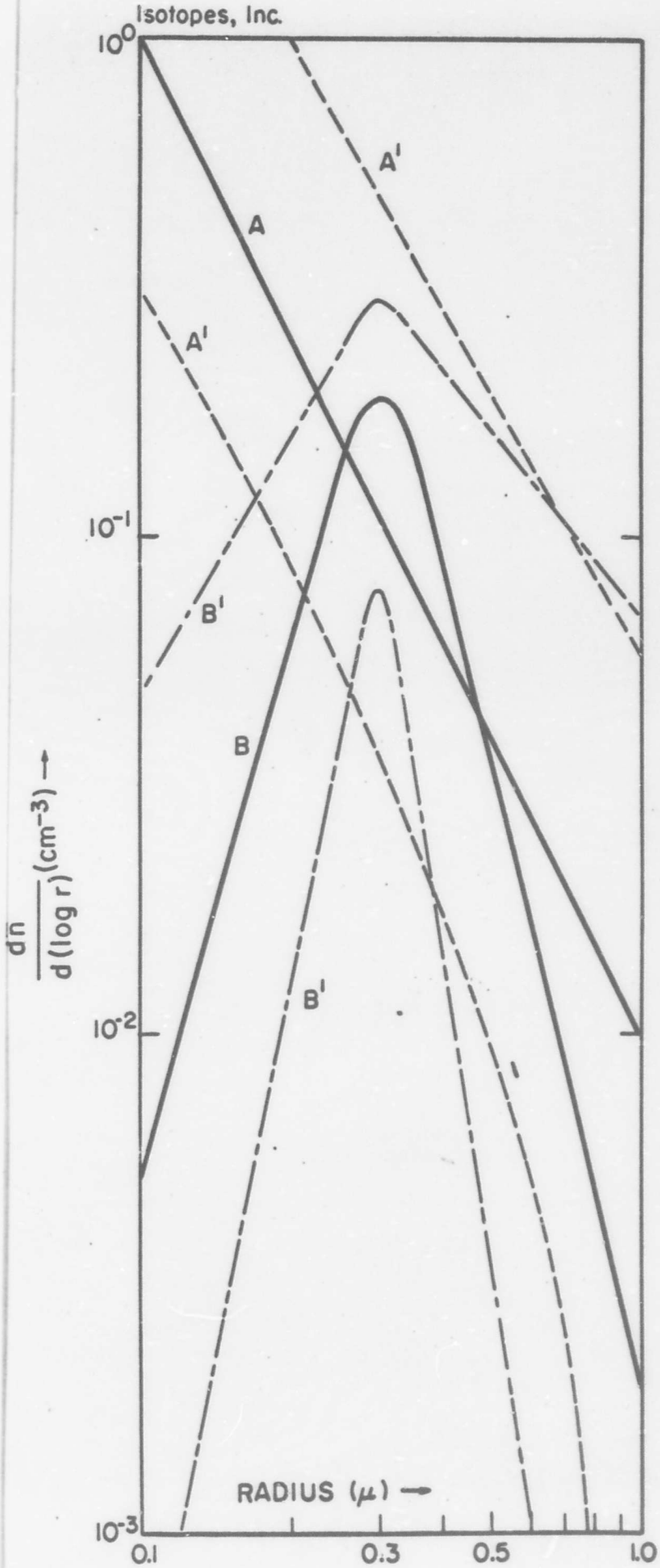

Figure 11 ·

Comparison of Particle Size-Concentration Spectra of Stratospheric Sulphate Particles

Curve A: AFCRL – Junge et al.
Curves A': Confidence Limits of Curve A
Curve B: Star Dust
Curves B': Confidence Limits of Curve B

The Origin of the Stratospheric Aerosol

We now turn our attention to consideration of the origin and history of stratospheric aerosol particles. On the basis of origin, three basic types of stratospheric particles may be distinguished, namely:

(1) Aitken nuclei with $r < 0.1$ micron,

(2) sulfate particles (or "large particles" based on size category) with $0.1 < r < 1.0$ micron, and

(3) extraterrestrial particles with radii of all sizes. (Only those with $r \geq 1$ micron are clearly discernible in direct samples since the sulfate particles dominate the population for $r < 1$ micron.)

Junge and his coworkers[7,9] have shown beyond doubt that the Aitken nuclei in the stratosphere are primarily of tropospheric origin and that they are probably introduced into the stratosphere by vertical eddy diffusion across the tropopause. The findings of Junge et al[7], Junge and Manson[10], Friend et al[1] and the present work constitute strong evidence that the sulfate particles, which comprise an overwhelming proponderance of the mass of solid material in the stratosphere, have their origin in the stratosphere.

This conclusion is mainly based upon composition data and upon the peak in the vertical profile of particle concentrations which is observed at about 20 km. altitude. Cadle[11] and Junge[12] have suggested that the sulfate particles result from photochemical oxidation of SO_2 in the stratosphere. The SO_2 is of tropospheric origin. (See Junge [13] for a discussion of SO_2 in the troposphere.) The first steps in the production of the aerosol would be

$$O_2 + h\nu = 2O \qquad (\nu = 1751\text{-}1200°A)$$

$$O + SO_2 + M = SO_3 + M$$

$$SO_3 + H_2O = H_2SO_4$$

Exactly how NH_4^+ (or possibly NH_3) enters into the reaction to produce $(NH_4)_2 SO_4$ is not understood. Similar comments pertain to the formation of the persulfate $(NH_4)_2 S_2O_8$. This latter compound has two SO_4 groups connected by a peroxide type linkage. Perhaps ozone plays a role in its production.

It is not known what role, if any, the Aitken nuclei may play in the formation and growth of the sulfate particles. Perhaps some fraction or particular type of the Aitken nuclei either constitute a very efficient third body (M) in the photochemical oxidation of SO_2, or they may be carriers for SO_2, or both. The Aitken nuclei may then become the centers of reaction so that the sulfate particles grow on them by condensation.

The shape of the particle size spectrum for radii greater than 0.3 micron may be explained by a quasi-stationary state in condensation-sedimentation processes.

Beyond these tentative suggestions no further speculation can be made concerning the mechanism of production and removal of the stratospheric aerosol particles. In all probability the exact mechanism, once understood, will account for all details of the shape of the distribution function of the particles.

The Association of Nuclear Debris with the Stratospheric Aerosol

In order to provide some insight into the possible association of nuclear debris with the stratospheric aerosol particles crude calculations of the coagulation half-times using the Smoluchowski relationship and analytical approximations to the Star Dust size-concentration distribution were carried out in a manner similar to that of Manson[14]. Our

calculations give half-times similar to those of Manson and show, e.g. that particles of 0.01 micron radius or less should quickly (relative to the time scale of air motions in the stratosphere) become attached primarily to the Aitken nuclei. The calculated value of the removal half-time for a particle of debris with a 0.01 micron radius by the natural aerosol at 20 km altitude is about 100 days. For debris particles of 0.001 micron radius the removal half-time is about 3 hours. One interesting result of the coagulation rate calculations was that a small fraction (about 1% or so) of the debris particles with $r < 0.001$ micron would be removed by the aerosol particles with radius greater than 0.3 micron, but a very much smaller fraction would be removed by aerosol particles with $0.1 < r < 0.3$ micron. Thus there is presented a rather peculiar possibility that relatively fresh nuclear debris which had been injected into the stratosphere, might be found to a large extent on particles with $r < 0.1$ micron, to a smaller extent on particles with $r > 0.3$ micron, but to practically no extent on particles with $0.1 < r < 0.3$ micron.

In conclusion it should be stated that there still remains much work to be done before we will have gained knowledge concerning the detailed history of the particles of nuclear debris in the stratosphere from the moment of introduction to the moment of removal. We have, however, gained some knowledge of the nature of the microscopic environment in which the nuclear debris which constitutes world wide fallout exists.

Isotopes, Inc.

CHAPTER 4. RADIOCHEMICAL ANALYSES OF STAR DUST FILTER SAMPLES

The filter samples of stratospheric and tropospheric air collected during Project Star Dust are analyzed radiometrically and radiochemically to determine the concentrations of various natural and artificial radionuclides in the sampled air.

The Purpose and Plan of the Filter Analyses

The plan followed in the radiochemical analysis of the Star Dust filter samples has been designed to accomplish two basic purposes: (1) the acquisition of data on atmospheric diffusion and circulation needed in the development of the Star Dust model, and (2) the delineation of the distribution of the nuclear debris in the stratosphere to permit the calculation of the stratospheric burden of such debris. The second of these purposes might be accomplished adequately if the analysis of the filter samples was limited to the measurement of strontium-90 and a few other fission products and "tracer" nuclides to delineate debris of different origins. In order to accomplish the first of these purposes, however; it is desirable that the stratospheric concentrations of a number of natural and artificial activities be measured. Thus natural activities, such as beryllium-7, lead-210 and polonium-210, and products of neutron activation, such as tungsten-185, rhodium-102, manganese-54 and antimony-124, have been measured in many Star Dust samples.

As soon as a filter sample is received at Isotopes, Inc. a disk, 2.86 cm in diameter, is cut from the sample and is subsequently beta-counted to determine the level of activity in the filter. The resulting information is used to detect possible sampling malfunctions or sample mix-ups as well as to group filters into composite samples for radiochemical analysis. A few filter samples are also selected each month for measurement on the 400 channel gamma spectrometer. The total gamma spectra reveal the relative abundances in the samples of some

radionuclides of special interest, such as barium-140, antimony-124, manganese-54 and yttrium-88. Thus these spectra are used in deciding whether short-lived fission products, such as barium-140, iodine-131 and molybdenum-99, or tracer nuclides, such as antimony-124 and yttrium-88, should be measured radiochemically in the samples collected in particular stratospheric regions.

The program of radiochemical analyses has evolved into a system which includes four basic sample groups. These are designated the "SF" group, which consists mainly of fission products, the "SZ" group, which consists mainly of products of neutron activation produced during the 1961 and 1962 Soviet test series, the "ST" group, which consists mainly of natural and artificial "tracer" nuclides, and the "SQ" group, which consists of long-lived potentially hazardous nuclides. Strontium-90 is included in all groups to provide cross-checking of data when aliquots of a set of filters are included in samples of more than one group.

An attempt has been made during Project Star Dust to reach a compromise between the desire to obtain detailed information on the stratospheric concentrations of many nuclides and the necessity of keeping the cost of the analytical program within reasonable bounds. During Project HASP almost every usable filter sample was analyzed individually for its content of fission products. Grouping of filters into composite samples was limited mainly to analyses of tracer nuclides such as rhodium-102, phosphorus-32 and, in the later stages of the program, tungsten-185 which could not be measured in individual filters. During Project Star Dust, however, aliquots of filters have been combined to form composite samples for radiochemical analysis, regardless of the levels of activity involved, whenever the loss of detailed knowledge caused by this combination could be justified. The meridional gradients of nuclide concentrations have generally not been steep except during or immediately after periods of

weapons testing, or in the vicinity of the tropopause. Thus it has visually been possible to combine, for analysis, filters collected at a single altitude but over a range of latitude. The vertical concentration gradients have frequently been rather steep, and since most missions have involved horizontal flight tracks the general rule followed has been not to combine filters collected at significantly different altitudes. Where a series of closely spaced altitudes has been sampled, as during some orbit missions flown at maximum altitude, the total beta activities have been used to distinguish significant breaks in the vertical profile and filters have been combined accordingly.

A major aim of Project Star Dust has been the monitoring of the stratospheric burden of nuclear debris in general, and of strontium-90 in particular. Thus almost all usable filter samples received, at least before mid-1963, have been analyzed for strontium-90 and for one or more additional fission products. Since the end of the 1958-1961 test moratorium this has meant the inclusion of aliquots of almost all filters in samples in the "SF" group. Usually only a single quadrant of each filter has been used for these fission product ("SF") analyses. Additional quadrants of many samples have been used in preparing samples in the "SZ", "ST" and "SQ" groups. Many portions of filters or whole filters have been supplied to other government agencies or their contractors to be used in other research programs.

The specific nuclides included within the analytical scheme of each sample group has varied from time to time, but these schemes have gradually evolved into a more permanent pattern as the potential usefulness and inherent limitations of each analysis have become clear. The "SF" group has included samples measured only for strontium-90 and cerium-144, but such samples have generally consisted of filters collected in tropospheric air characterized by very low activities. Almost all "SF" samples containing filters collected since

the first interception of debris from the 1961 Soviet tests have included shorter-lived fission products, such as strontium-89 or zirconium-95 in their analytical schemes. During much of the period since October 1961, cerium-141 and barium-140 have also been included, and a number of samples which contained very fresh debris were also analyzed for molybdenum-99 and iodine-131. During 1963 promethium-147, yttrium-91, yttrium-88 and silver-110 (the last two are products of neutron activation rather than fission products) were added to the analytical scheme of a set of "SF" samples selected from a range of latitudes and longitudes. This was done to provide a monitoring of stratospheric concentrations of these nuclides until their importance could be evaluated.

The selection of filters to be included in "SZ", "ST" and "SQ" samples has also been based on the desire to monitor stratospheric concentrations of the nuclides analyzed in these samples at a series of latitudes and altitudes. When it became apparent that the 1961 Soviet test series had produced unusually large amounts of neutron activation products, the analytical scheme of the "SZ" group of samples was designed to include measurements of strontium-90, manganese-54, iron-55, iron-59, cobalt-57, cobalt-58, cobalt-60 and thallium-204. Antimony-124 and antimony-125 were added when the activity of antimony-124 fell below the limits of detection in the total gamma spectra of untreated filters. Following the injection of cadmium-109 into the upper atmosphere by the 9 July 1962 rocket shot Starfish, this nuclide was added to the analytical scheme of some "SZ" samples. Later cadmium-113m and cadmium-115m were also added when the presence of these nuclides in stratospheric debris became apparent.

During the first few months of Project Star Dust most samples belonged to the "ST" group since data for the tracer nuclides rhodium-102, tungsten-181, beryllium-7, lead-210 and polonium-210 appeared to be more likely to prove of value in the development and testing of the Star Dust model than did data for

the long-lived fission products still measurable in stratospheric air samples. Strontium-90 and cerium-144 were the only fission products analyzed in these samples. Once fresh debris from the 1961 Soviet tests reached the Star Dust sampling corridor, however, the value of measurements of these nuclides diminished, both because of the relatively greater importance of obtaining information regarding the spread of debris from the Soviet tests and because of the added difficulty of analyzing low activities of the tracers in the presence of fission product contaminants. Tungsten-185 was added to the analytical scheme of some "ST" samples during period of testing, but concentrations comparable to those found during 1958 and 1959 were never found. From late 1961 to early 1963 only strontium-90, beryllium-7, lead-210, polonium-210 and rhodium-102 have been measured routinely in "ST" samples. During early 1963 the entire "ST" analytical scheme was revised with rhodium-102, lead-210 and polonium-210 being dropped in favor of the cosmic ray products phosphorus-32, phosphorus-33 and sodium-22. The new analytical scheme will be described in a future report.

Periodically a series of filters are taken for analysis as "SQ" samples. These are analyzed for cesium-137 and plutonium as well as for strontium-90, following the analytical scheme developed during Project HASP. The existence of the "SQ" samples as a group rather than having cesium-137 and plutonium included in the analytical scheme of some other group is justified only because the "SQ" analytical scheme already exists, and because neither of these nuclides need be measured too often. The Cs^{137}/Sr^{90} ratio shows little variation in stratospheric debris with either time, latitude or altitude. The Pu/Sr^{90} ratio has shown some variation with the source of the measured debris, but the plutonium isotopes measured have very long half lives and they have been produced by so many test series since 1952 that their use as tracers appears impracticable. Thus cesium-137 and plutonium concentrations are

monitored chiefly because of the potential hazard created by their presence in fallout.

Succeeding sections in this chapter present the detailed radiochemical procedures used in analyzing Star Dust filter samples. An outline of the radiometric procedures used is given at the end of the chapter.

Sample Pretreatment

Upon arrival at Isotopes, Inc., each filter paper is given a code number and the collection data accompanying the filter are recorded. Normally within a few hours after its arrival a small (2.86 cm diameter) disk for total beta is cut from each filter. The disk is beta assayed in an automatic sample changer for a 15 minute counting period. Each disk is routinely scheduled for three radioassays over a two week period.

In addition to removing the small (2.86 cm diameter) disk for total beta assay, three 3-inch diameter disks are removed from selected samples for which total gamma spectrometric analyses are required. The disks are placed in a special plastic holder which fits directly on top of the 3 inch by 3 inch NaI (Tl) crystal. The holder assures a reproducible geometry for all samples. Radioassay is at two settings, one to cover energies up to approximately 2.3 Mev and another to cover only energies up to approximately 0.9 Mev. Counting time is from 15 to 480 minutes, depending on the levels of activity.

Ashing Procedure

Upon completion of the total beta assay, it is possible to determine the type of analysis required for a particular composite sample. Then the following dissolution procedure is utilized preparatory to radiochemical separation and purification:

1. Cut the filter papers into small squares approximately two inches on a side and place in a 1 liter beaker (See Notes 1 and 2).
2. Slowly add 400 ml of fuming nitric acid and allow the mixture to stand for 30 minutes.
3. Evaporate the solution to approximately 50 ml, add another 50 ml of fuming nitric acid and evaporate to a volume of approximately 25 ml.
4. Add 25 ml of 70% $HClO_4$ and 25 ml of concentrated HNO_3 and evaporate to white fumes of perchloric acid.
5. Transfer the solution to a 100 ml Teflon beaker (See Note 3) using 7M HNO_3 as transfer agent. Thoroughly wash the glass beaker several times with 7M HNO_3 and combine the washings with the solution in the Teflon beaker.
6. Add 10 ml of concentrated HF and evaporate to white fumes of $HClO_4$. Repeat the concentrated HF addition and evaporation to fumes of $HClO_4$ two additonal times. Finally evaporate to a volume of approximately 2 ml.
7. Depending on the type of analysis desired prepare the final solution by one of the following methods:
   (a) If polonium-210 is to be determined, as in some samples in the "ST" group, the 2 ml of solution is transferred to a 150 ml glass beaker using 0.5M HCl as the transfer agent. Wash the Teflon beaker with 0.5M HCl until virtually all residual activity is removed (See Note 4). Combine all washings with the solution in the 150 ml glass beaker.
   (b) If antimony-124, 125 is to be determined, as in samples in the "SZ" group, the 2 ml of solution is transferred to a 25 ml volumetric flask utilizing 3M HCl as the transfer agent. Wash the Teflon

beaker with 3M HCl until virtually no residual activity remains. Combine all washings with the solution in the volumetric flask.

(c) If no polonium-210 or antimony-124, 125 analysis is required, as in samples in the "SF" and "SQ" groups, transfer the solution to a 150 ml glass beaker utilizing 7M HNO_3 as transfer agent. Wash the Teflon beaker with 7N HNO_3 until virtually no residual activity remains (See Note 4). Combine all washings with the solution in the volumetric flask.

Note 1. If antimony-124, 125 analysis is required, 30 mg of standardized antimony carrier are added directly to the cut filter paper. The carrier is added because experimental work has shown a 10 to 20% loss due to volatility during wet ashing.

Note 2. In order to minimize the cross contamination of samples with low activity levels by samples with higher activity levels, two types of equipment are employed. Pyrex glassware is used for samples which exhibit greater than 1×10^4 total beta counts per minute; Kimax glassware is used for samples which exhibit less than 1×10^4 total beta counts per minute. The Teflon beakers are also segregated by the same criterion as the glass equipment.

Note 3. Monitor the Teflon beakers in a beta counter prior to use.

Note 4. Monitor the Teflon beaker in a beta counter after the washings. The measurement is required to determine if any significant amount of activity remains. If greater than 0.1% of the gross beta activity remains, wash the beaker with the appropriate washing acid until an activity below this level is attained.

Isotopes, Inc.

Sequential Radiochemical Separation of Strontium-89, 90, Yttrium-91, Zirconium-95, Molybdenum-99, Barium-140 and Cerium-141, 144

After the addition of carriers, an hydroxycarbonate precipitation is used to separate molybdenum, which remains in the supernate. After dissolution of the hydroxycarbonates, the addition of ammonium hydroxide coprecipitates cerium and yttrium hydroxides. The supernate, containing barium and strontium activities, is buffered and barium chromate is precipitated. The strontium fraction is further purified by several ferric hydroxide scavengings, and the yttrium-90 is milked after an appropriate growth period. A flow chart is shown in Figure 12.

1. To the filter paper solution contained in a 40 ml centrifuge tube add 20 mg each of strontium, cerium and barium carriers. Also add 10 mg each of zirconium, yttrium and molybdenum carriers.

2. Add 1 ml of 5M $NH_2OH.HCl$ dropwise and stir carefully during the addition (Note 1). Evaporate the solution to a volume of approximately 10 ml and transfer to a 40 ml glass centifuge tube using water as a transfer agent.

3. Add 50% NaOH until pH 9-10 is obtained and place in a hot water bath. Add 10 ml of saturated Na_2CO_3 solution, with stirring, and allow the precipitate to digest for 5-10 minutes in the hot water bath.

4. Cool the mixture to room temperature, centrifuge and decant the supernate into a 250 ml beaker. Reserve the supernate for the molybdenum-99 purification procedure.

5. Wash the precipitate with 5 ml of water containing a few drops of 50% NaOH, centrifuge and add the wash solution to the molybdenum-99 fraction.

6. Dissolve the hydroxycarbonate precipitate in 5 ml of 6M HNO_3. Boil over a flame for 2 minutes to rid the solution of CO_2.

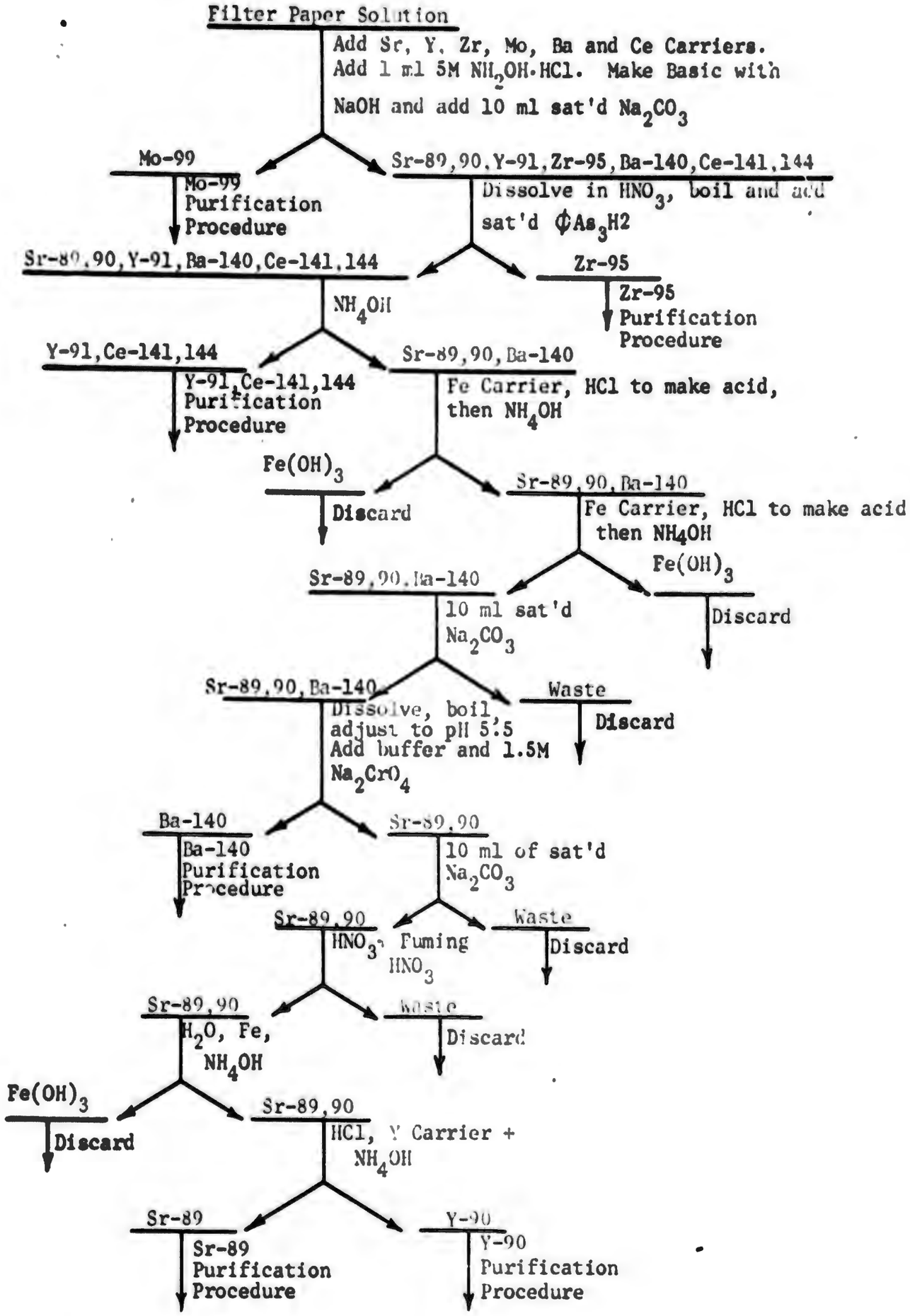

FIGURE 12 SEQUENTIAL RADIOCHEMICAL SEPARATION OF Sr-89, 90, Y-91, Zr-95, Mo-99, Ba-140 AND Ce-141, 144

Isotopes, Inc.

7. Repeat steps 3 to 6 combining all supernates with the molybdenum-99 fraction.

8. Dilute the solution from step 6 to 10 ml with water and add 2 ml of saturated phenylarsonic acid solution (ϕAsO_3H_2). Digest in a hot water bath until the zirconium phenylarsonate precipitate settles out (about 20 minutes).

9. Cool the mixture to room temperature, add a drop of aerosol reagent, and centrifuge thoroughly. Decant the supernate into a 40 ml centrifuge tube and reserve the precipitate for the zirconium-95 purification procedure described in DASA 1300, Volume 1, page 121 (1961).

10. To the supernate from step 9, add concentrated NH_4OH until $Ce(OH)_3$ and $Y(OH)_3$ precipitate. Place in a hot water bath for several minutes, cool to room temperature, centrifuge and reserve the supernate by decanting into a 40 ml centrifuge tube.

11. To the $Ce(OH)_3$ and $Y(OH)_3$ precipitate add 5 ml of 6M HNO_3. Boil over a flame to remove any CO_2 and again precipitate $Ce(OH)_3$ and $Y(OH)_3$ with concentrated NH_4OH. Digest in a hot water bath for several minutes, centrifuge and combine the supernate with the supernate from step 10. Reserve the $Ce(OH)_3$ and $Y(OH)_3$ precipitate for cerium-141, 144 and yttrium-91 purification procedures as described in DASA 1300, Volume 1, pages 119 and 140 (1961).

12. To the combined supernates from steps 10 and 11, add 5 mg of Fe^{+3} carrier. Add concentrated HCl dropwise with stirring until the solution clears and then make basic with concentrated NH_4OH until the precipitate reappears. (If the precipitate is slow in forming, place in a hot water bath for several minutes.) Centrifuge and transfer the supernate to a 40 ml centrifuge tube. Discard the precipitate.

13. Again add 5 mg of Fe^{+3} carrier and repeat step 12.

Isotopes, Inc.

14. To the supernate from step 13, add sufficient concentrated NH_4OH to exceed pH above 8.5. Heat the solution in a hot water bath and add 10 ml of saturated Na_2CO_3 with stirring. Digest until the precipitate settles, cool to room temperature in a water bath, centrifuge and discard the supernate.

15. To the carbonate precipitate from step 14, add 5 ml of 6M HNO_3 and boil over a flame for about 2 minutes to remove all the CO_2.

16. Cool the solution to room temperature and add 4-5 drops of alizarin. Add 6M NH_4OH until a color change from yellow to violet occurs.

17. Add 5 ml of "barium buffer solution" and heat nearly to boiling. Add 1 ml of 1.5M Na_2CrO_4 (via pipette) with stirring and digest in a hot water bath until the $BaCrO_4$ settles.

18. Cool the solution to room temperature, centrifuge and decant the supernate into a 40 ml centrifuge tube. Reserve the $BaCrO_4$ for the barium-140 purification procedure described in DASA 1300, Volume 1, page 135 (1961).

19. To the supernate from step 18, add 5 ml of concentrated NH_4OH with stirring. (The pH of the solution should be above 8.5.) Heat in a hot water bath for several minutes and add 10 ml of saturated Na_2CO_3 with stirring.

20. Digest in a hot water bath for 10 to 15 minutes until the $SrCO_3$ precipitate settles, cool to room temperature, centrifuge and discard the supernate.

21. Dissolve the precipitate in 5 ml of concentrated HNO_3 and boil over a flame to remove all CO_2. Cool in an ice bath for 5 minutes (Note 2). Add two to three drops of fuming nitric acid, centrifuge and discard the supernate.

22. Dissolve the precipitate in 15 ml of water. Add 5 mg of Fe^{+3} carrier and make basic with concentrated NH_4OH until $Fe(OH)_3$ precipitates. Centrifuge and transfer the supernate to a clean 40 ml centrifuge tube.

Discard the precipitate. Record the date and time of this last $Fe(OH)_3$ scavenge. (This represents the starting time of yttrium-90 growth.)

23. Acidify the supernate from step 22 with concentrated HCl and add, via pipette, 10 mg (1 ml) of standardized yttrium carrier. Set aside for yttrium-strontium separation. (Allow at least 3 days for sufficient yttrium-90 growth.)

24. To the solution which has been set aside for at least 3 days, add 7-8 drops of meta cresol purple indicator, stir well and make basic with 6M NH_4OH until one drop causes a color change from yellow to purple (pH 7.6).

25. Digest in a hot water bath for about 10 minutes, cool to room temperature, immediately centrifuge the $Y(OH)_3$ precipitate and decant the supernate into a 40 ml centrifuge tube. Reserve the supernate for strontium-89 analysis. Record the time and date of "milking", i.e. when the supernate (strontium fraction) is decanted.

26. Wash the $Y(OH)_3$ precipitate with 3 ml of water, using a stirring rod to slurry the precipitate. Centrifuge and combine the supernate with the "strontium supernate" from step 25. Retain the $Y(OH)_3$ precipitate for the yttrium-90 purification procedure described in DASA 1300, Volume 1, page 117 (1961).

27. Reserve the combined supernates from steps 25 and 26 for the strontium-89, 90 purification procedure as described in DASA 1300, Volume 1, page 118 (1961).

Note 1. Effervescence should occur at this point. If it does not, heat the solution and carefully add 1-2 drops of concentrated HNO_3.

Note 2. $Sr(NO_3)_2$ will precipitate. The fuming nitric acid step separates strontium from calcium.

Isotopes, Inc.

Iodine-131 Purification Procedure[15]

Some of the "SF" samples analyzed for short-lived fission products, such as molybdenum-99 and barium-140, have also been analyzed for iodine-131. The iodine-131 analysis has been performed using a separate portion of the filters to avoid introducing complications into the sequential analysis.

A portion of the previously untreated filter paper is digested in fuming nitric acid with iodide and iodate carriers. All oxidation states are converted to iodine with sodium nitrite and the iodine is distilled into sodium bisulfite where it is reduced to the iodide. Purification is further accomplished by extractions into carbon tetrachloride. The iodine is precipitated as palladium iodide and the activity assayed for the 8.05 day iodine-131.

The step-by-step procedure is as follows:

1. Cut a quadrant of filter paper into 1/2 inch squares and place in a distilling flask (Note 1) the side arms of which are stoppered. Chill the flask in an ice bath and add 5 ml of concentrated HCl, 14 mg of iodate carrier (Note 2) and 10 mg of iodide carrier. Add 45 ml of chilled fuming HNO_3 (Note 3) and allow the solution to stand in a hood overnight so that the filter paper is completely dissolved and a clear solution is obtained.
2. Place 25 ml of 6M NaOH and 5 ml of 1M $NaHSO_3$ in the receiving tube of the distillation apparatus, connect the distilling flask to the receiving tube and start the air flowing through the solution at a rate of 1 to 2 bubbles per second.
3. Dilute the contents of the distilling flask to 100 ml with water and add 10 ml of 2M $NaNO_2$.
4. Heat gently at first, then more vigorously until all of the iodine is distilled into the receiving tube and no iodine crystals remain in the side arm.
5. Remove the receiving tube, wash down the side arm with water into the receiving tube.

6. Neutralise the solution in the receiving tube with concentrated HNO_3 and add 3 ml of 6M HNO_3 in excess. Transfer the solution to a 250 ml separatory funnel containing 20 ml of CCl_4 .
7. Add 1 ml of 2M $NaNO_2$ and extract the iodine into the CCl_4 layer with shaking (the CCl_4 layer should be violet).
8. Transfer the organic (lower) phase to a 125 ml separatory funnel and discard the aqueous phase.
9. Add 15 ml of water and 1 ml of 1M $NaHSO_3$, shake and discard the CCl_4 layer (which should now be colorless).
10. Add 2 ml of 6M HNO_3, 15 ml of CCl_4 , 1 ml of 2M $NaNO_2$ and shake; transfer the organic phase to another 125 ml separatory funnel.
11. Repeat steps (9) and (10) and then step (9) again.
12. Transfer the aqueous phase from step (11) to a 40 ml centrifuge tube, add 3 drops of concentrated HCl and heat to boiling (Note 4.).
13. Add 15 ml of anhydrous "Anhydrol" and add 20 mg of palladium carrier; cool to room temperature, centrifuge and discard the supernate.
14. Wash the precipitate with 10 ml of anhydrous "Anhydrol", centrifuge and discard the wash solution.
15. Suspend the PdI_2 precipitate in 10 ml of anhydrous "Anhydrol" and filter onto a previously washed and weighed glass-fiber filter dish; dry in a vacuum desiccator for 30 minutes. Weigh, record the chemical yield of PdI_2 and mount on a brass planchet for counting.

Note 1. The distilling flask consists of a 1000 ml round-bottom 3 neck flask. One neck is for the air inlet, one neck is for an addition funnel and one neck is for an outlet to the receiving tube.

Note 2. Iodine-131 may also be present on the filter paper in the form of the iodate and hence iodate carrier is added before the iodide carrier

in order to establish equilibrium with any radioiodate. The iodate is then quantitatively converted in strong HNO_3 solutions and in the presence of iodide, to the iodide (or tri-iodide) and then to iodine.

Note 3. Additional fuming HNO_3 may be needed to completely decompose the paper.

Note 4. Boiling is necessary to insure the removal of SO_2 which interferes with the precipitation of the iodide.

Iodine-131 Counting Procedure

The iodine-131 is followed for beta decay and is accepted as radiochemically pure if its empirically determined half-life agrees to within $\pm$ 0.4 days with the theoretical half-life of 8.05 days. The disintegration rate is obtained by applying chemical yield and self-absorption and self-scattering factors.

The PdI_2 may be gamma assayed on a NaI (Tl) crystal coupled to a multi-channel gamma ray spectrometer. The absolute disintegration rate is obtained by subtracting the background from the 0.36 Mev photopeak and applying an efficiency determined by counting an absolute standard under the same conditions of geometry and sample thickness.

Isotopes, Inc.

Molybdenum-99 Purification Procedure[16]

Molybdenum is precipitated with α-benzoinoxime from 0.1 N nitric acid solution. After decomposition of the benzoinoxime with nitric acid and perchloric acid, the molybdenum is oxidized to Mo^{+6}, extracted into diethyl ether and back extracted with water. Further purification is accomplished by several ferric hydroxide scavenges and finally molybdenum quinolate is precipitated, mounted and radioassayed.

(a) To the separated molybdenum supernate add concentrated HNO_3 until the solution is approximately 0.1N. Cool in a cold water bath and add, with stirring, 5 ml of 5% α-benzoinoxime. Centrifuge and discard the supernate.

(b) To the precipitate carefully add 10 ml of concentrated HNO_3(Note 1) and evaporate to approximately 2 ml in a hot air or sand bath. Add 2 ml of 70% $HClO_4$ and evaporate to dryness.

(c) Heat the residue over a flame to remove all traces of $HClO_4$ (Caution) (Note 2), cool to room temperature, add 5 mg of iron carrier, 10 ml of water and heat in a hot water bath to dissolve all salts. Add 2 ml of concentrated NH_4OH, cool, centrifuge and transfer the supernate to a 40 ml centrifuge tube. Discard the precipitate.

(d) Neutralize the solution with concentrated HCl and then double the volume with concentrated HCl to make the solution 6N HCl. Add 5 mg of iron carrier and 5 mg of tellurium carrier.

(e) Transfer the solution to a 250 ml separatory funnel and add 1 ml of 2M Na_2 $)_3$. Add 100 ml of equilibrated diethyl ether (Note 3) and shake for 3 minutes. Discard the aqueous (lower) phase and wash the organic layer twice with 15 ml of 6N HCl containing 1 drop of 2M Na_2BrO_3. Discard the washings.

(f) Strip the molybdenum by adding 5 ml of water and shaking for 1 minute (solution should become colorless). Collect the aqueous phase in a 40 ml centrifuge tube. Add another 5 ml of water to the organic phase and shake for 1 minute. Add the second strip solution to the centrifuge tube containing the first strip solution.

(g) Add concentrated NH_4OH until $Fe(OH)_3$ precipitates. Centrifuge, transfer the supernate to a 40 ml centrifuge tube and discard the precipitate.

(h) Add 5 mg of iron carrier to the supernate from step (g), centrifuge, transfer the supernate to a 40 ml centrifuge tube and discard the precipitate.

(i) Neutralize the supernate from step (h) with 6M HCl and add 5 ml of buffer solution (1M $C_2H_4O_2$ - 3.6M $NaC_2H_3O_2$). Heat to boiling, add 1 ml of 5% 8-hydroxyquinoline reagent dropwise and 1 to 2 drops of Aerosol reagent.

(j) Digest the precipitate for 10 minutes in a hot water bath, allow to stand for several minutes and filter the precipitate onto a previously washed and weighed Whatman No. 42 filter disk.

(k) Wash the precipitate with 10 ml of water and then finally with 15 ml of anhydrous "Anhydrol". Dry in an oven at 110°C for 10 minutes, cool to room temperature in a desiccator. Weigh, record chemical yield of the 8-hydroxyquinolate derivative and mount on a brass planchet for counting.

Note 1. Add the concentrated HNO_3 dropwise applying heat. If the addition is too rapid the organic precipitate will decompose too quickly and bubble out of the centrifuge tube.

Isotopes, Inc.

Note 2. Exercise caution due to possibility of formation of organic perchlorates.

Note 3. The equilibration of the ethyl-ether is performed in the following manner: Add 100 ml of ethyl ether, 100 ml of 6N HCl and shake for 5 minutes. Withdraw the aqueous (lower) phase and retain the ether fraction for the purification procedure.

Cerium-141, 144 Purification Procedure[17]

The cerium hydroxide precipitate is dissolved in 9M nitric acid, oxidized to Ce^{+4} with sodium bromate and extracted into methyl isobutyl ketone. The cerium is back-extracted with hydrogen peroxide and precipitated as the oxalate. The oxalate is ignited at 850°C to produce CeO_2 which is mounted and radioassayed.

(a) Dissolve the $Ce(OH)_3$ precipitate in 5 ml of 9M HNO_3 and transfer to a 125 ml separatory funnel containing 50 ml of freshly equilibrated methyl isobutyl ketone (Note 1).

(b) Wash the glass storage vial with 6.5 ml of conc. HNO_3, 2 ml of 6M $NaBrO_3$ and 4.5 ml of water, add the washings to the separatory funnel and shake for 15-30 seconds.

(c) Withdraw the aqueous phase (bottom phase) and wash the methyl isobutyl ketone phase twice with 10 ml of 9M HNO_3 containing a few drops of 2M $NaBrO_3$ (Notes 1 and 2).

(d) Back-extract the cerium by shaking the methyl isobutyl ketone phase with 5 ml of water containing 3 drops of hydrogen peroxide (H_2O_2). (Notes 1 and 3)

(e) Withdraw the aqueous phase into a clean 40 ml centrifuge tube and neutralize by adding conc. NH_4OH(3 - 5 ml) until a precipitate just appears, and acidify with 1.5 ml of 6M HNO_3.

(f) Dilute the solution to a volume of 15 ml with water and heat just to boiling; add 5 ml of saturated $(NH_4)_2C_2O_4$, stir for several minutes and add gradually 10 ml more of saturated $(NH_4)_2C_2O_4$.

(g) Digest the solution in a hot water bath for about 10 minutes, cool to room temperature and filter the $Ce_2(C_2O_4)_3 \cdot 9\ H_2O$ on a Whatman No. 42 filter disk. Wash three times with 5 ml portions of water and three times with 5 ml portions of acetone.

(h) Transfer the precipitate and filter paper to a porcelain crucible and ignite for 1 hour at 850°C. On completion of ignition, transfer the precipitate to a previously washed and weighed glass fiber filter paper with acetone. Oven dry at 100°C for 15 minutes, cool in a desiccator, weigh as CeO_2 and mount on a brass planchet for beta counting.

Note 1. The equilibration of methyl isobutyl ketone (for use with ten samples) is performed in the following manner: to 400 mls of methyl isobutyl ketone, add 400 mls of 9M HNO_3 containing 16 mls of 2M sodium bromate ($NaBrO_3$) and shake or stir for five minutes. CAUTION: In extractions of strong HNO_3 solutions (6 to 12M) with methyl isobutyl ketone considerable amounts of HNO_3 pass into the organic phase. It has been observed that such solutions of HNO_3 in methyl isobutyl ketone are unstable and will undergo a vigorous reaction after standing for a few hours. The methyl isobutyl ketone phases remaining after back-extraction with 5 ml of water were observed to react similarly but only after standing for about 3 days. It is recommended, therefore, that the methyl isobutyl ketone not be equilibrated with HNO_3 until just before use and that it be washed thoroughly with water (three times with an equal volume) soon after use. It is also recommended that HNO_3 solutions which have been in contact with methyl isobutyl ketone be neutralized with NH_4OH before storing or discarding.

Note 2. Combine the aqueous phase and washings and neutralize with NH_4OH before discarding.

Note 3. Wash the methyl isobutyl ketone three times with 50 ml of water before discarding. Also neutralize washings before discarding.

Isotopes, Inc.

Sequential Radiochemical Separation of Beryllium-7, Strontium-89, 90, Rhodium-102, Cerium-141, 144, Tungsten-181, 185, Lead-210 and Polonium-210

Polonium is separated by plating on a silver disk at zero potential at 75°- 80° C from a 0.5 M hydrochloric acid solution. Strontium, barium, beryllium, cerium, lead and rhodium carriers are added and the solution is neutralized with sodium hydroxide. Tungsten carrier is added and tungstic oxide is precipated in strong nitric acid solution. Lead and rhodium are separated as iodides with sodium iodide and hydriodic acid, respectively. The resultant supernate is treated with sodium hydroxide and sodium carbonate, precipitating strontium-cerium hydroxycarbonates and leaving the soluble beryllium in the supernate. Finally the hydroxycarbonates are dissolved and the cerium separated as cerium hydroxide with concentrated ammonium hydroxide. (See Figure 13)

1. Transfer the 0.5 M HCl sample solution to a 70 ml plexiglass cup **(Note 1)**. Wash the beaker several times with 0.5 M HCL and add the washings to the cup. Add 0.5 M HCl until the cup is almost filled.

2. Lower a Teflon stirring rod, attached to a Welch Type B Stirrer, into the solution. The end of the rod should be approximately one-half inch from the bottom of the cup.

3. Add approximately 100 mg of ascorbic acid.

4. Start the stirrer. Allow the temperature to reach 75°- 80° C and plate for three hours (Note 2). Replace any loss due to evaporation during plating with 0.5 M HCL (usually about 5 ml during the three hours).

5. When plating is completed, decant the hot solution into the original 150 ml beaker and wash the cup and Teflon stirring rod several times with 0.5 M HCl and water. Add the washings to the original solution in the beaker and reserve for separation of the other radionuclides.

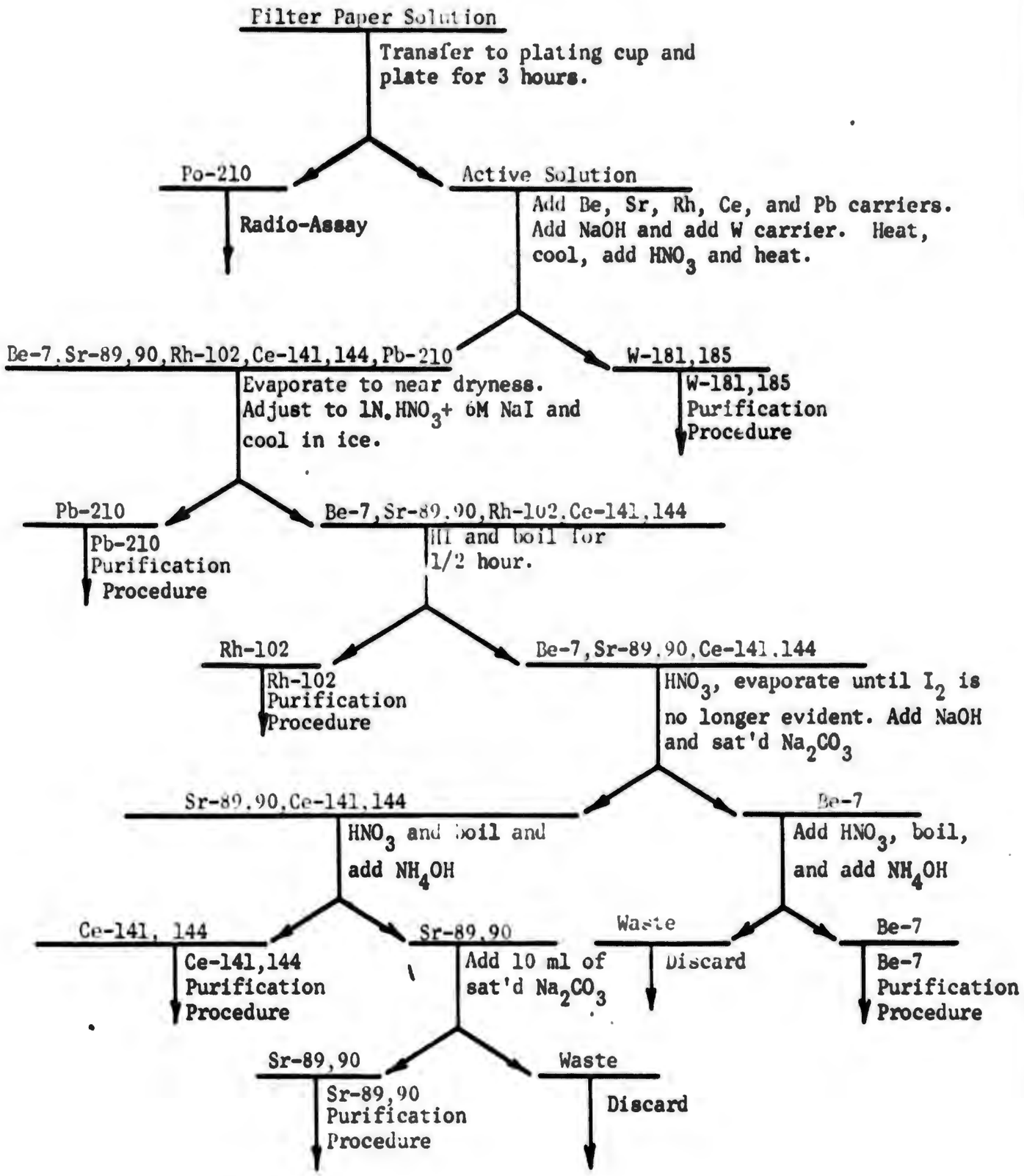

FIGURE 13 SEQUENTIAL RADIOCHEMICAL SEPARATION OF Be-7, Sr-89,90, Rh-102, Ce-141,144, W-181,185, Pb-210 AND Po-210

Isotopes, Inc.

6. Remove the silver disk (Note 3) from the plating cup, wash it with water, air dry and reserve for alpha counting. Clean the O - ring and cup for the next sample.

7. Evaporate the solution from the polonium-210 separation to approximately 10 ml.

8. Add 10 ml of standardized beryllium carrier (1 mg Be/ml), 30 mg of rhodium carrier, and 20 mg each of strontium, barium, cerium and lead carriers. Heat the solution to dissolve any precipitate (Note 4).

9. Carefully neutralize the solution with 50% NaOH, add 20 mg of standardized tungsten carrier and warm for 15 minutes.

10. Cool, add 25 ml of concentrated HNO_3 and digest for one hour on a hot plate to completely precipitate tungstic oxide.

11. Transfer the mixture, by portions, to a 40 ml centrifuge tube, centrifuge and decant the supernate into a 100 ml beaker. Wash the precipitate with 5 ml of 6N HNO_3, centrifuge and combine the wash with the supernate (Note 5). Reserve the precipitate for the tungsten-181, 185 purification procedure as described in DASA 1300, Volume 1, page 142 (1961).

12. Evaporate the supernate from step 11 to a volume at which salts appear, then carefully evaporate almost to dryness using low heat to avoid spattering. Cool, add enough water to dissolve all salts and transfer the solution to a clean 40 ml centrifuge tube. Wash the beaker with three 5 ml portions of water and combine the portions in the centrifuge tube.

13. Cool the solution in the centrifuge tube in an ice bath and add 2 ml of 6M NaI (6M NaI in a solution of 1N HNO_3) to precipitate PbI_2. Cool the mixture for five minutes, centrifuge and decant the supernate into a clean 40 ml centrifuge tube. Wash the precipitate with 3 ml of water

containing 6 drops of 6M NaI, centrifuge and combine the wash solution with the original supernate. Retain the precipitate for lead-210 purification.

14. To the supernate from step 13 add 2 ml of 47% HI and digest in a boiling water bath for one-half hour. Cool to room temperature, centrifuge and decant the supernate to a clean 100 ml beaker. Wash the RhI_3 precipitate with 5 ml of water containing 3 drops of 47% HI, centrifuge and transfer the wash solution to the supernate in the 100 ml beaker. Reserve the precipitate for rhodium-102 purification as described in DASA 1300, Volume 1, page 127 (1961).

15. To the solution from step 14, add 5 ml of concentrated HNO_3 and evaporate until I_2 fumes are no longer evident (Note 6). Continue to evaporate until salts appear, cool, add enough water to dissolve the salts and transfer the solution to a 40 ml centrifuge tube. Wash the beaker with three 5 ml portions of water and transfer the washings to the centrifuge tube.

16. Add 12N NaOH until pH 8.5 is attained, heat in a hot water bath and add 10 ml of saturated Na_2CO_3. Digest in the hot water bath until the precipitate settles, cool to room temperature, centrifuge and transfer the supernate to a clean 100 ml beaker.

17. To the precipitate from step 16, add 5 ml of 6N HNO_3 and boil the solution over a flame for approximately 2 minutes to expel all CO_2. Cool, add 12N NaOH until a pH of 8.5 is reached and repeat step 16. Combine the supernate from step 16.

18. Add 5 ml of 6N HNO_3 and heat over a flame for 2 minutes to expel CO_2. Cool, add concentrated NH_4OH until $Ce(OH)_3$ is precipitated. Digest in a hot water bath for 10 minutes, cool to room temperature, centrifuge and transfer the supernate to a 40 ml centrifuge tube.

Isotopes, Inc.

19. Redissolve the $Ce(OH)_3$ precipitate in 3 ml of 6N HNO_3 and heat to remove any CO_2. Reprecipitate the $Ce(OH)_3$ with concentrated NH_4OH, digest in a hot water bath, cool and centrifuge. Combine the supernate with the supernate in the 40 ml centrifuge tube from step 18. Reserve the $Ce(OH)_3$ precipitate for cerium-141, 144 purification.

20. Warm the combined supernates from steps 18 and 19 in a hot water bath, add 10 ml of saturated Na_2CO_3 and digest the precipitate until it settles. Cool, centrifuge and discard the supernate. Reserve the precipitate for strontium-89, 90 purification as described in DASA 1300, Volume 1, pages 107, 117, 118 (1961).

21. Acidify the combined supernates from steps 16 and 17 with concentrated HNO_3, heat on a hot plate to remove CO_2 (Note 7), cool and add concentrated NH_4OH to precipitate $Be(OH)_2$. Transfer the solution to a 40 ml centrifuge tube (by portions), centrifuge and discard the supernate. Reserve the precipitate for beryllium-7 purification.

Note 1. The plating cup is assembled in the following manner:

(a) Polish a 1 inch diameter silver disk with International Silver polish until a bright, clean surface is obtained.

(b) Hold the disk against an O - ring and install the unit in the plastic plating cell. (The ring forms a seal between the disk and cell.)

Note 2. The required plating temperature is attained by wrapping a Brisheat Flexible Heating tape around the Plexiglass cup. The tape is connected to a voltage regulator which has been calibrated at 75°- 80°C. Calibration is accomplished by filling the cup with water, inserting a thermometer under the surface of the liquid and adjusting the voltage regulator until the desired temperature is reached.

Isotopes, Inc.

Note 3. The polonium-210 is deposited in a circle with a diameter of 13/16 of an inch.

Note 4. If the precipitate does not completely dissolve add concentrated HNO_3 dropwise until a true solution is obtained.

Note 5. The WO_3 precipitate may entrain some rhodium as evidenced by a red coloration. The rhodium is removed by washing the precipitate with 5 ml of 6N HCl. Centrifuge and add the wash solution to the supernate.

Note 6. The amount of added nitric acid may not be sufficient to completely oxidize the iodine. If necessary, additional concentrated HNO_3 may be added.

Note 7. Care must be taken during the neutralization due to effervescence of CO_2 which may expel some of the solution from the vessel. It is advisable to partially cover the beaker with a cover glass during the neutralization.

Beryllium-7 Purification Procedure[18,19]

Beryllium is purified by a lanthanum hydroxide scavenge, a molybdenum sulfide and tellurium sulfide scavenge and subsequent extraction into acetylacetone-benzene. The beryllium is back-extracted with 6M hydrochloric acid whereupon beryllium hydroxide is precipitated with ammonium hydroxide and the precipitate radioassayed. The recovery of beryllium carrier is determined colorimetrically with 4(p-nitrophenylazo) orcinol.

The step-by-step procedure is as follows:

(a) To the $Be(OH)_2$ precipitate add 5 mg of lanthanum carrier and 10 ml of 3M NaOH and digest in a hot water bath for not more than five minutes(Note 1). Cool, centrifuge and decant the supernate into a clean 40 ml centrifuge tube. Repeat washing with another 10 ml of 3M NaOH combining supernates. Discard the $La(OH)_3$ precipitate.

(b) Neutralize the solution with dropwise addition of concentrated HCl and then make strongly ammoniacal with concentrated NH_4OH (Note 2).

(c) Digest the solution in a hot water bath for 10 minutes, cool, centrifuge the $Be(OH)_2$ and discard the supernate.

(d) Dissolve the $Be(OH)_2$ in 3 ml of 6M HCl and dilute to 10 ml with water. Add 0.5 ml of molybdenum (10 mg Mo/ml) and 0.5 ml of tellurium (10 mg Te/ml) carriers and heat in a hot water bath for five minutes.

(e) Bubble hydrogen sulfide gas through the solution for five minutes and heat for an additional five minutes. Filter the solution through a Whatman No. 42 filter paper (9 cm diameter) in a 2", 60^{o} glass funnel and collect the filtrate in a clean 125 ml erlenmeyer flask. Evaporate the filtrate to a volume of approximately 3 ml and transfer the solution to a 40 ml centrifuge tube with water.

(f) Add 2 ml of "acetate buffer solution" and 2 ml of 10% E.D.T.A. solution; adjust to pH 5.5 - 6.0 by dropwise addition of concentrated NH_4OH. Transfer the solution to a 60 ml cylindrical separatory funnel, add 2 ml of acetylacetone and stir mechanically for several minutes.

(g) Add 7 ml of benzene and stir mechanically for two minutes, withdraw the aqueous (lower) phase into a 40 ml centrifuge tube and transfer the organic phase into a second 40 ml centrifuge tube. Transfer the aqueous fraction back into the same separatory funnel after adjusting, if necessary, to pH 5.5 - 6.0 with concentrated NH_4OH.

(h) Repeat step (g) twice and combine the benzene fractions in the centrifuge tube.

(i) Transfer the combined benzene fractions to the original separatory funnel. Wash the benzene fraction three times with 10 ml of saturated E.D.T.A. solution and discard all the wash solutions.

(j) To the benzene fraction, add 7 ml of 6M HCl; mechanically stir for several minutes and withdraw the HCl layer (lower) into a 125 ml erlenmeyer flask.

(k) Repeat step (j) twice combining the HCl fractions in the erlenmeyer flask and discard the benzene fraction.

(l) Evaporate the HCl fraction almost to dryness. Add 5 ml of concentrated HNO_3 and evaporate just to dryness.

(m) Dissolve the $Be(NO_3)$ residue in 2 ml of 6M HCl, dilute with 5 ml of water and transfer the solution to a 40 ml centrifuge tube. Wash the flask with three 3 ml portions of water and add the washings to the centrifuge tube.

(n) Make the solution strongly ammoniacal with concentrated NH_4OH, centrifuge and discard the supernate. Wash the $Be(OH)_2$ twice with 5 ml of water, centrifuge and discard the washing.

(o) Dissolve the precipitate in a minimum of concentrated HCl and transfer the solution to a 10 ml test tube (12 x 100 mm) with a minimum of water. Make the solution strongly ammoniacal with concentrated NH_4OH, centrifuge and discard the supernate. Measure the height of the $Be(OH)_2$ precipitate in centimeters and gamma count the sample.

(p) After completion of the radioassay, dissolve the $Be(OH)_2$ in 5 ml of 6N HCl, dilute to volume in a 100 ml volumetric flask and determine the recovery of beryllium colorimetrically.

Note 1. It has been observed that digesting for longer than five minutes may result in some dissolution of the $La(OH)_3$.

Note 2. The addition of HCl will cause the precipitation of $Be(OH)_2$, the solution is neutral when the $Be(OH)_2$ redissolves.

Isotopes, Inc.

Beryllium Colorimetric Procedure[20] (4-p-nitrophenylazo) orcinol Method)

The beryllium complex of 4-(p-nitrophenylazo) orcinol is formed in a buffered solution at pH 12.0 containing E.D.T.A. chelating agent. Measurement is made at 515 mμ. Interfering elements are removed prior to the measurement. The color is stable for approximately one hour. The concentration range is 20 to 200 γ/100 ml for the 1 cm cell.

(a) Dissolve the $Be(OH)_2$ in 5 ml of 6N HCl and dilute to volume in a 100 ml volumetric flask.

(b) Pipette a 2.00 ml aliquot of the solution into a 100 ml beaker. Adjust the volume to 15 ml with water.

(c) Add 5 ml of the chelating solution (Note 1) and adjust the pH to 5.5 using 2M HCl or 2M NaOH as required.

(d) Add 10 ml of beryllium buffer solution (Note 2), stir and let stand for five minutes.

(e) Transfer the solution to a 100 ml volumetric flask. Add exactly 10.0 ml of dye solution (Note 3) mix and let stand for ten minutes. Dilute to mark with distilled water.

(f) Record the absorbance of each solution in a 1 cm cell at 515 mμ.

(g) Divide the absorbance reading by the average slope value obtained from the calibration (Note 4) and multiply by 50.0 to obtain milligrams of beryllium.

Note 1. Chelating Solution: Saturated Disodium E.D.T.A.

Note 2. Buffer solution (pH 12): Prepared by dissolving 116 grams of citric acid, 61.5 grams of sodium borate decahydrate, 216 grams of sodium hydroxide in water and dilute to 1 liter.

Note 3. Dye Solution: Prepared by dissolving 0.150 grams of 4-(p-nitrophenylazo) orcinol (Chemical Procurement Laboratories, Inc.) in 500 ml

of 0.1N sodium hydroxide solution by stirring on a mechanical stirrer for five hours. Filter the solution through a sintered glass filter and finally through a Millipore HA filter (0.45u). A new solution has to be made up for each run.

Note 4. A calibration curve must be obtained, using a standard solution, with each set of samples. To prepare the standard solution, dissolve 1.0000 gram of high purity beryllium metal in 10 ml of 6N HCl. Boil until effervescence stops. Cool, dilute to 1 liter with water in a volumetric flask and mix thoroughly. Dilute 10 ml of this solution to 250 ml in a volumetric flask and mix thoroughly. This solution, 40 ɣ Be/ml, is used to calibrate the 1 cm cells. Transfer 1.00, 2.00, 3.00, 4.00 and 5.00 ml of this standard beryllium solution into a 100 ml beaker. Adjust the volume to 15 ml with the water. Concurrently run a 15 ml water blank. Proceed as in steps (c) through (f) of the procedure.

Lead-210 Purification Procedure[21]

Lead is purified by successive precipitations of lead nitrate, lead chromate and lead sulfate. The lead-210 activity is separated from the bismuth-210 daughter by several lead sulfate precipitations with bismuth hold-back carrier. After an appropriate growth period, the lead is milked from the bismuth and the bismuth fraction mounted and radioassayed.

(a) Dissolve the PbI_2 precipitate in 10 ml of concentrated HNO_3 and boil over an open flame until all the I_2 is removed. (Note 1)

(b) Cool in an ice bath and add 2 ml of fuming HNO_3, stir vigorously, centrifuge and discard the supernate.

(c) Dissolve the $Pb(NO_3)_2$ precipitate in 5 ml of water and transfer the solution with a minimum of water to a 40 ml centrifuge tube. Add 20-25 drops of concentrated H_2SO_4 , heat over an open flame for two minutes, cool, wash down the walls of the centrifuge tube with water. Centrifuge and discard the supernate.

(d) Dissolve the $PbSO_4$ precipitate in a minimum amount of 6M $NH_4C_2H_3O_2$ and heat to a rolling boil. Add 2 ml of 1.5M Na_2CrO_4 and place in a hot water bath for 10 minutes. Centrifuge and discard the supernate.

(e) Add 10 mls of concentrated HNO_3 to the $PbCrO_4$ precipitate and 5 drops of concentrated HCl. Boil the solution until a color of blue-green is obtained.

(f) Repeat step (b).

(g) Add 10 ml of water to the $Pb(NO_3)_2$ precipitate and add 1 ml of Zr carrier. Heat in a hot water bath, add 2 ml of saturated phenylarsonic acid and digest in the hot water bath for a minimum of 20 minutes.

(h) Cool, centrifuge and transfer the supernate to a clean 40 ml centrifuge tube. Discard the precipitate.

(i) Add 20-25 drops of concentrated H_2SO_4 and heat over an open flame for 2 minutes. Cool to room temperature, centrifuge and discard the supernate.

(j) Dissolve the $PbSO_4$ with a minimum amount of 6M $NH_4C_2H_3O_2$ (Note 2). Add 10 mg of bismuth scavenge carrier and if a precipitate forms, dissolve it with glacial acetic acid and heat.

(k) Add 20-25 drops concentrated H_2SO_4 , heat over an open flame, cool, centrifuge and discard the supernate.

(l) Repeat steps (j) and (k) twice.

(m) Wash the precipitate three times with 10 ml of water containing 3 drops of concentrated H_2SO_4. Centrifuge after each wash, discarding the first two wash solutions. Check the last wash solution (Note 3) and record the time and date (Note 4).

(n) Dissolve the $PbSO_4$ precipitate in a minimum amount of 6M $NH_4C_2H_3O_2$ and add 10 mg of standardized bismuth carrier. If a precipitate forms, add a few drops of glacial acetic acid and heat the solution until it dissolves.

(o) After at least ten days have elapsed, add 20-25 drops of concentrated H_2SO_4 and heat over a flame for two minutes. Cool, wash down the sides of the centrifuge tube with water. Centrifuge and transfer the supernate to a clean 40 ml glass centrifuge tube. Record this time and date as the time of milking of Bi^{210} from Pb^{210}. Wash the $PbSO_4$ precipitate with 5 ml of water containing 1 drop of concentrated H_2SO_4 , centrifuge and combine the wash and the supernate.

(p) Make the supernate from step (o) ammoniacal (pH 9-10) with concentrated NH_4OH. Digest in a hot water bath for ten minutes to coagulate the $Bi(OH)_3$ precipitate. Cool, centrifuge and discard the supernate.

(q) Dissolve the $Bi(OH)_3$ in 3 ml of glacial acetic acid, 5 ml of 6M $NH_4C_2H_3O_2$ and place in a hot water bath for ten minutes. Add 5 ml of saturated E.D.T.A. solution, 0.2 ml of saturated $CaCl_2$ solution and heat over a flame for two minutes.

(r) Add concentrated NH_4OH to precipitate $Bi(OH)_3$. Digest the precipitate in a hot water bath for ten minutes, cool, centrifuge and discard the supernate. Slurry the precipitate in 5 ml of water, centrifuge and discard the wash.

(s) Add 6 drops of concentrated HCl and a minimum of water to dissolve the precipitate (Note 5). Add 6N NH_4OH until a precipitate is observed and add dropwise 6N HNO_3 until the precipitate is dissolved. Add water until a volume of 40 ml is obtained and place in a hot water bath for thirty minutes. Cool, centrifuge and discard the supernate.

(t) Add 10 ml of anhydrous "Anhydrol", slurry the BiOCl precipitate and filter onto a previously washed and weighed Whatman No. 42 filter disk. Wash the precipitate three times with "Anhydrol". Dry in an oven at 110°C for fifteen minutes, cool to room temperature in a dessicator, weigh, record the chemical yield of BiOCl and mount on a brass planchet.

(u) After the radioassay of Bi-210 has been completed, slurry the $PbSO_4$ precipitate from step (o) with anhydrous "Anhydrol". Filter onto a previously washed and weighed Whatman No. 42 filter disk.

Dry in an oven at 110°C for fifteen minutes, cool to room temperature in a dessicator and record the chemical yield recovery of lead.

Note 1. During the removal of I_2 a precipitate of $Pb(NO_3)_2$ may form. Do not try to dissolve this precipitate.

Note 2. In order to minimize the volume, start with 2 ml of 6M $NH_4C_2H_3O_2$. Add additional 6M $NH_4C_2H_3O_2$ in increments of 1 ml until the precipitate completely dissolves. Heat should be used at all times to facilitate the dissolution.

Note 3. To the supernate from the third wash add sufficient concentrated NH_4OH to make the solution basic. If a precipitate appears, continue to wash the $PbSO_4$ precipitate until the ammoniacal supernate is clear.

Note 4. This is the time and date of separation of Bi^{210} from Pb^{210}.

Note 5. The Bi may be mounted as Bi(Q uniolate)$_3$ instead of BiOCl.

Bismuth-210 Counting Procedure

The BiOCl is counted three times on a low level beta counter at approximately 48 hour intervals. The counting time for each measurement is 8 hours. The activity at each counting time is corrected back to milking time of Bi^{210} using the theoretical Bi^{210} half life of 5.0 days. If the corrected activities agree to within one standard deviation of the counting error, the sample is considered radiochemically pure.

The absolute disintegration rate is obtained by applying self-scattering self absorption factors and chemical yield corrections.

Isotopes, Inc.

Sequential Radiochemical Separation of Manganese-54, Iron-55, 59, Strontium-89, 90, Cadmium-109, 113m, 115m, Antimony-124, 125, Cobalt 57, 58 and Thallium-204

After the addition of carriers thallium is precipitated as thallium iodide. Antimony and cadmium are precipitated and separated as sulfides; the cadmium at pH 1.5. After the separation of manganese as the dioxide, cobalt is precipitated as cobaltinitrite. The supernate from the cobalt separation is treated with ammonium hydroxide separating iron as ferric hydroxide. The supernate contains the strontium activity. A flow chart is shown in Figure 14.

1. From the sample contained in a 25 ml volumetric flask (Note 1), remove two 2 ml aliquots for elemental iron spectrophotometric determination.

2. Pipette 20 ml of the sample solution into a 40 ml centrifuge tube and add 20 mg each of thallium, strontium, iron, cadmium, cobalt and manganese carriers.

3. Add 5 ml of 6% H_2SO_3 and 3 or 4 crystals of NaI. Stir and allow to stand at room temperature for 10 minutes. Centrifuge, decant the supernate to a clean 100 ml beaker and retain the precipitate for thallium-204 purification.

4. Heat the supernate from step 3 on a hot plate for approximately 3/4 hour to expel SO_2, then bubble H_2S through the solution for two minutes. Cool to room temperature, transfer to a 40 ml centrifuge tube, centrifuge and decant the supernate to another 40 ml centrifuge tube. Reserve the antimony sulfide precipitate for antimony-124, 125 purification.

5. Evaporate the supernate from step 4 to almost dryness, dilute with water to a pH of 1.5 (approximately 15 ml of water), heat and bubble H_2S gas through the solution for 2 minutes. If a yellow precipitate does not form, increase the volume of water. Cool, centrifuge and decant the supernate.

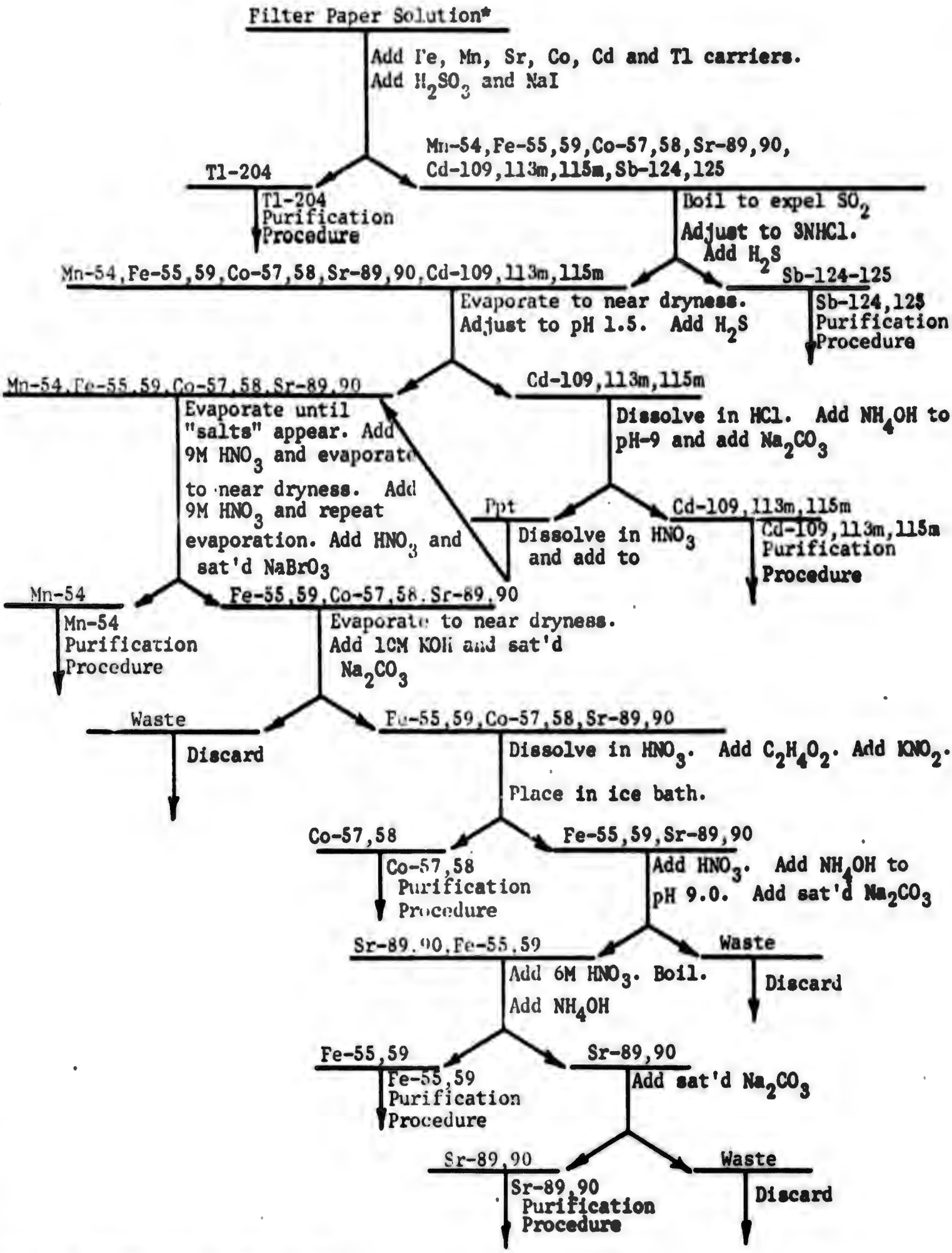

b carrier is added prior to ashing

FIGURE 14 SEQUENTIAL RADIOCHEMICAL SEPARATION OF Mn-54, Fe-55,59, Co-57,58, Sr-89,90, Cd-109,113m,115m, Sb-124,125 AND Tl-204

6. Dissolve the cadmium sulfide precipitate in 5 ml of 6M HCl, boiling until the precipitate is completely dissolved. Adjust the volume to approximately 15 ml with water and add concentrated NH_4OH to pH 9. Heat in a hot water bath for 5 minutes and add 10 ml of saturated Na_2CO_3. Digest in a hot water bath for 20 minutes, cool, centrifuge and transfer the supernate to a 40 ml centrifuge tube. Reserve the supernate for cadmium-109, 113m and 115m purification.

7. Dissolve the carbonate precipitate from step 6 in 5 ml of 6M HNO_3, boil to expel CO_2 and combine with the supernate from step 5 in the 15C ml beaker (Note 2).

8. Evaporate the combined supernate from steps 5 and 7 until "salting out" occurs. Add 20 ml of 9N HNO_3 and again evaporate until salts appear. Add 20 ml of 9M HNO_3 and repeat the evaporation.

9. Add 5 ml of concentrated HNO_3, dilute to 100 ml with water, heat almost to boiling, and add 2 ml of saturated $NaBrO_3$ with stirring. Digest for approximately 20 minutes or until the MnO_2 precipitate settles.

10. Cool to room temperature, transfer to a 40 ml centrifuge tube and centrifuge in portions. Combine the supernates in a 150 ml beaker. Retain the precipitate for manganese-54 purification.

11. Evaporate the combined supernates to almost dryness and transfer the solution to a clean 40 ml centrifuge tube with approximately 25 ml of water. Adjust the pH to 9.0 with 10M KOH, place the tube into a hot water bath of several minutes and add 10 ml of saturated Na_2CO_3. Digest the precipitate for 15-20 minutes, cool, centrifuge and discard the supernate.

12. Dissolve the precipitate with 6 to 10 drops of concentrated HNO_3 and 2 ml of 6N CH_3COOH. Boil over flame for 2 minutes to remove the CO_2 and dilute to 20 ml with water. (If the solution does not turn clear add 2 to 3 drops of H_2O_2 and boil slowly.) Add 6 ml of 3N CH_3COOH saturated with KNO_3 and digest in an ice bath for 30 minutes. Centrifuge and decant the supernate into a clean 100 ml beaker. Wash the $K_3Co(NO_2)_6$ precipitate with 10 ml of water, centrifuge and discard the wash. Retain the precipitate for cobalt-57, 58 purification.

13. Add concentrated HNO_3, cautiously with stirring, until effervescence stops and the solution turns green. Then evaporate to a small volume. Transfer the solution to a clean 40 ml centrifuge tube with water, adjust the pH to 9.0 using concentrated NH_4OH and heat in a hot water bath for five minutes. Add 10 ml of saturated Na_2CO_3, digest the precipitate for 15-20 minutes in the hot water bath, cool, centrifuge and discard the supernate.

14. Dissolve the precipitate from step 13 with 5 ml of 6N HNO_3 and boil over a flame for two minutes to remove all of the CO_2. Cool, dilute to 10 ml with water and add sufficient concentrated NH_4OH to precipitate $Fe(OH)_3$. Digest the precipitate in a hot water bath for ten minutes, cool, centrifuge and decant the supernate into a clean 40 ml centrifuge tube. Retain the $Fe(OH)_3$ precipitate for iron-55, 59 purifcation.

15. To the supernate from step 13 add concentrated NH_4OH until pH 9.0 is obtained. Heat in a hot water bath for five minutes, add 10 ml of saturated Na_2CO_3 solution, digest for 10 minutes in a hot water bath, cool, centrifuge and discard the supernate. Retain the $SrCO_3$ precipitate for strontium-89, 90 purification as described in DASA 1300, Volume 1, pages 108, 117, 118 (1961).

Note 1. On standing, an insoluble antimony precipitate may appear (antimony carrier is added prior to ashing). This precipitate may be dissolved by the addition of concentrated HCl and heating. The precipitate must be dissolved prior to the removal of the aliquot for elemental iron determination.

Note 2. Some strontium is entrained in the cadmium sulfide. Steps 6 and 7 are designed to separate this strontium.

Manganese-54 Purification Procedure[22]

The manganese dioxide precipitate is dissolved in concentrated HCl and manganese carbonate is precipitated. After oxidation to MnO_4^{-2} with $NaBiO_3$ and a ferric hydroxide scavenge, the manganese is finally precipitated and radioassayed as MnO_2. Chemical yield recovery is ascertained by ignition to Mn_3O_4 at 850°C.

The step-by-step procedure is as follows:

(a) Dissolve the MnO_2 precipitate in 4 ml of concentrated HCl and evaporate the solution to near dryness. If the solution is not clear or a very light green during evaporation, again add 4 ml of concentrated HCl and evaporate until the solution turns light green.

(b) Dilute the solution to 10 ml with water and add solid Na_2CO_3 slowly until all the $MnCO_3$ has precipitated. Heat vigorously to insure complete precipitation. Centrifuge and discard the supernate. Wash the precipitate with 10 ml of water, centrifuge and discard the wash.

(c) Dissolve the precipitate in 3 ml of concentrated HNO_3, add 1 ml of iron carrier (10 mg Fe/ml) and dilute to 15 ml with water. Cool the centrifuge tube in an ice bath and add 0.5 grams of $NaBiO_3$ (in portions, with stirring) to oxidize Mn^{+2} to MnO_4^-. Continue stirring for 1 minute and then add 2 drops of 85% phosphoric acid to stabilize the permanganate.

(d) Make the solution basic with 6M NaOH (pH 9 to 10 with pH paper), centrifuge and decant the supernate into a 100 ml beaker (Note 1). Wash the precipitate with 5 ml of water containing several drops of 6M NaOH, centrifuge and combine the wash with the supernate in the 100 ml beaker. Discard the precipitate.

(e) To the combined supernate and wash from step (d) add 3 ml of concentrated HNO_3. Heat, add 2 ml of saturated oxalic acid solution and heat until the solution becomes colorless (Note 2).

(f) Heat the solution almost to boiling, add 2 ml of saturated $NaBrO_3$ and stir vigorously until all the MnO_2 has precipitated.

(g) Transfer the precipitate by portions to a 40 ml centrifuge tube. Centrifuge and discard the supernate. Wash the precipitate with 10 ml of 1N HNO_3 , centrifuge and discard the wash.

(h) Filter the precipitate onto a Whatman No. 42 filter disk using water and finally anhydrous "Anhydrol" as transfer agents. Dry in an oven at 110°C for 20 minutes and mount on a nylon planchet for radioassay.

(i) On completion of radioassay, place the filter paper and precipitate in a previously heated and tared procelain crucible and heat gently until the paper is completely charred, making sure that the paper does not ignite.

(j) Heat the crucible in an electric muffle furnace at 850°C for 1 hour, cool in a desiccator and determine the chemical yield of Mn_3O_4 .

Note 1. The solution should remain a deep purple.

Note 2. The permanganate is reduced to Mn^{+2}.

23

Iron-55, 59 Purification Procedure

The ferric hydroxide precipitate is dissolved in 10M nitric acid and extracted into 0.6M thenoyltrifluoroacetone-xylene. The organic phase is washed with 4M nitric acid and 0.25M hydrofluoric-nitric acid mixture in order to remove zirconium-95. The iron is back-extracted with concentrated hydrochloric acid and finally plated onto a copper disk for radioassay.

(a) Dissolve the $Fe(OH)_3$ precipitate from the sequential separation in 3 ml of concentrated HNO_3, add 10 ml of 10M HNO_3 and 1.3 ml of 30% H_2O_2. Transfer the solution with water to a 60 ml cylindrical separatory funnel and add 15 ml of freshly prepared 0.6M 2-thenoyltrifluoroacetone(TTA)-xylene solution (Note 1). Stir the mixture for 15 minutes with a high speed motor stirrer.

(b) Withdraw and discard the aqueous phase. Wash the sides of the separatory funnel with several ml of water, stir for one minute. Withdraw and discard the aqueous wash solution.

(c) Add 15 ml of freshly prepared 4M HNO_3 - 3% H_2O_2 solution and perform a one minute scrub. Centrifuge and withdraw and discard the aqueous scrub solution. Wash the sides of the separatory funnel with several ml of water. Withdraw and discard the wash.

(d) Repeat step (c).

(e) Add 15 ml of 0.25M HF-0.25M HNO_3 solution, perform a one minute scrub and discard the aqueous scrub solution. Repeat this step twice more.

(f) Add 7 ml of concentrated HCl and stir until the organic phase is decolorized (about 10 minutes). Withdraw the aqueous phase and repeat the back-extraction with an additional 5 ml portion of concentrated HCl.

(g) Combine both aqueous portions and precipitate $Fe(OH)_3$ with excess concentrated NH_4OH. Centrifuge and discard the supernate.

(h) Dissolve the precipitate from step (g) in 5 drops of concentrated HCl and evaporate to dryness by gently heating over a flame. Dissolve the residue in 2 ml of water, add 1.5 ml of "Phosphate Buffer" (2.32M $NH_4H_2PO_4$) and 8 ml of "Carbonate Buffer"(Note 2).

(i) Transfer the solution to the electrodeposition unit containing a tared copper disk (Note 3) with 5 ml of "Carbonate Buffer" solution. Electrodeposit for 2 hours, starting at 450 m.a. for 15 minutes, and increasing to 500 m.a.

(j) On completion of plating, remove the copper disk and wash immediately with water and anhydrous "Anhydrol". Pat dry with a Kimwipe and weigh for chemical yield (Note 4). Immediately cover the disk with a thin coating of Krylon, dry, mount and radioassay.

Note 1. 0.6M TTA-xylene: 12 gm TTA/100 ml of xylene.

Note 2. The "Carbonate Buffer" solution is made by dissolving 392.5 g $(NH_4)_2 CO_4$ in 175 ml of concentrated NH_4OH and diluting to 1 liter with water.

Note 3. The copper disk has to be thoroughly washed with a cleansing compound, distilled water and anhydrous "Anhydrol" prior to taring.

Note 4. Adjust the yield utilizing the elemental iron value derived by spectrophotometric analysis.

Isotopes, Inc.

Iron Colorimetric Procedure (Ortho-Phenanthroline Method)[24]

The iron is reduced with hydroxylamine hydrochloride, the orange-red Fe(ll) complex of 0-phenanthroline is formed and the spectrophotometric determination is made at 510 mμ. Oxidizing agents cause the major interference. The color is stable for about 12 hours after a 5-10 minute color development. The recommended range is from 25 to 100γ of iron in 25 ml of solution using a 1 cm cell.

(a) Transfer an aliquot of the sample to a 25 ml volumetric flask (Notes 1 and 2) add 1 ml of 35% hydroxylamine hydrochloride solution, 1 ml of 1% ortho-phenanthroline in anhydrol solution and 15 ml of 40% ammonium acetate solution.

(b) Dilute to the mark and mix well.

(c) Rinse a 1 cm cell with three portions of the solution and transfer the solution to the cell.

(d) Convert the photometric readings to milligrams of iron as follows:

$$\text{Total milligrams Fe} = \frac{A \times B \times 1000}{C}$$

Where A = original volume of sample in milliliters.

B = micrograms of Fe in the aliquot used (from calibration curve)

C = volume of aliquot in milliliters

Note 1. Two aliquots of the standard solution and 5 ml of water should be transferred to separate 25 ml volumetrics and processed with the sample.

Note 2. To prepare the standard solution dissolve 0.5000 gm of pure iron in 50 ml of HCl (2:1) and dilute to 1 liter in a volumetric flask. Dilute 100 ml of this solution to 1 liter in a volumetric flask. This solution is used for calibration. Transfer 1.0, 2.0, 3.0, 4.0 and 5.0 ml of standard solution to separate 25 ml volumetric flasks. Transfer 5 ml of water to a separate 25 ml flask for use as a blank. Proceed with steps (a) through (d) of the procedure. Plot the photometric absorbance readings versus micrograms of ml of solution.

Isotopes, Inc.

Cobalt-57, 58, 60 Purification Procedure[25]

Cobalt is purified by two potassium cobaltinitrite precipitations, a palladium sulfide and copper sulfide scavenge plus two ferric hydroxide scavenges. Finally the cobalt is plated on a copper disk and radioassayed.

(a) Dissolve the $K_3Co(NO_2)_6$ precipitate in 5 ml of concentrated HCl and boil for several minutes to remove decomposition products. Add 10 mg of nickel carrier and dilute to 25 ml with water.

(b) Precipitate nickel and cobalt hydroxides with 10M KOH. Centrifuge and discard the supernate.

(c) Dissolve the precipitate in 3 ml of 6M $HC_2H_3O_2$ and heat slightly if necessary in order to dissolve the precipitate. Dilute to 25 ml with water and cool to room temperature.

(d) Precipitate $K_3Co(NO_2)_6$ by adding 6 ml of 3M $HC_2H_3O_2$ that is freshly saturated with KNO_2 (Note 1). Allow 30 minutes for complete precipitation. Centrifuge and discard the supernate. Wash the precipitate with 30 ml of water, centrifuge and discard the wash.

(e) Dissolve the $K_3Co(NO_2)_6$ precipitate in 5 ml of concentrated HCl, boil almost to dryness, add 2 drops of palladium carrier (10 mg Pd/ml) and 4 drops of copper carrier (10 mg Cu/ml). Dilute to 20 ml with water and add 2 ml of 1M HCl to make the solution approximately 0.1M.

(f) Heat the solution almost to boiling and bubble H_2S gas through the solution for 5 minutes. Filter the sulfide precipitate through Whatman No. 42 filter paper (9 cm) contained in a 2", 60° glass funnel and collect the filtrate in a 125 ml erlenmeyer flask. Wash the original centrifuge tube with 5 ml of water, pass the water solution through the filter funnel and combine with the filtrate in the erlenmeyer flask. Discard the sulfide precipitate.

(g) Boil the filtrate almost to dryness (Note 2) to remove excess H_2S, add 5 ml of water and transfer the solution to a 40 ml centrifuge tube using about 10 ml of 1N HCl as a transfer agent. Add 4 drops of iron carrier (10 mg Fe/ml) and precipitate $Fe(OH)_3$ by addition of concentrated NH_4OH (Note 3). After the $Fe(OH)_3$ has been completely precipitated, add about 0.5 ml of NH_4OH in excess. Centrifuge and discard the precipitate.

(h) Acidify the supernate with 6M HCl, add 4 drops of iron carrier and repeat the scavenge as in step (g).

(i) Transfer the supernate from the $Fe(OH)_3$ scavenge to a clean 40 ml centrifuge tube and precipitate CoS by bubbling H_2S gas through the solution for 2 minutes. Centrifuge and discard the supernate.

(j) Transfer the CoS precipitate with 5-10 ml of water to a 125 ml erlenmeyer flask, add 10 ml of concentrated HNO_3 and evaporate to approximately 5 ml. Transfer the solution to a 100 ml beaker and wash the erlenmeyer twice with water, adding the washes to the beaker and evaporate to 1-2 ml.

(k) Add 3 ml of concentrated H_2SO_4 and heat to SO_3 fumes. Cool, slowly add 5-10 ml of water and again cool. Neutralize the solution with concentrated NH_4OH, add 2 grams $(NH_4)_2SO_4$ and electroplate the cobalt on a tared 7/8" diameter copper disk. Begin plating at 3-4 volts and 0.10 amps. After the first half-hour increase the current to 0.20 amps and plate for 4 hours. Upon completion of plating the solution should be colorless.

(l) Dismount the copper disk from the plating cell, wash the disk with water and acetone, dry in a desiccator and weigh the Co metal for chemical yield. Mount on a nylon planchet for radioassay.

Isotopes, Inc.

Note 1. Maintain a saturated solution by repeated addition of KNO_2.

Note 2. The H_2S is removed to prevent precipitation of CoS in the $Fe(OH)_3$ scavenge step.

Note 3. If, at the addition of NH_4OH, the green color of $Co(OH)_2$ appears, add HCl until the color disappears and proceed with the $Fe(OH)_3$ precipitation.

Cadmium-109, 113m, 115m Purification Procedure[26]

The cadmium fraction is purified by several cadmium sulfide precipitations and iron, silver and palladium scavenges. The cadmium is electroplated on copper for radioassay.

(a) To the supernate containing the separated cadmium, add 6N HCl until the pH is 1.5. Bubble H_2S gas through the solution for 5 minutes, centrifuge and discard the supernate.

(b) Dissolve the CdS precipitate in 5 ml of 6N HCl and boil over a flame for approximately 2 minutes. Add 2 drops of palladium carrier (10 mg Pd/ml), heat to boiling and saturate the solution with H_2S gas for 3 minutes.

(c) Digest the precipitate in a hot water bath for 5 minutes, cool to room temperature, add 2 drops of aerosol and centrifuge. Transfer the supernate to a clean 40 ml centrifuge tube and discard the precipitate.

(d) Evaporate the supernate to dryness in a hot sand bath or over a flame. Dissolve the residue in 15 ml of water, add 3 drops of iron carrier (10 mg Fe/ml) and 1 ml of 6M $NH_4C_2H_3O_2$. Heat the solution to boiling over a flame and digest for 5 to 10 minutes in a hot water bath.

(e) Cool the solution to room temperature, centrifuge and discard the precipitate. To the supernate add 1 ml 6M $NH_4C_2H_3O_2$, heat to boiling over a flame, add 3 drops of iron carrier (10 mg Fe/ml) and digest in a hot water bath for 5 to 10 minutes.

(f) Cool the solution to room temperature, centrifuge, transfer the supernate to a clean 40 ml centrifuge tube and discard the precipitate.

(g) To the supernate add 6N HCl until a pH of 1.5 is reached and heat in a hot water bath. Saturate the solution with H_2S gas for three minutes (Note 1). Cool to room temperature, centrifuge and discard the supernate.

(h) Add 2 ml concentrated HNO_3 and boil over a flame until the CdS precipitate is dissolved. Dilute to 5 ml with water, add 5 drops of silver carrier (10 mg/ml), 1 ml of 1M HCl, stir and digest in a hot water bath for 5 minutes. Cool, centrifuge and discard the precipitate.

(i) Add water until a pH of 1.5 is obtained and heat in a hot water bath for 5 minutes. Saturate the solution with H_2S gas for 3 minutes, cool to room temperature, centrifuge and discard the supernate.

(j) Repeat steps (b) through (g), twice.

(k) Dissolve the CdS precipitate in 5 ml of 6N HCl and evaporate to dryness.

(l) Wash down the walls of the centrifuge tube with approximately 1 ml of water, add 6 drops of concentrated H_2SO_4 and boil over a flame until SO_3 fumes are given off. Cool, again wash the sides of the centrifuge tube with 1 ml of water and heat to SO_3 fumes.

(m) Cool, add 3 ml of water to dissolve the $CdSO_4$. Again cool and add 12M NaOH, a drop at a time, until the first permanent $Cd(OH)_2$ precipitate is formed.

(n) Add 10% solution of KCN until the precipitate dissolves and transfer the solution to the electrodeposition unit containing a tared copper disk (Note 2). Wash the centrifuge tube with 5 to 7 ml of 0.03% solution of gelatin and transfer the wash to the electrodeposition unit. Electroplate for 3.5 hours at 6.0 volts.

(o) On completion of plating, remove the copper disk and wash for several minutes with hot water and then with anhydrous "Anhydrol". Dry the disk and weigh the cobalt metal for chemical yield. Mount on a brass planchet for radioassay.

Note 1. If a precipitate does not form, add water until it does.

Note 2. The copper disk should be thoroughly washed with a cleaning compound, distilled water and anhydrous "Anhydrol" prior to taring.

Antimony-124, 125 Purification Procedure[27]

The separated antimony sulfide is dissolved and another sulfide precipation is performed. The antimony is finally precipitated as metal with "Oxsorbent". The metal is mounted and radioassayed.

(a) Dissolve the separated Sb_2S_5 precipitate in 4 ml of concentrated HCl and boil over a flame for two minutes. If the precipitate does not completely dissolve, add 4 to 5 drops of 30% H_2O_2 and boil.

(b) Add 10 mg of rhodium carrier, 10 mg of ruthenium carrier and 4 drops of 30% H_2O_2. Heat the solution to boiling, cool, add 4 drops of 3% H_2O_2 and evaporate to dryness in a hot air bath.

(c) While still hot add 20 ml 6N H_2SO_4, bubble H_2S gas into the solution for ten minutes, cool, centrifuge and discard the supernate.

(d) Wash the precipitate from step (c) with 5 ml of 3N H_2SO_4, centrifuge and discard the wash. Add 5 ml of concentrated HCl and heat the solution to boiling. Cool, dilute to a total of 15 ml with water. Centrifuge and filter the supernate through Whatman No. 42 filter paper, collecting the filtrate in a 125 ml erlenmeyer flask.

(e) Add another 5 ml of concentrated HCl and heat the solution to boiling. Cool, dilute to 15 ml with water and filter through the same Whatman filter paper used in step (d). Combine the filtrate with the filtrate in the erlenmeyer flask.

(f) Wash the precipitate with concentrated HCl, filter through the Whatman No. 42 filter paper and combine the filtrate with the filtrates from steps (d) and (e).

(g) Add 5 ml of "Oxsorbent" ($CrCl_2$ solution) (Note 1) to the erlenmeyer flask, heat to boiling, cool and add an additional 5 ml "Oxsorbent".

Cool, centrifuge and carefully decant and discard the supernate.

Wash with 10 ml of water, centrifuge, decant and discard the wash. Filter the antimony metal onto a tared Whatman No. 42 filter paper using water as a transferring agent. Wash the precipitate with three 5 ml portions of anhydrous "Anhydrol". Dry in an oven at 110°C for 10 minutes, cool in a desiccator, weigh and mount on a brass planchet.

Note 1. The 5 ml of "Oxsorbent" is added to the solution via a 5 ml pipette. The tip of the pipette is immersed in the solution and the "Oxsorbent" is allowed to enter the solution without coming into contact with air. A clean pipette is used for each addition to each sample.

Isotopes, Inc.

Thallium-204 Purification Procedure[28]

The separated TlI precipitate is dissolved in 6M HNO_3 and subjected to a series of tellurium metal and lanthanum hydroxide scavengings. Finally, after several TlI precipitations, the thallium activity is mounted as thallium chromate and is radioassayed.

(a) Dissolve the separated TlI precipitate in 5 ml of 6M HNO_3 by boiling over an open flame. Heat until iodine vapors are no longer evident. Transfer the solution to a 125 ml erlenmeyer flask with water as transfer agent.

(b) Add 1 ml of tellurium carrier (10 mg Te/ml), 5 ml of concentrated HCl and evaporate to dryness. Add 5 ml of concentrated HCl and evaporate to dryness three more times.

(c) While still warm, add 20 ml of 3M HCl, approximately 1 ml of $N_2H_2H_2O$ (hydrazine-hydrate) and heat to boiling. Add 1 ml of 6% H_2SO_3, continue to boi. and make four to five successive 1 ml additions of H_2SO_3 (Note 1).

(d) While still warm filter the solution through a 2" 60° funnel using No. 42 Whatman filter paper. Collect the solution in a clean 125 ml erlenmeyer flask (Note 2). Wash the original flask and the precipitate with dilute H_2SO_3. Combine the wash with the filtrate and discard the precipitate.

(e) Bring the volume of solution to approximately 75 ml with water, add 1 to 2 gm. of NaI. Transfer to a 40 ml centrifuge tube, centrifuge and discard the supernate.

(f) Add 5 ml of 6M HNO_3 and heat the solution over an open flame until the I_2 vapors are no longer evident; then add 7 drops of lanthanum carrier (10 mg La/ml).

(g) Dilute the solution to 20 ml with water, heat over an open flame until the solution is hot and add 1 ml of H_2SO_3 . While still warm make the solution ammoniacal by the dropwise addition of concentrated NH_4OH; then add 1 ml of NH_4OH in excess.

(h) Centrifuge, transfer the supernate to a clean 40 ml centrifuge tube and discard the precipitate.

(i) To the supernate add approximately 1 gram of NaI, centrifuge and discard the supernate. To the precipitate add 3 ml of 6M HNO_3 and heat over an open flame until I_2 vapors are no longer evident. Transfer the solution to a 125 ml erlenmeyer flask with water.

(j) Repeat steps (b) through (i).

(k) To the supernate, again add 1-2 grams of NaI,centrifuge and discard the supernate.

(l) Repeat steps (f), (g) and (h).

(m) To the supernate from step (l) add 5 ml of 10% Na_2CrO_4 and allow the precipitate to stand at room temperature for 10 minutes.

(n) Centrifuge and discard the supernate. Filter the precipitate onto a tared Whatman No. 42 filter disk with water. Wash the precipitate with 10 ml of water and three 5 ml portions of anhydrous "Anhydrol". Dry in an oven at 110° C for ten minutes. Cool in a desiccator and weigh for chemical yield. Mount on a brass planchet for radioassay.

Note 1. Particular care must be given to insure complete precipitation of tellurium metal. When the tellurium has been completely precipitated, the supernate is clear with no bluish tint.

Note 2. If the solution stands too long before filtering white crystals will form. If this happens add 1 ml of H_2SO_3 and heat.

Isotopes, Inc.

Sequential Radiochemical Separation of Strontium-90, Cesium-137 and Plutonium-239

Strontium, cesium and iron carriers are added and ferric hydroxide and strontium carbonate are precipitated, leaving cesium in the supernate. The precipitate is dissolved, and the plutonium is separated by a ferric hydroxide scavenge with ammonium hydroxide. A flow chart is shown in Figure 15.

1. To an aliquot of the filter paper solution contained in a 40 ml glass centrifuge tube add 20 mg of strontium carrier, 1 ml of strontium-85 spike solution (Note 1), 20 mg of cesium carrier and 10 mg of iron carrier.

2. Make the solution basic to pH 9 with 50% NaOH, digest in a hot water bath for 20 minutes, add 10 ml of saturated Na_2CO_3 solution, digest for 10 minutes in a hot water bath, cool, centrifuge and reserve the supernate for cesium-137 purification as described in DASA 1300, Volume 1, page 133 (1961).

3. Dissolve the precipitate in 5 ml of 6M HNO_3, boil over a flame for two minutes to expel all CO_2, dilute to 15 ml with water and make basic to pH 8.5 with concentrated NH_4OH. Centrifuge and reserve the ferric hydroxide precipitate for plutonium-239 purification, as described in DASA 1300, Volume 1, page 145 (1961).

4. Reserve the supernate for strontium-90 purification as described in DASA 1300, Volume 1, pages 107 (step 13) and 117 (1961).

Note 1. Strontium-85 spike is added to determine the recovery of strontium. This eliminates the need for a gravimetric determination of $SrCO_3$. The strontium-85 yield method is described in DASA 1300, Volume 5, page 231 (step m) (1961).

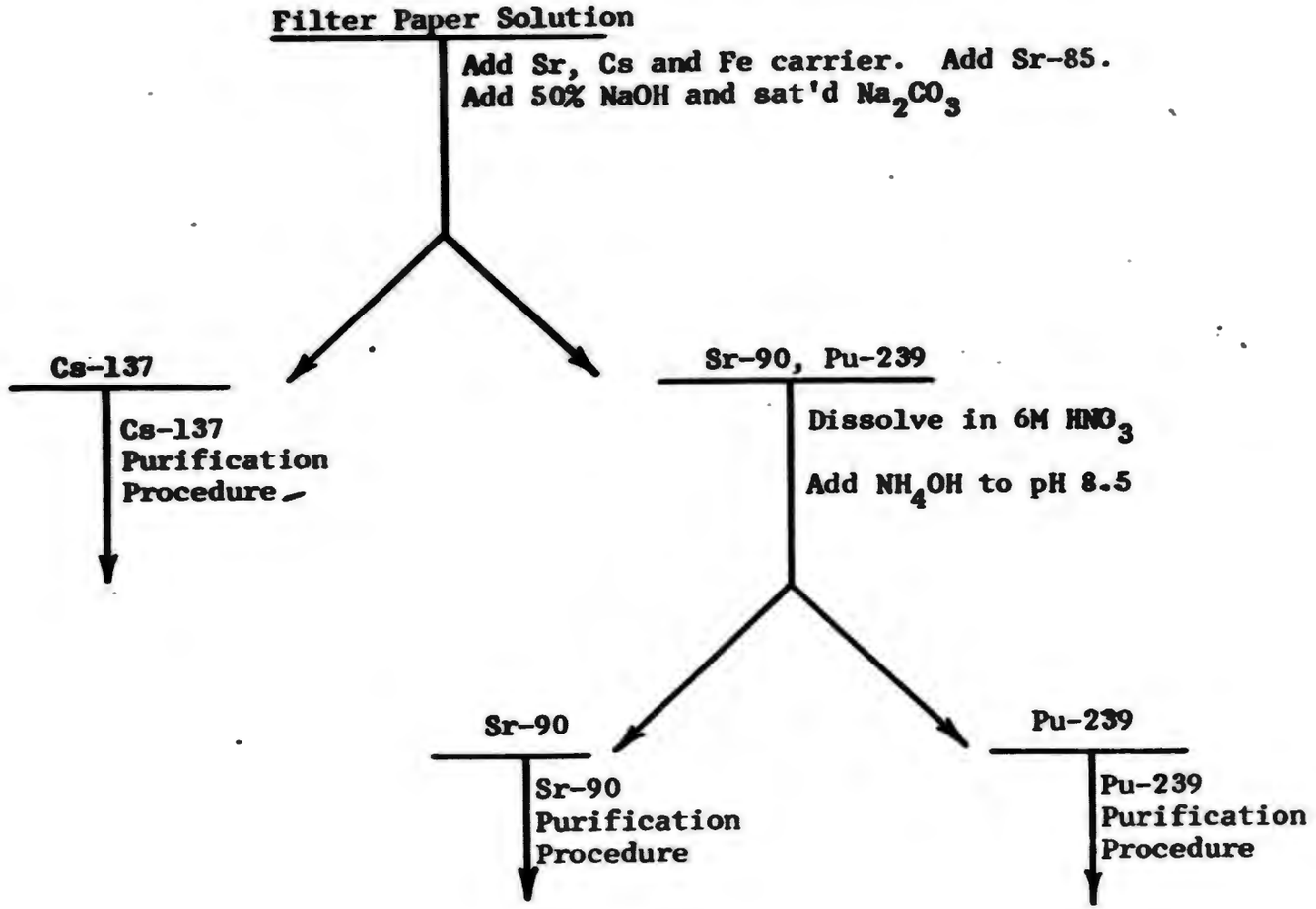

FIGURE 15 · SEQUENTIAL RADIOCHEMICAL SEPARATION OF Sr-90, Cs-137 AND Pu-239

Isotopes, Inc.

List of Reagents

1. Carriers

(a)	Antimony:	SbF_3	(30 mg Sb/ml)
(b)	Thallium:	Tl_3O_2	(20 mg TI/ml)
(c)	Cadmium:	$Cd(NO_3)_2 \cdot 6H_2O$	(10 mg Cd/ml)
(d)	Cobalt:	$Co(NO_3)_2 \cdot 6H_2O$	(20 mg Co/ml)
(e)	Iron:	$FeCl_3 \cdot 6H_2O$	(20 mg Fe/ml), (10 mg Fe/ml), (5 mg Fe/ml)
(f)	Manganese:	$MnCl_2 \cdot 4H_2O$	(20 mg Mn/ml)
(g)	Tellurium:	TeO_2	(10 mg Te/ml)
(h)	Lanthanum:	$La(NO_3)_3 \cdot 6H_2O$	(10 mg La/ml), (5 mg La/ml)
(i)	Rhodium:	$RhCl_3$	(10 mg Rh/ml)
(j)	Ruthenium:	Ru	(10 mg Ru/ml)
(k)	Palladium:	$PdCl_2$	(10 mg Pd/ml), (20 mg Pd/ml)
(l)	Copper:	$CuCl_2 \cdot 2H_2O$	(10 mg Cu/ml)
(m)	Strontium:	$Sr(NO_3)_2 \cdot 4H_2O$	(20 mg Sr/ml)
(n)	Barium:	$Ba(NO_3)_2$	(20 mg Ba/ml), (50 mg Ba/ml)
(o)	Zirconium:	$ZrOCl_2 \cdot 8H_2O$	(10 mg Zr/ml)
(p)	Yttrium:	$Y(NO_3)_3 \cdot 6H_2O$	(10 mg Y/ml)
(q)	Beryllium:	$Be(NO_3)_2 \cdot 3H_2O$	(1 mg Be/ml)
(r)	Molybdenum:	$(NH_4)_2MoO_4$	(10 mg Mo/ml)
(s)	Tungsten:	H_2WO_4	(20 mg W/ml)
(t)	Bismuth:	$BiCl_3$	(10 mg Bi/ml)
(u)	Niobium:	$Nb(HC_2O_4)_5$	(10 mg Nb/ml)
(v)	Cerium:	$Ce(NO_3)_3 \cdot 6H_2O$	(20 mg Ce/ml)
(w)	Iodide:	NaI	(10 mg I/ml)
(x)	Iodate:	$NaIO_3$	(14 mg IO_3/ml)
(y)	Lead:	$Pb(NO_3)_2$	(20 mg Pb/ml)
(z)	Cesium:	CoCl	(20 mg Cs/ml)

2. Sodium Iodide (NaI)
3. Sulfurous Acid (H_2SO_3)
4. Hydrogen Sulfide gas (H_2S)
5. Sodium Bromate ($NaBrO_3$, saturated, 1M, 2M)
6. Sodium Carbonate (Na_2CO_3, saturated)
7. Potassium Nitrate (KNO_3)
8. Hydrazine Hydrate ($N_2H_2 \cdot H_2O$)

Isotopes, Inc.

9. Sodium Chromate (Na_2CrO_4, 10%, 1.5M)
10. Anhydrous "Anhydrol" (commercial product of denatured 95% ethyl alcohol available from C.P. Commercial Solvents, Inc., Newark, New Jersey)
11. Hydrogen Peroxide (H_2O_2, 30%, 3%)
12. Oxsorbent ($CrCl_2$ solution)
13. "Aerosol" solution (1% wetting agent)
14. Ammonium Acetate ($NH_4C_2H_3O_2$, 6M, 40%)
15. Potassium Cyanide (KCN, 10%)
16. Phenolpthalein indicator
17. Gelatin solution (0.03%)
18. Ammonium Sulfate ($(NH_4)_2SO_4$)
19. Sodium Bismuthate ($NaBiO_3$)
20. Phosphoric Acid (H_3PO_4)
21. Oxalic Acid ($C_2H_2O_2 \cdot 2H_2O$, saturated)
22. 2-Thenoyltrifluoroacetone, T.T.A. (0.6M in xylene)
23. "Phosphate Buffer" (2.32 $NH_4H_2PO_4$)
24. "Carbonate Buffer" (392.5g $(NH_4)_2CO_3$, 175 concentrated NH_4OH diluted to one liter with H_2O)
25. o-phenanthroline (1% in "Anhydrol" solution)
26. Hydroxylamine Hydrochloride ($NH_2OH \cdot HCL$, 35%, 5M)
27. Diethyl Ether ($C_2H_5O\ C_2H_5$)
28. Barium Buffer (1.1M $C_2H_4O_2$ and 2.8M $NH_4C_2H_3O_2$)
29. Hydrafluoric Acid (HF)
30. Boric Acid (H_3BO_3 , saturated)
31. dl-Mandelic Acid ($C_6H_5CH(OH)COOH$, 16%)
32. Tri-n-butylphosphate
33. Ligroin (petroleum ether)
34. Meta-Cresol purple indicator
35. Ammonium Oxalate ($(NH_4)_2C_2O_4$, saturated
36. Acetone
37. Fuming Nitric Acid (HNO_3, 90%)
38. "Acetate Buffer Solution" ($2MC_2H_4O_2$ - 4M $NH_4C_2H_3O_2$)
39. Disodium Ethylenediaminetetra-acetate (saturated solution)
40. Acetylacetone
41. Benzene

Isotopes, Inc.

42. "Beryllium Buffer Solution" (116 Citric Acid, 61.5 grams of sodium borate decahydrate, 216 grams of sodium hydroxide, diluted to 1 liter)
43. "Beryllium Dye Solution" (0.150 gram of 4-(p-nitrophenylazo) orcinol in 500 ml of 0.1N NaOH. Filter through a Millipore H.A. filter (0.45 mμ)
44. Pyridine
45. Phenylarsonic Acid (saturated solution)
46. Dowex 1 x 2 Anion Exchange resin, 100 to 200 mesh
47. Perchloric acid ($HClO_4$, 70%)
48. Magnesium Metal (Mg, powder)
49. Tartaric acid ($C_4H_6O_6$, saturated)
50. Ammonium Nitrate (NH_4NO_3)
51. Chloroform ($CHCl_3$)
52. Cupferron (6% solution)
53. Glacial Acetic Acid ($C_2H_4O_2$)
54. "Tungsten Buffer Solution" (1M $C_2H_4O_2$ - 3.6M $NaC_2H_3O_2$)
55. 8-Hydroxyquinoline (5% solution in "Anhydrol")
56. Sulfuric Acid (H_2SO_4)
57. Methyl isobutyl ketone
58. Sodium Nitrite ($NaNO_2$, 2M)
59. Carbon Tetrachloride (CCl_4)
60. Sodium Bisulfite ($NaHSO_3$, 1M)
61. α -benzoin oxime (5% solution in "Anhydrol")
62. Ammonium Hydroxide (NH_4OH)
63. Sodium Hydroxide (NaOH)
64. Nitric Acid (HNO_3, 70%)
65. Hydrochloric Acid (HCl)

Radiometric Assay Techniques

The final phase of the radiochemical analysis is the radiometric assay of the purified radionuclides. The diversity of samples measured necessitated the use of various beta, alpha, gamma and "X"-ray detecting devices which are described in the following sections.

Beta Counting

Beta emitting nuclides are counted on one of four types of counters designed to give optimum net count rates and backgrounds. These types of counters are designated as:

1. "X" Counters - (20 counters)

   Thin window, Geiger made, gas flow (99% helium, 1% 180 isobutane) detectors with anti coincidence guards and four inches of load shielding around each bank of 4 detectors. The backgrounds are approximately 0.5 cpm. The usual counting period is 5 hours. The limit of detection is 0.15 cpm.

2. "L" Counters - (12 counters)

   Sealed, Geiger made detectors with anti coincidence guard tubes and lead shielding. The backgrounds are approximately 2 cpm and the counting periods are up to 5 hours.

3. "H" Counters - (4 counters)

   Sealed, Geiger made detectors with 2" of lead shielding. The dead time is less than 50 micro seconds. The backgrounds are approximately 5 cpm. The usual counting periods are 5-30 minutes.

4. "A" Counters - (2 counting systems)

   Automatic sample changers, with the detectors operating in the proportional mode and shielded with lead. Gas flow detectors using 10% methane - 90% argon. The backgrounds are approximately 10 cpm.

The counters are calibrated for efficiency with known activity standards for the nuclides listed in Table 10. The radiochemically separated nuclide from

a sample is mounted on a brass planchet and counted on the appropriate counter to give the optimum count rate consistent with the level of activity. The purity of the sample is checked either by the absorber ratio method with aluminum absorbers or by following the half life for a minimum of 3 counts for nuclides with half lives of less than a few weeks.

Samples which contain more than one beta-emitting isotope of the same element are measured either by counting a daughter product of one of the isotopes or by absorber discrimination if the isotopes have markedly different energies. For example, in samples containing strontium-90 and strontium-89, the yttrium-90 daughter of strontium-90 is measured, and the strontium-89 activity is calculated by subtracting from the total count of the strontium fraction the contribution attributable to strontium-90 and yttrium-90. The absorber technique is used to measure samples containing phosphorus-32 and phosphorus-33. The phosphorus-32 activity is obtained by counting the sample with an absorber thick enough to remove the 0.26 Mev beta of phosphorus-33. This activity, corrected for counting efficiency, is then subtracted from the counting rate obtained when the sample is counted without absorbers, and the phosphorus-33 activity is calculated.

Table 10. Summary of Beta Counting Procedures

Nuclide	Predominant Energy (Mev)	Half Life	Purity Measurement	Limit of Detection (cpm)
Na^{22}	0.55	2.7 y.	Absorber ratio	4
P^{32}	1.7	14 d.	Half life*	1.2
P^{33}	0.26	25 d.	Half life*	5
Co^{60}	0.31	5.3 y.	Absorber ratio	4
Sr^{89}	1.5	54 d.	Half life	1.2
Sr^{90}	0.6	19.9 y.	Y^{90} counted	4
Y^{90}	2.2	62 h.	Half life	1.2
Y^{91}	1.55	60 d.	Absorber ratio	1.2
Zr^{95}	0.37	65 d.	Absorber ratio	5
Mo^{99}	1.2	67 h.	Half life	1.2
Cd^{113m}	0.5	5 y.	Absorber ratio*	4
Cd^{115m}	1.6	43 d.	Half life*	1.2
I^{131}	0.61	8.1 d.	Half life	3
Cs^{137}	0.52	33 y.	Absorber ratio	4
Ba^{140}	1.0	12.8 d.	Half life	2
La^{140}	1.32	40 h.	Half life	1.2
Ce^{141}	0.44	32 d.	Half life*	4
Ce^{144}	0.30	282 d.	Absorber ratio* (Pr^{144} counted)	5
Pm^{147}	0.227	2.4 y.	Absorber ratio	5
Tl^{204}	0.77	3 y.	Absorber ratio	2
Bi^{210}	1.17	5 d.	Half life	1.2

*Absorber discrimination between isotopes is used.

Isotopes, Inc.

Gamma-ray Spectrometry

There are three NaI(Tl) crystals presently being used for gamma ray spectrometry: a 3" x 3" cylindrical NaI(Tl) crystal, a 2 1/2" x 1 3/4" "well" type NaI(Tl) crystal and a 0.020" x 1 1/4" "thin" NaI(Tl) crystal. The thin cyrstal is used to assay weak gamma or x-radiation. Each crystal is used with a multi-channel pulse height analyzer.

Samples are mounted on planchettes and either counted on top of the 3" x 3" crystal or the "thin" crystal or placed in a culture tube and counted in the well of the "well" type crystal.

The spectrum from the gamma radioassay is stored and displayed in the multi-channel analyzer. The spectrum will normally consist of a photopeak for each energy gamma radiation present in the nuclide. There is also associated with each photopeak a compton which is seen as a continuum on the low energy side of the peak. Other peaks may also be produced as a result of annihilation (0.51 Mev. gamma rays), coincidence summing, pair production, etc.

The method of calculating the disintegration rate after background subtraction is to sum the total number of counts under the curve of one or more photopeaks and applying a previously determined detection efficiency.

For spectra that contain photopeaks of more than one nuclide, spectrum stripping may be required. To accomplish this the spectra of radiochemically pure samples of the nuclides represented are used, beginning with the one which contributes to the highest energy peak and proceeding to those which contribute peaks of lower energy. These spectra, which are stored on magnetic tape, may be fed back into the analyzer as needed. The spectrum of a standard sample of the appropriate nuclide is normalized to make the total count under the highest energy photopeak equal to the total count under the same photopeak in the spectrum which is to be stripped. The entire normalized spectrum of the

standard is then subtracted from the spectrum of the sample being analyzed, using the electronic memory of the multi-channel pulse-height analyzer. The process is then repeated using the spectrum of a standard sample of the nuclide which contributes the highest energy peak in the residual spectrum of the sample being analyzed. The activity of each of the nuclides present in the sample is determined by measuring the activity under its highest energy photopeak before it is stripped.

The spectra of radiochemically pure standard samples of the nuclides being measured are compared to the spectra for the samples being analyzed to check their purity. In addition, about 10 per cent of all beryllium-7 and yttrium-88 samples are followed for decay to determine their purity by half life measurements. Corrections are made for aliquot and chemical yield. The activities are corrected to collection date by using the proper half life. Table 11 lists the nuclides and pertinent information for samples assayed via gamma ray spectrometry.

Table 11. Summary of Gamma Counting Procedures

Nuclide	Photopeak Energy(Mev)	Half Life	Detector	Geometry	Limit of Detection for 2 hour Count (dpm)
Be^{7}	0.48	52.9 d.	Well	1-2 ml solution	198.9
Mn^{54}	0.84	310 d.	3x3	Planchet	63.8
			Well	1-2 ml solution	39.8
Co^{57}	0.122	270 d.	3x3	Planchet	15.5
			Well	1-2 ml solution	5.3
Co^{58}	0.81	71 d.	3x3	Planchet	58.8
			Well	1-2 ml solution	39.5
Fe^{59}	1.10 and 1.30	45 d.	3x3	Planchet	55.0
			Well	1-2 ml solution	78.0
Co^{60}	1.17 and 1.33	5.3 y.	3x3	Planchet	44.4
			Well	1-2 ml solution	26.0
Y^{88}	1.85	108 d.	3x3	Planchet	57.3
			Well	1-2 ml solution	50.9
Zr^{95}	0.76	65 d.	3x3	Planchet	60.1
			Well	1-2 ml solution	39.0
Cd^{109}	0.024	470 d.	Thin	Planchet	2.76*
Sb^{124}	0.605	60 d.	3x3	Planchet	37.5
			Well	1-2 ml solution	20.8
Sb^{125}	0.60	2.7 y.	Well	1-2 ml solution	88.4
Ce^{141}	0.145	33 d.	3x3	Planchet	37.8
Ce^{144}	0.134	280 d.	3x3	Planchet	149.3
			Well	1-2 ml solution	51.6

*The inter laboratory calibration of a cadmium-109 tracer solution resulted in an assigned value of 2.5×10^{6} dpm/gram.[29] Using this value the detection efficiency of the cadmium-109 x-ray is 38.0%.

X-Ray Proportional Counting

Iron-55 (half life = 2.9 years) is measured using an internal gas flow proportional counter with 10% methane and 90% argon as the counting gas. The background of the detector is reduced to approximately 1 cpm by an anti-coincidence guard and 4 inches of lead shielding. The iron-55, with the iron carrier, is plated onto a disk and is placed 1/4 inch from the thin window of the proportional counter. The 6.4 Kev x-rays produced by electron capture are critically absorbed in the counting gas and the counting rate is recorded.

From a calibration of the counter with known samples of varying weights the variation of detection efficiency as a function of sample weight is established, permitting assaying of samples of unknown activity. The purity of the sample is established by absorber counting with beryllium absorbers.

Isotopes, Inc.

Alpha Counting

Alpha emittors such as polonium-210 and plutonium-239 are measured using a scintillating phosphor (ZnS) coat on the face of a photomultiplier tube. The alpha emittor, plated on a disk, is placed close to the phosphor surface and the alpha radiations are detected and counted.

The 5.3 Mev alpha from polonium-210 (half life = 138 days) and the 5.2 Mev alpha from plutonium-239 (half life = 24,000 years) are assayed. As a check, alpha samples are counted with both ZnS detectors. The backgrounds are about 0.2 to 0.3 counts per minute and the counting efficiencies approximately 40 per cent for each detector.

CHAPTER 5. THE STRATOSPHERIC DISTRIBUTION OF NUCLEAR DEBRIS

By the end of the 1958-1961 test moratorium the stratosphere contained only rather low concentrations of nuclear debris from test series performed during 1958 and previous years. The concentrations in the Northern and Southern Hemispheres were approximately equal. The resumption of atmospheric testing by the Soviet Union in September 1961 resulted in the presence of high concentrations of nuclear debris in the Northern Hemisphere during the last third of 1961 and the first third of 1962. However, the stratosphere of the Southern Hemisphere continued to display mainly low concentrations of old debris.

This pattern was changed during the second third of 1962 by the resumption of atmospheric testing of nuclear weapons by the United States at Christmas Island. Debris from these tests was injected into the equatorial stratosphere, from which it gradually spread toward both poles. During the final third of 1962 atmospheric tests by the Soviet Union again injected large quantities of nuclear debris into the northern polar stratosphere producing very high concentrations of strontium-90 and of other fission products in that region. The stratospheric concentrations in the Northern Hemisphere continued to exceed those in the Southern Hemisphere throughout the first two-thirds of 1963.

In the succeeding sections of this chapter we will discuss the distribution within the Star Dust sampling corridor during 1961 to 1963 of total beta activity, of strontium-90 and other fission products, and of several "tracer" nuclides, such as rhodium-102, manganese-54 and antimony-124. While total beta activity may be used to indicate the presence of fresh debris, strontium-90 may be used as a measure of the burden of long-lived activity

from all past injections. Short-lived fission products may also be used as indicators of fresh debris and fission product ratios may be used to distinguish debris from different injections. Rhodium-102 may be used as a tracer for debris from the 1958 rocket shot Orange, and manganese-54, Iron-55, antimony-124 and several other products of neutron activation serve as tracers for debris from high yield Soviet tests during 1961 and 1962.

The Concentrations of Total Beta Activity

The mean 6 month distribution of total beta activity in the Star Dust sampling corridor for the period June-September 1961, and the mean monthly distributions from October 1961 to August 1962 are shown in Figures 16 to 27.

Because of the high specific activity of short-lived fission products, the total beta activity increases enormously when fresh debris from recent nuclear tests is injected into the stratosphere. High concentrations of fresh debris are reflected in the very high total beta activities encountered in the Star Dust sampling corridor during the months following the Soviet tests of late 1961 (Figures 16,17 and 18), the United States tests of mid-1962 (Figures 20,21 and 22), and the Soviet tests of late 1962 (Figures 22,23,23 and 25). On the other hand, as the stratospheric debris ages and mixes with the surrounding air the total beta concentrations decrease, at first quite rapidly and then more slowly. Such decreases are evident in the northern polar stratosphere during the first half of 1962 (Figures 18,19,20 and 21), in the tropical stratosphere during the latter half of 1962 (Figures 21,22 and 23), and in the northern polar stratosphere during 1963 (Figures 24,25,26 and 27).

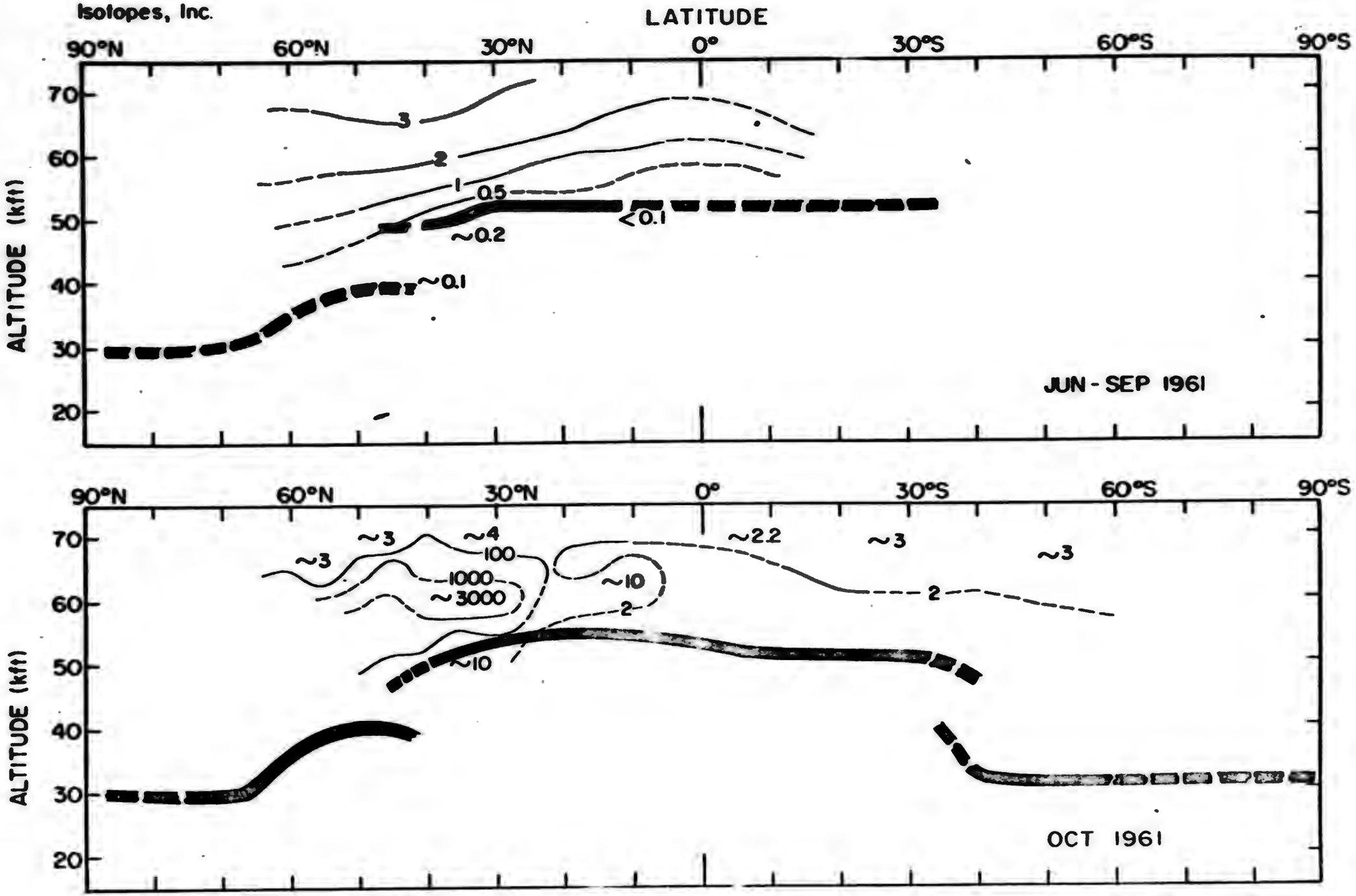

FIGURE 16 · THE MEAN DISTRIBUTION OF TOTAL BETA ACTIVITY (dpm/SCF) IN THE STAR DUST SAMPLING CORRIDOR DURING JUNE - SEPTEMBER, 1961 AND OCTOBER, 1961

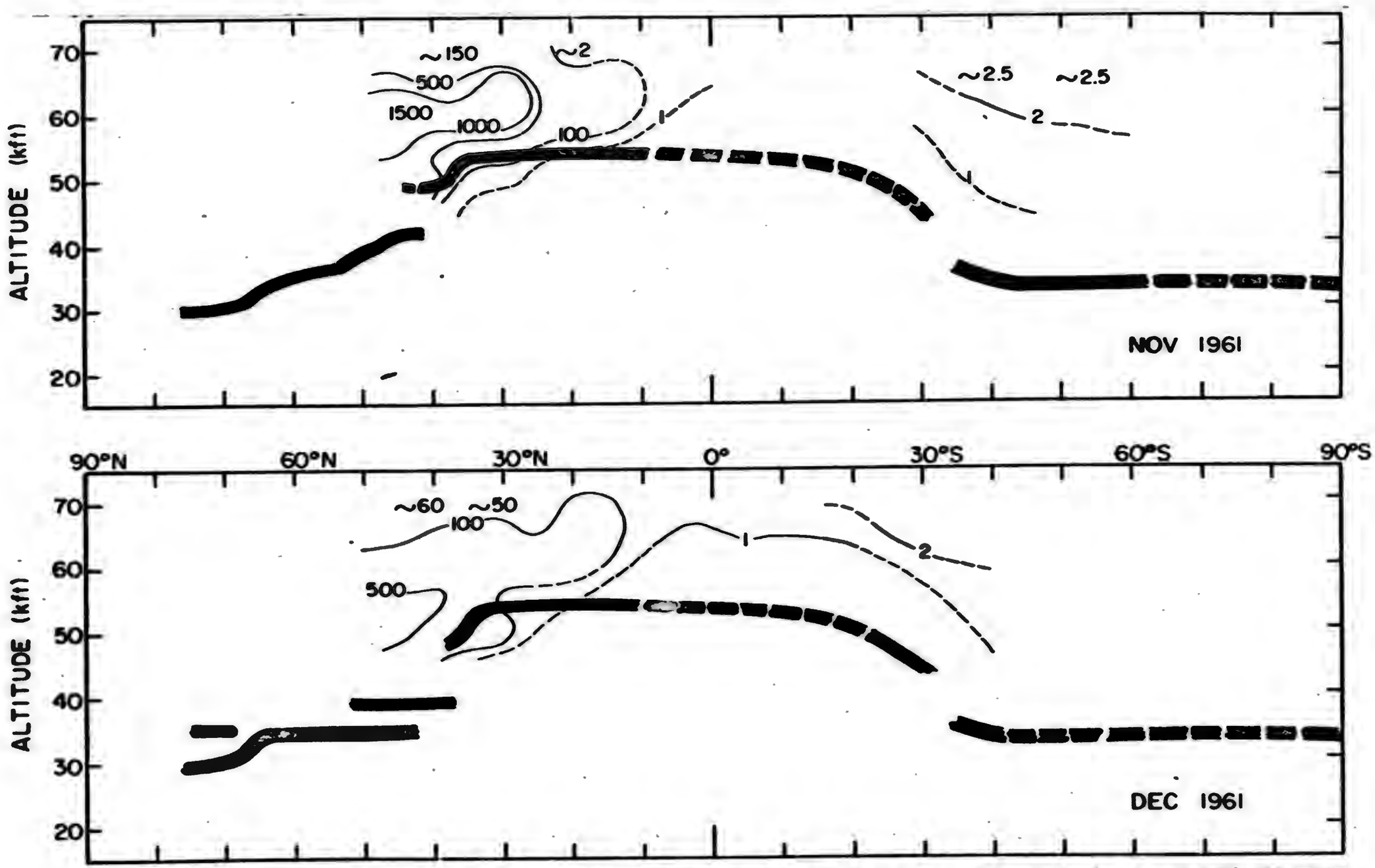

FIGURE 17 · THE MEAN DISTRIBUTION OF TOTAL BETA ACTIVITY (dpm/SCF) IN THE STAR DUST SAMPLING CORRIDOR DURING NOVEMBER AND DECEMBER, 1961

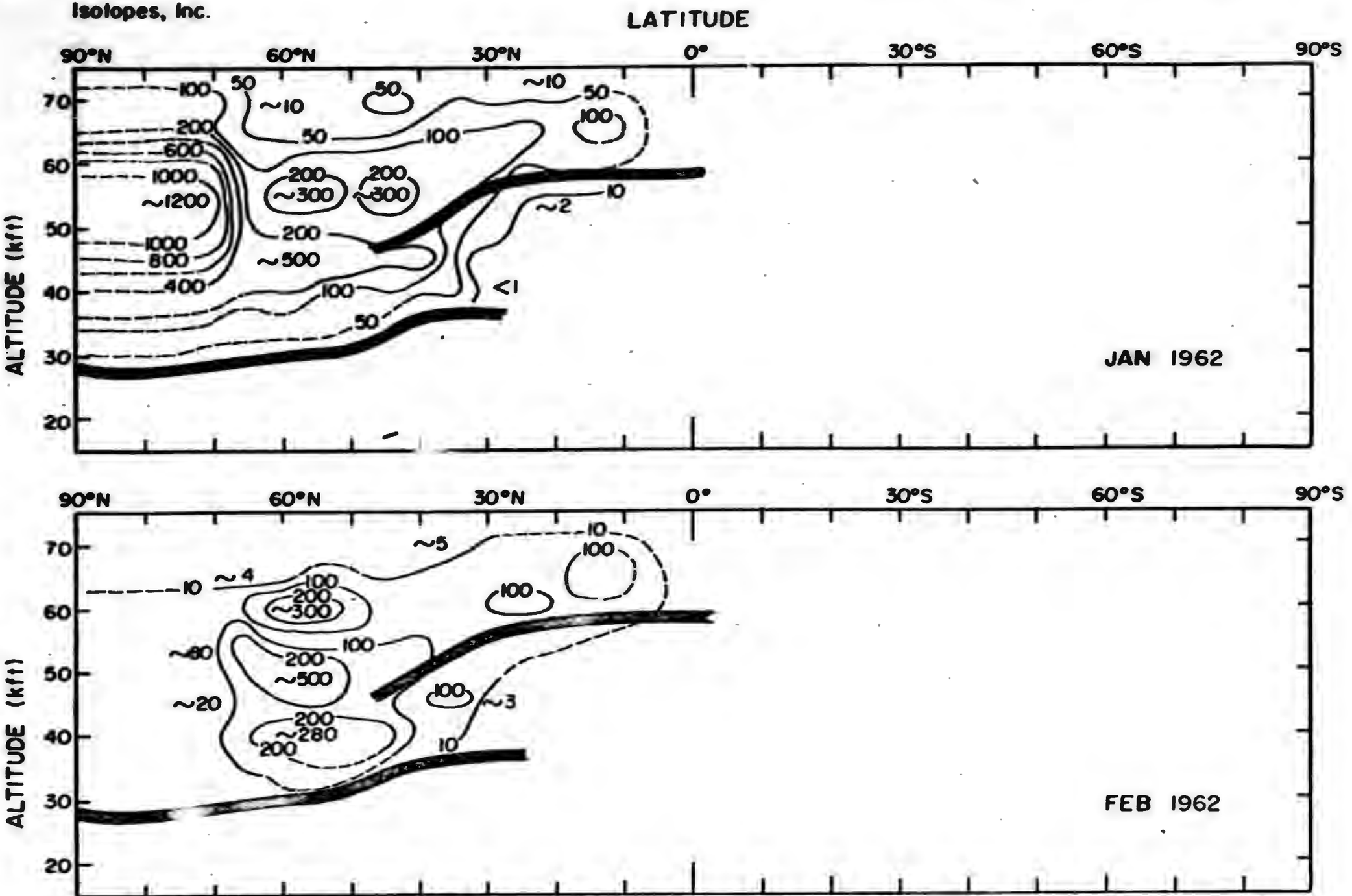

FIGURE 18 · THE MEAN DISTRIBUTION OF TOTAL BETA ACTIVITY (dpm/SCF) IN THE STAR DUST SAMPLING CORRIDOR DURING JANUARY AND FEBRUARY, 1962

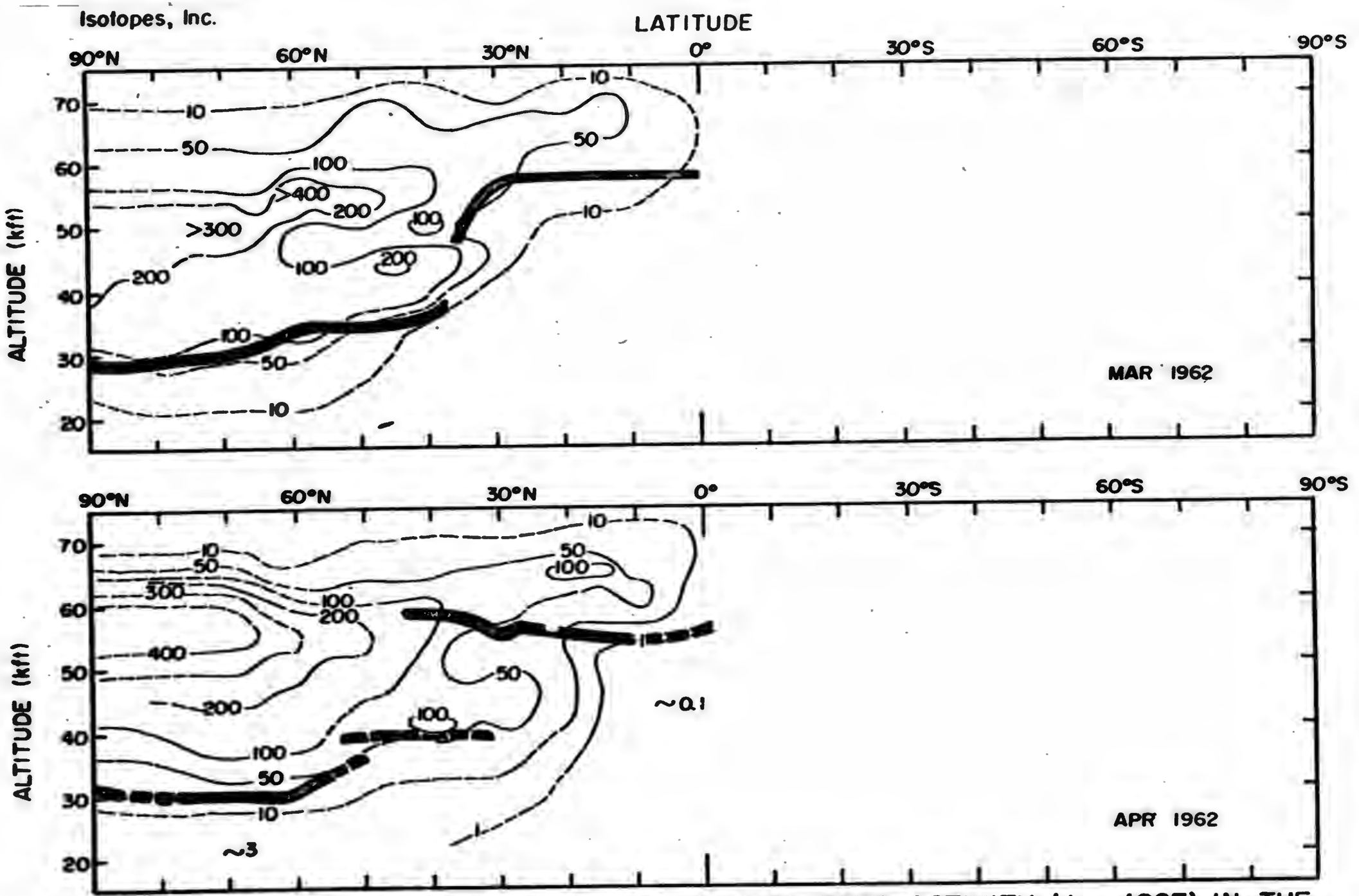

FIGURE 19 · THE MEAN DISTRIBUTION OF TOTAL BETA ACTIVITY (dpm/SCF) IN THE STAR DUST SAMPLING CORRIDOR DURING MARCH AND APRIL, 1962

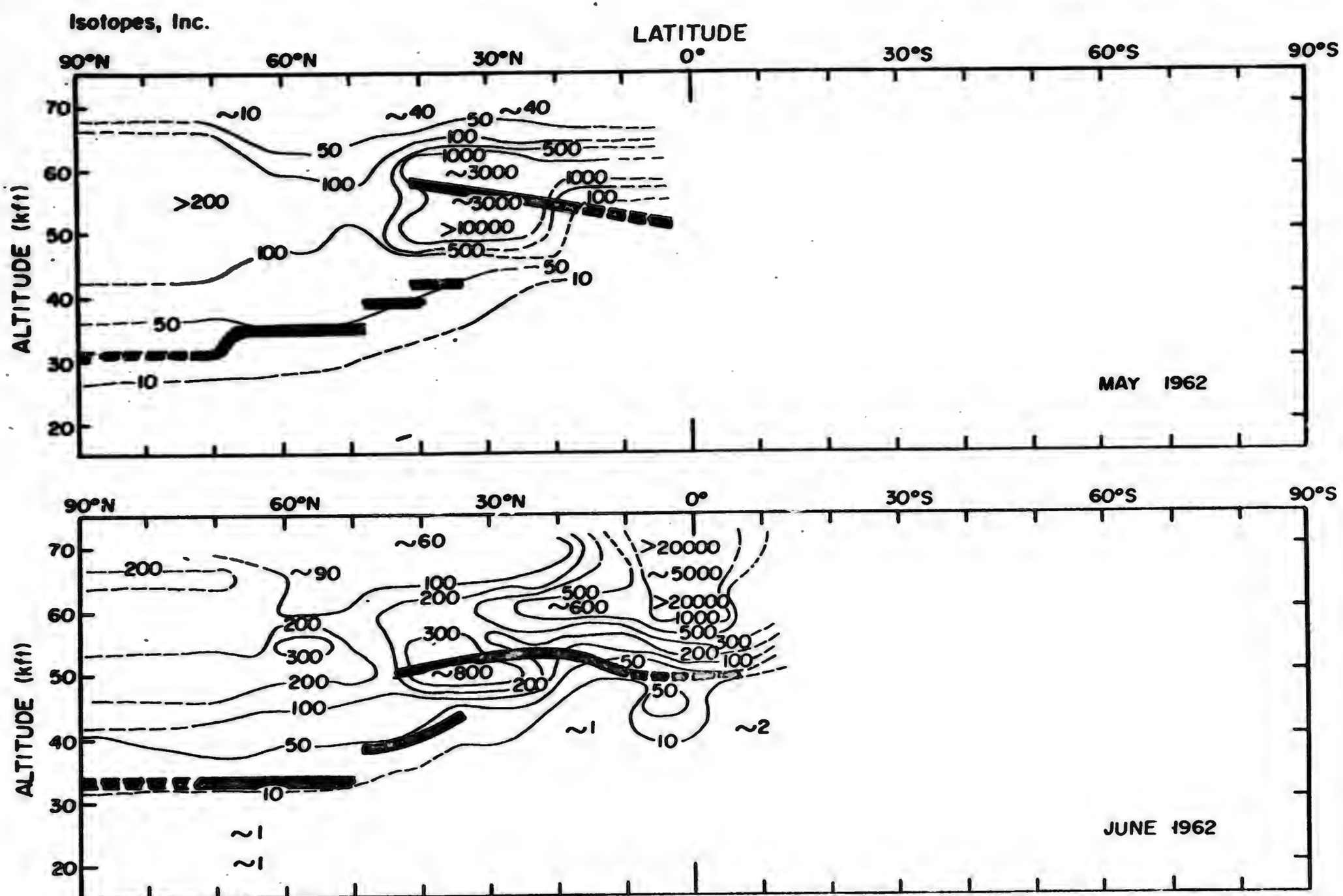

FIGURE 20 · THE MEAN DISTRIBUTION OF TOTAL BETA ACTIVITY (dpm/SCF) IN THE STAR DUST SAMPLING CORRIDOR DURING MAY AND JUNE, 1962

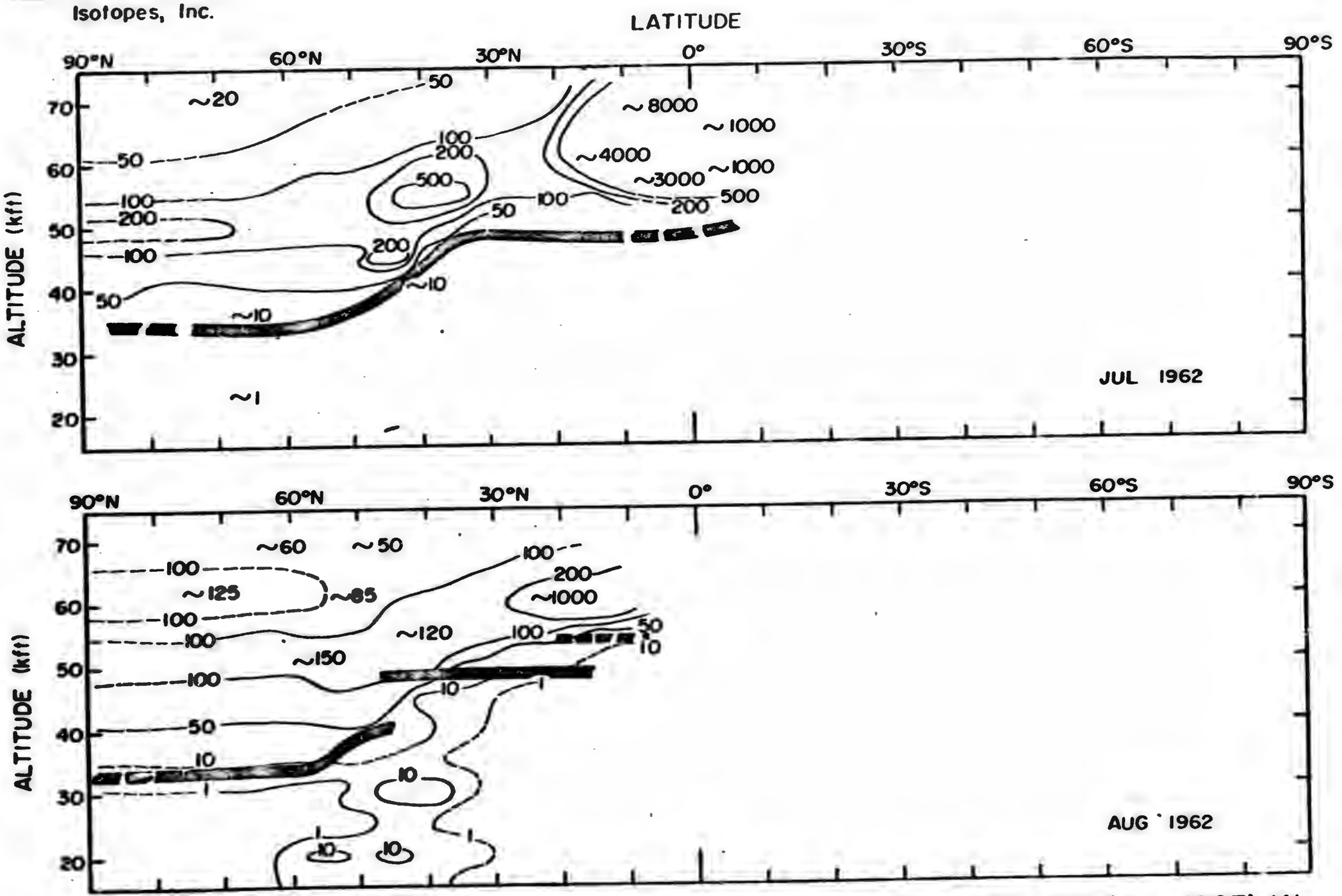

FIGURE 21. THE MEAN DISTRIBUTION OF TOTAL BETA ACTIVITY (dpm/SCF) IN THE STAR DUST SAMPLING CORRIDOR DURING JULY AND AUGUST, 1962

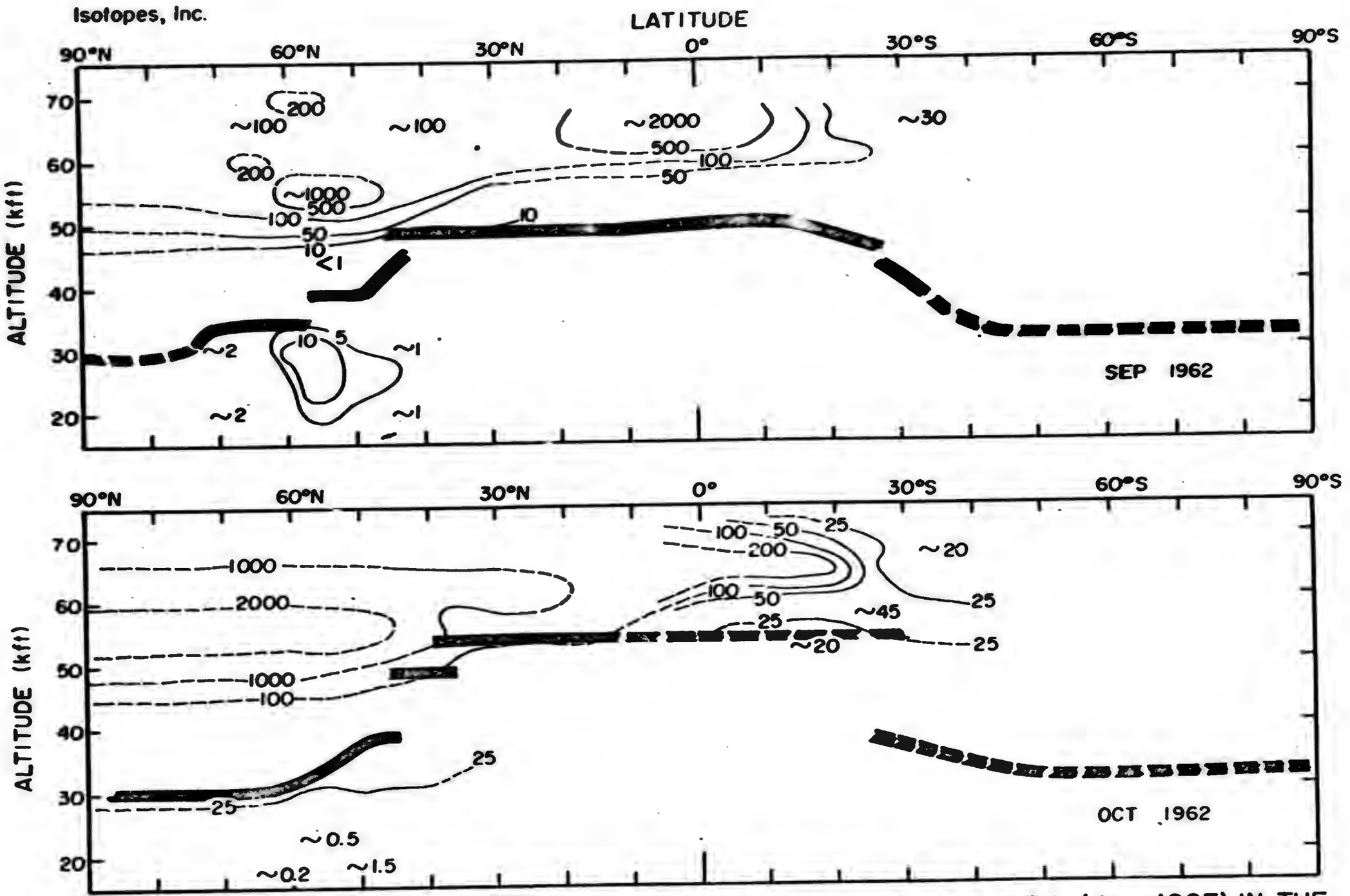

FIGURE 22 · THE MEAN DISTRIBUTION OF TOTAL BETA ACTIVITY (dpm/SCF) IN THE STAR DUST SAMPLING CORRIDOR DURING SEPTEMBER AND OCTOBER, 1962

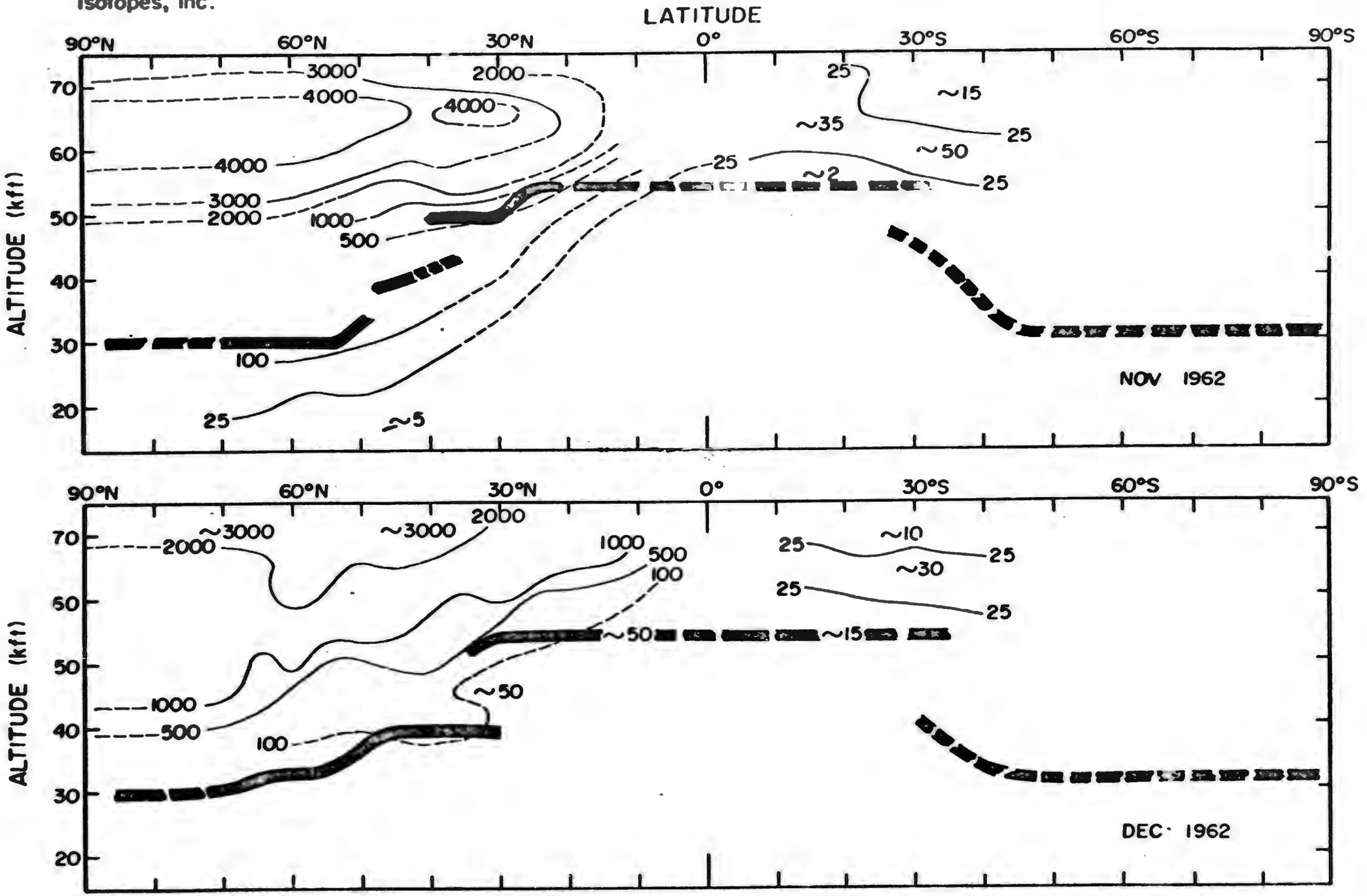

FIGURE 23· THE MEAN DISTRIBUTION OF TOTAL BETA ACTIVITY (dpm/SCF) IN THE STAR DUST SAMPLING CORRIDOR DURING NOVEMBER AND DECEMBER 1962

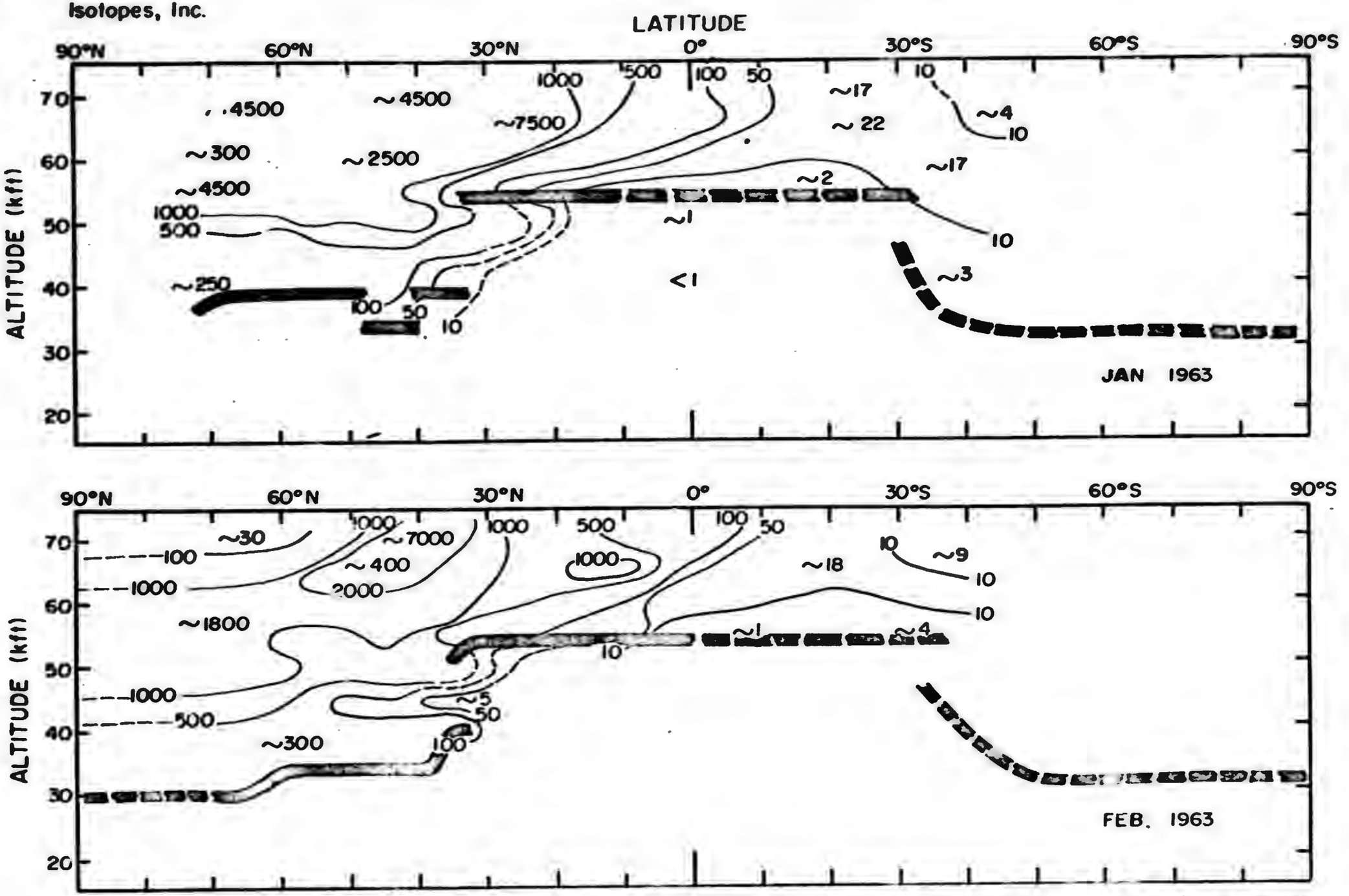

FIGURE 24 · THE MEAN DISTRIBUTION OF TOTAL BETA ACTIVITY (dpm/SCF) IN THE STAR DUST SAMPLING CORRIDOR DURING JANUARY AND FEBRUARY, 1963

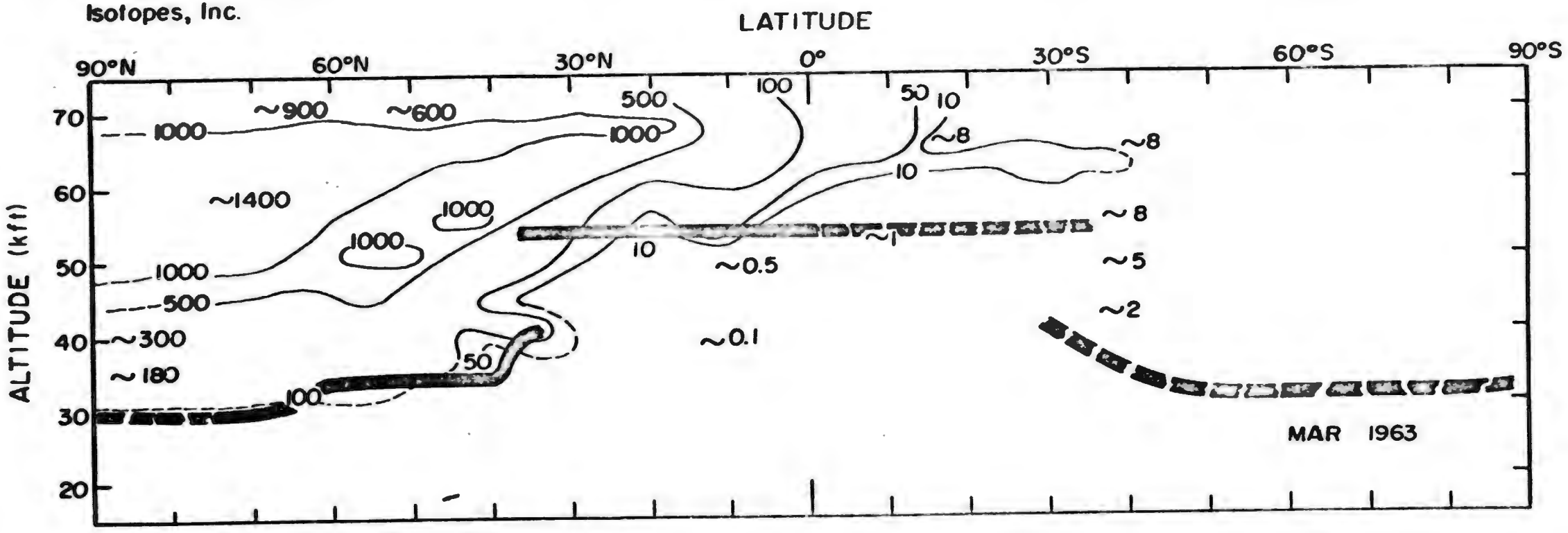

FIGURE 25. THE MEAN DISTRIBUTION OF TOTAL BETA ACTIVITY (dpm/SCF) IN THE STAR DUST SAMPLING CORRIDOR DURING MARCH AND APRIL, 1963

Isotopes, Inc

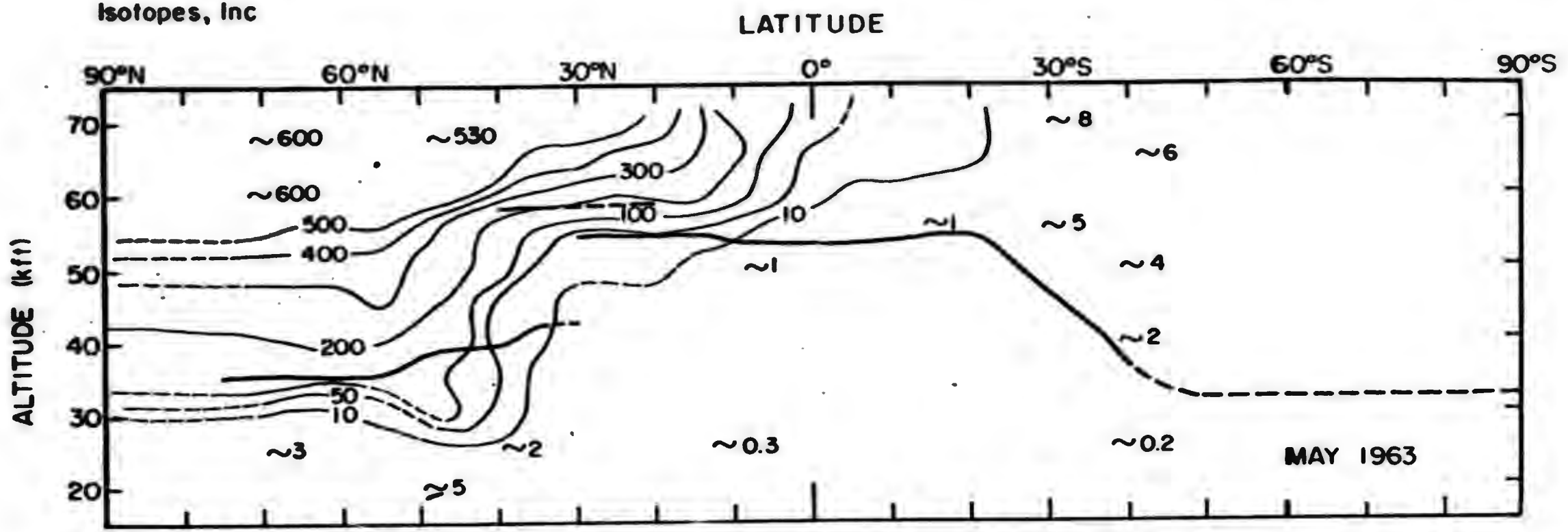

FIGURE 26 · THE MEAN DISTRIBUTION OF TOTAL BETA ACTIVITY (dpm/SCF) IN THE STAR DUST SAMPLING CORRIDOR DURING MAY AND JUNE, 1963

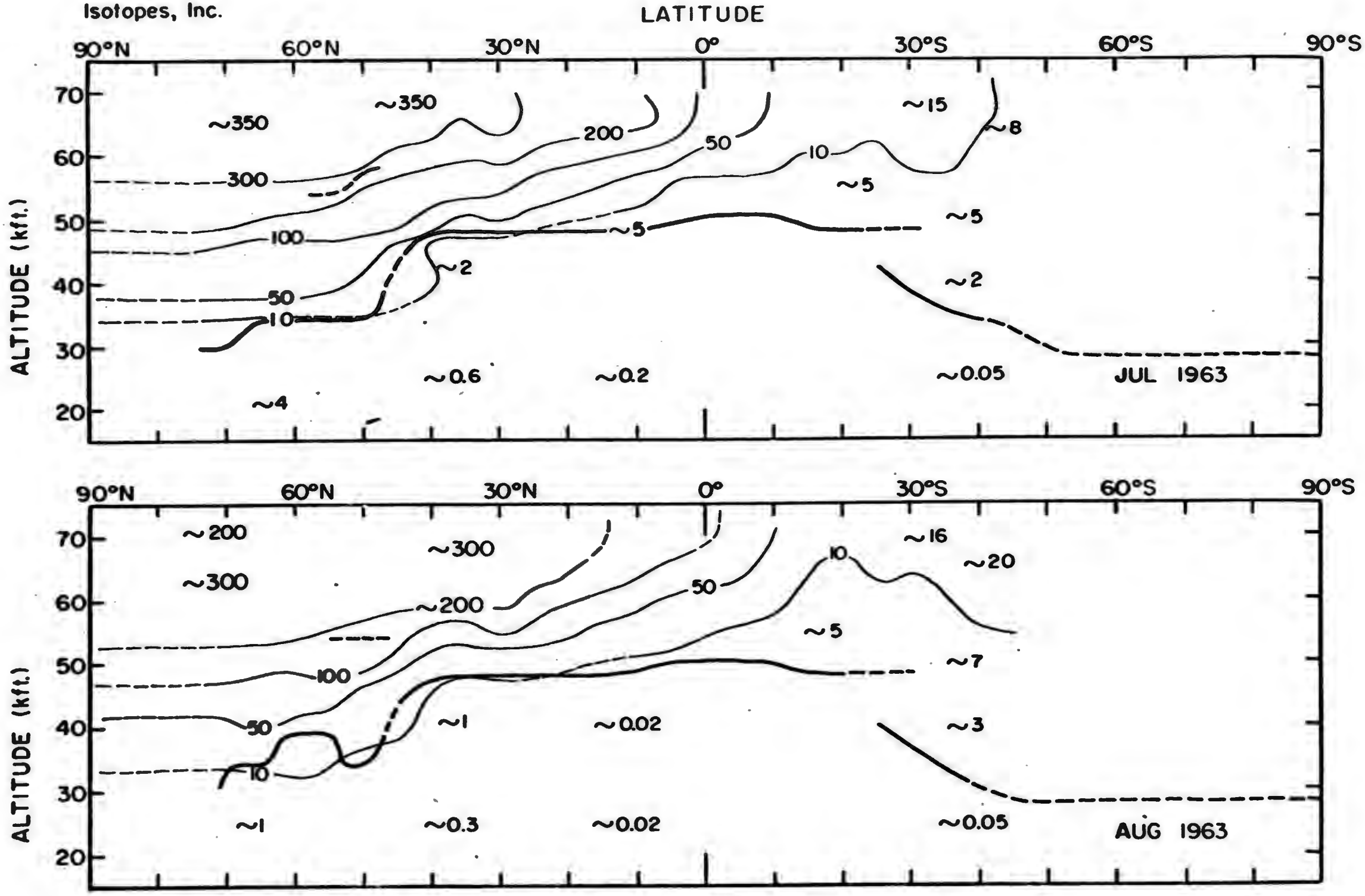

FIGURE 27· THE MEAN DISTRIBUTION OF TOTAL BETA ACTIVITY (dpm/SCF) IN THE STAR DUST SAMPLING CORRIDOR DURING JULY AND AUGUST, 1963

The Concentrations of Short-Lived Fission Products

During the periods of weapon testing, when fresh debris has been encountered by Star Dust missions, several short-lived fission products have been added to the scheme of analysis of the filter samples. These have included barium-140, iodine-131 and molybdenum-99. The distributions of these nuclides indicate the distribution of the fresh debris, but they are useful especially for determining the apparent age of the youngest component of the sampled debris.

Figures 28 and 29 show the distributions of barium-140 in the Star Dust sampling corridor during mid-1962, when debris from the United States tests at Christmas Island was being intercepted. The similarity of the patterns of these distributions to those of the total beta activity during these months (Figures 20 and 21) is not unexpected. The barium-140 data, like the total beta data, suggest that in the layer between 45 and 55 thousand feet the debris injected at low latitudes show rapid movement toward the pole, but in the layer between 60 and 65 thousand feet it shows only relatively slow poleward movement.

The distributions of barium-140 during December 1962 to March 1963, when debris from the late 1962 Soviet tests was being intercepted, are shown in Figures 30 and 31. The general pattern of these distributions resembles that of the total beta activity during these months (Figures 23, 24 and 25). During December 1962 to February 1963 barium-140 activities encountered at 25° to 50°N often exceeded those encountered poleward of 50°N, but by March 1963 the highest activities were found near the latitude of injection in the polar stratosphere. An explanation of the phenomenon may be sought in the configuration of the polar night circulation and in

the changes which occurred in this circulation during the first few months of 1963.

It is noteworthy that while fresh debris moving poleward from an equatorial injection is most likely to be encountered at about 50 thousand feet at 30°N (Figures 28 and 29), fresh debris moving equatorward from a polar injection appears more likely to be encountered at 60 thousand feet or higher at 30°N (Figures 30 and 31, and also Figures 16,17 and 18). This could indicate the existence of an organized circulation affecting the movement of debris in the vicinity of the tropopause gap. An attempt is being made in the development of the Star Dust model to introduce terms for a limited circulation which will duplicate these observations.

If two or more relatively short-lived fission products are measured in a sample, the fission product ratios may be used to calculate the apparent age of the youngest component of nuclear debris contained in the sample. The fission product ratios in the sample are compared with those expected in nuclear debris at the time of its production.[30] If all of the debris in the sample were from a single event and it were unfractionated, any fission product ratio could be used. The greatest precision would be obtained, however, by using the ratio between a short-lived nuclide and a long-lived nuclide, since this ratio would change rapidly with time. In practice we are limited in our choice of nuclides by the necessity that the short-lived nuclides still be present in the samples in measurable quantities when they are received for analysis. Molybdenum-99 (half life=2.75 days) and iodine-131 (half life=8.0° days) have been used successfully for age determinations of Star Dust samples, but even they have been measurable in only a fraction of

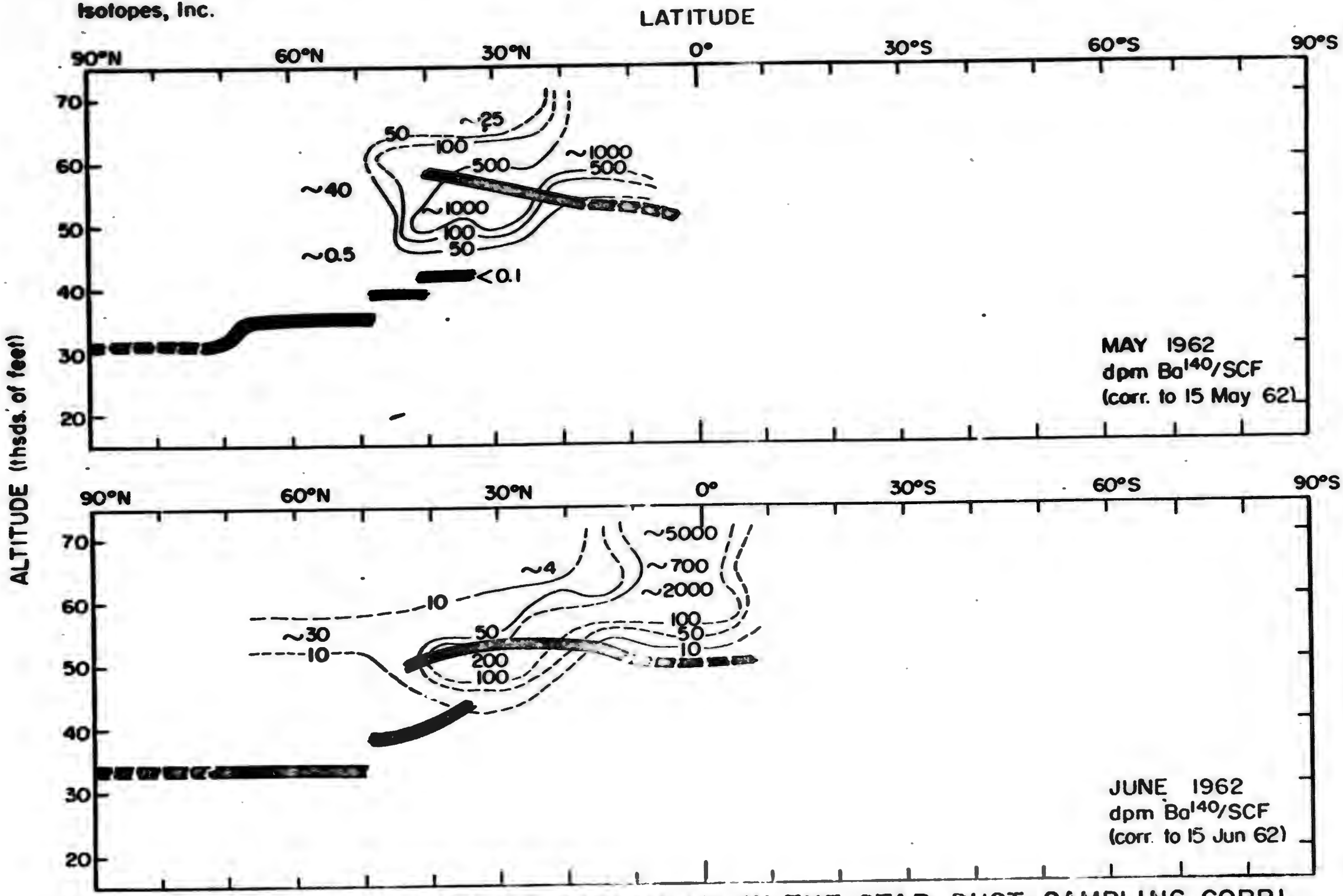

FIGURE 28 · DISTRIBUTION OF BARIUM-140 IN THE STAR DUST SAMPLING CORRIDOR, MAY AND JUNE 1962

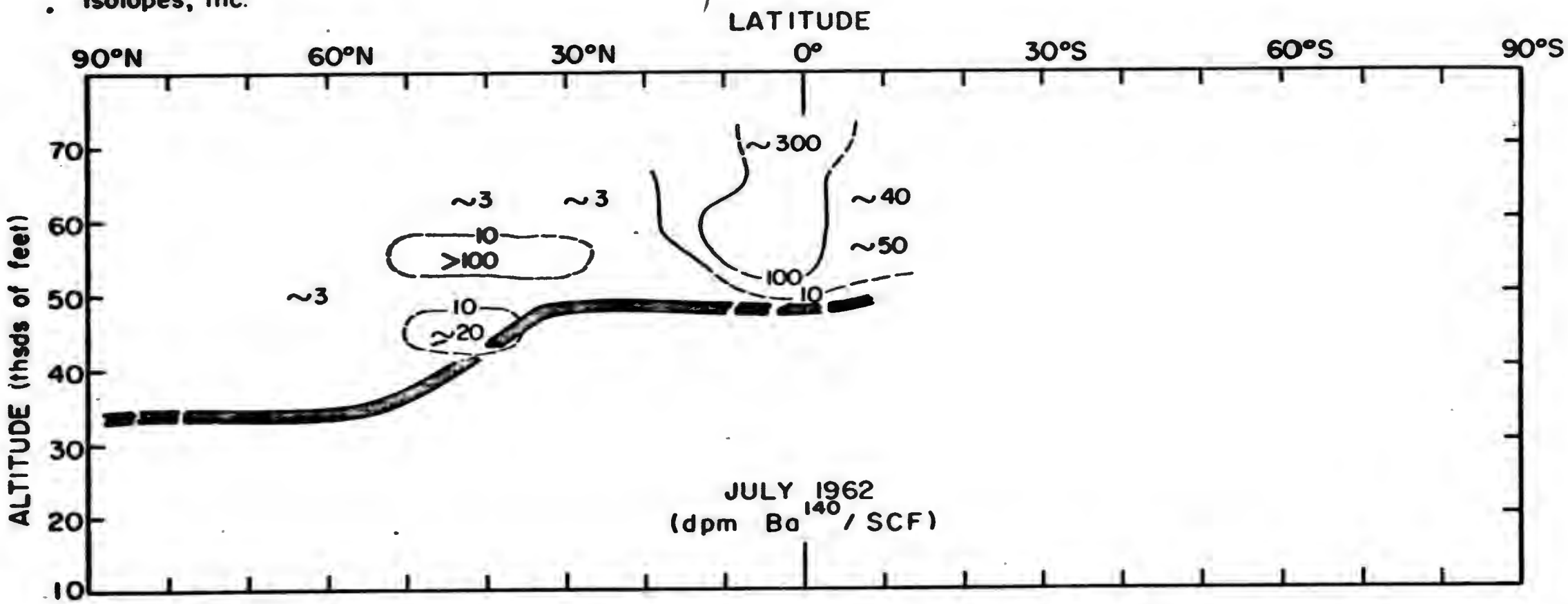

FIGURE 29· DISTRIBUTION OF BARIUM-140 IN THE STAR DUST SAMPLING CORRIDOR, JULY 1962

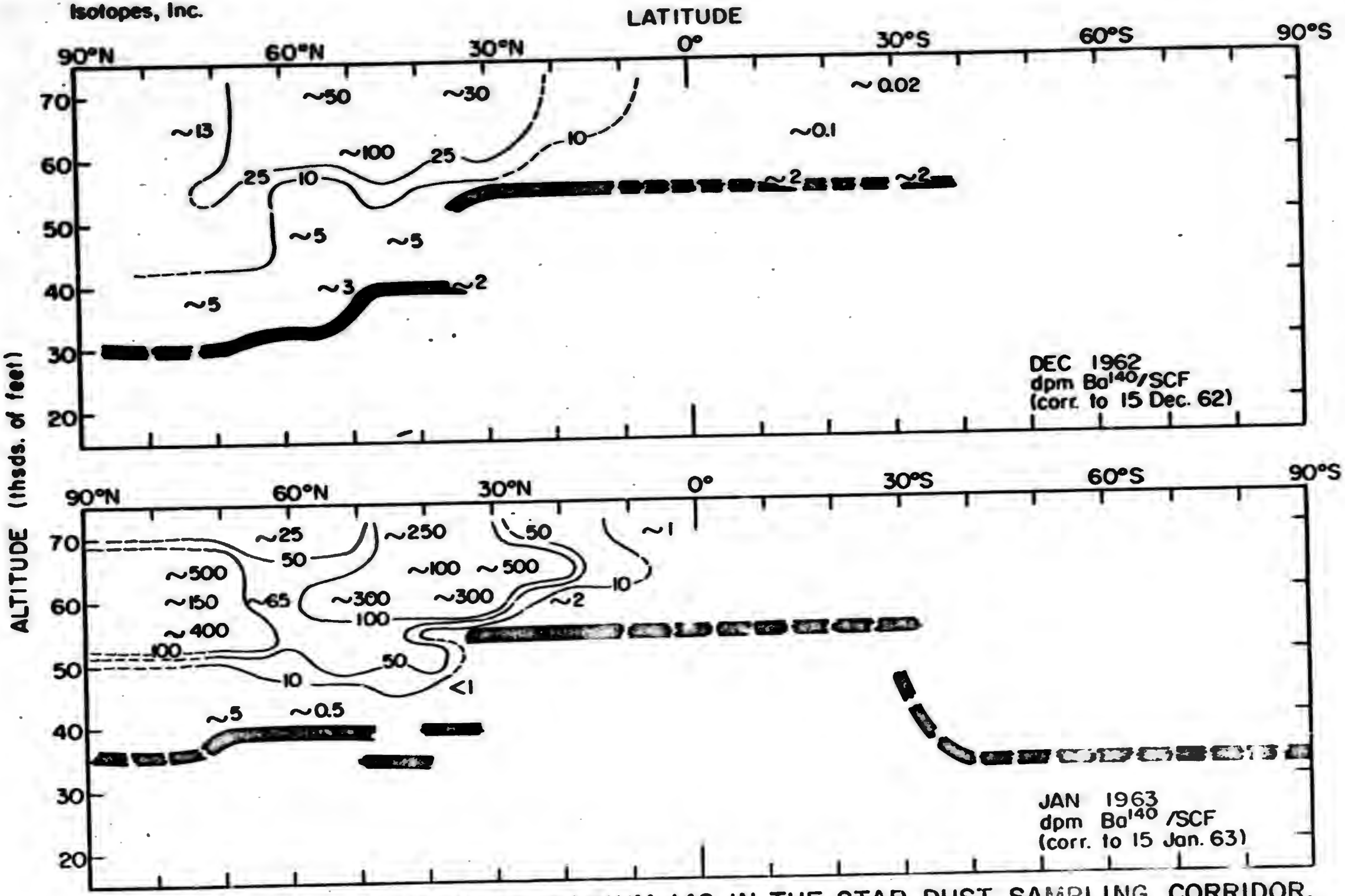

FIGURE 30 · DISTRIBUTION OF BARIUM-140 IN THE STAR DUST SAMPLING CORRIDOR, DECEMBER 1962 AND JANUARY 1963

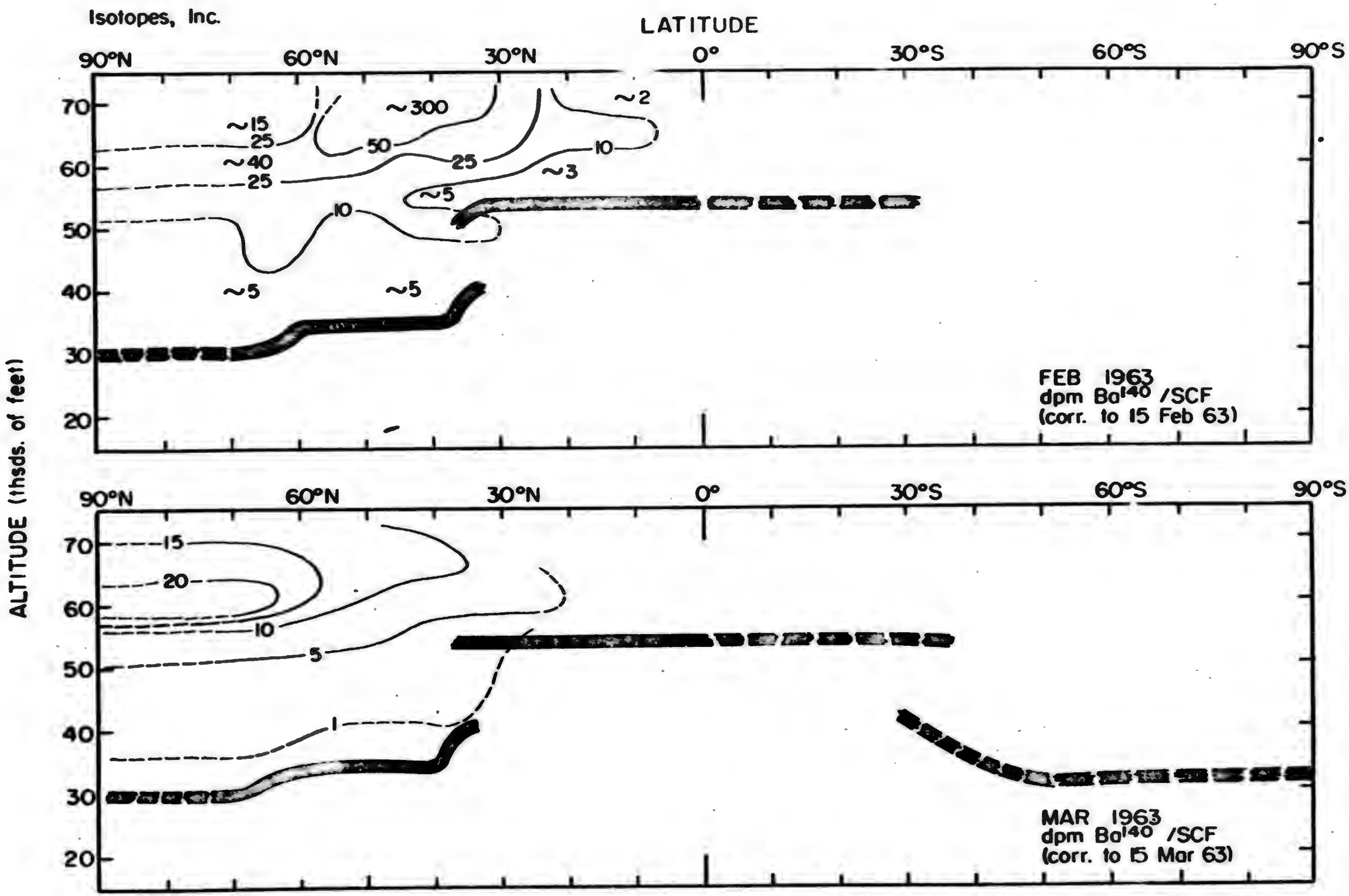

FIGURE 31· DISTRIBUTION OF BARIUM-140 IN THE STAR DUST SAMPLING CORRIDOR, FEBRUARY AND MARCH 1963

the samples in which they have been sought. The choice of the long-lived nuclide is limited by the necessity that virtually all of it in the sample should have originated in the event being dated. This criterion limits the usefulness of strontium-90, cerium-144 and other nuclides which tend to be present in the stratosphere in significant quantities as a "background" from past test series. During late 1961, following the 34 month test moratorium, the "background" of cerium-144 (half life=285 days) was negligible. On the other hand, during January and February 1963 when we were intercepting fresh debris from the December 1962 Soviet tests, the "background" of even zirconium-95 (half life=65 days) and strontium-89 (half life=50.5 days) were high enough to limit their usefulness.

Some examples of the results of calculating the apparent age of debris in Star Dust samples are given in Tables 12 to 14. Data for three samples collected during early May 1962 are shown in Table 12. Differences in apparent age indicated by the various nuclide ratios are attributable mainly to fractionation of the debris and to analytical errors, since the samples were all collected in the atmospheric layer beneath the tropical tropopause (but above the polar tropopause) where the "background" of older debris is not especially great and should not significantly affect the ratios used. This fresh debris was attributed to the 4 May 1962 intermediate yield shot at Christmas Island [31], both on the basis of the data in Table 12 and on the basis of trajectories calculated by the United States Weather Bureau[32].

Data for a series of samples collected during late June and early July 1962 are given in Table 13. Some of the variations in apparent age of these samples probably result from the presence in the samples of debris

from more than one of the events during the mid-1962 United States test series as well as debris from the 1961 Soviet test series. Effects due to fractionation of the debris and to analytical errors are no doubt also present. Since events of intermediate or low-megaton yield took place on the 8th, 9th, 10th, 12th, 15th, 17th and 22nd of June 1962 [31], there is a good deal of uncertainty involved in the assignment of the debris to the specific events. It would appear, however, that fresh debris from two or more events (probably from June 8th or 9th, from June 15th, and possibly from June 17th) is represented.

Molybdenum-99 was measured in three samples collected during early January 1963. The calculated apparent ages, given in Table 14, show fair agreement with an assigned shot date of 24 December 1962, the date of the only megaton events in the December 1962 Soviet test series [31]. The "background" of debris from the earlier Soviet tests was so high that all ratios in Table 14 are doubtlessly affected.

Despite that limitations on the use of fission product ratios for dating nuclear debris, the information obtained is usually extremely valuable. The data permit us to estimate rates of movement and of dilution of clouds of fresh debris, and to identify the sources represented.

Isotopes, Inc.

Table 12. Apparent Age of Fresh Debris Intercepted During Early May 1962

Sample	Collection Date	Latitude	Longitude	Altitude (K ft)	Activity (dpm/SCF) Total B	Activity (dpm/SCF) Ba^{140}	Nuclide Ratios	Apparent Age (days)	Apparent Shot Date
SF-644	8 May 1962	31°/37°N	101°/104°W	51	26,900	1,320	Mo^{99}/Ce^{144}=51.9	3	5 May 1962
							Mo^{99}/Zr^{95} =10.8	4	4 May 1962
							Mo^{99}/Ce^{141}= 6.22	4	4 May 1962
							Mo^{99}/Ba^{140}= 3.22	2	6 May 1962
SF-645	8 May 1962	38°/43°N	104°/108°W	50	56,100	3,100	Mo^{99}/Ce^{144}=39.1	5	3 May 1962
							Mo^{99}/Zr^{95} = 8.43	5	3 May 1962
							Mo^{99}/Ce^{141}= 5.54	4	4 May 1962
							Mo^{99}/Ba^{140}= 2.66	3	5 May 1962
							I^{131}/Sr^{89} = 5.93	2	6 May 1962
							I^{131}/Ba^{140}= 1.71	-	-
SF-647	10 May 1962	30°N	100°W	50	33,200	6,920	Mo^{99}/Ce^{144}=22.8	7	3 May 1962
							Mo^{99}/Zr^{95} = 3.77	8	2 May 1962
							Mo^{99}/Ce^{141}= 2.40	8	2 May 1962
							Mo^{99}/Ba^{140}= 0.39	13	27 Apr 1962

Isotopes, Inc.

Table 13. Apparent Ages of Fresh Debris Intercepted During Late June and Early July 1962

Sample	Collection Date	Latitude	Longitude	Altitude (K ft)	Activity (dpm/SCF) Total B	Activity (dpm/SCF) Ba^{140}	Nuclide Ratios	Apparent Age (days)	Apparent Shot Date
SF-676	19 Jun 1962	$36^{o}/44^{o}N$	$103^{o}/109^{o}W$	50	1,480	293	Mo^{99}/Ce^{144} = 11.4	9	10 Jun 1962
							Mo^{99}/Zr^{95} = 1.82	11	8 Jun 1962
							Mo^{99}/Ce^{141} = 1.29	11	8 Jun 1962
							Mo^{99}/Ba^{140} = 0.19	16	3 Jun 1962
							Mo^{99}/I^{131} = 1.40	9	10 Jun 1962
							I^{131}/Sr^{89} = 1.48	21	29 May 1962
SF-680	22 Jun 1962	$30^{o}N$	$100^{o}W$	51	753	146	Mo^{99}/Ce^{144} = 4.38	13	9 Jun 1962
							Mo^{99}/Zr^{95} = 1.52	12	10 Jun 1962
							Mo^{99}/Ce^{141} = 0.78	13	9 Jun 1962
							Mo^{99}/Ba^{140} = 0.12	19	3 Jun 1962
							Mo^{99}/I^{131} = 0.75	12	10 Jun 1962
							I^{131}/Sr^{89} = 1.63	20	2 Jun 1962
SF-683	23 Jun 1962	$2^{o}S/2^{o}N$	$81^{o}/79^{o}W$	60	23,200	1,580	Mo^{99}/Ce^{144} = 16.0	8	15 Jun 1962
							Mo^{99}/Zr^{95} = 3.07	9	14 Jun 1962
							Mo^{99}/Ce^{141} = 2.24	8	15 Jun 1962
							Mo^{99}/Ba^{140} = 0.77	10	13 Jun 1962
							Mo^{99}/I^{131} = 1.49	8	15 Jun 1962
							I^{131}/Sr^{89} = 1.93	18	5 Jun 1962

Isotopes, Inc.

Table 13 (Continued)

Sample	Collection Date	Latitude	Longitude	Altitude (K ft)	Activity (dpm/SCF) Total B	Activity (dpm/SCF) Ba^{140}	Nuclide Ratios	Apparent Age (days)	Apparent Shot Date
SF-693	29 Jun 1962	4°S/2°N	82°/79°W	68	5,620	338	Mo^{99}/Ce^{144} = 2.63	15	14 Jun 1962
							Mo^{99}/Zr^{95} = 0.64	15	14 Jun 1962
							Mo^{99}/Ce^{141} = 0.54	14	15 Jun 1962
							Mo^{99}/Ba^{140} = 0.32	14	15 Jun 1962
							Mo^{99}/I^{131} = 0.74	12	17 Jun 1962
							I^{131}/Sr^{89} = 1.12	25	4 Jun 1962
SF-695	3 Jul 1962	9°/15°N	80°/83°W	60	5,460	344	Mo^{99}/Ce^{144} = 0.83	20	13 Jun 1962
							Mo^{99}/Zr^{95} = 0.23	19	14 Jun 1962
							Mo^{99}/Ce^{141} = 0.18	19	14 Jun 1962
							Mo^{99}/Ba^{140} = 0.13	18	15 Jun 1962
							Mo^{99}/I^{131} = 0.53	14	19 Jun 1962
							I^{131}/Sr^{89} = 0.47	37	27 May 1962
SF-699	3 Jul 1962	4°/10°S	82°/79°W	56	1,290	100	Mo^{99}/Ce^{144} = 2.74	15	18 Jun 1962
							Mo^{99}/Zr^{95} = 0.91	14	19 Jun 1962
							Mo^{99}/Ce^{141} = 0.47	15	18 Jun 1962
							Mo^{99}/Ba^{140} = 0.31	14	19 Jun 1962

Isotopes, Inc.

Table 14. Apparent Age of Fresh Debris Intercepted During January 1963

Sample	Collection Date	Latitude	Longitude	Altitude (K ft)	Activity (dpm/SCF) Total B	Activity (dpm/SCF) Ba^{140}	Nuclide Ratios	Apparent Age (days)	Apparent Shot Date
SF-2194	9 Jan 1963	24°/21°N	97°/96°W	65	22,600	763	Mo^{99}/Ce^{144} = 0.843	20	20 Dec 1962
							Mo^{99}/Zr^{95} = 0.302	18	22 Dec 1962
							Mo^{99}/Ba^{140} = 0.188	17	23 Dec 1962
SF-2200	11 Jan 1963	32°/37°N	100°/103°W	64	5,330	178	Mo^{99}/Ce^{144} = 0.253	25	17 Dec 1962
							Mo^{99}/Zr^{95} = 0.054	26	16 Dec 1962
							Mo^{99}/Ba^{140} = 0.130	18	24 Dec 1962
SF-2202	11 Jan 1963	37°/31°N	103°/100°W	68	2,590	122	Mo^{99}/Ce^{144} = 0.181	26	16 Dec 1962
							Mo^{99}/Zr^{95} = 0.082	24	18 Dec 1962
							Mo^{99}/Ce^{141} = 0.181	19	23 Dec 1962
							Mo^{99}/Ba^{140} = 0.121	19	23 Dec 1962

The Concentrations of Strontium-90 Activity

Because it has a relatively long radioactive half life, Strontium-90 may be used as a more or less conservative tracer for stratospheric nuclear debris. While concentrations of total beta activity or short-lived fission products are indicative of the amount of the most recent debris, concentrations of strontium-90 are indicative of the total burden from all past stratospheric injections.

The stratospheric concentrations of strontium-90 which have been found at two altitudes at each of two latitudes in the Northern Hemisphere during Projects HASP and Star Dust are shown in Figure 32. Mean bimonthly concentrations for 50 and 65 thousand feet at 65°N and for 55 and 65 thousand feet at 25°N are shown. While the 1961 Soviet test series and the 1962 United States test series resulted in large increases in the stratospheric concentrations of strontium-90, especially at 50 thousand feet in the polar stratosphere, it is evident that concentrations of unprecedented size were found within the northern polar stratosphere following the 1962 Soviet tests.

The mean distribution of strontium-90 within the Star Dust sampling corridor during June to September 1961, before our first interception of debris from the 1961 Soviet test series, and during October to December 1961 are portrayed in Figure 33. The strontium-90 distribution during June to September 1961 still resembled that which had been found in the HASP sampling corridor during early 1960, but the concentrations had decreased and the horizontal concentration gradients had become less steep . Nevertheless concentrations still increased with latitude and altitude in both hemispheres. A mean value of 34 was found for the activity ratio Ce^{144}/Sr^{90} (corrected for decay to 15 August 1958) in nuclear debris in the lower stratosphere of the Northern Hemisphere during June to September 1961. We have assumed that

the Ce^{144}/Sr^{90} ratio in debris from the 1958 rocket shots Teak and Orange[31] was approximately 47.5 on 15 August 1958 (based on fission yields reported by Hallden et al [30]), and that this ratio corrected to 15 August 1958 was approximately 23.1 in debris from other sources (based on measurements made during Project HASP). We have then calculated that nearly half of the strontium-90 present in the stratosphere of the Northern Hemisphere during June to September 1961 had been produced by the 1958 rocket shots [33].

The distributions of strontium-90 in the Star Dust sampling corridor during October to December 1961, as shown in the lower half of Figure 33, and during January to April 1962, as shown in the upper half of Figure 34, indicate the validity of two conclusions which were reached during Project HASP regarding the injection and later movement in the stratosphere of debris from Soviet weapons tests . Firstly, it would appear that Soviet debris injected into the stratosphere by weapons of megaton yield stabilizes, for the most part, at altitudes below 60 thousand feet. Secondly, it appears from the configuration of isopleths of strontium-90 concentration at 40°N to 10°N that the Soviet debris increases in altitude as it moves equatorward (whereas debris from tropical injections decreases in altitude as it moves poleward [34]). It is evident also from these distributions that while debris injected at high latitudes may be spread laterally quite rapidly within the polar stratosphere, its transport through the tropical stratosphere is rather slow.

In the lower half of Figure 34 is shown the distribution of strontium-90 in the Star Dust sampling corridor during May to August 1962. High concentrations of strontium-90 resulting from the mid-1962 United States weapons tests at Christmas Island appear to be mainly restricted to

the tropical stratosphere, although it appears that in the layer between 45 and 55 thousand feet some of this debris had moved into the northern polar stratosphere. The highest concentrations of strontium-90 in the northern polar stratosphere at this time were found in the layer between 45 and 60 thousand feet, as they had been during January to April 1962. While a small fraction of the strontium-90 in this layer had been contributed by the 1962 United States injections, most was a residue from the 1961 Soviet injections. (In the following section of this chapter we will discuss the use of fission product ratios to calculate the contributions to the stratospheric burden by the 1961 Soviet tests and the 1962 United States tests.)

The distributions of strontium-90 during September to October 1962 and November to December 1962 are portrayed in Figure 35. During most of the final third of 1962 the altitude coverage in the Star Dust sampling corridor was rather limited, so that the representativeness of the data which were used to construct Figure 35 might be questioned. Since a series of high yield devices was tested by the Soviet Union during this period and fresh debris was passing through the sampling corridor, there is, of course, no guarantee that better coverage in the corridor would have produced data which was substantially more representative of the mean distribution of strontium-90 in the whole stratosphere. There is an indication in the cross-section for November to December 1962 that, outside of the equatorial region, the stratospheric strontium-90 concentrations in the Northern Hemisphere were at least ten times as high as those in the Southern Hemisphere. This appears to be correct, for the cross-section for January to April 1963 (Figure 36) shows the same situation.

Isotopes, Inc.

During the first third of 1963 the Star Dust sampling program was again expanded to provide good altitude and latitude coverage. Thus the strontium-90 distribution shown in Figure 36 should, at least in its general outlines, be representative of the whole stratosphere.

If we assume that debris from the 1962 United States test series was distributed evenly between the Northern and Southern Hemispheres because it was injected into the equatorial stratosphere, we may assume that the difference in strontium-90 concentrations between the Northern Hemisphere and the Southern represents debris produced by the 1961 and 1962 Soviet tests. If this is true it is evident that in the northern polar stratosphere during January to April 1963 the strontium-90 concentration attributable to these tests exceeded 2000 dpm/1000SCF at altitudes above 50 thousand feet, and exceeded 200 dpm/1000SCF even in the vicinity of the tropopause. In the northern tropical stratosphere also, excess concentrations of strontium-90 attributable to the Soviet tests ranged from a few hundred to 2000 dpm/1000SCF. Never before during either Project HASP or Project Star Dust had such high concentrations been found except when fresh debris was intercepted within a few weeks following its production.

Isotopes, Inc.

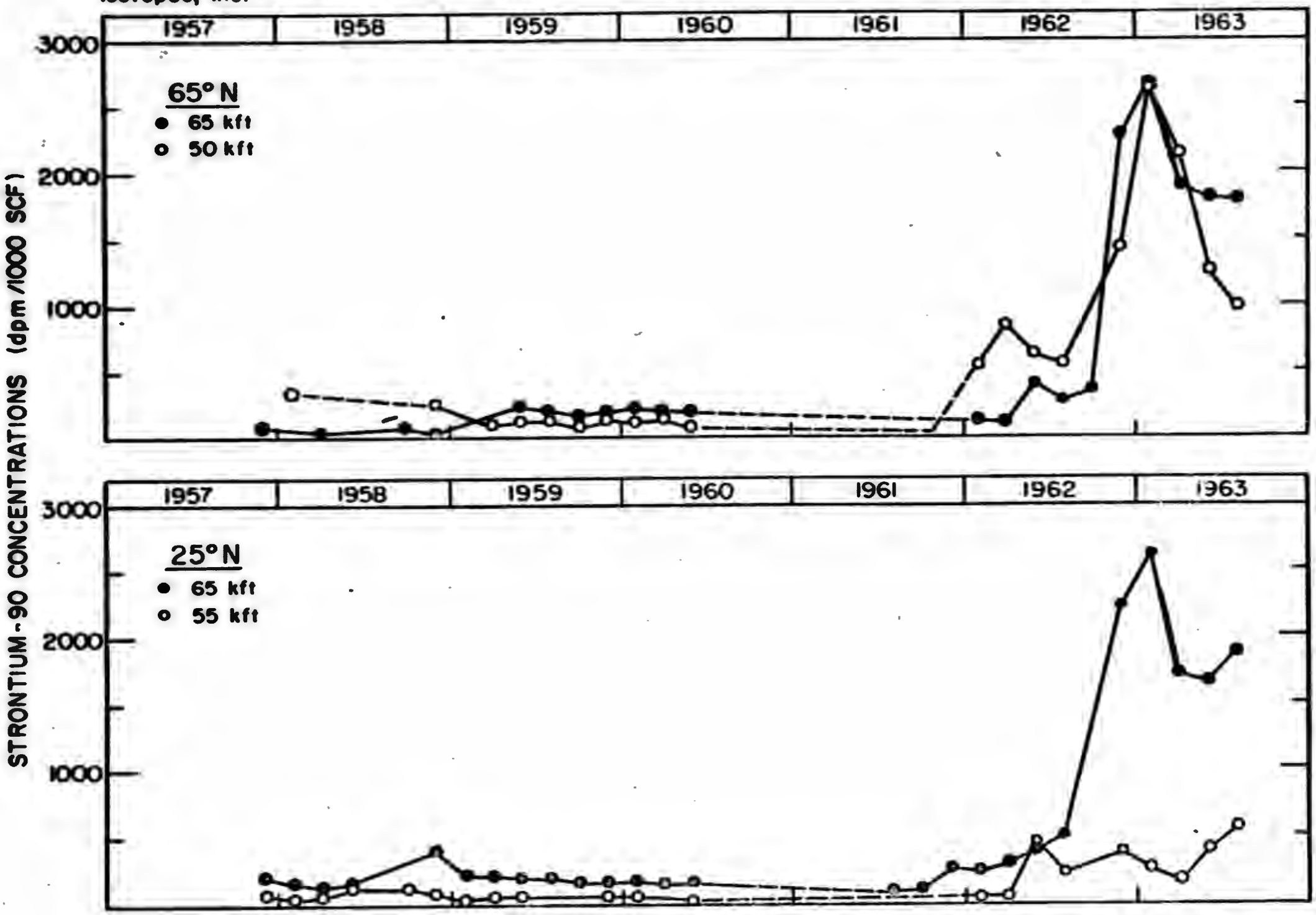

FIGURE 32 · VARIATION WITH TIME OF STRONTIUM-90 CONCENTRATIONS AT 65°N AND 25°N

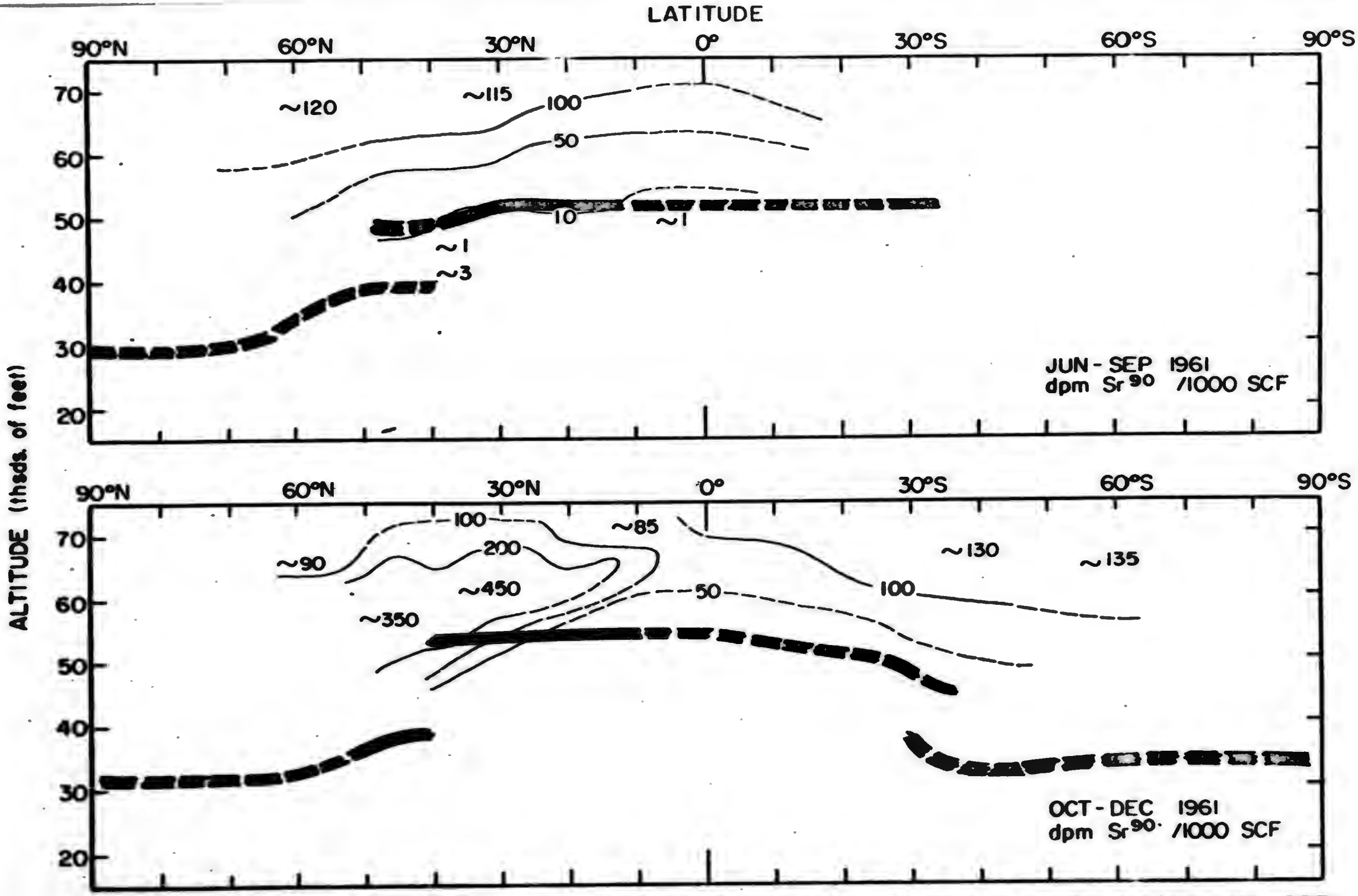

FIGURE 33. DISTRIBUTION OF STRONTIUM-90 IN THE STAR DUST SAMPLING CORRIDOR DURING JUNE-SEPTEMBER 1961 AND OCTOBER-DECEMBER 1961

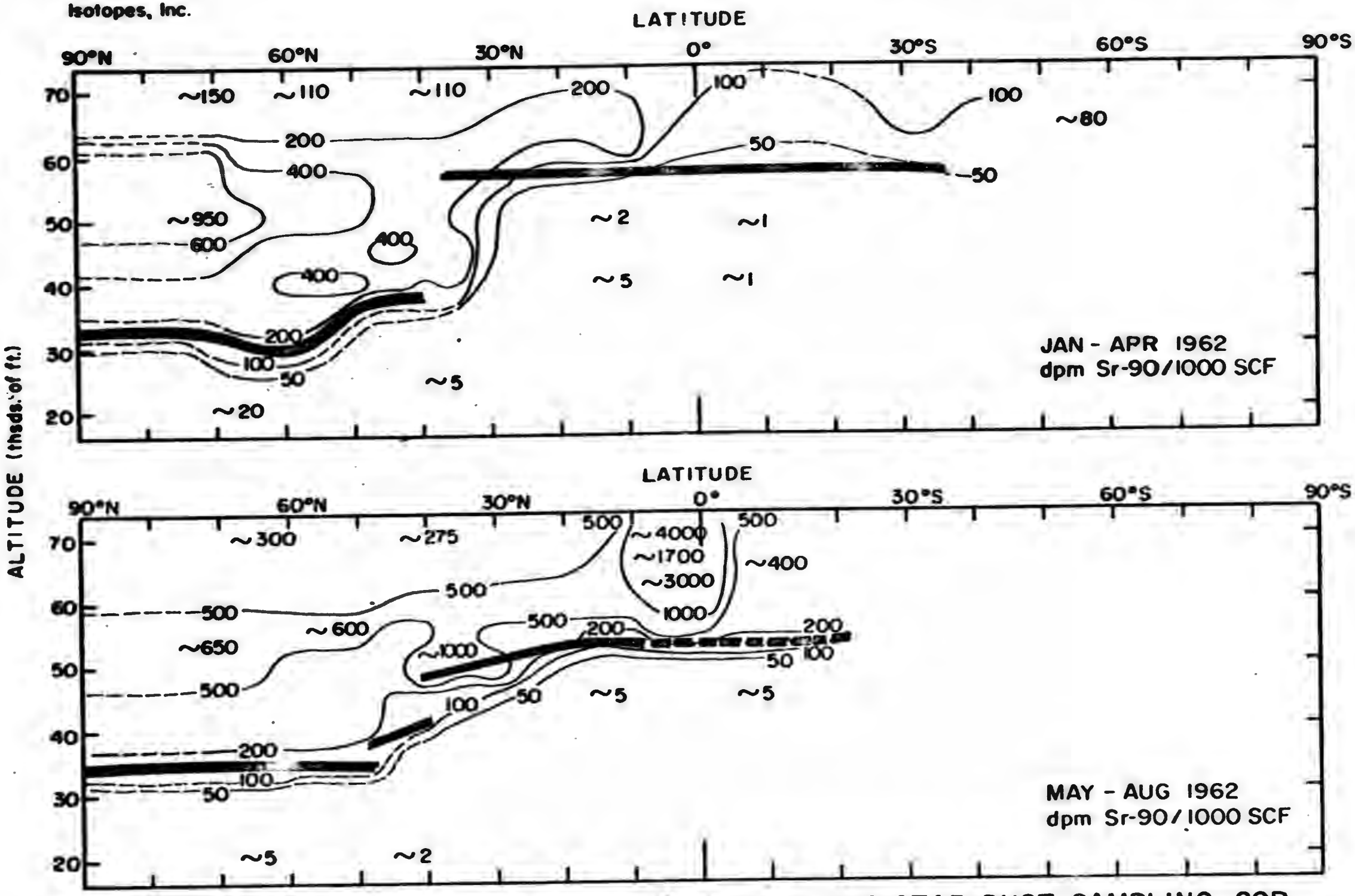

FIGURE 34 · DISTRIBUTION OF STRONTIUM-90 IN THE STAR DUST SAMPLING CORRIDOR, JAN TO APR AND MAY TO OCT 1962

Isotopes, Inc.

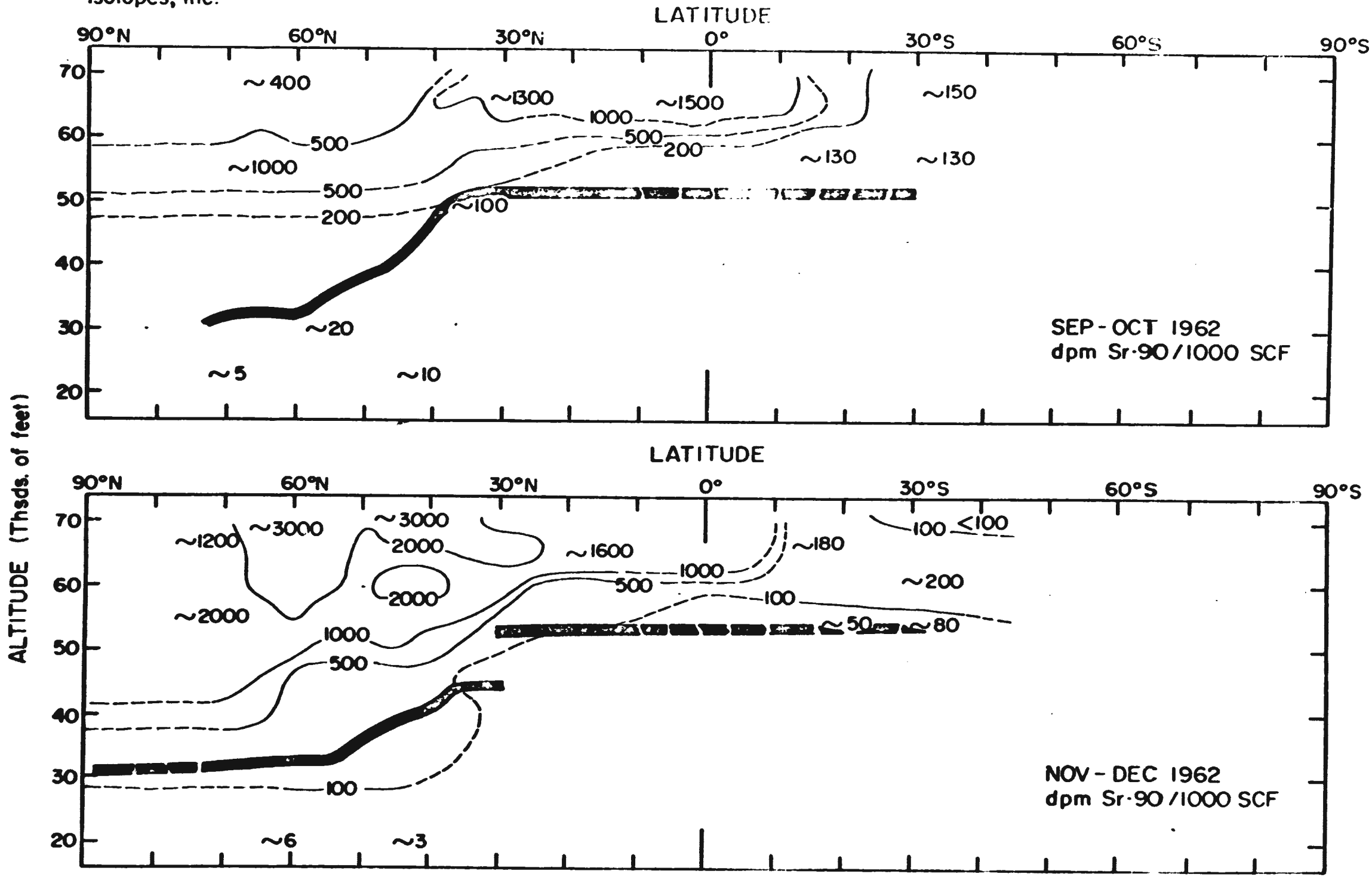

FIGURE 35· DISTRIBUTION OF STRONTIUM-90 IN THE STAR DUST SAMPLING CORRIDOR DURING SEPTEMBER-OCTOBER AND NOVEMBER-DECEMBER 1962

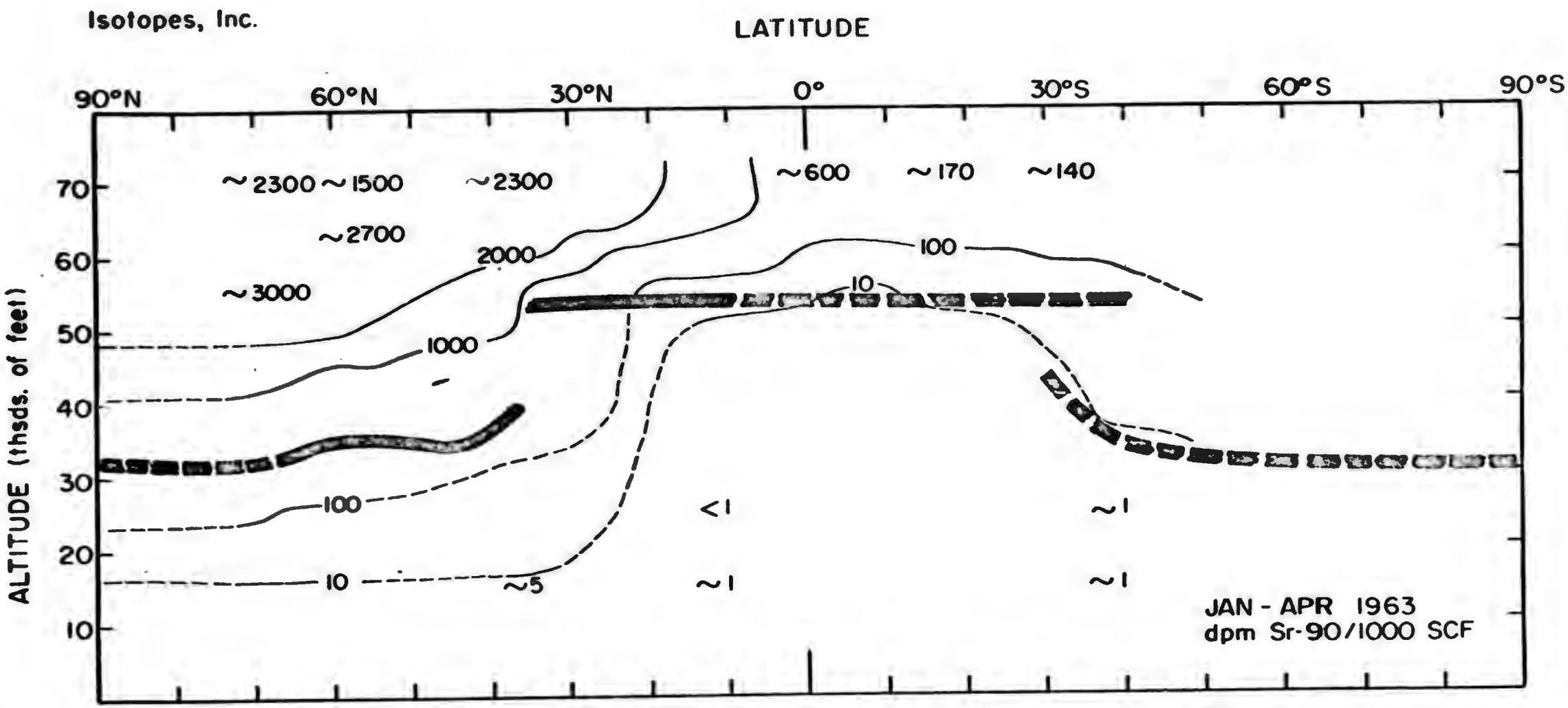

FIGURE 36 · DISTRIBUTION OF STRONTIUM-90 IN THE STAR DUST SAMPLING CORRIDOR DURING JANUARY - APRIL, 1963

Isotopes, Inc.

The Stratospheric Burden of Strontium-90

The stratospheric distributions of strontium-90 shown in Figures 33 to 36 have been used as the basis for calculating the stratospheric burden of strontium-90. Data from the Atomic Energy Commission's balloon sampling program[35] have been used to extrapolate the Star Dust data to altitudes above 100 thousand feet. Additional data from WU-2 sampling during 1961 have been used to extrapolate Star Dust data for 1961 to high northern latitudes[36]. The results of the burden calculations are summarized in Table 15.

The estimated maximum errors given with the calculated burdens are based mainly upon our judgment of the adequacy of sampling during the intervals covered. They are largely subjective, but they should be realistic if the assumptions made in extrapolating the Star Dust data to unsampled regions are approximately correct. The most important of these assumptions is that the concentrations of debris from low altitude detonations decrease with increasing altitude from approximately 100 thousand feet (the highest altitude reached by the balloon sampling) to the top of the atmosphere, and that within the polar stratosphere, at least from 45° to 90°, there is only a slight change in the concentration of debris as a function of latitude at any one altitude. Thus far we have seen no evidence that these assumptions are not generally true.

The burdens in the Southern Hemisphere during June-September 1961, and May-August 1962, when there was no Star Dust sampling of the Southern Hemisphere, are based on the burden calculated for the succeeding months when there was sampling. Similarly, the data for succeeding months have been used to supplement the limited amount of Star Dust measurements of the

strontium-90 concentrations in the northern polar stratosphere during October-December 1961.

In the previous section we discussed the use of the fission product ratio Ce^{144}/Sr^{90} to divide the stratospheric burden of strontium-90 in the Northern Hemisphere during mid-1961 into two components, one attributable to the 1958 rocket shots Teak and Orange and the other attributable to other pre-1961 weapons tests. A similar calculation was used to divide the strontium-90 burden of the Southern Hemisphere stratosphere during October-December 1961 into the same two components. The reliability of this calculation was limited by the scarcity of Star Dust data for the Southern Hemisphere and by some uncertainty in the value of the Ce^{144}/Sr^{90} ratio in non-rocket shot debris in the southern polar stratosphere.

The division of the January-April 1962 burden into a component attributable to pre-1961 weapons tests and a component attributable to the 1961 Soviet tests has been based on the Sr^{89}/Sr^{90} and Ce^{144}/Sr^{90} ratios found in Star Dust samples collected during the first third of 1962. We have assumed that the Sr^{89}/Sr^{90} ratio in debris from the Soviet tests, corrected for decay to 15 October 1961, would equal 176, the ratio in fresh debris [37], and that this ratio in all other debris, corrected to the same date, would equal zero. The calculated distributions of Soviet strontium-90 and of strontium-90 from pre-1961 weapons tests are shown in Figure 37. We have performed an alternative calculation assuming that the Ce^{144}/Sr^{90} ratio in the Soviet debris, corrected for decay to 15 October 1961, would equal 47.5 and that this ratio in all other debris, corrected to the same date, would equal 2.0. The strontium-90 distributions obtained from this calculation are portrayed in Figure 38. The January-April 1962 strontium-90

burden given in Table 15 may be calculated either from the distributions given in Figure 37 or from those given in Figure 38.

The main limitation on the accuracy of these calculations is the probability that debris from the 1961 Soviet tests was not yet well mixed in the northern polar stratosphere during January-April 1962. In addition, the frequency of sampling during this period was less than would be needed to assure that the samples collected were completely representative of the debris in the sampling corridor. Nevertheless there is adequate reason to believe that the calculated burdens are approximately correct, for the distribution of strontium-90 found in the northern polar stratosphere during the second quarter of 1962 is quite similar to that found there during the first quarter.

We have employed the same principle which was used to calculate the distributions of strontium-90 shown in Figures 37 and 38 to distinguish between debris from the 1962 United States tests and older debris present in the Star Dust sampling corridor during May-August 1962. Because testing was continuing during this period and successive injections of fresh debris continually changed the nuclide ratios in the stratospheric debris, the assumptions used in the calculation were somewhat more complicated and considerably less reliable than those used to divide the January-April 1962 strontium-90 burden into its components.

We have assumed a value of 146 on shot date for the Sr^{89}/Sr^{90} ratio in debris from the 1962 United States tests[30]. The following assumed shot dates have then been used: 1 May 1962 for samples collected during May 1962; 15 May 1962 for samples collected during June 1962; 15 June 1962 for samples collected during July 1962; 1 July 1962 for samples collected

during August 1962. All pre-1962 debris was assumed to have had a Sr^{89}/Sr^{90} ratio of 146 on an assigned shot date of 15 October 1961. This last assumption, of course, has greater validity when applied to samples collected in the lower northern polar stratosphere than when applied to samples collected elsewhere in the stratosphere.

The results of this calculation are shown in Figure 39. (They have been modified in the equatorial stratosphere at 0° and 5°N where the calculation attributed all debris to the 1962 tests. Interpolated values bases on data at 10°N and farther north and at 5°S and farther south have been substituted in this region.) The approximate correctness of the calculation is suggested by the correspondence of the distribution of "pre-1962" strontium-90 during May-August 1962, as indicated in Figure 39, to the distribution of strontium-90 during January-April 1962, as indicated in Figure 34. The distributions shown in Figure 39 have been used to calculate the stratospheric burdens of strontium-90 during May-August 1962 which are included in Table 15. The burden from "pre-1962 debris" agrees well enough with the total burden for January-April 1962. The calculated burden from "1962 U.S. debris" is, as has been mentioned above, especially subject to error because of the difficulty of obtaining representative sampling while the test series was still in progress.

The same difficulty applies to the burdens calculated for September-October 1962 and November-December 1962. In addition these calculations are based on relatively sparse sampling at all altitudes except 55 thousand feet. Thus the calculated burdens for both of these bimonthly periods are especially subject to error. Unless there is something fundamentally wrong with our assumptions, however, the actual errors in the

calculated burdens should not exceed the estimated errors given in Table 15.

The calculated burden for January-April 1963 should be relatively accurate since atmospheric weapons tests had ceased by the end of December 1962. However, it would appear from the measurements of barium-140 in Star Dust samples (Figures 30 and 31) that debris from the December 1962 Soviet tests was still unevenly distributed within the northern polar stratosphere before March 1963. The same conclusion may be obtained based on the antimony-124 data which are described in a following section of this chapter. Indeed, the rapid decrease after January-February 1963 in the strontium-90 concentrations encountered at 65°N and 25°N (Figure 32) must be attributed to dilution of debris from the late 1962 Soviet tests by mixing with uncontaminated air, probably following the breakdown of the polar night circulation. In spite of these limitations the estimated burden for January-April 1963 which is given in Table 15 should be approximately correct.

It is planned that in a later Star Dust report the stratospheric burdens which are summarized in Table 15 will be recalculated using improved assumptions and more complete data, and an attempt will be made to calculate the contribution by the 1962 Soviet tests to the January-April 1963 stratospheric strontium-90 burden.

Table 15. Apparent Stratospheric Burdens of Strontium-90 (in Megacuries) During 1961 to 1963

	Northern Hemisphere	Southern Hemisphere	Total
June-September 1961			
1958 Rocket Shot Debris	0.18 ± 0.09	-	-
Debris from other sources	0.19 ± 0.10	-	-
	0.37 ± 0.13	~0.5	~0.9
October-December 1961			
1958 Rocket Shot Debris	-	0.19 ± 0.10	-
Debris from other sources	-	0.28 ± 0.14	-
	~1.6	0.47 ± 0.17	~2.1
January-April 1962			
Pre 1961 Debris	0.4 ± 0.1	0.4 ± 0.1	0.8 ± 0.1
1961 Soviet Debris	1.2 ± 0.3	< 0.01	1.2 ± 0.3
	1.6 ± 0.3	0.4 ± 0.1	2.0 ± 0.3
May-August 1962			
Pre 1962 Debris	1.5 ± 0.3	-	-
1962 U.S. Debris	1.0 ± 0.4	-	-
	2.5 + 0.5	~1.0	~3.5
September-October 1962			
TOTAL	2.2 ± 0.7	1.0 ± 0.3	3.2 ± 0.8
November-December 1962			
TOTAL	5.6 ± 1.9	0.8 ± 0.3	6.4 ± 1.9
January-April 1963			
TOTAL	6.7 ± 1.7	0.7 ± 0.3	7.4 ± 1.7

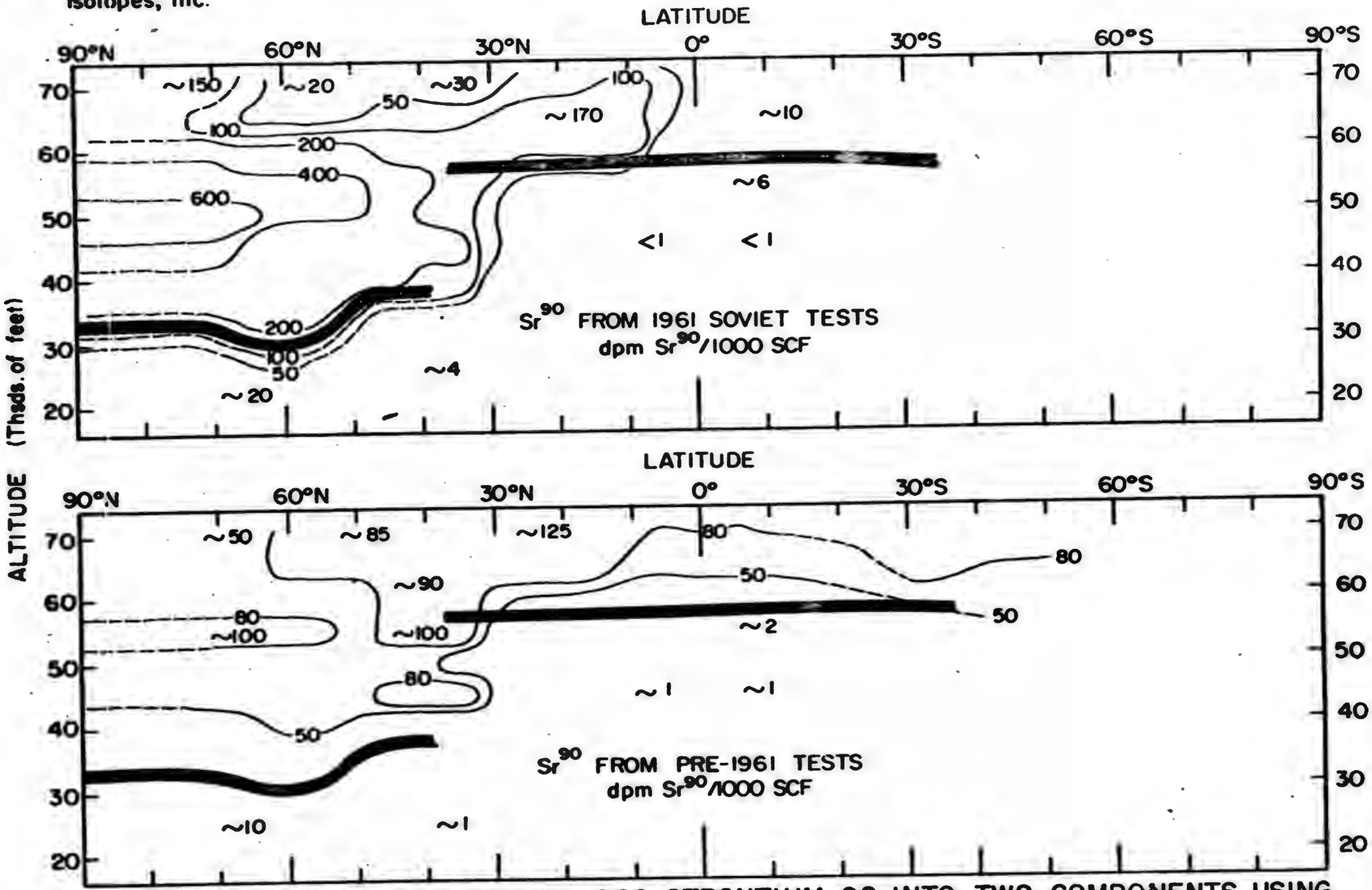

FIGURE 37· DIVISION OF JAN-APR 1962 STRONTIUM-90 INTO TWO COMPONENTS USING THE RATIO Sr-89/Sr-90 (WITH Sr-89/Sr-90 = 176 ON 15 OCT 1961 IN SOVIET DEBRIS)

Isotopes, Inc.

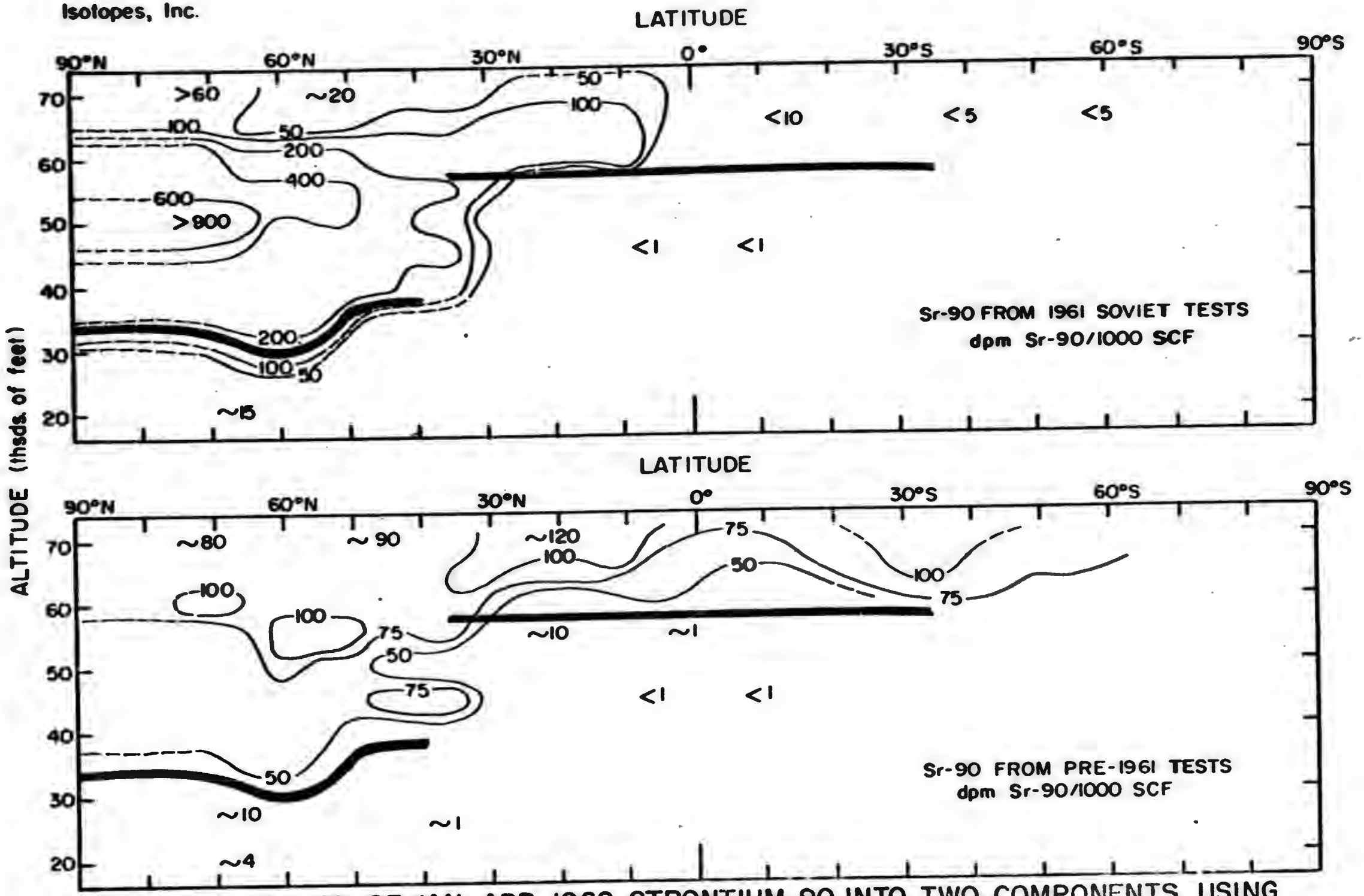

FIGURE 38·DIVISION OF JAN-APR 1962 STRONTIUM-90 INTO TWO COMPONENTS USING Ce-144 / Sr-90 (WITH Ce-144/Sr-90 = 47.5 ON 15 OCT 1961 IN SOVIET DEBRIS)

Isotopes, Inc.

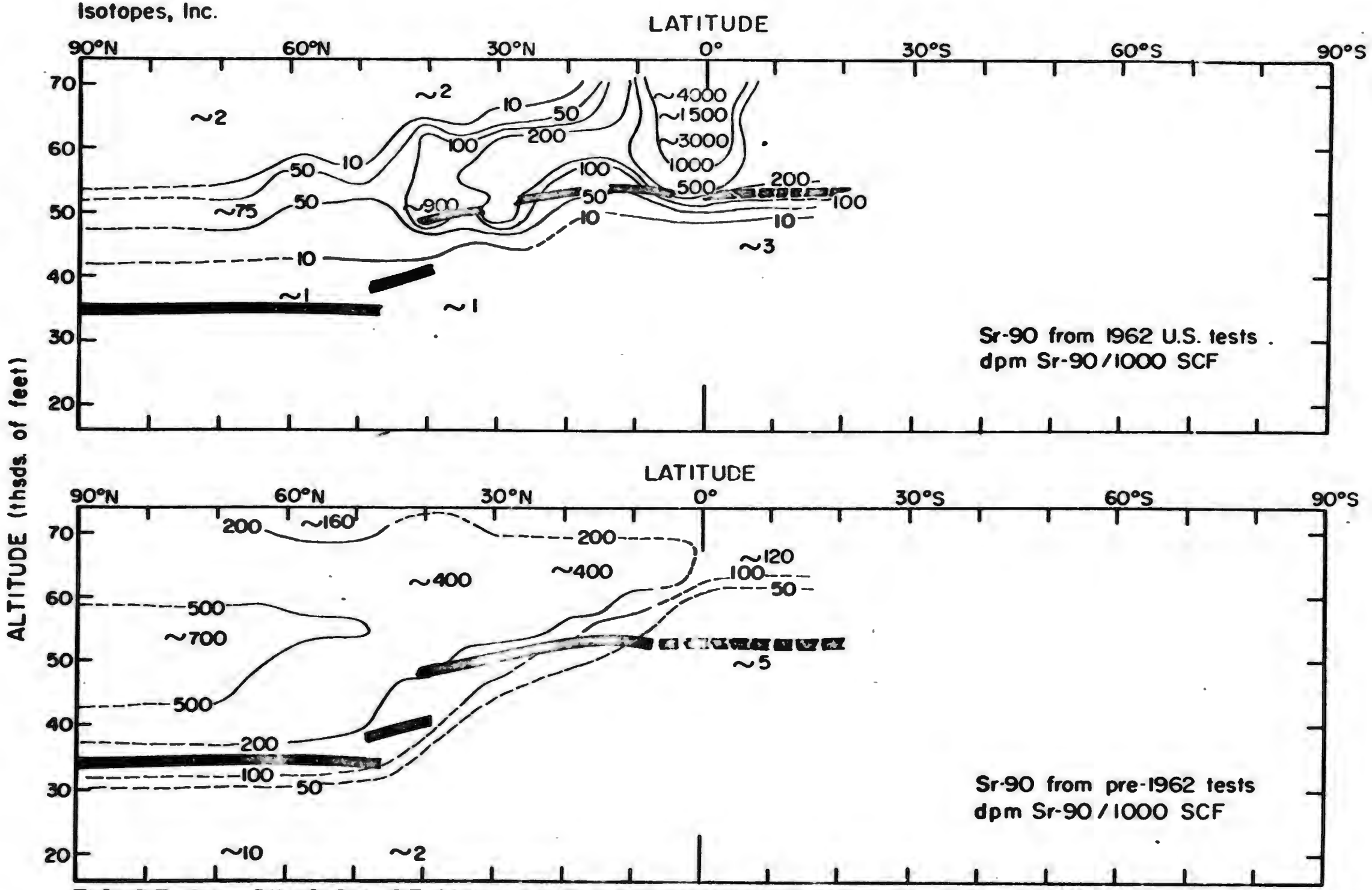

FIGURE 39 · DIVISION OF MAY-JUNE STRONTIUM-90 INTO TWO COMPONENTS USING THE Sr-89 / Sr-90 RATIO IN THE DEBRIS

The Concentrations of Rhodium-102

The tracer nuclide rhodium-102 which was injected into the mesosphere by the 12 August 1958 Orange shot[31,38] has been measured in HASP and Star Dust samples since 1960. The frequency of such measurements on Star Dust samples was high during the early months of the program, but it decreased after the resumption of atmospheric testing of nuclear weapons in late 1961 and remained low during 1962 and early 1963.

Several laboratories have measured this nuclide in stratospheric filter samples[36,38,39], but the results of these analyses have not shown satisfactory agreement. An intercalibration of the rhodium-102 analyses performed at different laboratories was begun about a year ago, and it is hoped that it will soon be completed. For the present all HASP and Star Dust rhodium-102 data should be considered preliminary.

The concentrations of rhodium-102 encountered at a series of latitudes and altitudes within the Star Dust sampling corridor during 1961 to 1963 are shown in Figure 40. The distributions of rhodium-102 in the sampling corridor during December 1959-June 1960, June-December 1961 and January-August 1962 are portrayed in Figure 41. Kalkstein has reported that additional rhodium-102 was injected into the lower stratosphere by the 1962 United States test series. Evidence may be found in the Star Dust data that an increase in stratospheric rhodium-102 concentrations occurred in mid-1962, so that the usefulness of this nuclide as a tracer for debris from the 1958 rocket shots appears to have ended after the first half of 1962.

The significance of the rhodium-102 data for the development of theories of atmospheric mixing and circulation has been discussed elsewhere by us and by Kalkstein[38]. The most significant observation

concerning the rhodium-102 is that this debris from a high altitude injection at low latitudes first entered the lower stratosphere at high latitudes in both hemispheres, apparently during the winter season, and subsequently moved equatorward in the lower stratosphere.

In the northern polar stratosphere the concentrations of rhodium-102 at altitudes of 65 thousand feet and higher appeared to decrease during the interval between June 1960 and June 1961 (see Figure 41), probably because of dilution of the rhodium-102 as it was transported downward and equatorward. There is no indication in Figure 40 that there was any similar decrease during the interval 1961-1962. Nevertheless at 50 thousand feet the rhodium-102 concentration did increase during the first half of 1962. Presumably the new rhodium-102 which reached the 50 thousand foot level at this time came from the higher levels in the polar stratosphere. From the data in the bottom diagram of Figure 40 one might conclude that rhodium-102 concentrations in the southern polar stratosphere, at least at 65 thousand feet, were approximately the same as those in the northern polar stratosphere during 1961 to early 1963. The suggestion in Figure 41 that the Northern Hemisphere concentrations exceeded the Southern Hemisphere concentrations during January-August 1962 may result from a preferential sampling in the Northern Hemisphere during the second-third of 1962 of new rhodium-102 produced by the 1962 United States tests at Christmas Island. There was no Star Dust sampling in the Southern Hemisphere (except at low latitudes) at this time.

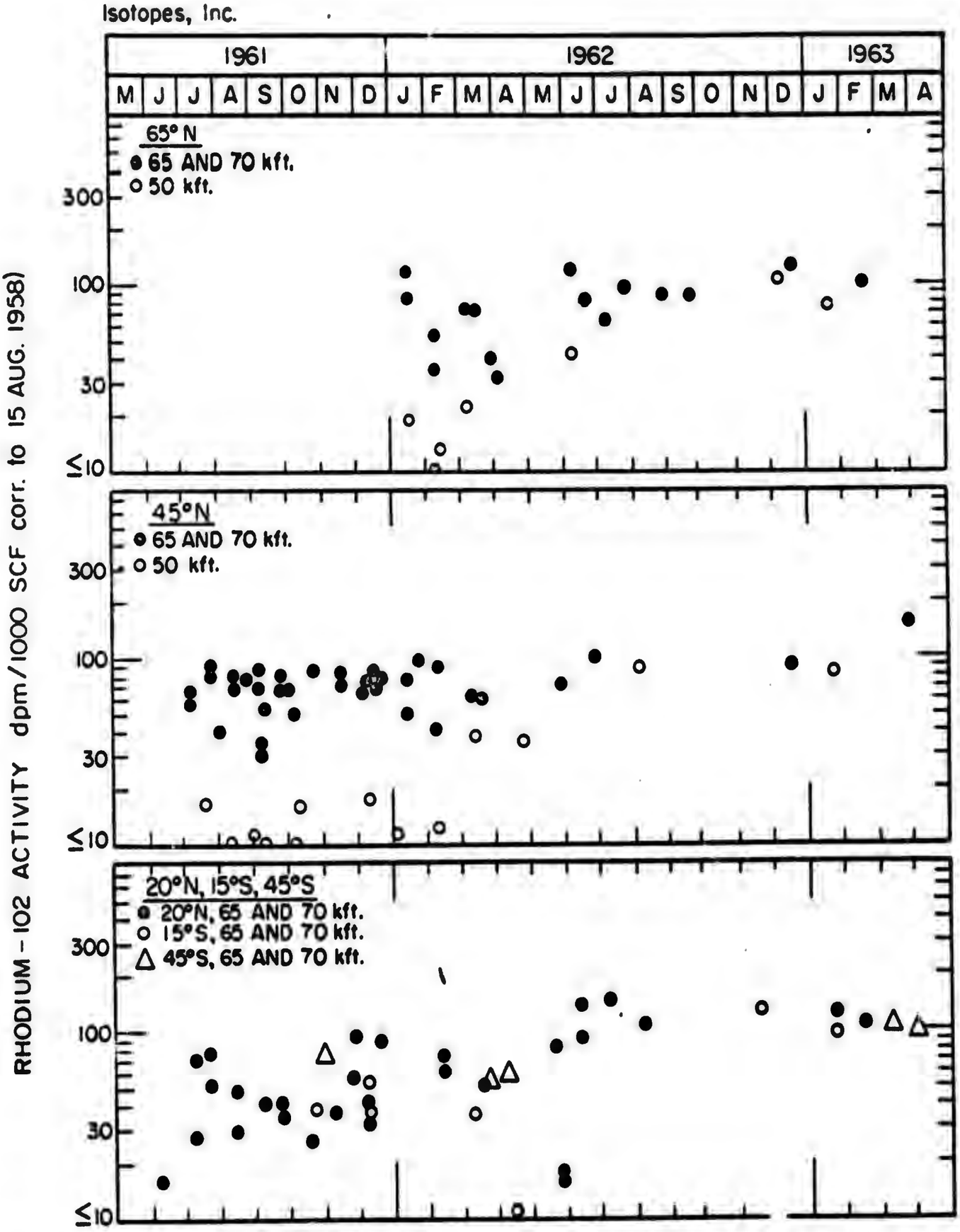

FIGURE 40·VARIATION WITH TIME OF RHODIUM-102 CONCENTRATIONS IN THE STAR DUST SAMPLING CORRIDOR

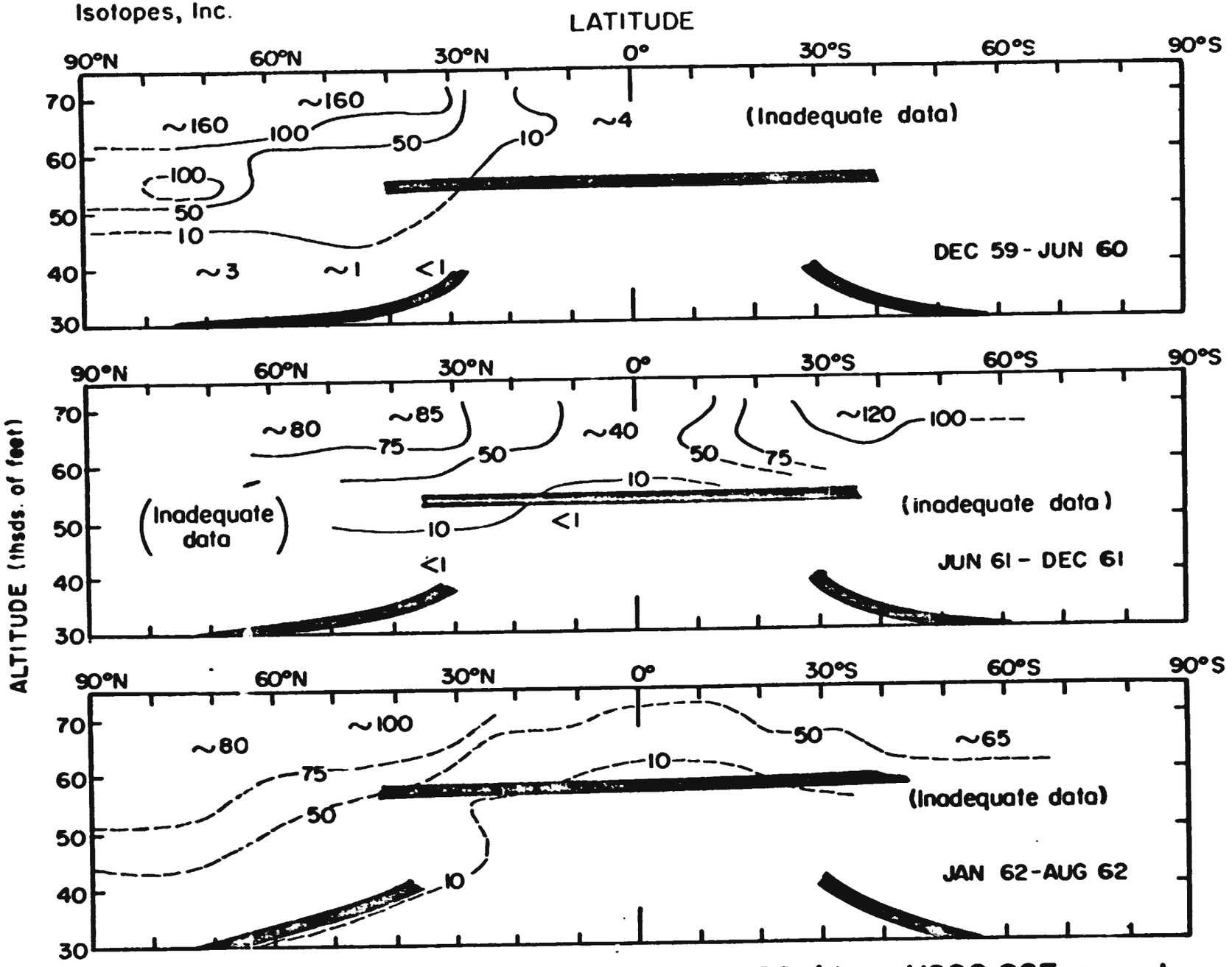

FIGURE 41 · DISTRIBUTION OF RHODIUM-102 (dpm / 1000 SCF corr. to 12 Aug 58) IN THE STAR DUST SAMPLING CORRIDOR

The Concentrations of Manganese-54, Iron-55 and Antimony-124

In previous quarterly reports we have discussed the stratospheric concentrations of several products of neutron activation which were injected at relatively high altitudes in the northern polar stratosphere by one or more events during the 1961 Soviet test series. Presumably the late October 1961 high yield devices were the source, for a very high neutron flux would be required to produce the observed amounts of these nuclides, and the activation products were injected higher into the stratosphere than was most of the fission product debris from that test series.

The vertical distributions of some of the activation products (manganese-54, iron-55 and antimony-124) in the vicinity of Fairbanks, Alaska on four dates in 1962 are shown in Figures 42 and 43. The vertical distributions of the fission product strontium-90 are shown for comparision. From these and similar data it has been concluded that a number of activation products, including manganese-54, iron-55, cobalt-57, antimony-124 and thallium-204, measured in samples collected before September 1962 had a common origin. For samples collected during 1962 the data for the activation products have been corrected for decay to 15 October 1961. In Star Dust samples the mean values for several nuclide ratios, so corrected, are: $Fe^{55}/Mn^{54}=1.58$, $Co^{57}/Mn^{54}=0.055$, $Sb^{124}/Mn^{54}=3.4$ and $Mn^{54}/Tl^{204}=790$.

The data for the samples collected near Fairbanks on 7 December 1962 show the effects of the late 1962 Soviet injections. Not only are the strontium-90 concentrations at all altitudes higher than at any time since the first few months of 1962, but the concentrations of the activation products at the lower altitudes sampled are also higher than at any time during the first two-thirds of 1962. It would appear, then, that some events

during the 1962 Soviet test series injected additional activation products into the lower polar stratosphere. Confirmation of this is found in data for a series of samples collected at about 60°N and 55 thousand feet during the second half of 1962. These data are shown in Figure 44. The total beta and strontium-90 activities have been corrected for decay to collection date, and the antimony-124, iron-55 and manganese-54 activities have been corrected to 15 October 1961. A sample of fresh debris collected on 13 October 1962 contained extremely high activities of the activation products as well as of fission products. Evidently the event which had produced this debris produced large quantities of manganese-54 and iron-55 and some antimony-124. The data for samples collected at this location during November and December 1962 show no definite evidence that further major injections of the activation products occurred during 1962, but a number of Star Dust samples collected during January 1964 and succeeding months contained high activities of antimony-124. This new antimony-124 was evidently produced during the December 1962 Soviet test series. In a preceding section of this chapter we have presented data on the Mo^{99}/Ba^{140} ratios in this debris which suggest a shot date of about 23 December or 24 December 1962 (see Table 14).

The vertical profiles of activity in the vicinity of Fairbanks during December 1962 and April 1963 are shown in Figure 45. The activities are corrected for decay to 31 December 1962. The high concentrations of antimony-124 at 55 thousand feet and higher altitudes are the result of the late December 1962 injections. It would appear that antimony-124, measured in samples collected during 1963, can be used as a tracer for a late December 1962 Soviet injection, but the usefulness of data for the longer lived nuclides is more limited. It may be possible to use nuclide ratios to distinguish

between manganese-54, iron-55 and cobalt-57 produced by the 1962 Soviet tests and the same nuclides produced by the 1961 Soviet tests. Nevertheless it is apparent that the determination of the extent of the vertical motion of the 1961 activation products during the winter of 1962-1963 will not be easily accomplished.

The trends with time in the manganese-54 concentrations at three altitudes at 65°N and 35°N are shown in Figure 46. These curves show several interesting features which are of significance in the study of stratospheric motions. During the first quarter of 1962 there was considerable variation in manganese-54 activities encountered from one mission to another. During May and June 1962 a pulse of manganese-54 activity appeared to reach the sampling corridor, and by July relatively high levels of activity, which varied relatively little from mission to mission, characterized most of the polar stratosphere of the Northern Hemisphere. By December 1962 there had been a pronounced increase in activity in the lowest stratospheric layers, as evidenced by data from 45 thousand feet at 65°N and 55 thousand feet at 35°N. As discussed above, this increase most likely resulted from new injections of manganese-54 during the 1962 Soviet test series. Some fluctuations in activities occurred at 65°N during the first third of 1963. These fluctuations, like those which were observed during the first third of 1962, almost certainly resulted from changes in the polar night circulation which commonly occur at this time. There appears to have been a general gradual decrease in stratospheric activities during subsequent months.

The mean distributions of manganese-54 in the Star Dust sampling corridor during January-April and May-August 1962 are shown in Figure 47. It is evident that there was more manganese-54 in the corridor during the

later interval and that it had spread farther south. The mean distributions during September-October and November-December 1962 are shown in Figure 48. The restricted Star Dust sampling during these intervals limits the reliability of the indicated distributions. Two month mean values have been calculated because additional manganese-54 wa injected into the stratosphere during the last third of 1962. The mean distributions for the four month intervals, September-December 1962 and January-April 1963 are shown in Figure 49. Since new manganese-54 was present in the stratosphere during both of these intervals, and correction of the data to October 1961 tends to magnify the concentrations actually present, Figure 50 has also been plot fed with the data corrected to 31 December 1962. Mean bimonthly distributions of manganese-54 during January-February and March-April 1963, which are shown in Figure 51, have been calculated because fresh debris was being intercepted in the Star Dust sampling corridor during these months. Mean bimonthly distributions of antimony-124 for the same intervals are shown in Figure 52. A comparison of Figures 51 and 52 shows that by early 1963 there were significant differences in the stratospheric distributions of these two activation products.

There appears to be some evidence in the manganese-54 data that at some time between August 1962 and March 1963 withing the northern polar stratosphere there was a subsidence of the debris containing the activation products. In spite of the new injections of manganese-54 during late 1962, the concentrations of that nuclide at about 65 thousand feet altitude at high northern latitudes during the first third of 1963 (Figure 49) were lower than they had been during May-August 1962 (Figure 47). The usefulness of measurements of manganese-54 during the winter of 1962-1963 to detect subsidence in the polar stratosphere was hindered, of course, by the repeated

interception of newly injected manganese-54 in this region.

The apparent stratospheric burden of manganese-54 during each of a series of four month intervals during 1962 and early 1963 has been calculated, based on the manganese-54 distributions shown in Figures 47 and 49. The results, corrected for decay both to 15 October 1961 and to 31 December 1962, are given in Table 16. The 140 percent increase in the apparent burden between the first and second thirds of 1962 must be attributed to inadequate sampling during January-April 1962 of the debris which contained the high concentrations of activation products. Changes in the stratospheric circulation which occurred by early February 1962 caused air which was relatively uncontaminated with debris from the 1961 Soviet tests to displace air which was contaminated in the sampling corridor. By late February contaminated air was again encountered at all levels, but high concentrations of the activation products were not commonly found in the Star Dust samples collected before May 1962. A few samples collected in January, March and April 1962 did contain high concentrations of these nuclides, however, suggesting that the variations in concentration observed from one mission to the next resulted from the presence in the lower stratosphere of masses of highly contaminated air and masses of virtually uncontaminated air, either of which might be intercepted on a particular mission depending upon the position of the aircraft flight track relative to the circulation cells in the lower stratosphere. Extensive mixing between these masses of air appears to have occurred by the second half of 1962, for by then large variations between missions in activity encountered were no longer common.

The 25 percent increase in the apparent burden of manganese-54 between the second and final thirds of 1962 and the additional 40 percent

increase by the first third of 1963 are probably attributable to the injection of new debris by the 1962 Soviet tests. By March and April 1963 this new debris was apparently fairly evenly distributed within the northern polar stratosphere, so that the calculated burden should be relatively accurate.

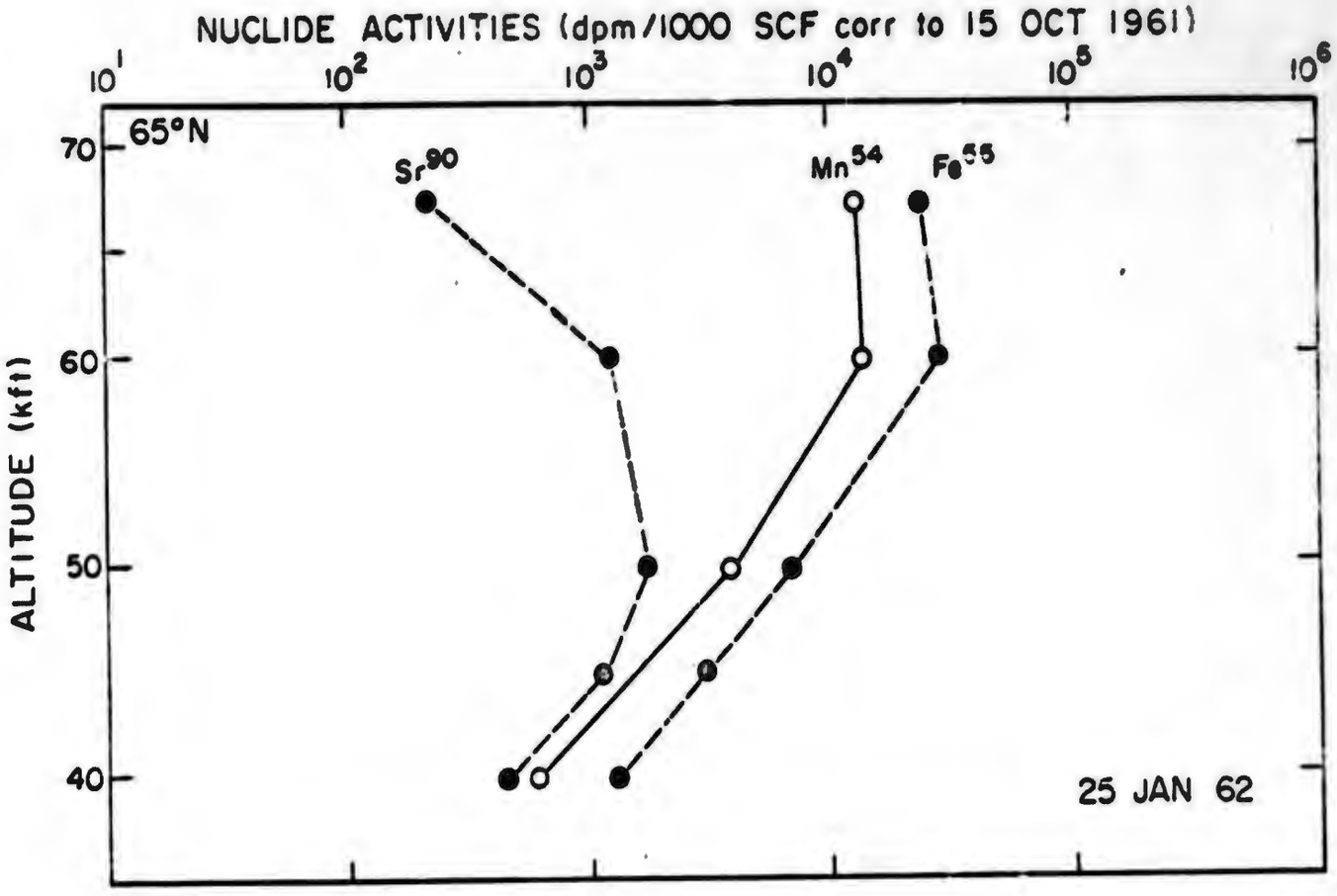

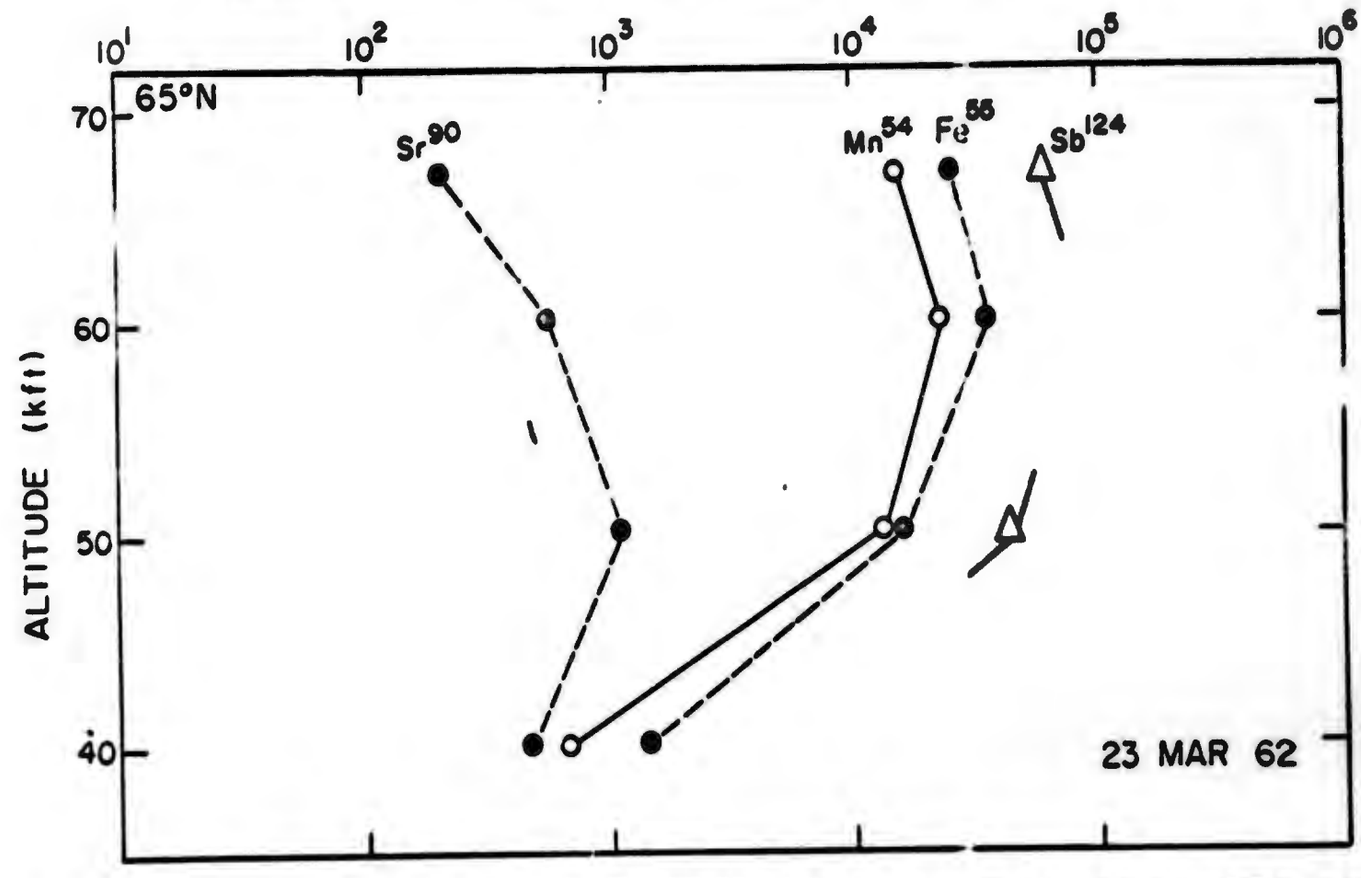

FIGURE 42 · VERTICAL DISTRIBUTION OF ACTIVATION PRODUCTS AND STRONTIUM-90 AT 65°N, 25 JAN 1962 AND 23 MAR 1962

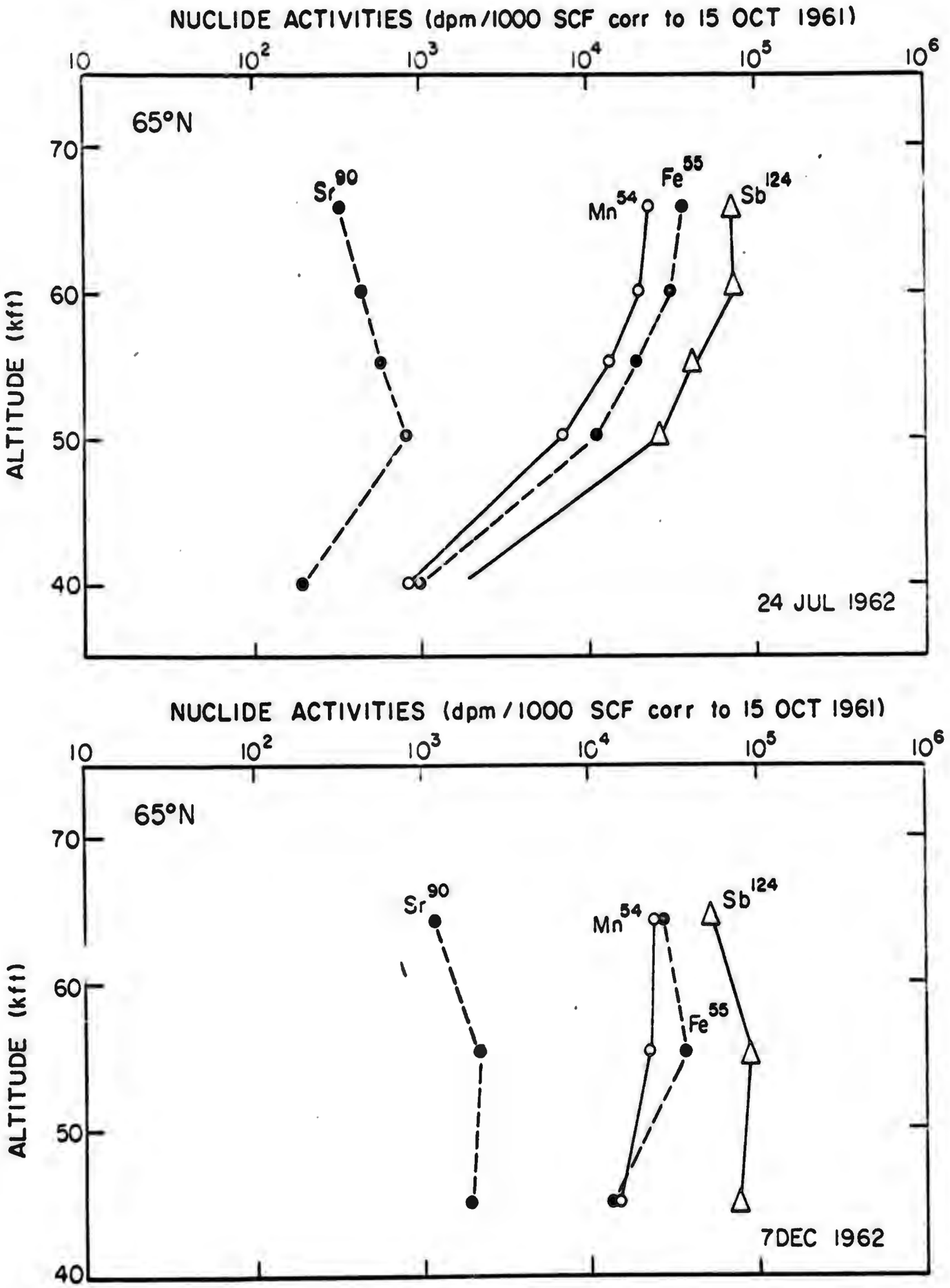

FIGURE 43 · VERTICAL DISTRIBUTION OF ACTIVATION PRODUCTS AND STRONTIUM-90 AT 65°N, 24 JUL 1962 AND 7 DEC 1962

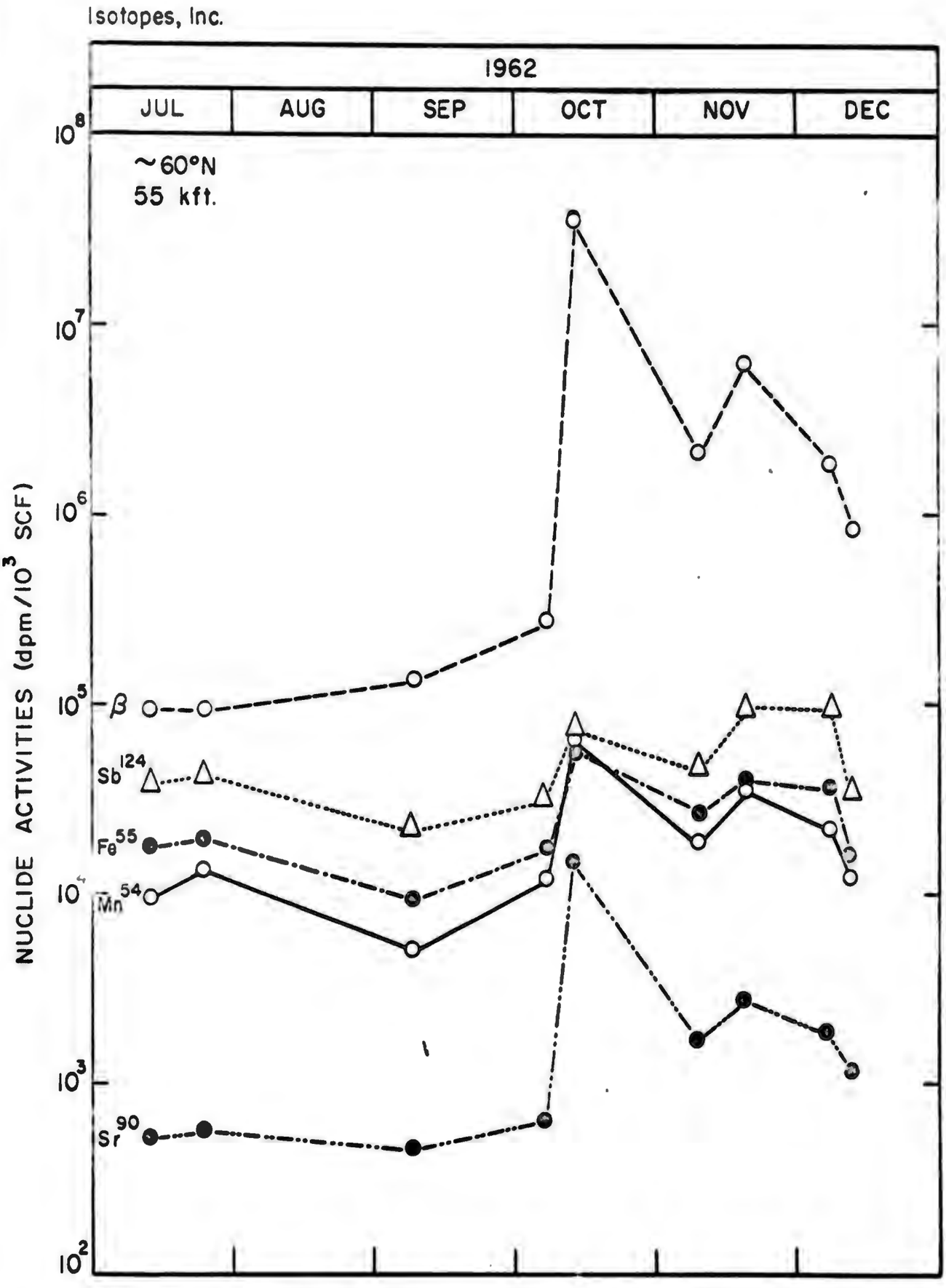

FIGURE 44 · CHANGE WITH TIME OF SOME NUCLIDE ACTIVITIES AT 60°N, 55 kft. DURING JULY TO DECEMBER 1962

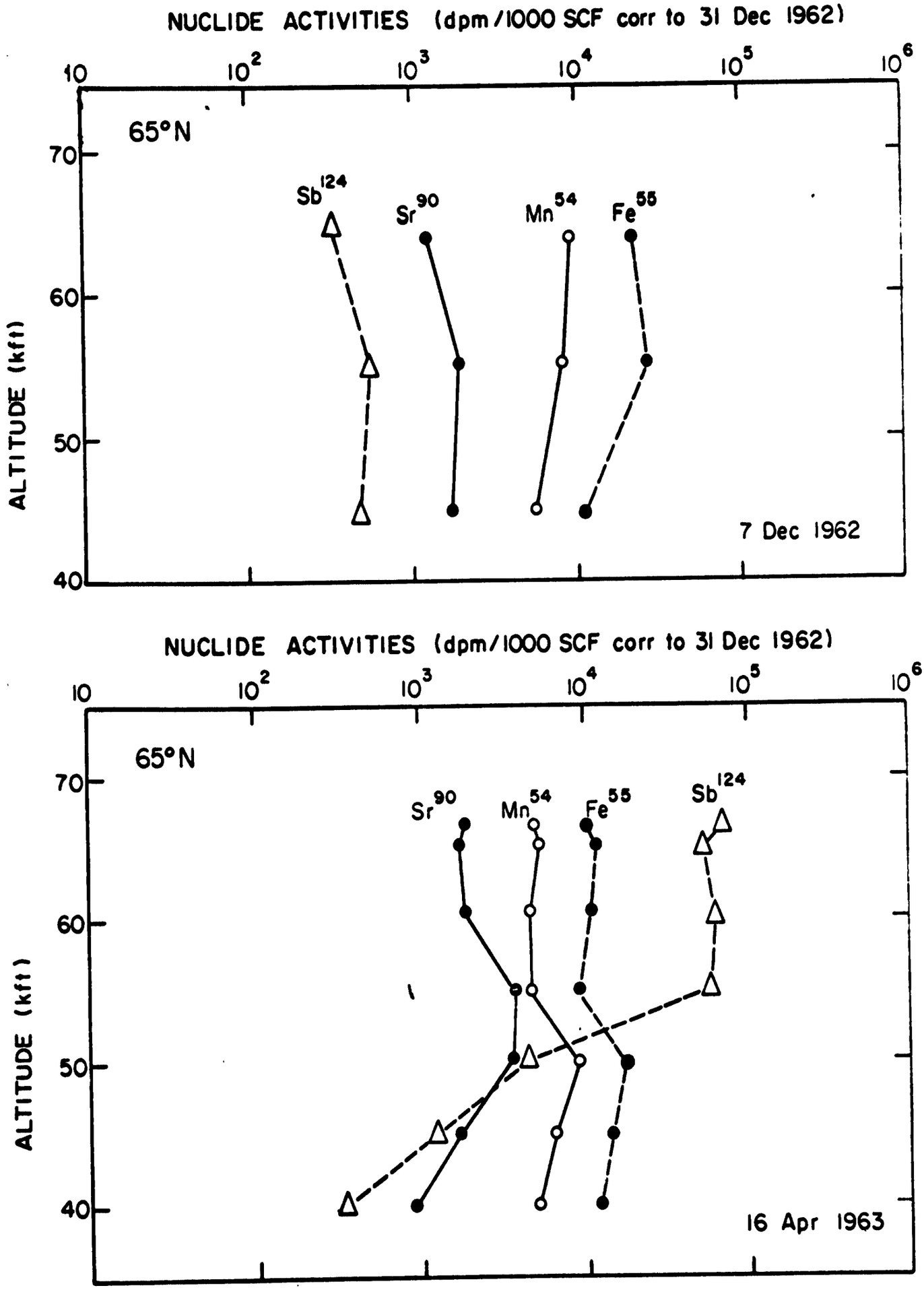

FIGURE 45 · VERTICAL DISTRIBUTION OF ACTIVATION PRODUCTS AND STRONTIUM-90 AT 65°N, 7 DEC 1962 AND 16 APR 1963

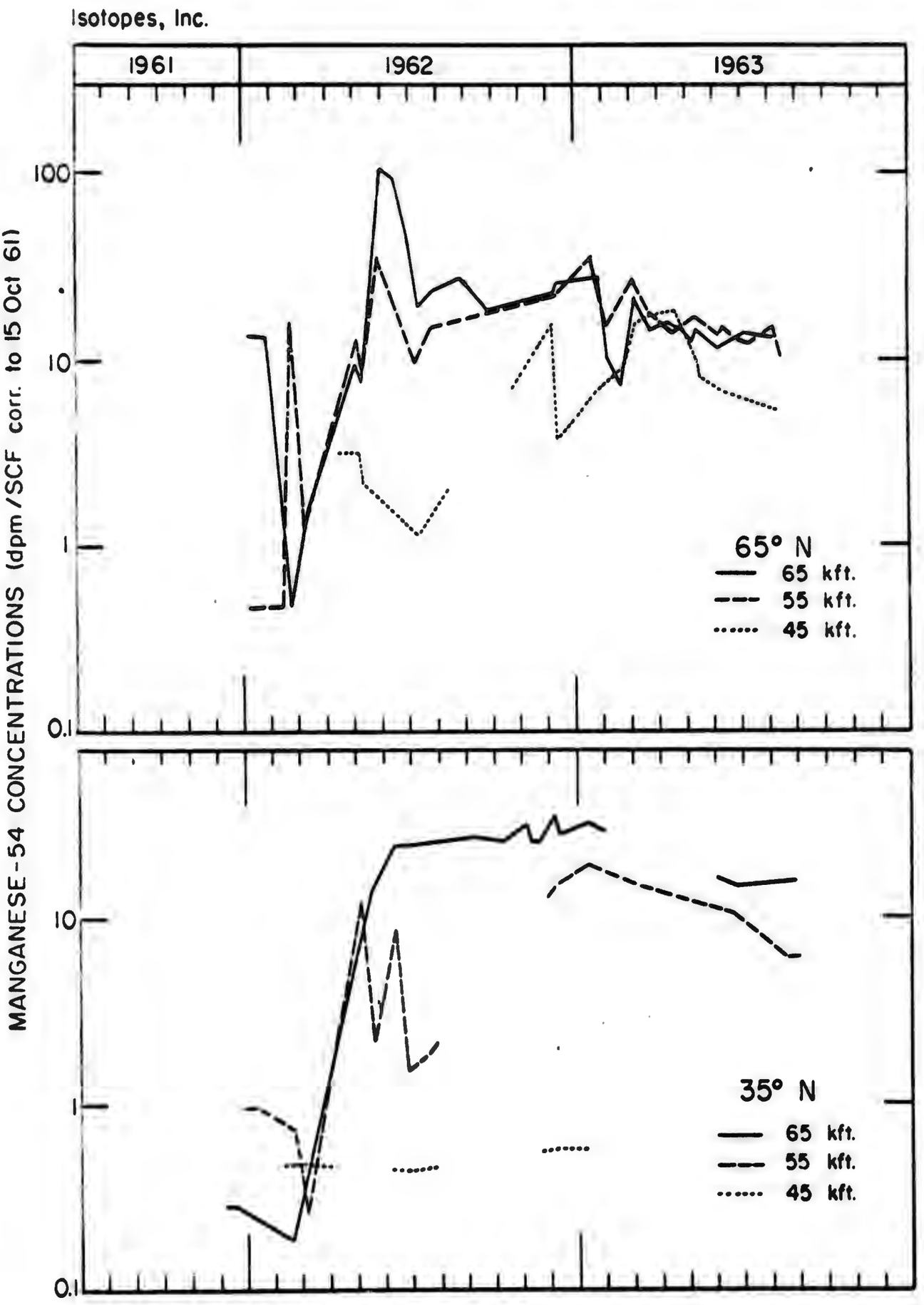

FIGURE 46 · VARIATION WITH TIME OF MANGANESE-54 CONCENTRATIONS AT 65°N AND 35°N

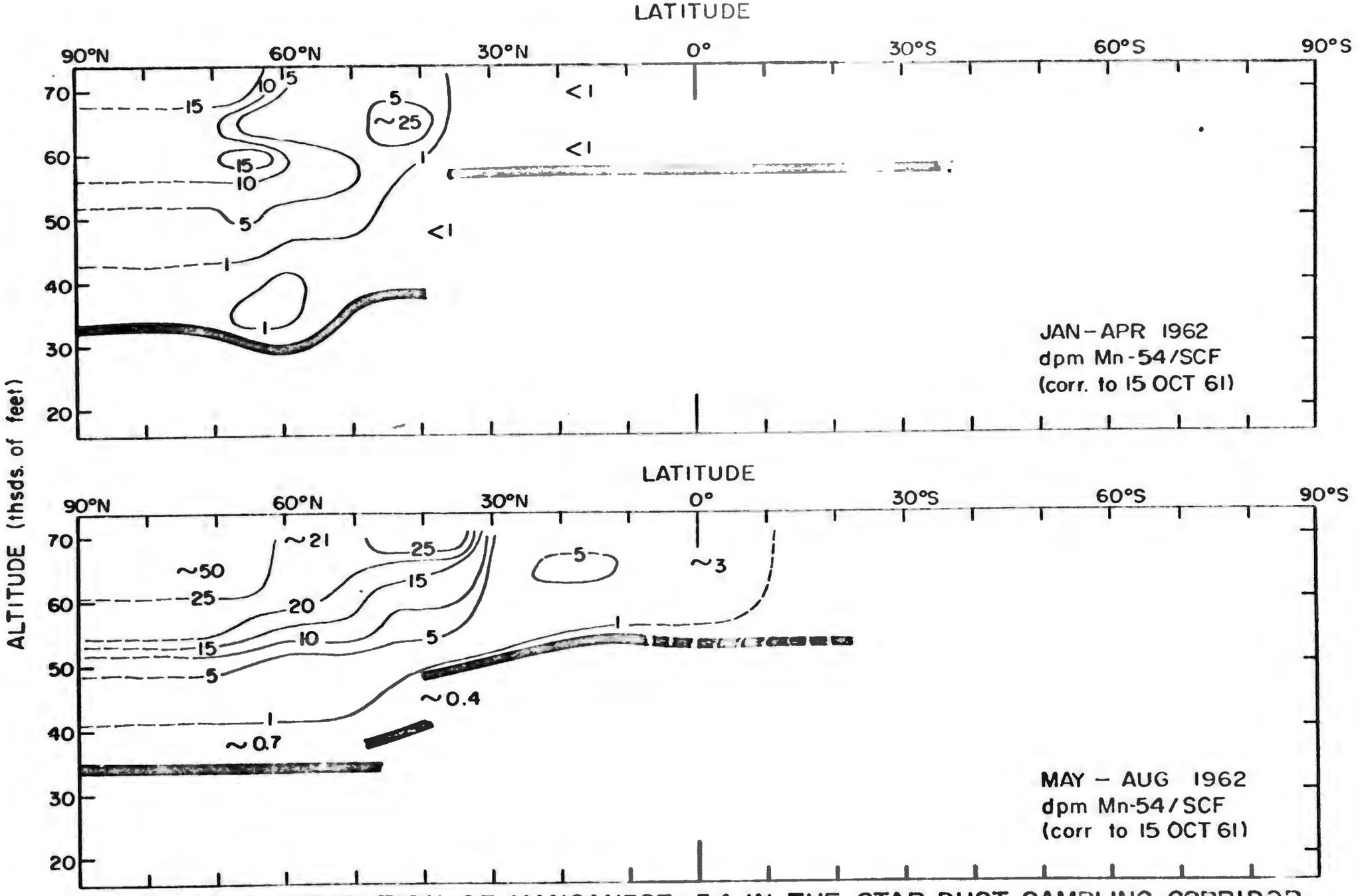

FIGURE 47 · DISTRIBUTION OF MANGANESE-54 IN THE STAR DUST SAMPLING CORRIDOR, JAN TO APR AND MAY TO AUG 1962

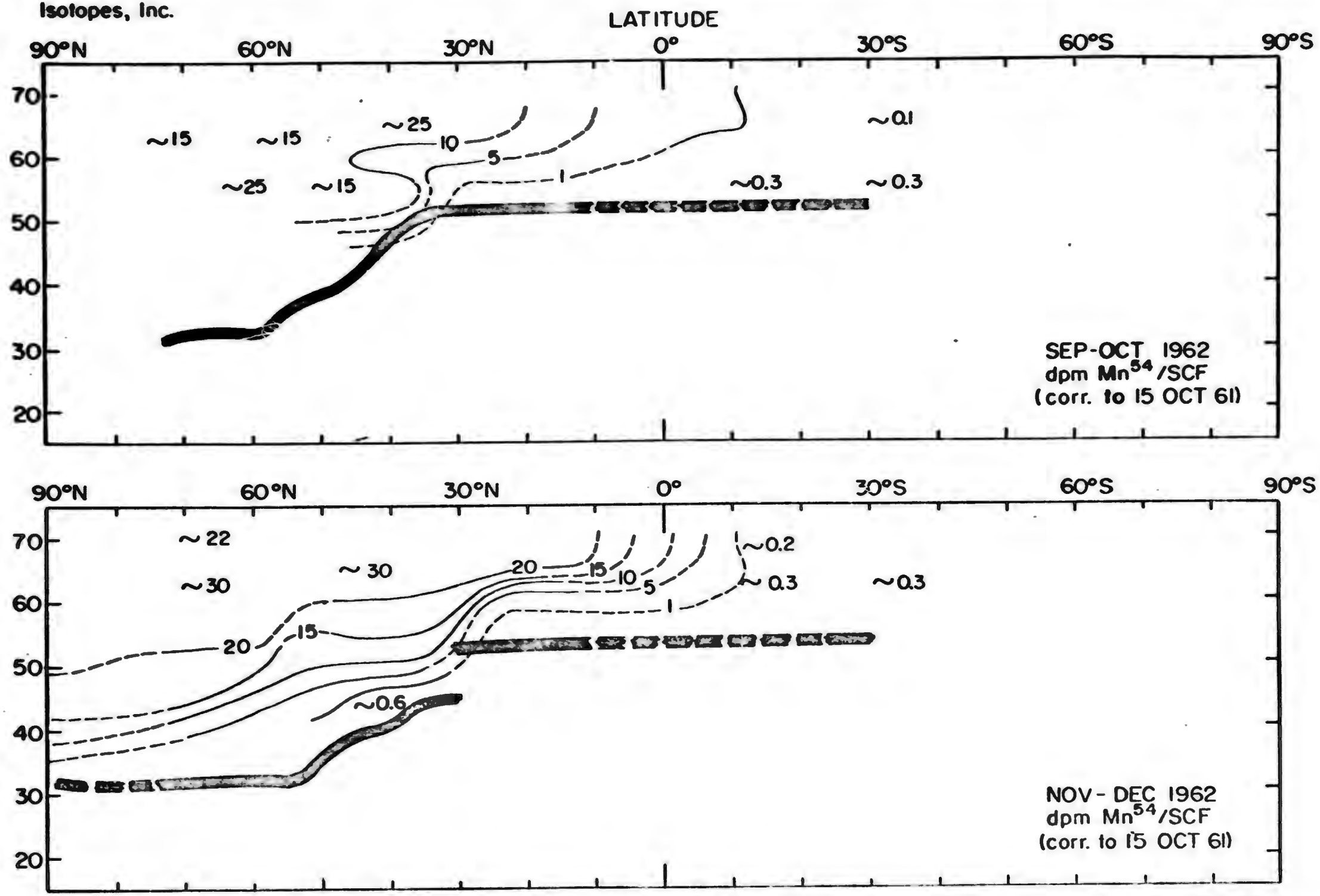

FIGURE 48· DISTRIBUTION OF MANGANESE-54 IN THE STAR DUST SAMPLING CORRIDOR DURING SEPTEMBER - OCTOBER AND NOVEMBER - DECEMBER, 1962

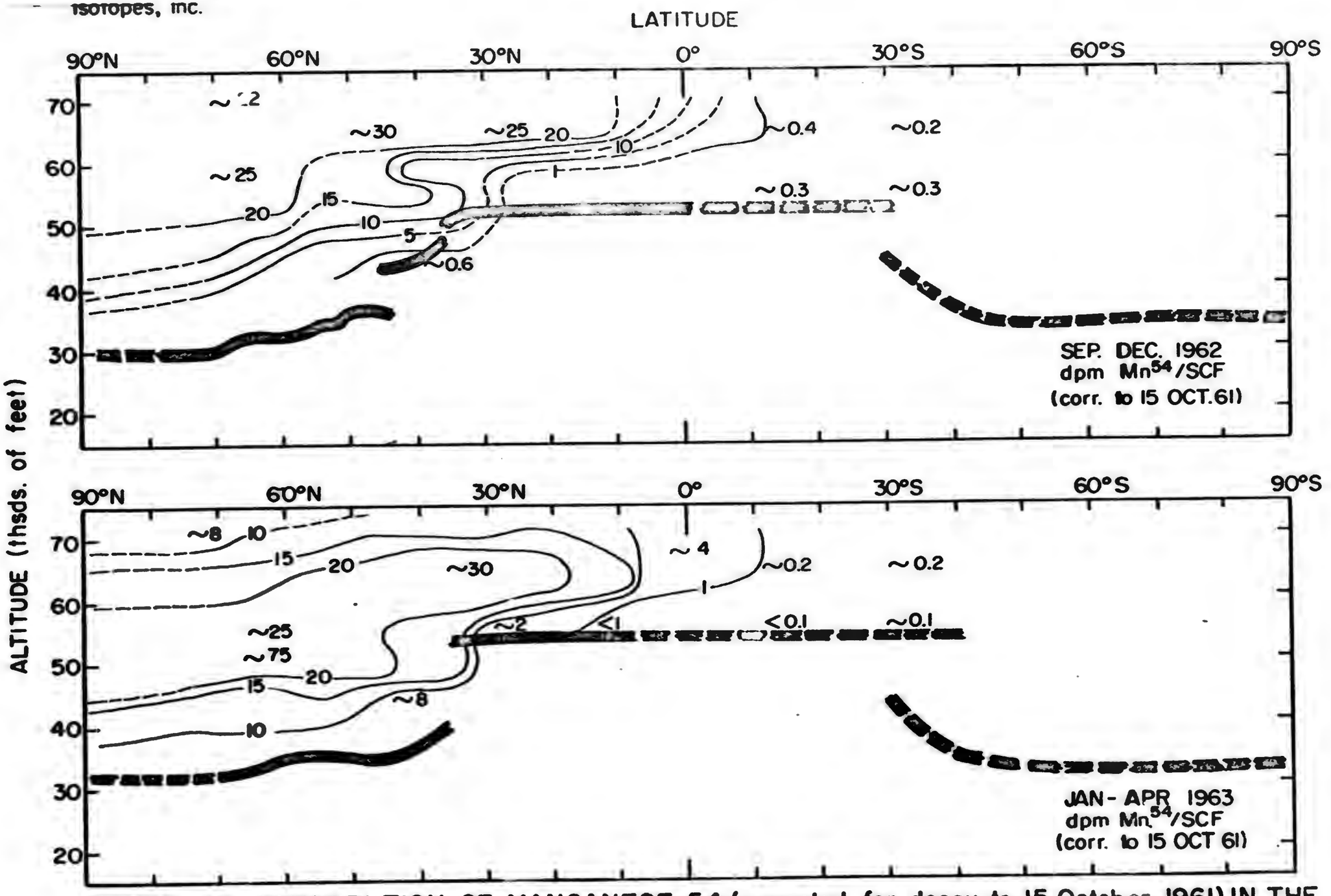

FIGURE 49 · DISTRIBUTION OF MANGANESE-54 (corrected for decay to 15 October 1961) IN THE STAR DUST SAMPLING CORRIDOR DURING SEPTEMBER - DECEMBER, 1962 AND JANUARY-APRIL, 1963

Isotopes, Inc.

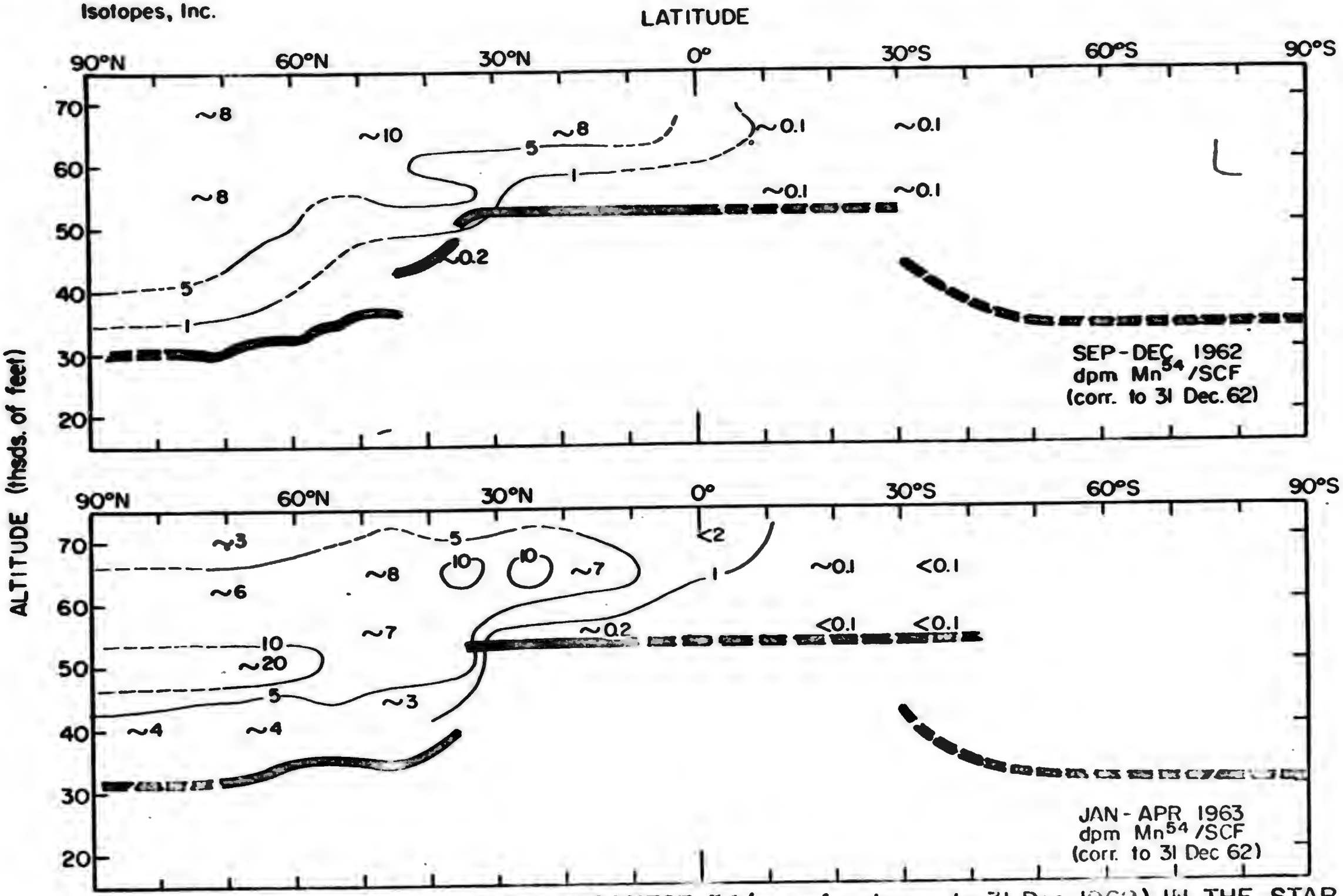

FIGURE 50 · DISTRIBUTION OF MANGANESE-54 (corr. for decay to 31 Dec. 1962) IN THE STAR DUST SAMPLING CORRIDOR DURING SEPTEMBER-DECEMBER, 1962 AND JANUARY — APRIL, 1963

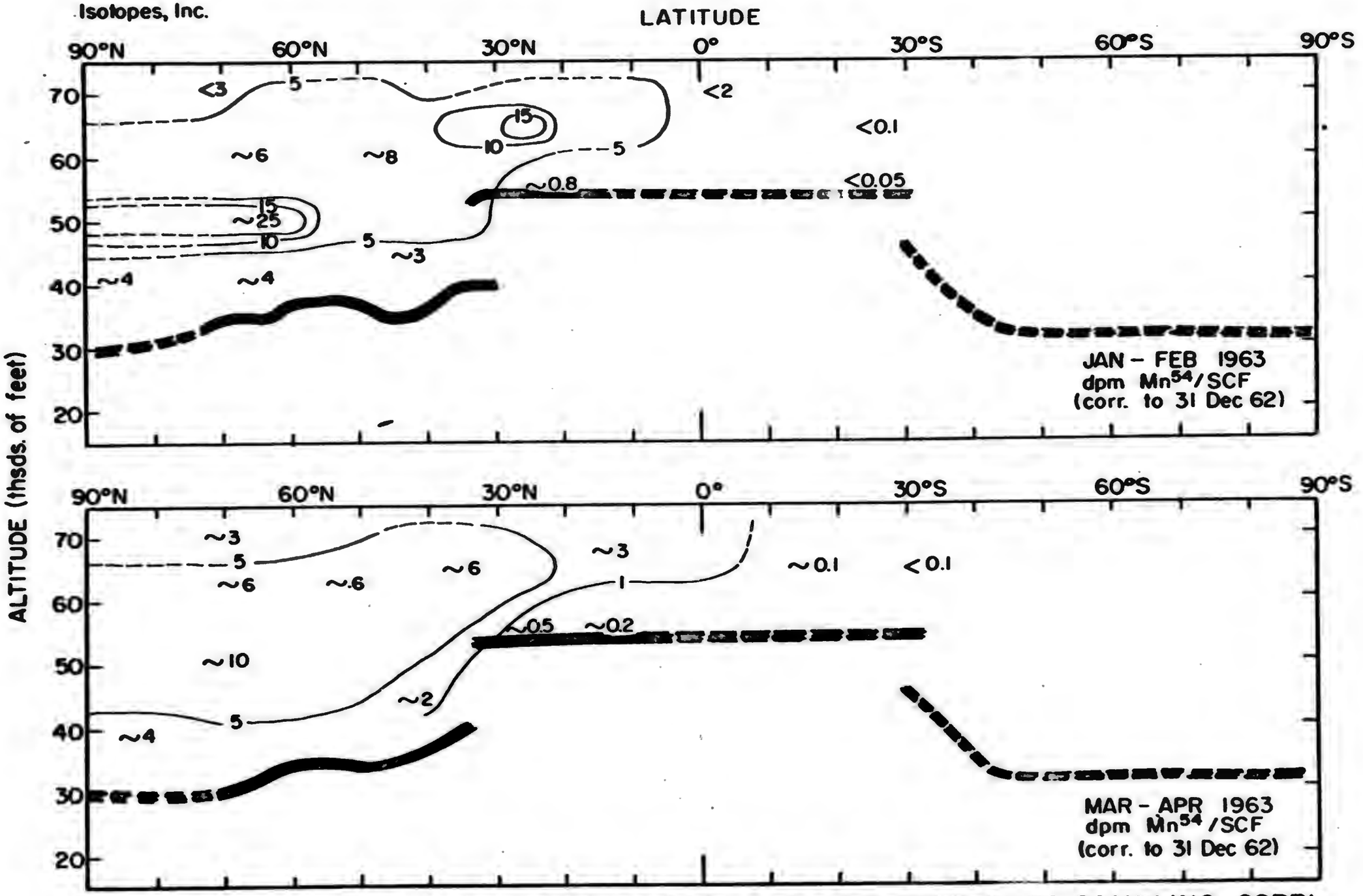

FIGURE 51 · DISTRIBUTION OF MANGANESE-54 IN THE STAR DUST SAMPLING CORRIDOR DURING JANUARY-FEBRUARY AND MARCH-APRIL, 1963

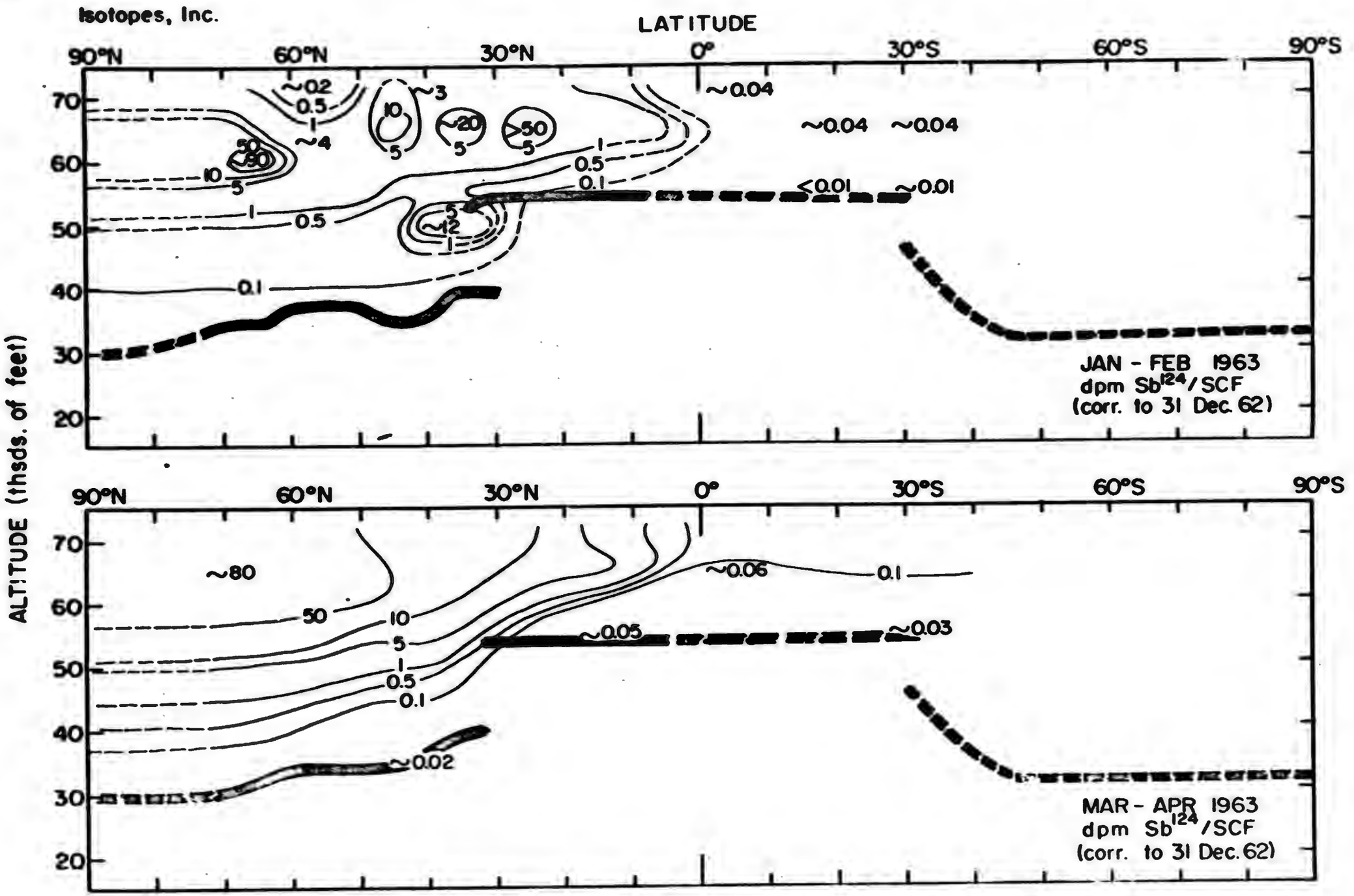

FIGURE 52 · DISTRIBUTION OF ANTIMONY-124 IN THE STAR DUST SAMPLING CORRIDOR DURING JANUARY - FEBRUARY AND MARCH - APRIL, 1963

Table 16. Apparent Stratospheric Burdens of Manganese-54 (in Megacuries) in the Northern Hemisphere During 1962 and Early 1963

Interval	Corrected for Decay to 15 Oct 1961	Corrected for Decay to 31 Dec 1962
January - April 1962	15 MC	5.3 MC
May - August 1962	36 MC	13.1 MC
September - December 1962	45 MC	16.0 MC
January - April 1963	63 MC	22.8 MC

CHAPTER 6. THE STRATOSPHERIC DISTRIBUTION OF NATURAL ACTIVITY

Three radionuclides which are produced in the atmosphere by natural processes have been measured in Star Dust samples since the program began in 1961. One of these, beryllium-7, is a product of the cosmic-ray induced spallation of atmospheric nitrogen and oxygen. The others, lead-210 and polonium-210, are daughter products of radon. Lead-210 is produced in the atmosphere by the decay of radon which escapes from soil, rocks and bodies of water at the surface of the earth. Polonium-210 results from the further decay of the lead-210. The stratospheric concentrations of these nuclides have been measured in the hope that their distributions would yield information on the directions and magnitudes of atmospheric motions.

The Concentrations of Beryllium-7

The mean distribution of beryllium-7 in the Star Dust (or HASP) sampling corridor has been calculated for each of a series of time intervals during Project Star Dust (and Project HASP). These distributions are shown in Figures 53, 54 and 55. A theoretical distribution in a stagnant atmosphere, based on beryllium-7 production rates calculated by Lal and Peters[40], is included in each of these figures for purposes of comparison.

The mean distributions shown in Figure 53 are for October 1959 - June 1960 and June - September 1961. The concentrations found in the vicinity of the tropopause and of the tropopause gap were generally lower than predicted for a stagnant atmosphere. This was expected, of course, for the tropopause acts as a sink for beryllium-7 just as it does for debris from nuclear weapons tests. At the higher levels sampled the concentrations found in the polar stratosphere were lower than the theoretical, but those found in the tropical stratosphere were slightly higher than the theoretical. This situation could result from eddy diffusion in the meridional direction.

Isotopes, Inc.

In Figure 54 are shown the mean distributions for January - April 1962 and May - August 1962. During the first of these intervals rather high concentrations of beryllium-7 were found in the northern polar stratosphere. Bleichrodt[41] has described the presence of artificial beryllium-7, produced by the 1961 Soviet test series, at 42 thousand feet in the stratosphere during October - November 1961. The high concentrations of beryllium-7 in the Star Dust sampling corridor during the first third of 1962 are consistent with Bleichrodt's conclusion that beryllium-7 is produced by atmospheric nuclear explosions. Even stronger evidence for such artificial production of this nuclide is found in the very high concentrations of the tropical stratosphere during the interval May - August 1962. These high concentrations of beryllium-7 were associated with fresh debris from the mid-1962 United States weapons tests at Christmas Island.

The mean distribution of beryllium-7 in the sampling corridor during January - March 1963, which is shown in Figure 55, shows anomalously high concentrations in the northern polar stratosphere. These, no doubt, resulted from the artificial production of beryllium-7 by the 1962 Soviet test series. It would appear from Figure 55 that the artificial beryllium-7 had reached at least 10°S at high altitudes where concentrations more than twice as high as the theoretical value were found. This might, in part at least, represent a remnant of artificially produced beryllium-7 from the 1962 United States tests. South of 20°S the concentrations found approximated the theoretical values.

The beryllium-7 analysis utilizes gamma spectrometric measurement of the 0.48 Mev gamma ray, and inspection of the gamma spectrum for each sample assures its radiochemical purity. Nevertheless, it was decided that additional evidence for the purity of the samples should be obtained, since the samples

which appeared to contain excess beryllium-7 were those which also contained high activities of short-lived fission products. To provide such evidence the decay of a series of samples collected during late 1962 and early 1963 was monitored. Data for four such samples are shown in Figure 56. Decay curves for the 53 day half life of beryllium-7 are drawn through them. The fit of the curves to the data is adequate even though the measurements suffered from several factors, including the passage of several months between the collection of the samples and their analysis. In addition,relatively small aliquots of the samples were used in the analyses because they contained high activities of fission products. In the analyses of more recent samples larger aliquots, processed sooner after sample collection, have been measured. As a result higher counting rates and better decay curves have been obtained.

Commencing with samples collected in May 1963, samples analyzed for beryllium-7 are also being analyzed for sodium-22, phosphorus-32 and phosphorus-33. It is expected that the resulting data will permit quantitative estimation of rates of meridional movement of stratospheric air. Measurements made during the winter season should also allow estimates to be made of rates of vertical motion if subsidence of air within the polar stratosphere occurs during this season.

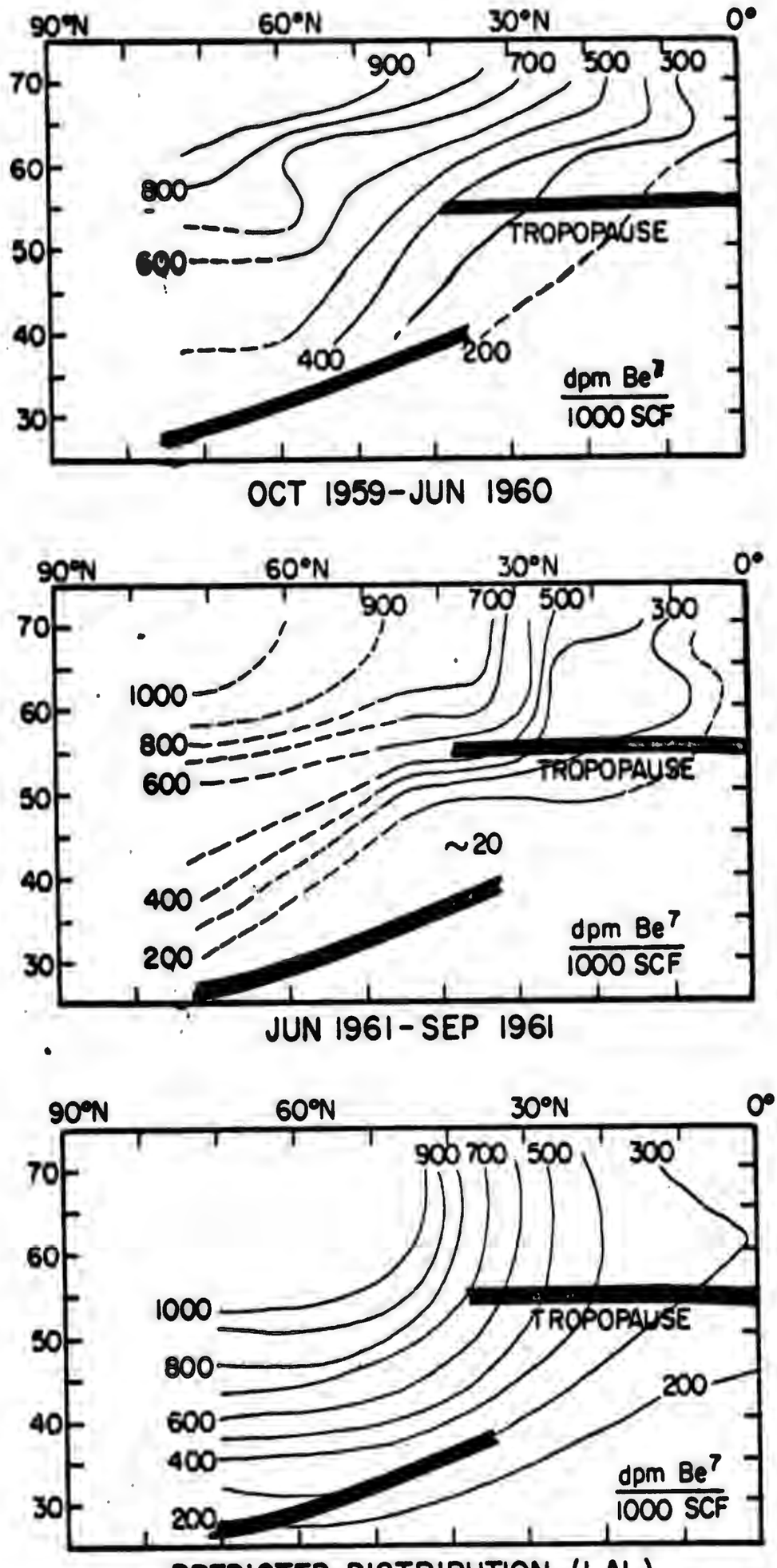

FIG. 53.
STRATOSPHERIC DISTRIBUTION OF BERYLLIUM-7

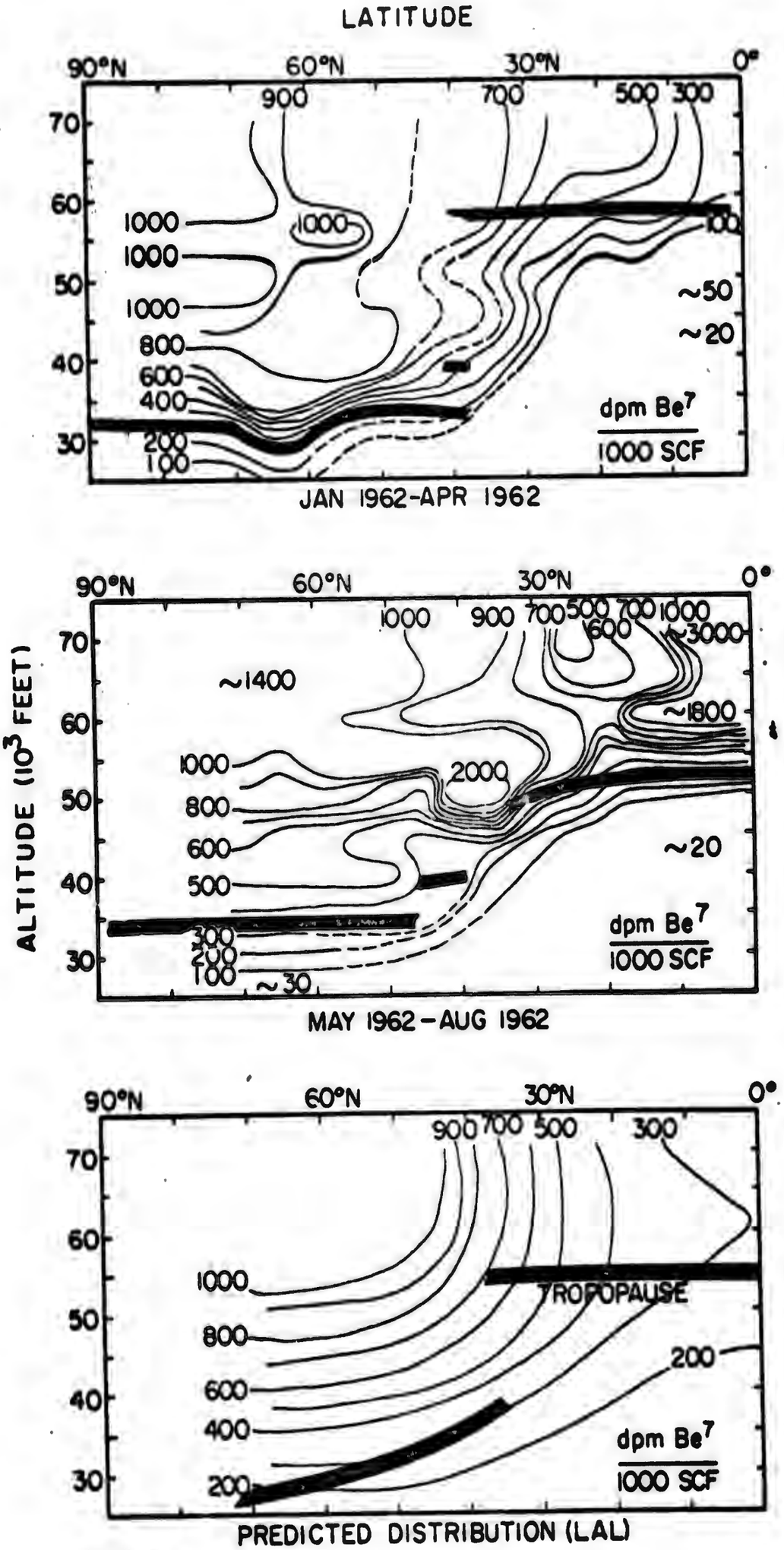

FIG. 54.
STRATOSPHERIC DISTRIBUTION OF BERYLLIUM-7

Isotopes, Inc.

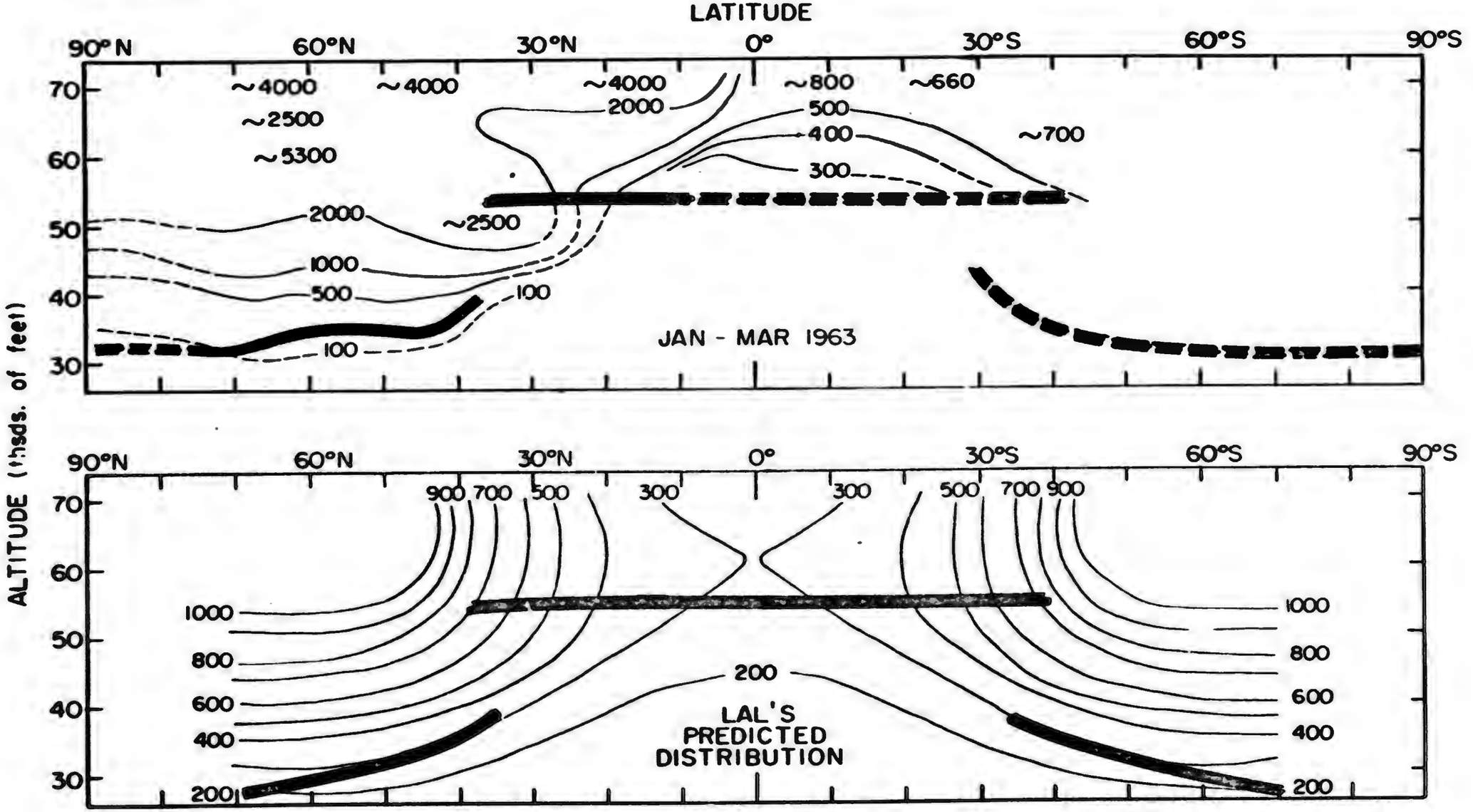

FIGURE 55 · STRATOSPHERIC DISTRIBUTION OF BERYLLIUM - 7 (dpm / 1000 SCF)

Isotopes, Inc.

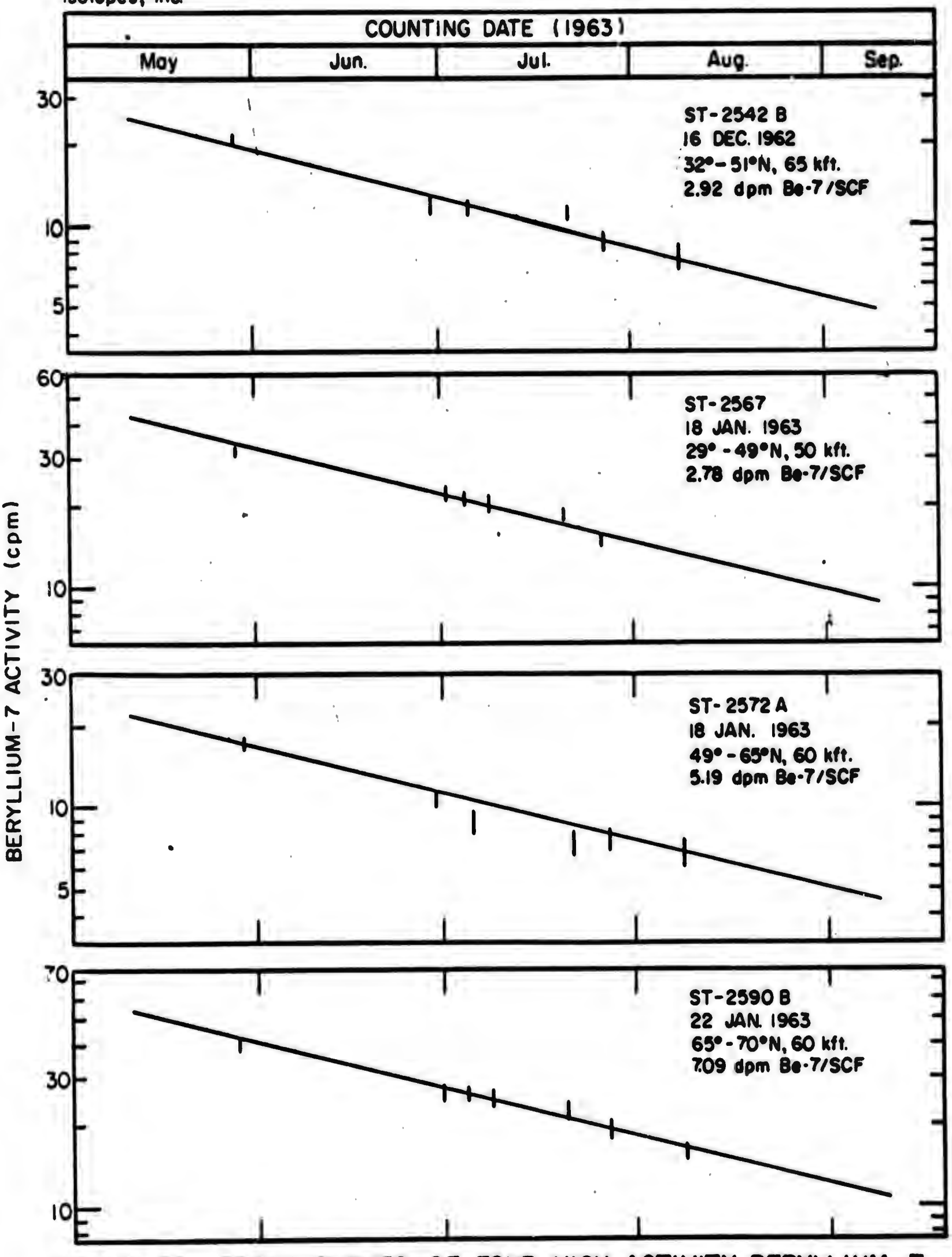

FIGURE 56 · DECAY CURVES OF FOUR HIGH ACTIVITY BERYLLIUM-7 SAMPLES

Isotopes, Inc.

The Concentrations of Lead-210 and Polonium-210

Analyses of lead-210 and polonium-210 have been performed on a large number of Star Dust samples collected between June 1961 and March 1963. The frequency of analysis of these nuclides was decreased during 1962 as it became evident that it would be difficult to obtain useful data because of contamination of the samples by high activities of fission products from the atmospheric nuclear weapons tests performed during late 1961 and during 1962. Indeed the levels of activity of natural lead-210 and polonium-210 in the samples are so low that even contamination by natural lead from the glassware used in the analyses or from laboratory dust may constitute a problem. In any event the data obtained have been less than satisfactory. Nevertheless some useful conclusions may be drawn from them.

The predominant decay scheme of radium is given in Table 17. Radium is present, of course, in rocks, in soil and in natural waters at and below the surface of the earth. The noble gas, radon, which is produced by the decay of radium has a half life of 3.8 days. Because it is chemically inert, radon produced in porous soil or rock or within surface waters may migrate to the surface and enter the atmosphere. Should the radon be carried into the upper troposphere before it decays, it or its decay products may enter the stratosphere. Measurements of radon and of its long-lived daughter products, lead-210 and polonium-210, in the stratosphere have been reported.[42,43,44] Because of their short half lives the members of the decay series between radon and lead-210 do not occur in the stratosphere in significant quantities.

Lead-210 which enters the stratosphere from the troposphere or is produced in the stratosphere by decay of radon may experience a long stratospheric residence time. In this event its daughter product bismuth-210 will rapidly grow into equilibrium with it and, eventually, so will polonium-210.

The curve shown in Figure 57 represents the increase in the activity ratio Po^{210}/Pb^{210} to be expected in lead-210 following its formation. If the stratospheric residence time of lead-210 is on the order of several years the ratio Po^{210}/Pb^{210} in stratospheric samples should approach 1.0. If the residence time is significantly shorter, much lower ratios should be found.

Data points for a series of samples collected in the Southern Hemisphere during October 1961 - April 1962 are plotted in Figure 58. The curves drawn through the data points represent the locus of points for samples in which polonium-210 and lead-210 are approximately in radioactive equilibrium. The data points for samples which are not yet in equilibrium should fall below the curves. Much of the scatter of the points must be attributed to analytical errors. The fact that most points for stratospheric samples fall above the curves suggests that a bias, perhaps due to a calibration error, exists in the data.

In spite of their limitations the data in Figure 58 do permit some conclusions to be drawn. The mean values of the lead-210 concentrations in the tropical stratosphere (0°- 30°S) and the polar stratosphere (30°- 60°S) are virtually the same: 0.32 ± 0.13 and 0.31 ± 0.12 dpm/1000 SCF respectively. The polonium-210 concentrations also agree within the standard deviation. They are 0.46 ± 0.14 dpm/1000 SCF in the tropical and 0.37 ± 0.16 in the polar stratosphere. The Po^{210}/Pb^{210} activity ratio in samples collected in the tropical troposphere and in the tropical tropopause layer is 0.35 ± 0.17. This is much lower than the ratio found in stratospheric samples: 1.44 ± 0.73 in the tropical and 1.19 ± 0.69 in the polar stratosphere.

The mean distributions of lead-210 and polonium-210 in the stratosphere of the Northern Hemisphere during June to September 1961, before debris from the 1961 Soviet tests reached the sampling corridor, are shown

in Figure 59. The data suggest that the highest concentrations of these nuclides occur in the tropical stratosphere and in the lower polar stratosphere. Within the polar stratosphere at least, the concentrations appear to be higher in the 10 thousand feet thick layer,which is immediately above the tropopause layer, than they are in the higher stratosphere.

Perhaps the data presented in Figures 58 and 59 are too uncertain to support a detailed interpretation. It is interesting, however to compare our results with the predictions of Jacobi and Andre[45] who calculated the vertical distribution of radon-220 and its decay products in the atmosphere by means of a solution of the diffusion equation which permitted them to use any vertical profile of the turbulent diffision coefficient. For the calculation of vertical distribution of lead-210 and polonium-210,they used a profile of the turbulent diffusion coefficient which they believed to be representative of normal turbulence conditions throughout the troposphere. They have assumed a series of tropospheric residence times for lead-210 varying from 5 days to infinity and have calculated a distribution for each. While none of these actually fits the Star Dust data, the best agreements result from the use of 5 or of 20 days residence times. Longer residence times result in predicted tropospheric concentrations of lead-210 which are much too high. The predicted lead-210 concentrations obtained using a 5 day residence time are lower than the Star Dust results at all altitudes from 40 to 70 thousand feet, and those obtained using a 20 day residence time are higher than the Star Dust results for altitudes below 60 thousand feet but agree with the Star Dust results at about 60 thousand feet. Above 60 thousand feet the predicted concentrations decrease very rapidly with altitude, a situation not confirmed by the Star Dust measurements. The predicted Po^{210}/Pb^{210} ratios increase rapidly with altitude above about 20 thousand feet, approaching 1.0 at about 50 thousand

feet in the case of the 5 day residence time and at about 60 thousand feet in the case of the 20 day residence time.

Although the Star Dust measurements do not confirm the details of the distributions calculated by Jacobi and Andre, they do appear to show two features of those distributions: a decrease of lead-210 concentrations with altitude above the tropopause layer, and an increase of the Po^{210}/Pb^{210} activity ratio to an equilibrium value of about 1.0 in the stratosphere.

Table 17. The Predominant Decay Series of Radium

Nuclide	Name	Half Life	Mode of Decay	
Ra^{226}	Radium	1,590 years		
Rn^{222}	Radon	3.825 days		
Po^{218}	Radium A	3.05 minutes		(99.97%)
Pb^{214}	Radium B	26.8 minutes	β	
Bi^{214}	Radium C	19.7 minutes	β	(99.96%)
Po^{214}	Radium C'	1.5×10^{-4} seconds		
Pb^{210}	Radium D	22 years	β	
Bi^{210}	Radium E	5.0 days	β	(~ 100%)
Po^{210}	Polonium	140 days		
Pb^{206}	Stable Lead	-	-	

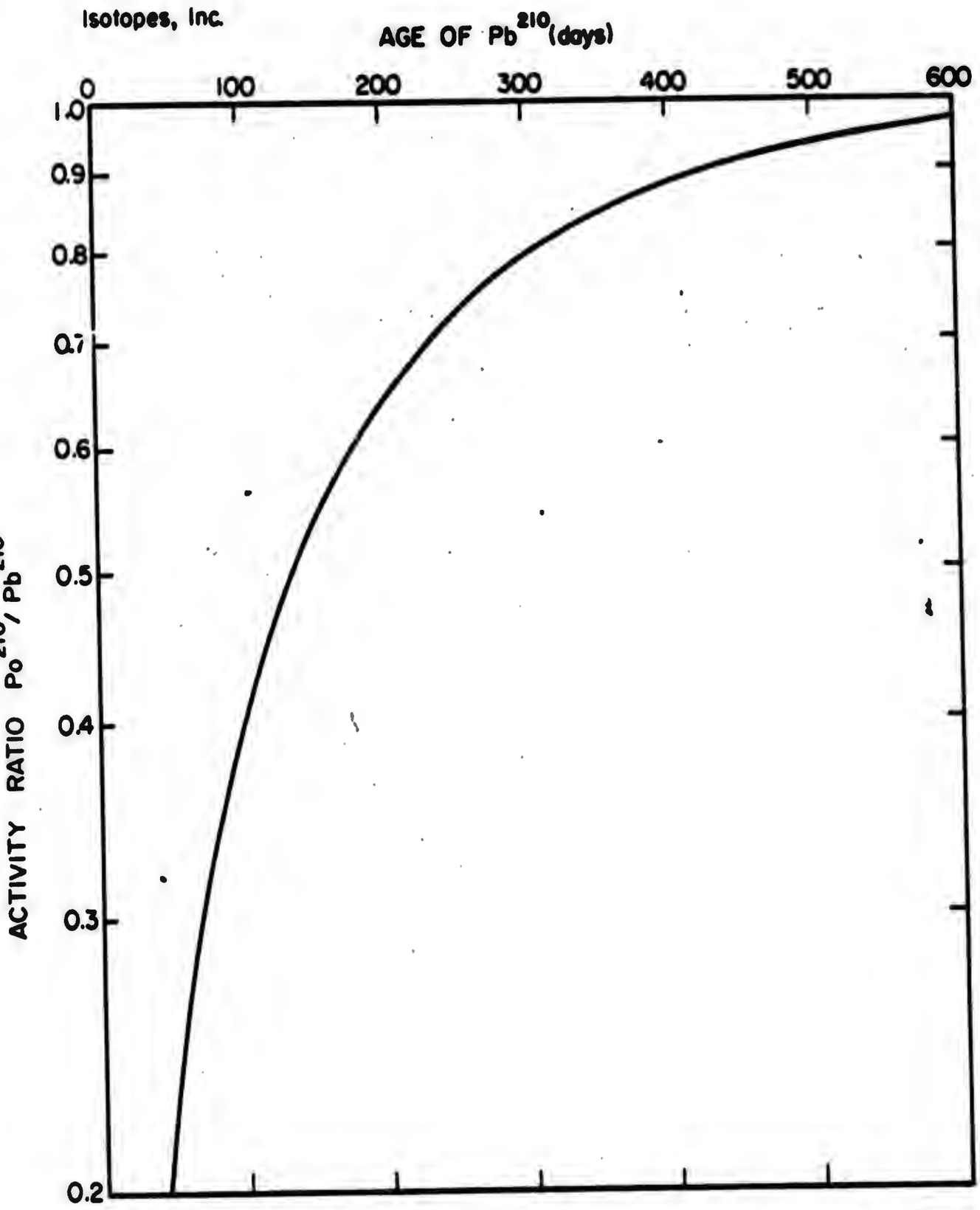

FIGURE 57 · VARIATION OF THE ACTIVITY RATIO Po^{210} / Pb^{210} WITH THE AGE OF THE LEAD-210

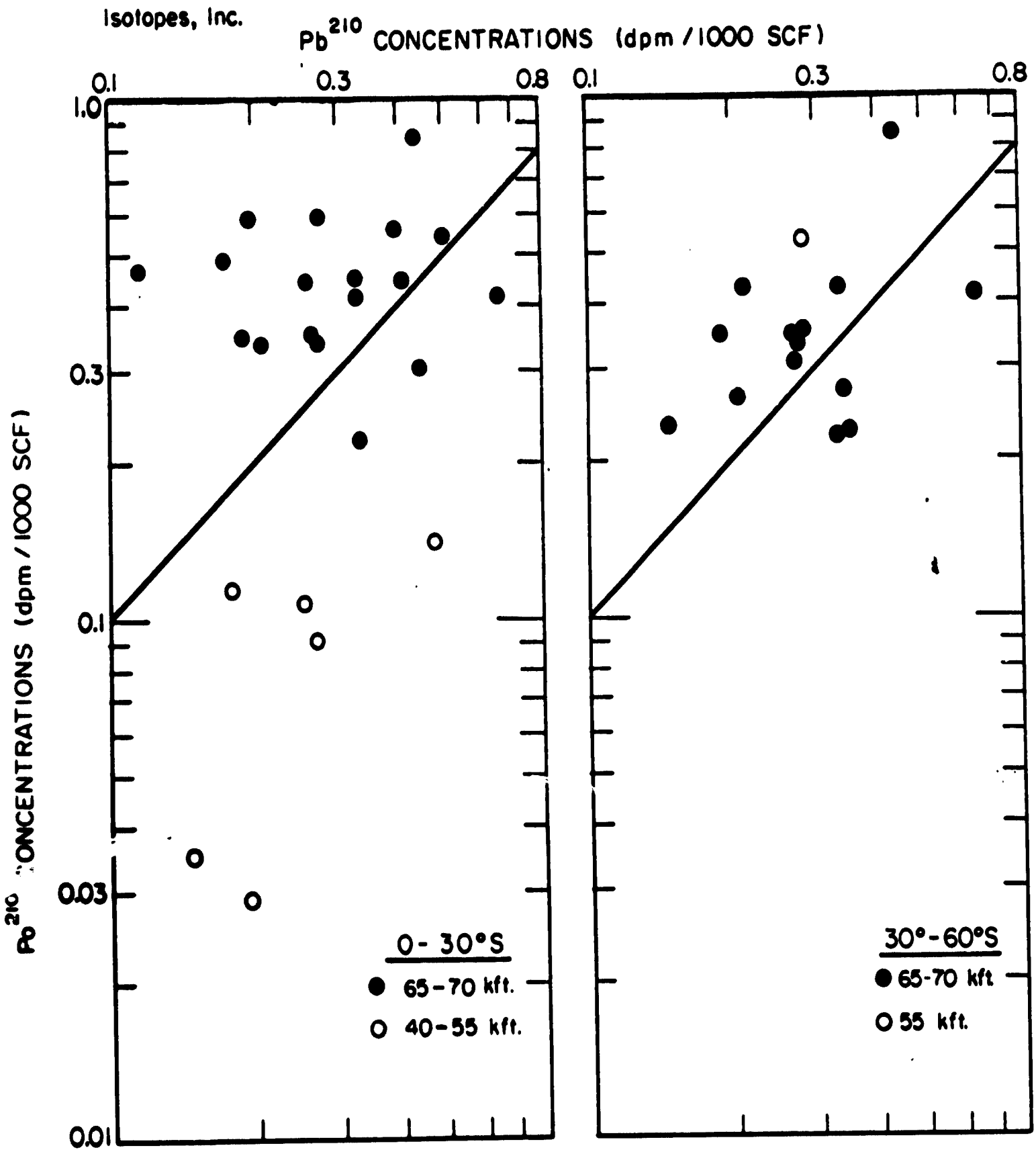

FIGURE 58 · CONCENTRATIONS OF Pb^{210} AND Po^{210} COLLECTED IN THE SOUTHERN HEMISPHERE DURING OCTOBER, 1961-APRIL, 1962

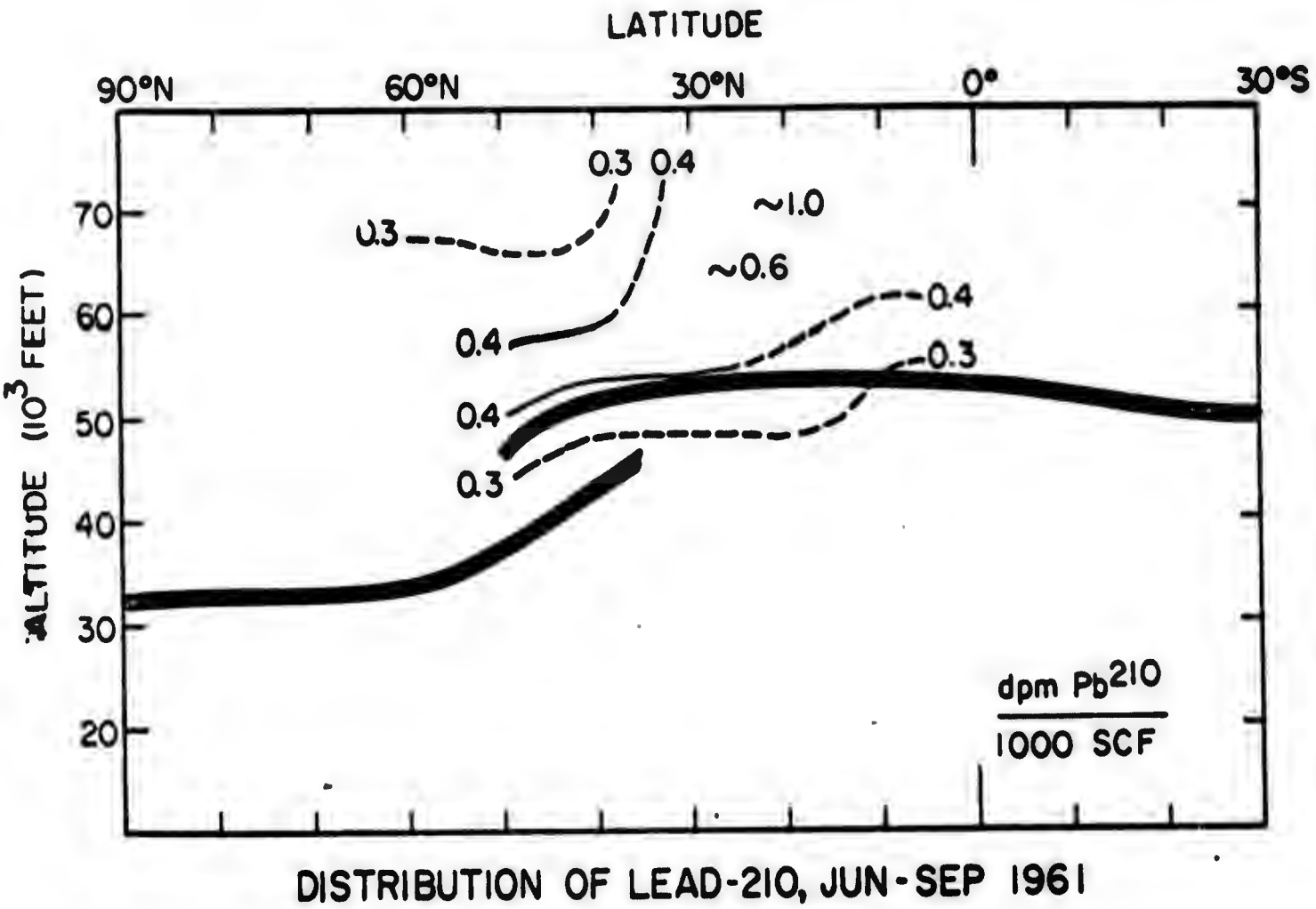

DISTRIBUTION OF LEAD-210, JUN-SEP 1961

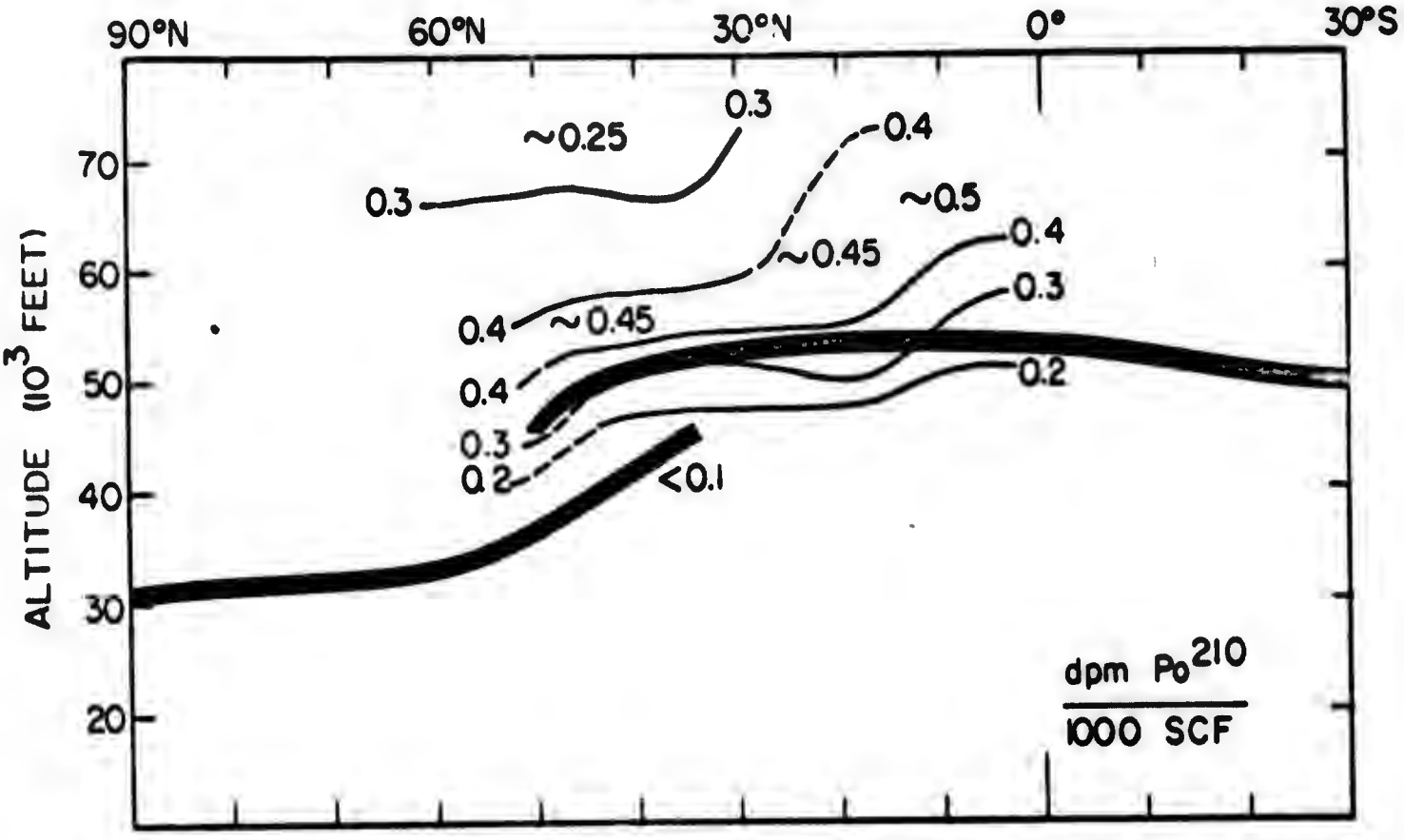

FIGURE 59·DISTRIBUTION OF POLONIUM-210, JUN-SEP 1961

CHAPTER 7. PROGRESS IN THE DESIGN OF THE STAR DUST MODEL

The purpose of the numerical diffusion-general circulation model described in the Fifth Quarterly Progress Report is to provide a rational basis for predicting diffusion and deposition patterns resulting from atmospheric inputs of radioactive materials at arbitrary height, latitude and time of year. The numerical model provides an objective method of experimentation so that the relative importance of the various factors which contribute to the time history of concentration and deposition at fixed points in space and on the ground may be properly evaluated. These experiments are performed by judiciously varying the parameters of the model and then comparing the differences in output with available observational material. The ultimate objective of the numerical experiments is to produce a model with known parameters which correctly reproduces all of the observed data. Only in this manner can one be reasonably confident that the model will correctly predict the results of an arbitrary injection.

The numerical model is capable of handling the following physical processes:

(1) diffusion (with arbitrary coefficients in poleward and vertical directions),

(2) general circulation advective terms (connected in the poleward and vertical directions by the equation of continuity),

(3) finite settling velocity of the particles (and dry fallout at the ground),

(4) arbitrary tropospheric removal mechanisms, and

(5) arbitrary source configurations.

The Initial Series of Experiments

The objective of the initial series of experiments was to attempt to reproduce the significant features of the tungsten-185 experiment as closely as

possible with a pure diffusion-rain out model. The equation to be solved was therefore

$$\frac{\partial q}{\partial t} = \frac{1}{\rho}\frac{\partial}{\partial r}\left(\rho K_r \frac{\partial q}{\partial r}\right) + \frac{1}{r_0^2}\frac{\partial}{\partial \mu}\left[(1-\mu^2) K_\mu \frac{\partial q}{\partial \mu}\right] \qquad (1)$$

where μ = sine of the latitude,

q = concentration (g/g air),

ρ = density of air,

r_0 = mean radius of the earth, and

K_r, K_μ = diffusion coefficients (cm^2/sec) in the r and μ directions respectively.

The rainout mechanism was simulated by removing a certain fraction of the material which had diffused down to rain cloud level after each complete cycle. The removal fraction was assumed to be proportional to the mean annual rainfall in appropriate latitude belts. The factors employed in all the studies reported here are given in Table 18.

The removal levels were assumed to be 6 km, 6 and 8 km, or 4, 6 and 8 km depending upon the specific model. For example, 22% of the material at 6 km (or 6 and 8 km, or 4, 6 and 8 km) and latitude 30^{o}S was removed at every second time step. This material was considered to have been deposited on the ground. For purposes of comparison between the observed spread and deposition of tungsten-185 and individual model predictions, the following were considered essential features of the observed distribution:

Table 18.

Removal Factors Used to Simulate Mechanism

Southern Hemisphere			Northern Hemisphere		
Sin ϕ	ϕ	(REMF)	Sin ϕ	ϕ	(REMF)
-1.0	90°S	0.00	0	0°N	0.45
-0.97	75°S	0.00	0.1	6°N	0.50
-0.9	64°S	0.15	0.2	12°N	0.37
-0.8	53°S	0.33	0.3	17°N	0.25
-0.7	44°S	0.37	0.4	24°N	0.20
-0.6	37°S	0.25	0.5	30°N	0.22
-0.5	30°S	0.22	0.6	37°N	0.25
-0.4	24°S	0.22	0.7	44°N	0.25
-0.3	17°S	0.29	0.8	53°N	0.22
-0.2	12°S	0.32	0.9	64°N	0.12
-0.1	6°S	0.37	0.97	75°N	0.00
-0	0°S	0.45	1.0	90°N	0.00

(a) the decrease of the central concentration with time,

(b) the pattern of concentration in the stratosphere, and

(c) the time history of the deposit of tungsten-185 on the earth's surface.

The two important features of the pattern of concentration in the stratosphere were taken to be:

(1) the behavior of the following concentration ratios:

$$R_1 = \frac{C_{m30°}}{C_m}, \quad R_2 = \frac{C_{m45°}}{C_m}, \quad R_3 = \frac{C_{m60°}}{C_m}$$

where C_m is the maximum value of concentration in the stratosphere, found usually at the injection level, and C_{m30}, C_{m45}, etc. are the maximum value found at 30°N, 45°N, etc., and

(2) the observed decrease in height of the region of maximum concentration as one proceeds from the equator to the poles of both hemispheres.

The finite difference scheme employed was described in the Fifth Quarterly Progress Report. It was found that the time step had to be decreased from one week (6.048×10^5 secs.) to 1/3 week (2.016×10^5 secs.) whenever K_μ was greater than 10^{10} or K_r greater than 5×10^4.

About twenty diffusion-rainout models have been run to date. None of these models reproduces all of the features of the observed distribution and deposit of tungsten-185. It is useful, however, to discuss some aspects of these models. The specific models to be discussed are numbered 8, 10E, 10F and 12C. The diffusion coefficients and removal levels for each model are indicated in Figures 60 to 63. All diffusion coefficients are symmetrical with respect to the equator.

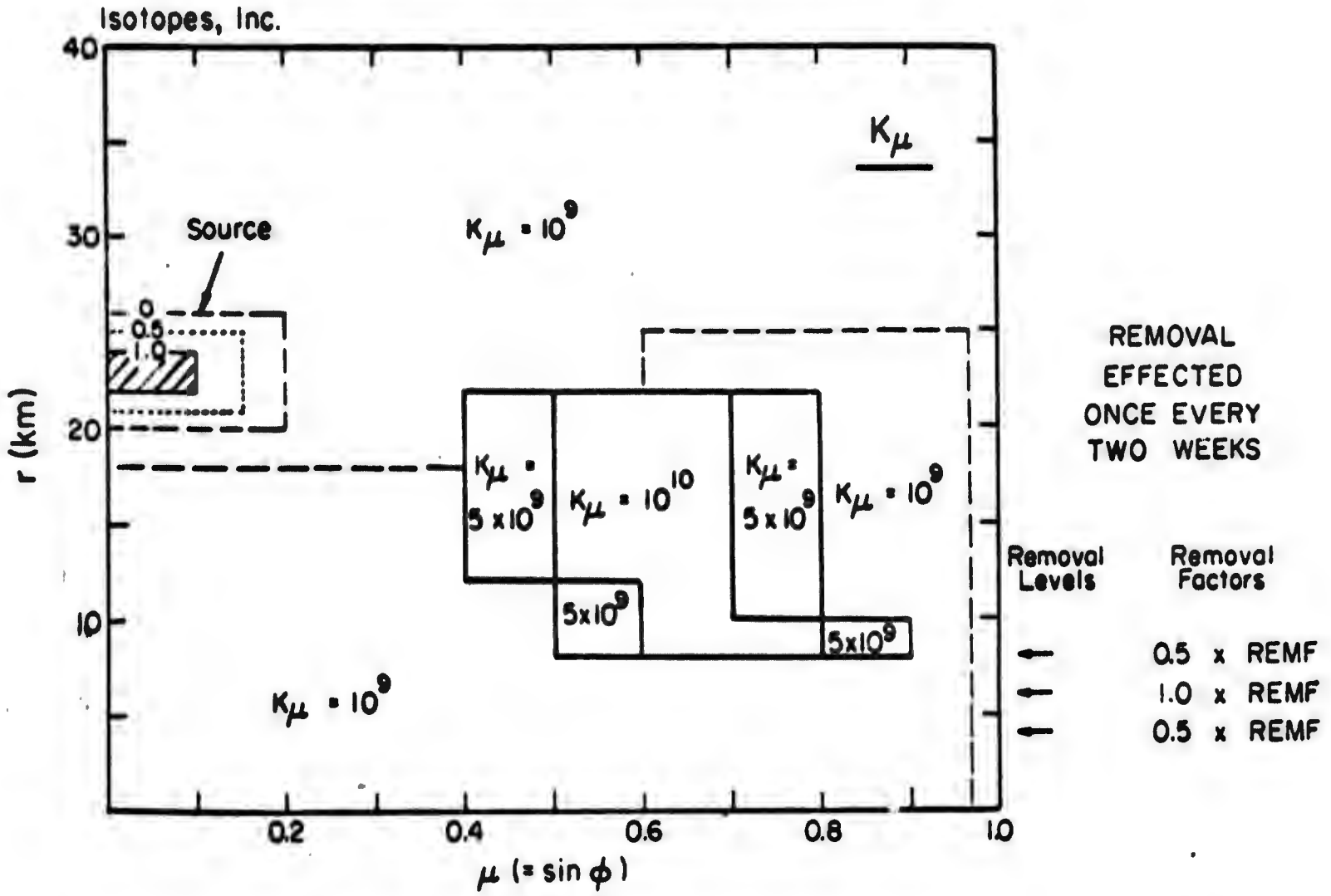

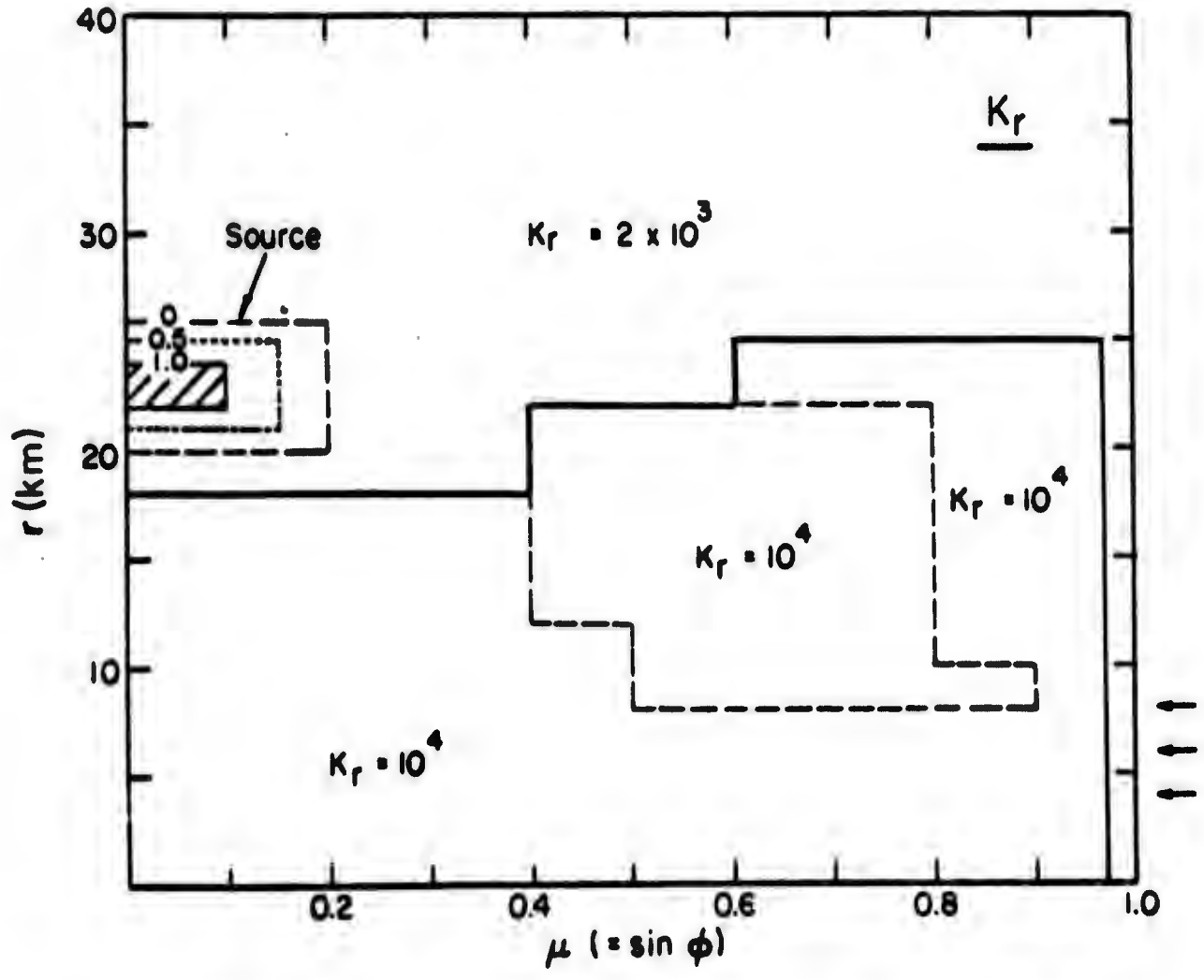

FIGURE 60 · DISTRIBUTION OF K AND REMOVAL FACTORS FOR MODEL 8

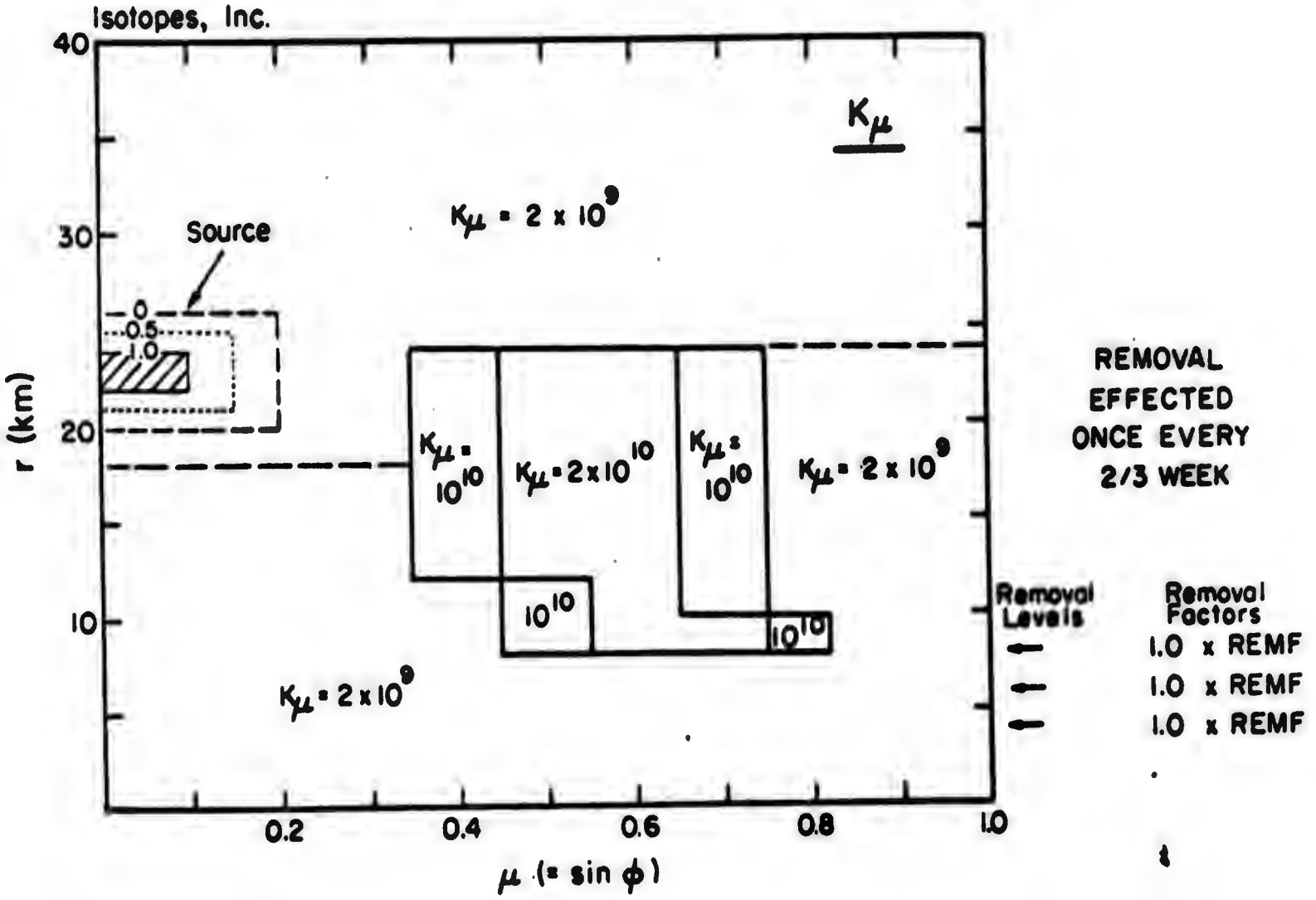

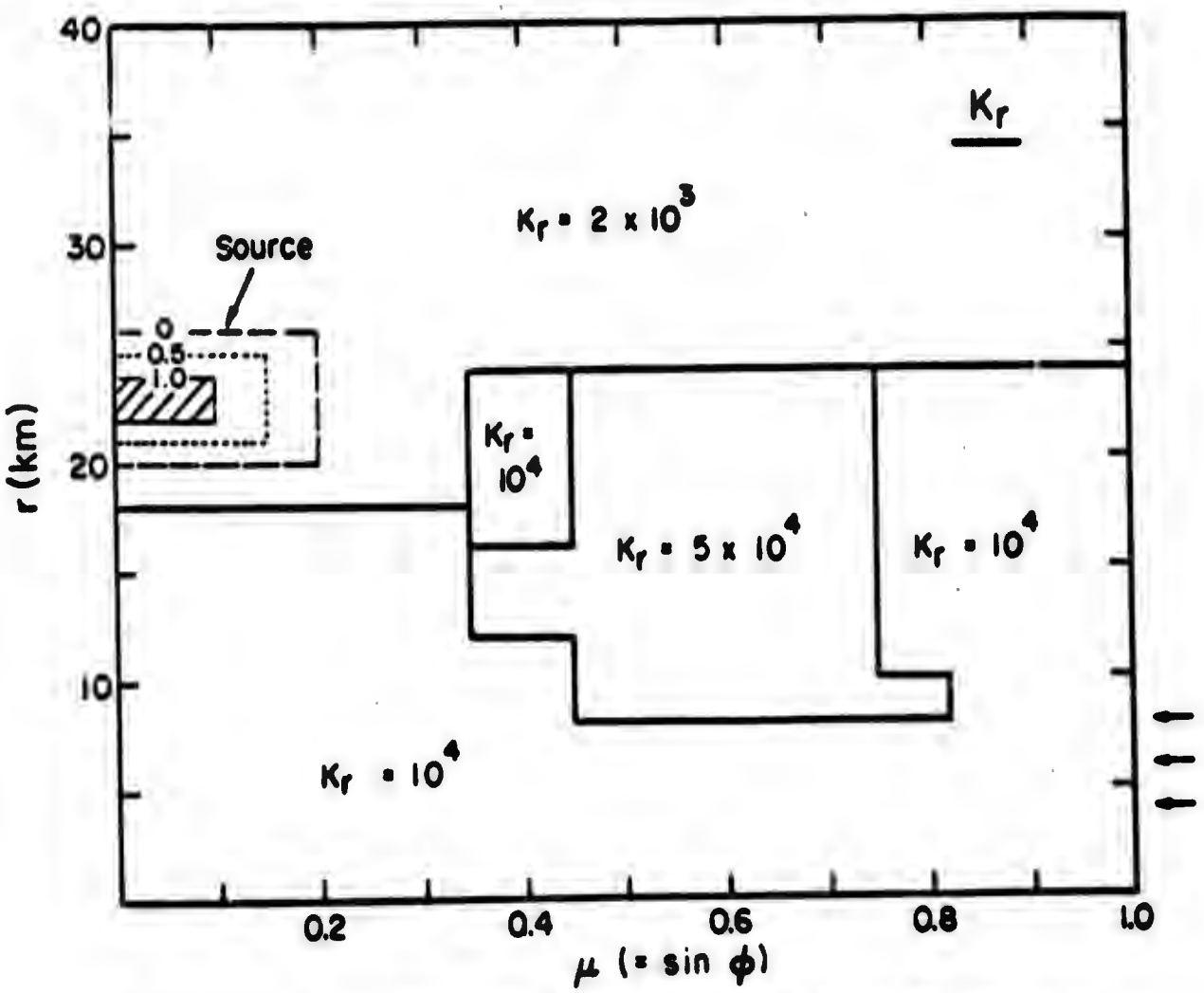

FIGURE 61 · DISTRIBUTION OF K AND REMOVAL FACTORS FOR MODEL 10E

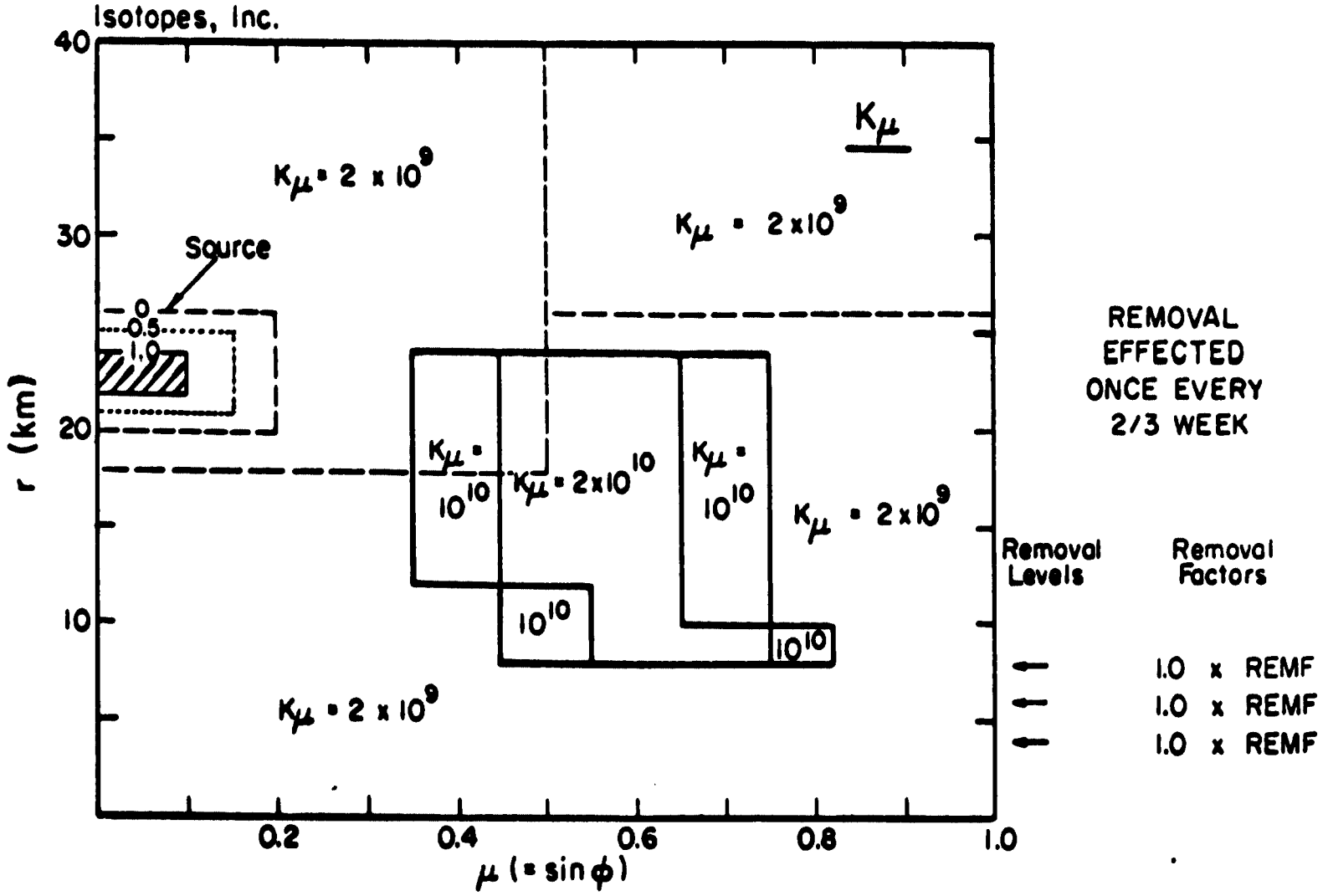

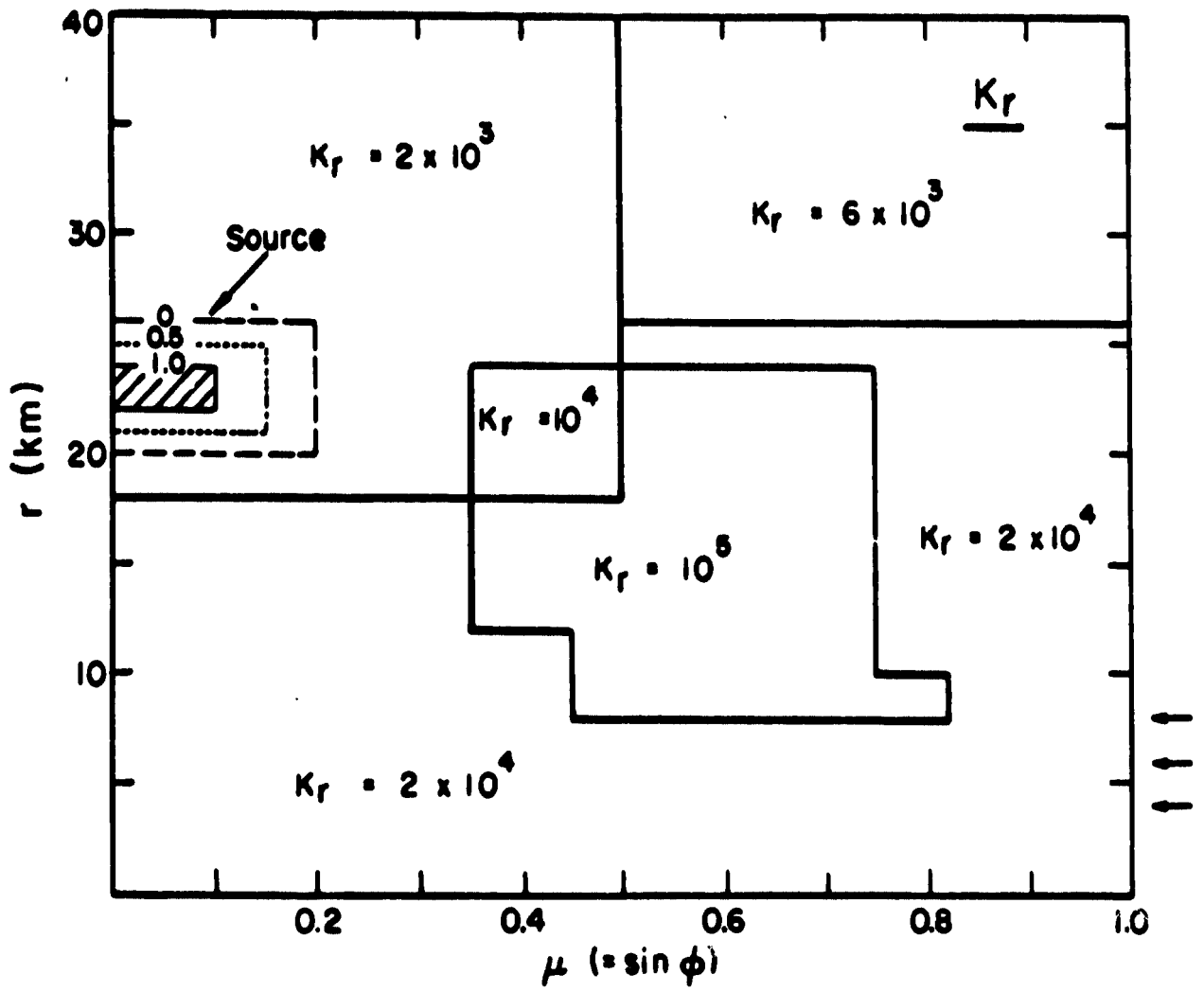

FIGURE 62 · DISTRIBUTION OF K AND REMOVAL FACTORS FOR MODEL 10F

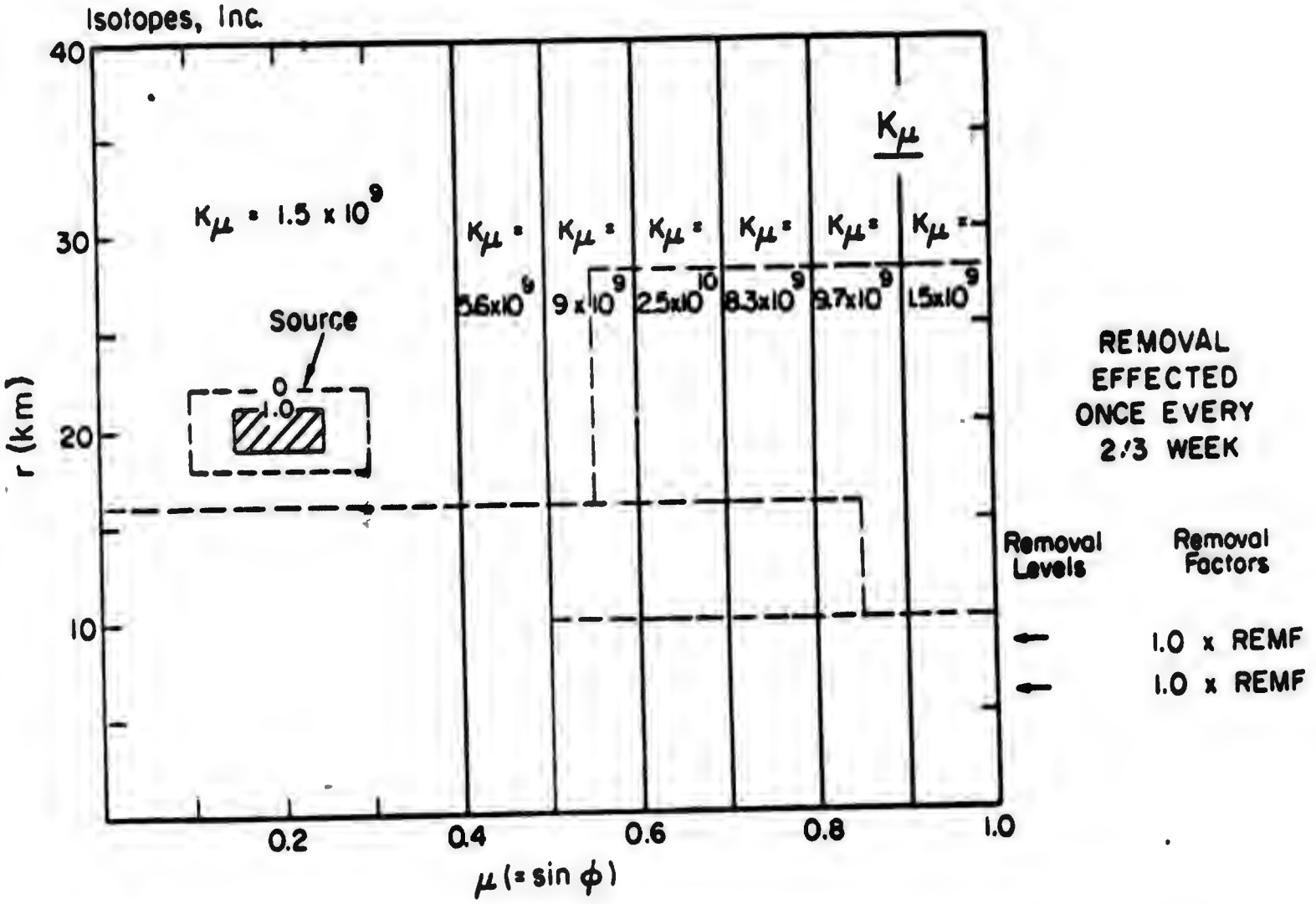

FIGURE 63 · DISTRIBUTION OF K AND REMOVAL FACTORS FOR MODEL 12C

The per cent of total injection removed by the rain process at indicated times after injection for the models described in Figures 60 to 63 is shown in Figure 64. For comparison, estimates of the same quantity observed for the tungsten-185 experiment are shown on the same graph. The latter data are taken from Volume 4 of DASA 1300. It was assumed that the total injection, corrected for decay to 1 July 1958 was 177 megacuries. Despite the differences in the amount of deposition, it may be seen that the curves are roughly parallel on the log-log plot. The curves can be made to coincide by a simple shift in the logarithm of time. The fact that the mathematical forms of the curves are so similar to the observed curve is quite encouraging and indicates that the rainout mechanism employed in the present models is fairly realistic. The comparisons should not be taken too literally, since the source conditions are probably not the same for the experiments and for the numerical models. Subsequent numerical experiments indicated that for exactly the same diffusion coefficients the removal at 40 weeks after injection was 25% for a source 13,000 feet above the tropical tropopause, but was only 9.5% for a source 19,000 feet above the tropical tropopause.

It may be deduced from Figure 64 that the removal curves are quite sensitive to the values of K_r. Doubling the value of K_r in the troposphere and tropopause gap effectively doubles the removal 40 weeks after injection.

The meridional distribution of the deposit for the various latitude belts in the Northern Hemisphere is shown in Figure 65. The solid curves are the observed data (obtained from Volume 4 of DASA 1300) while the dashed curves are those for model 10F. Since the total per cent deposited

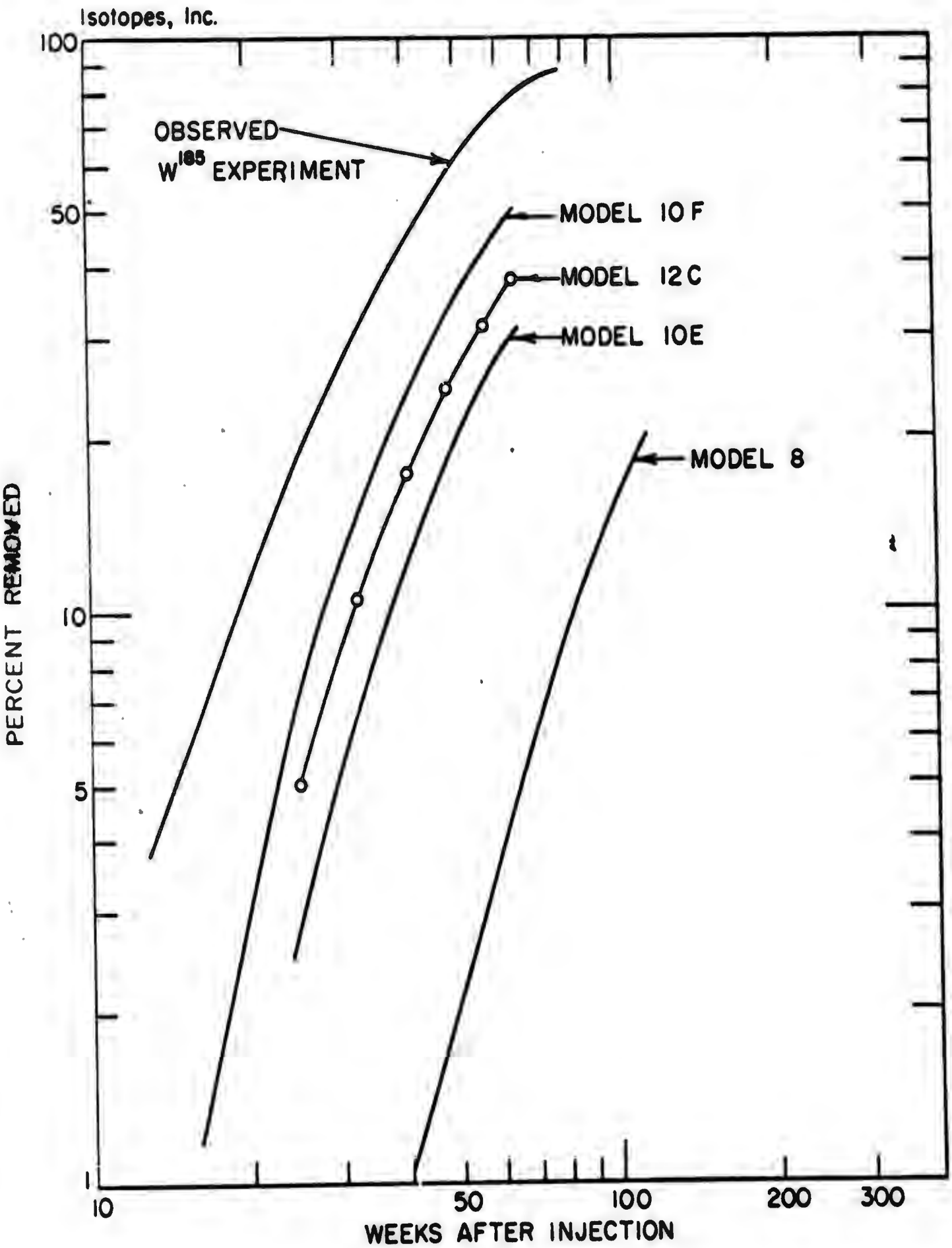

FIGURE 64·PERCENT OF TOTAL INJECTION REMOVED AS A FUNCTION OF TIME

is not the same, the strength of the source for model 10F was arbitrarily raised so that the absolute value of the total deposit over the hemisphere after 40 weeks would be the same for model and experiment. This procedure is arbitrary, but it does allow a visual comparison of the curves. It may be seen that model 10F closely reproduces the observed meridional distribution of rainout. A shift of the model curves about 4^{o} to the north would make the comparison after one year almost perfect except for the equatorial region.

The response of the meridional distribution of rainout to changes in tropospheric vertical diffusion coefficients is quite dramatic. For example, if the basic tropospheric K_r in model 10F is increased from 2×10^4 to 4×10^4, the distribution of the deposit with latitude becomes much flatter than that shown in Figure 65. All in all, however, the rainout mechanism assumed in the model has at least the inherent ability to reproduce the observed deposit data. The problem now is to justify the height distribution of K_r.

For example, a value of $K_r = 10^5$ at 22 km (above both the polar and tropical tropopause) seems unreasonably large. The present model assumes that the principal axes of the diffusion tensor are along the horizontal and vertical directions respectively. It is entirely possible and almost probable that a principal axis for large scale diffusion is along an isentropic surface. One possible way of modelling this effect is to assume that $K_r \approx K_r' + K_y \eta$ where η is the slope of the isentropic surface and K_r' is the diffusion coefficient in the radial direction. Since K_y is of the order of 10^9, $K_y \eta$ is of the order 10^4 if the slope of the isentropic surface is 10^{-5}, a not unreasonable value. This matter will be investigated further as the work proceeds.

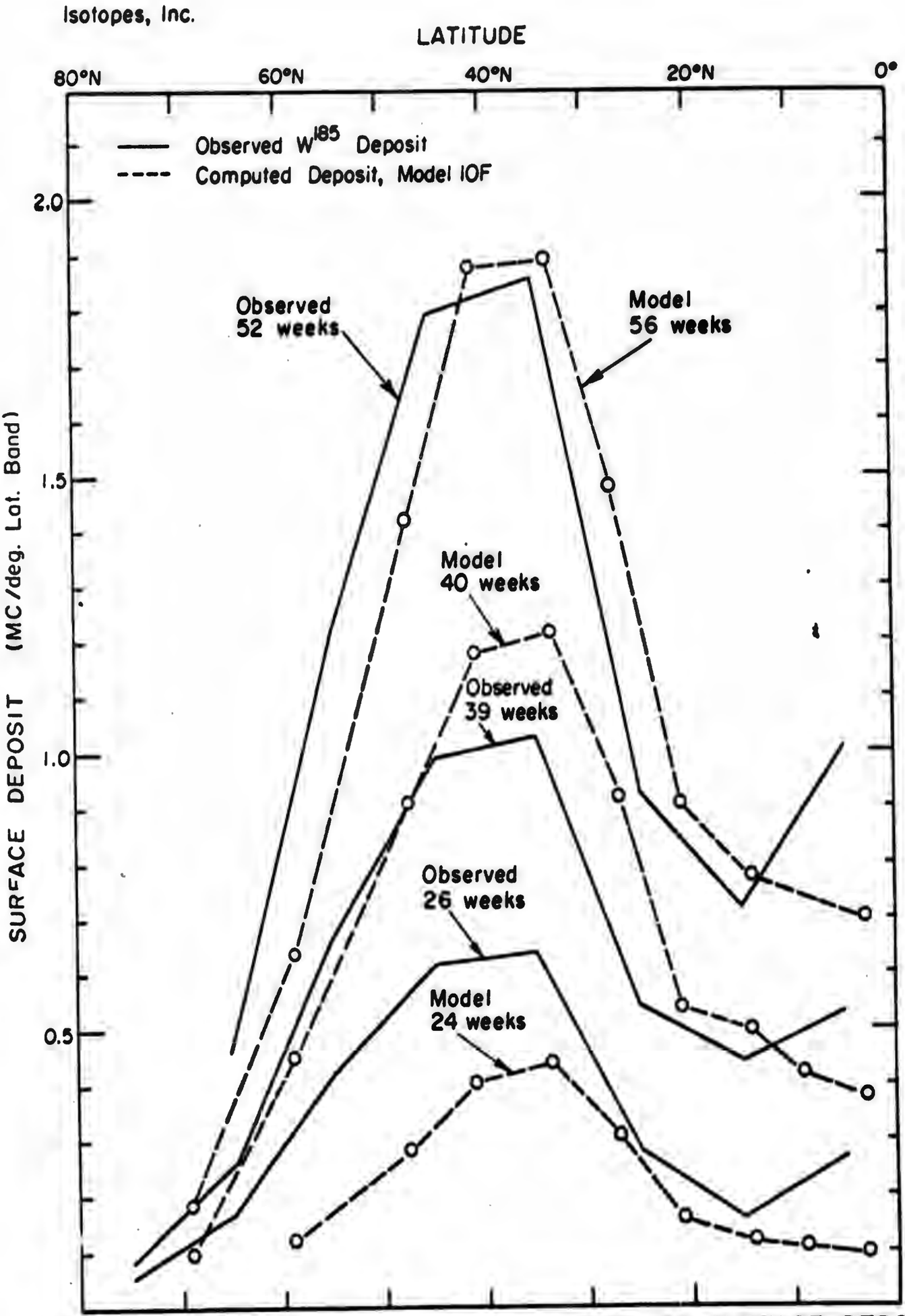

FIGURE 65 · DISTRIBUTION OF TUNGSTEN-185 SURFACE DEPOSIT AT VARIOUS TIMES

The decrease of central concentration with time in the models run thus far is rather slower than the observed decrease. This is shown in Figure 66, where the slopes of the decrease of central concentration with time are compared for models 8, 10F and 12C, with an estimated slope for the observed data. The scale of concentration here is arbitrary. The only purpose is to show how the slope of the curve varies from model to model. It is evident that the observed slope is steeper than is the slope for any of the models. The slope is evidently a function of the source (point or square), of the variation of K_μ with latitude, and of the rainout mechanism. The later models suggest that with more rapid rainout and perhaps a larger variation of K_μ with latitude, the model slopes may approach the observed slope.

The observed values of R_1, R_2 and R_3 are not too difficult to reproduce in the models. A basic value of K_μ of about 1.5×10^9 at the equator can reproduce these features of the observed distribution. The most difficult feature of the observed distribution to reproduce is the decrease in the height of the maximum concentration as one proceeds from equator to pole. It was possible to reproduce this feature in the early stages of a model by suitable variation of K_r with height in the polar stratosphere and of K_μ with latitude and height. For example, the pattern of concentration in the stratosphere for model 8 at 16 weeks after injection is shown in Figure 67, while the pattern of concentration 120 weeks after injection is shown in Figure 68. It is apparent from Figure 67 that the level of maximum concentration decreases by about 2 km from the equator to 53°N. But as time progresses and the rainout mechanism becomes more important, the level of maximum concentration in the stratosphere begins to rise (see Figure 68)

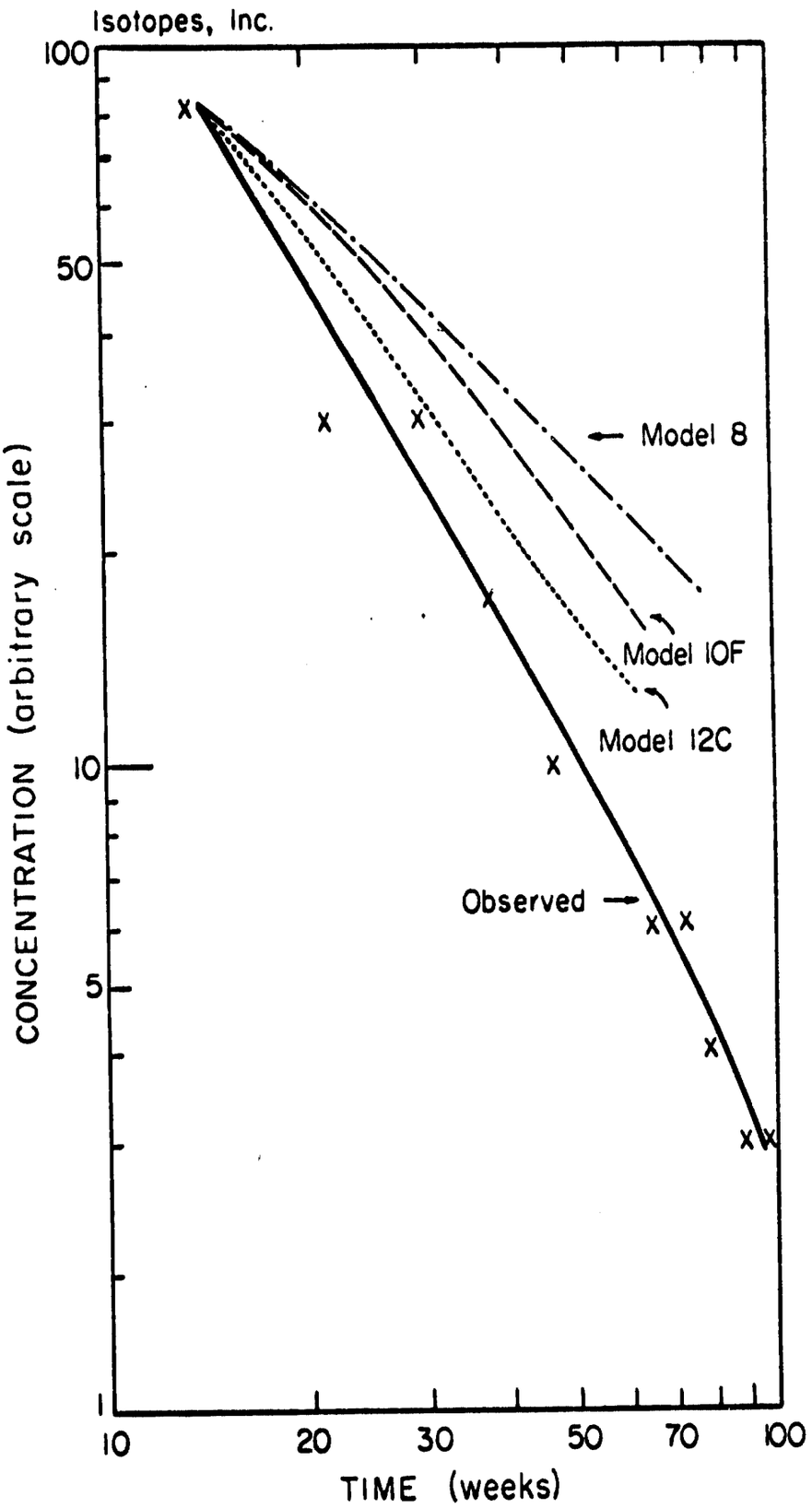

FIGURE 66 · CENTRAL CONCENTRATION AS A FUNCTION OF TIME

Isotopes, Inc.

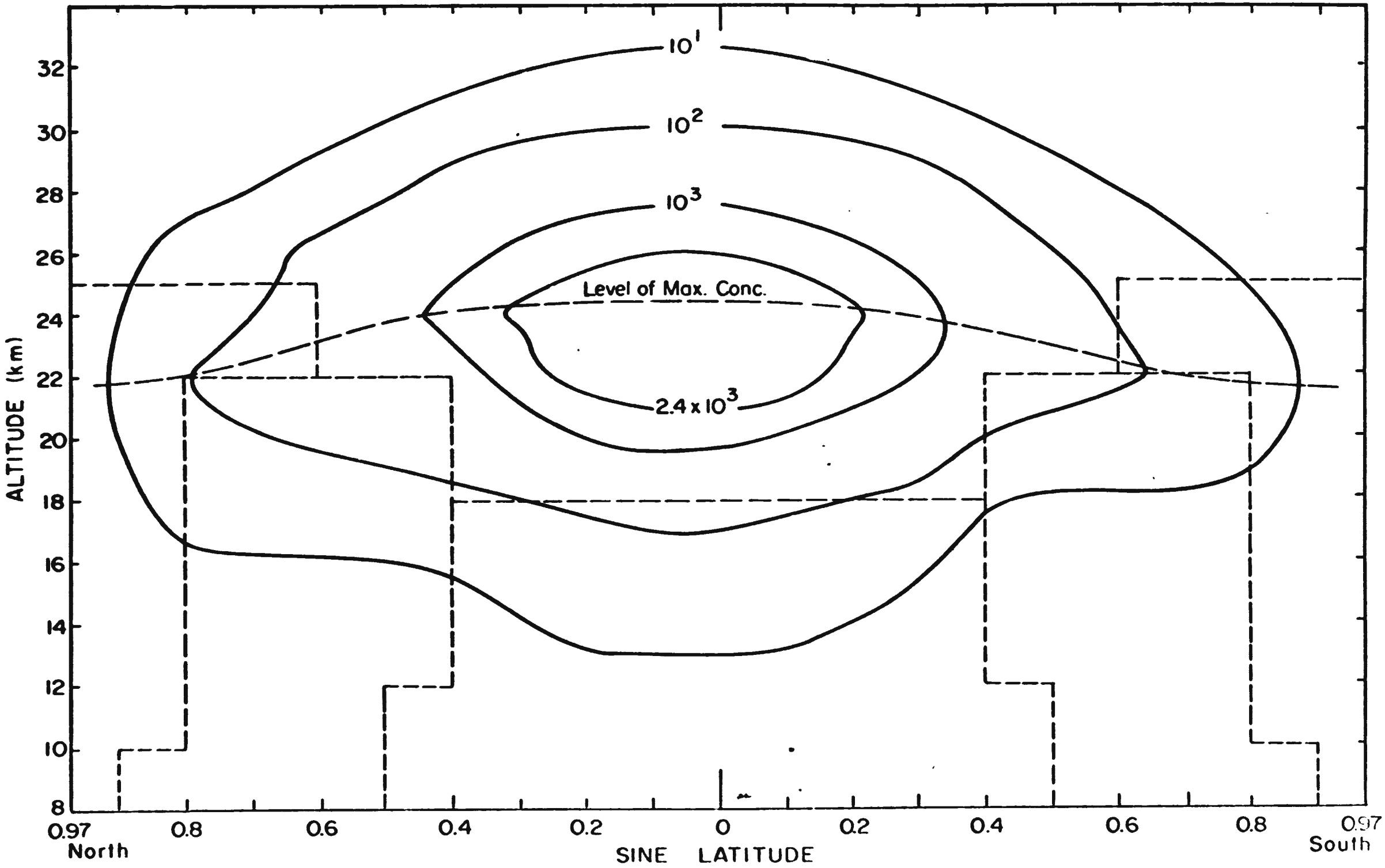

FIGURE 67 · DISTRIBUTION OF q AFTER 16 WEEKS, MODEL 8

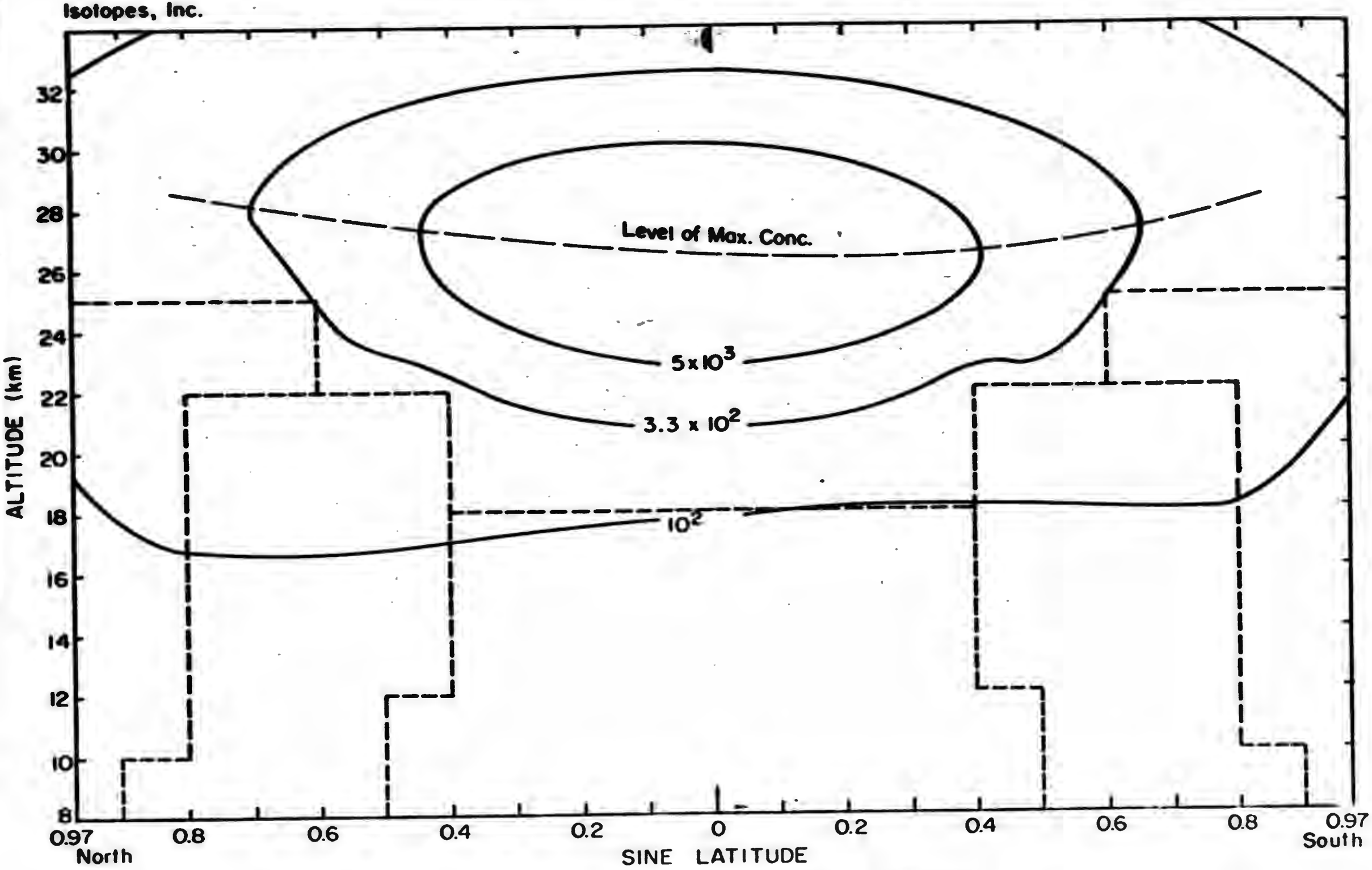

FIGURE 68 · DISTRIBUTION OF q AFTER 120 WEEKS, MODEL 8

and eventually rises above the level of the equatorial maximum. The more rapid the removal, the more rapidly does the level of maximum concentration in the stråtosphere rise at 45° and 50°N. Attempts to remedy this situation by adjusting K_r within a reasonable range in the polar stratosphere have met with little success.

Subsequent Experiments

At this stage in the development of the model, it was decided to incorporate the effect of both particle terminal velocity and non-zero values of V and W into the model. The initial experiments in this phase dealt only with the effect of particle terminal velocity which was made to be a function of altitude. The relevant term as it appears in the left hand side of the equation is

$$\frac{1}{\rho}\frac{\partial}{\partial r}(\rho\Omega q) \tag{2}$$

It was quickly found that the finite difference scheme sketched in the Fifth Progress Report yielded negative concentrations near the top of the model, especially when Ω was relatively large. Decreasing the time step helped this situation not at all. After some experimentation the following finite difference scheme for handling this term was found to yield positive values of concentration for values of Ω of interest to us. Thus, at the point j, k

$$\frac{1}{\rho}\frac{\partial}{\partial r}(\rho\Omega q) = \left[(\rho\Omega q^n)_{j,k+1} - (\rho\Omega q^n)_{j,k}\right] \Big/ \rho_k (r_{k+1} - r_k) \tag{3}$$

Since Ω is always negative, this scheme amounts to a simple upstream differencing technique. This term is always treated explicitly.

The few experiments run with values of Ω indicate that the rainout rate is quite sensitive to this term and that the tendency for the level of maximum concentration at the source to rise due to the variation of density with height can be exactly counterbalanced with an appropriate field of Ω .

Experimentation continued now with incorporation of general circulation velocities into the basic diffusion model. The relevant terms as they appear on the left hand side of the basic equation are

$$\frac{v \cos\phi}{r_0} \frac{\partial q}{\partial \mu} + w \frac{\partial q}{\partial r} \qquad (4)$$

where v is the mean meridional velocity and w the mean vertical velocity. Both v and w are subject to the continuity constraint

$$\frac{1}{r_0} \frac{\partial}{\partial \mu} (\rho v \cos\phi) + \frac{\partial}{\partial r} (\rho w) = 0 \qquad (5)$$

It soon became apparent that the finite difference scheme outlined in the Fifth Quarterly Progress Report for the two terms in equation (4) was defective in at least two respects. In the first place, negative concentrations are often produced, and in the second place it is almost impossible to write a simple but consistent finite difference scheme for equation (5) which will not locally distort the concentration field at a point (j, k) when inserted into equation (4). Upstream advection techniques were tried with equation (4). These resulted in positive concentrations throughout the field but failed to

conserve the total amount of diffusing material. The upstream differencing techniques will not conserve mass and in certain configurations of the initial conditions, the change in mass with time is intolerable.

It was finally decided to treat the two terms of equation (4) as follows: First, the equation of continuity is added to (4) resulting in

$$\frac{1}{\rho}\frac{\partial}{\partial r}(\rho w q) + \frac{1}{\rho r_0}\frac{\partial}{\partial \mu}(\rho v \cos\phi\, q) \tag{6}$$

Centered differencing techniques are used for (6) such that evaluating q^{n+1} at the point (j, k)

$$\frac{1}{\rho}\frac{\partial}{\partial r}(\rho w q) = \left[(\rho w q^n)_{j,k+1} - (\rho w q^n)_{j,k-1}\right] \Big/ \rho_k (r_{k+1} - r_{k-1}) \tag{7}$$

$$\frac{1}{\rho r_0}\frac{\partial}{\partial \mu}(\rho v \cos\phi\, q) = \left[(v\cos\phi\, q^n)_{j+1,k} - (v\cos\phi q^n)_{j-1,k}\right] \Big/ r_0(\mu_{j+1} - \mu_{j-1})$$

The terms in equation (7) are handled explicitly for all time steps. It can be shown that, if the boundary conditions are treated correctly, equation (7) will conserve the mass of the diffusing substance, although there is no guarantee now that q will be positive.

In order to ensure that no local distortions occur, the equation of continuity in consistent finite difference form is

$$(\rho w)_{j,k+1} = (\rho w)_{j,k-1} - \left[\frac{r_{k+1} - r_{k-1}}{r_0(\mu_{j+1} - \mu_{j-1})}\right]\left[(\rho v\cos\phi)_{j+1,k} - (\rho v\cos\phi)_{j-1,k}\right] \tag{8}$$

The field of **W** may be computed from a given field of **V**, or the field of **V** from a given field of **W** provided that **V = 0** at the poles and that **W** at the two lowest grid points is assumed to be zero.

Models run with assumed but mutually consistent fields of **V** and **W** indicate that for certain circulations the height of maximum concentration can decrease from equator to pole. More important, the latitudinal variation of the height of maximum concentration in the stratosphere can be maintained for at least two years with a strong mid-tropospheric sink (rainout process). One such circulation which can produce the desired result in the Northern Hemisphere with a source at 12°N is downward motion at 30°N, poleward motion from 30° - 60°N at 40 to 55 thousand feet, upward motion at 60°N and equatorward motion from 60 to 80 thousand feet between latitudes 60° and 30°N.

Incorporation of general circulation terms in the model increases the possible number of degrees of freedom considerably. At this point, therefore it was decided to begin experimenting with north polar tracer injections. The aim here is to provide a model which will agree with the observed results of both polar and near-equatorial injections. In order to be able to handle polar injections, it was necessary to provide many more grid points in polar latitudes than was the case in the first version of the model. Accordingly, the model was reprogrammed to minimize storage requirements and a grid of 30 x 28 points was adopted. The height interval was reduced from 2 to 1.5 km. There are 17 latitudinal points in the Northern Hemisphere and 12 in the Southern Hemisphere. The latitudinal definition in the Northern Hemisphere corresponds to a latitudinal grid spacing of slightly more than 5° per grid point. The reprogramming process was far more efficient than was

thought possible at the beginning and, if necessary, there is room now for an even greater number of grid points than 30 x 28 without resort to tape memory. The new program is in the process of being checked out.

CHAPTER 8. MEASUREMENTS OF CARBON-14 CONCENTRATIONS IN GROUND LEVEL AIR

The measurement of the concentration of carbon-14 in the carbon dioxide of ground level air in northern New Jersey which was begun during Project HASP, has been continued during Project Star Dust. Two samples are collected each month at the Township of Washington, Bergen County, New Jersey.

The samples are collected by exposing to the atmosphere approximately 150 ml. of 4N KOH solution contained in two Petri dishes. Approximately every third day the Petri dishes are emptied into a polyethylene bottle and are then refilled with fresh KOH solution. On about the first and fifteenth day of each month the accumulated sample, consisting of about 750 ml is taken to the laboratory and is processed. The solution is acidified with phosphoric acid to release the dissolved carbon dioxide. The evolved gas is collected and is purified twice using calcium oxide furnaces. It is then admitted to a two liter proportional counter and is counted twice, the first time for approximately 300 minutes and the second time for approximately 900 minutes.

The results of measurements of samples collected since January 1963 are listed in Table 19. Results of measurements of earlier samples were given in the sixth quarterly report. The concentrations are expressed in per cent above the activity of the National Bureau of Standards oxalic acid carbon-14 standard.

A pronounced rise in the carbon-14 concentrations began in April 1963, no doubt as the result of the release into the troposphere during the spring of 1963 of carbon-14 injected into the stratosphere by the 1961 and 1962 weapons test series. A concentration of + 91.0 per cent was reached in early August 1963. This was more than twice as high a concentration of artificial carbon-14 as was found during any year before 1963.

Isotopes, Inc.

The results of all carbon-14 measurements performed during Projects HASP and Star Dust have been used in preparing Figure 69, which shows the dramatic increase which occurred in ground-level carbon-14 concentrations during 1963. The tendency for carbon-14 concentrations in northern New Jersey to decrease during the late autumn and early winter season, only to increase again during the late winter, is evident from the data in Figure 69. Presumably this pheonomenon is related to the dilution of carbon-14 in ground-level air during the autumn and winter by "dead" carbon dioxide released by the consumption of fossil fuels. Bergen County lies within the heavily populated, highly industrialized region of the northeastern United States.

The accumulated strontium-90 deposit at Westwood, New Jersey, which is calculated from measurements on samples of rain and snow, is plotted in Figure 70 together with a curve drawn through the mean monthly carbon-14 activities in ground level air at the Township of Washington. Both curves show the increasing rate of fallout accumulation during 1962 and 1963.

Table 19. Carbon-14 Concentrations* in Ground-Level Air at Washington Township, Bergen County, New Jersey

Star Dust No.	Collection Interval	δC^{14}
SD-34	1 Jan 63 - 16 Jan 63	+ 30.0
SD-35	16 Jan 63 - 1 Feb 63	+ 26.0
SD-36	1 Feb 63 - 16 Feb 63	+ 35.0
SD-37	16 Feb 63 - 1 Mar 63	+ 38.1
SD-38	1 Mar 63 - 16 Mar 63	+ 38.0
SD-39	16 Mar 63 - 1 Apr 63	+ 34.5
SD-40	1 Apr 63 - 17 Apr 63	+ 50.8
SD-41	22 Apr 63 - 1 May 63	+ 53.3
SD-42	1 May 63 - 14 May 63	+ 64.0
SD-43	14 May 63 - 31 May 63	+ 66.5
SD-44	31 May 63 - 14 Jun 63	+ 65.6
SD-45	14 Jun 63 - 2 Jul 63	+ 80.2
SD-46	2 Jul 63 - 15 Jul 63	+ 90.0
SD-47	15 Jul 63 - 31 Jul 63	+ 81.5
SD-48	31 Jul 63 - 15 Aug 63	+ 91.0
SD-49	15 Aug 63 - 31 Aug 63	+ 90.0

*The concentrations are expressed in per cent above the activity of the National Bureau of Standards oxalic acid carbon-14 standard.

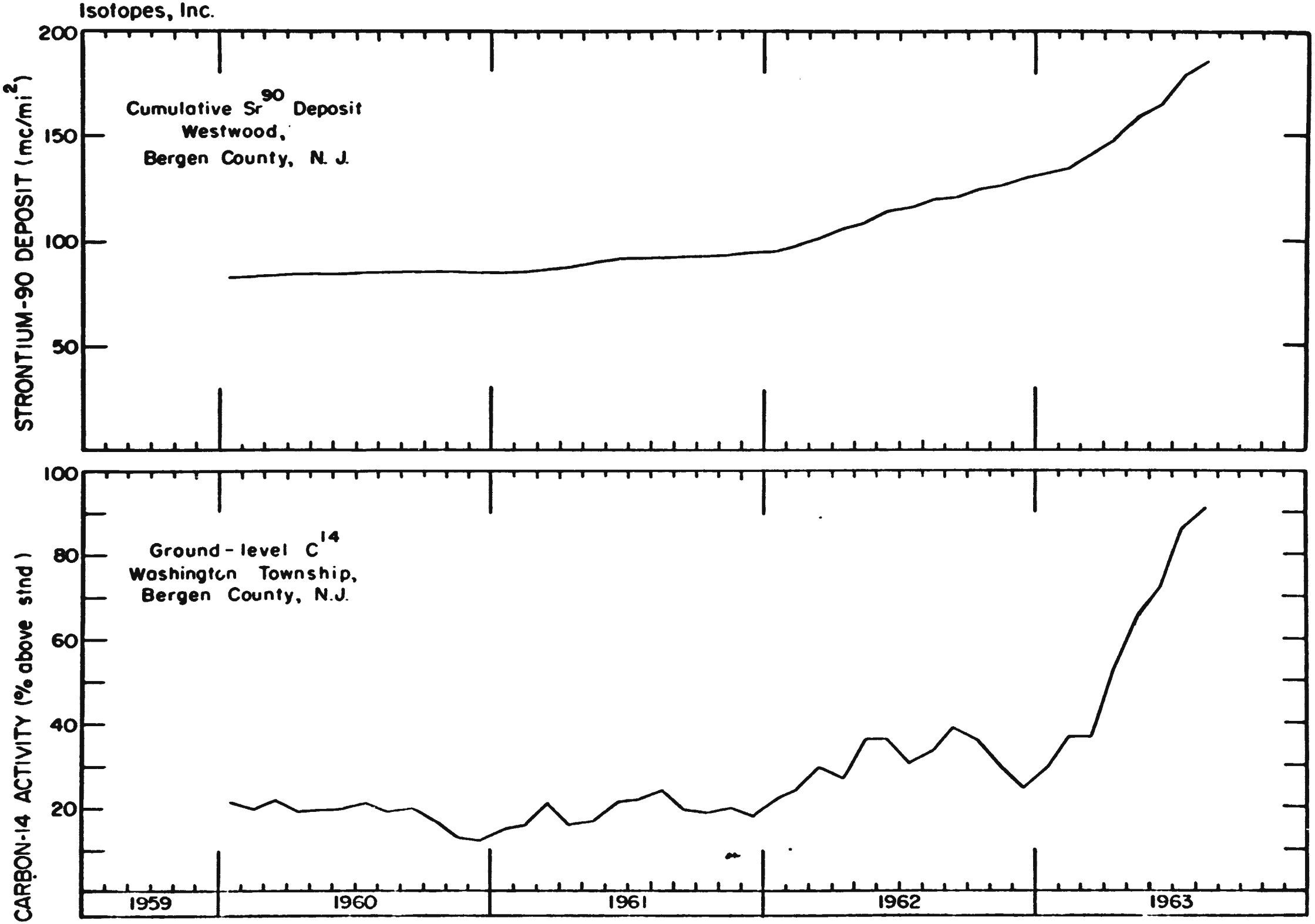

FIGURE 70 · TRENDS IN CUMULATIVE STRONTIUM-90 DEPOSIT AND IN GROUND-LEVEL CARBON-14 CONCENTRATIONS

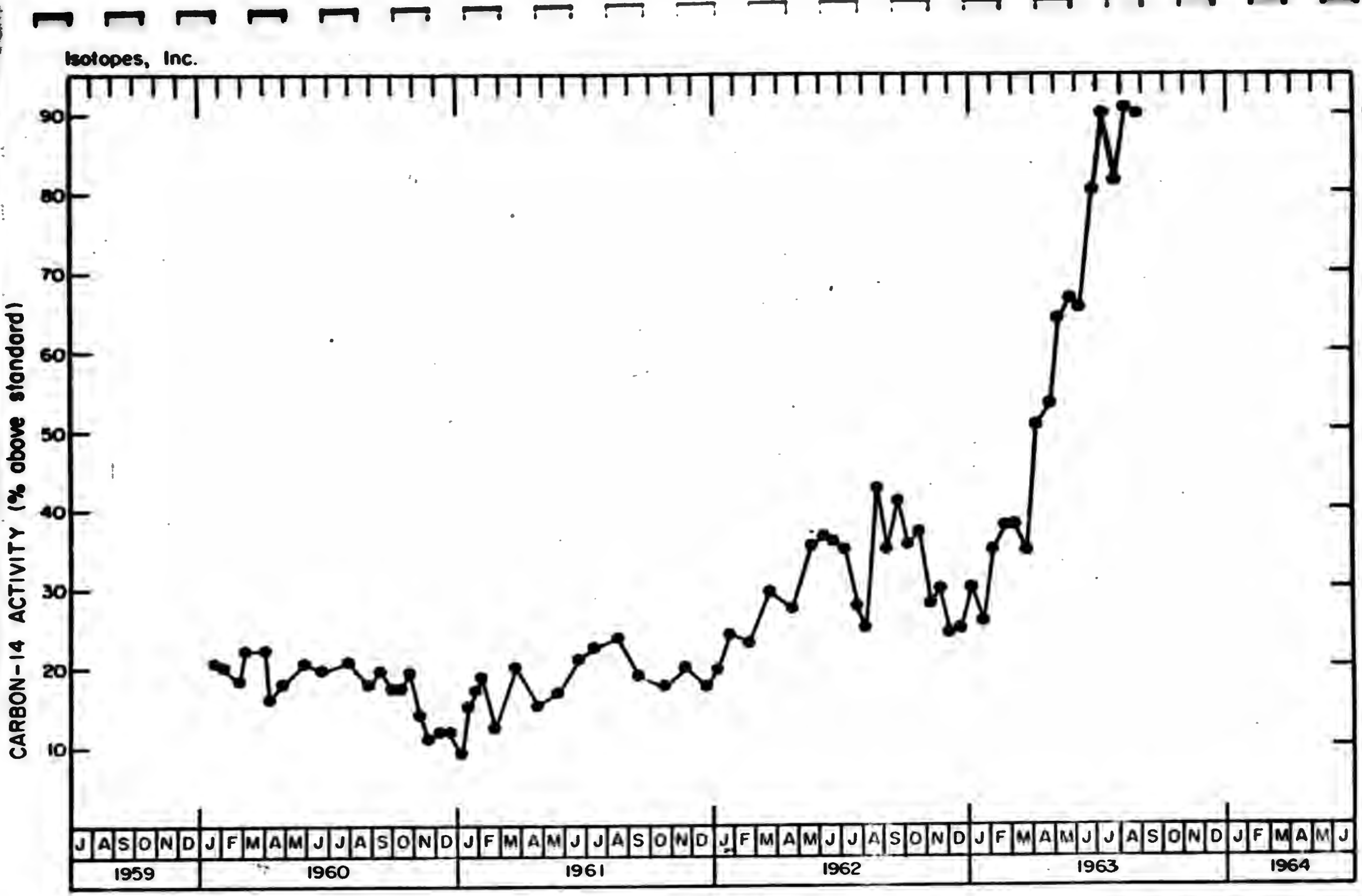

FIGURE 69 · CONCENTRATIONS OF ARTIFICIAL CARBON-14 IN GROUND-LEVEL AIR, TOWNSHIP OF WASHINGTON, BERGEN COUNTY, NEW JERSEY

Isotopes, Inc.

CHAPTER 9. THE DISTRIBUTION OF FISSION PRODUCTS IN KANSAS SOILS COLLECTED IN 1960

A limited study was undertaken during Project HASP of the vertical distribution of several fission products in a series of soil samples. Results were given in the final report on Project HASP[1] for the analyses of samples taken from several depths at each of 11 sampling sites in New Jersey and 2 sampling sites in Kansas during 1960. Additional analyses have been performed during Project Star Dust on samples collected in Kansas during 1960. A brief discussion of these new data will be presented here. In a later report we will review these data together with the results of analyses of soil samples collected in New Jersey during 1962 and 1963.

Plan of the Analyses

The purpose of the soil analysis program in Projects HASP and Star Dust has been the determination of the vertical distribution in the soil of gamma-emitting fission products, such as cesium-137, ruthenium-106 and cerium-144, which contribute to the external radiation health hazard from radioactive fallout from nuclear weapons tests, and the vertical distribution of strontium-90, which has generally been considered to be, potentially, the most hazardous fallout nuclide. In the selection of sites to be sampled, an effort was made to obtain samples which would exhibit wide ranges in as many compositional and structural characteristics as possible. Eastern Kansas was chosen for the collection of samples because the soils found there are significantly different from those found in the eastern half of the United States (including New Jersey where sampling was also being performed) but the climate is sufficiently humid to make the area an important agricultural region. The lesser importance of agriculture in most of the semi-arid and arid regions of the Western United States

and the lower fallout rates there combined to make the states west of Kansas appear less desirable as sampling locales.

The sampling apparatus and techniques used to collect the samples were described in DASA-1300, the final report on Project HASP. The collected cores were 24 inches long and 12 inches in diameter. For the radiochemical analyses a core 8 inches in diameter was taken from the 12 inch core. The outer margins of the 12 inch diameter core, which might have suffered contamination of the lower layers by material from the higher layers during core collection, were discarded. Each core was sliced into a series of layers, which were taken as separate samples. Since most of the fission product activity in the cores was in the upper few inches, thinner layers were taken from the tops than from the bottoms of the cores. The layers generally taken were, starting at the top of the cores, 0 to 1/2 inch, 1/2 to 1 inch, 1 to 2 inches, 2 to 3 inches, 3 to 4 inches, 4 to 6 inches, 6 to 9 inches and 9 to 12 inches. In one of the cores discussed here the layers between 12 and 18 inches and between 18 and 24 inches were also sampled and were analyzed. Generally it was expected that the quantities of fission products in these lower layers would be negligible and therefore it would not be necessary to analyze the layers taken from depths below 12 inches.

The fission products measured in the Kansas soils, strontium-90, ruthenium-106, cesium-137 and cerium-144, were the same nuclides which had been measured in the New Jersey soils. As with the New Jersey soils, all data were corrected for decay to 1 July 1960. Unfortunately, the data obtained, and especially those for ruthenium-106 and cerium-144, were inferior in accuracy and precision to those obtained for the New Jersey samples and reported in DASA-1300. Nevertheless most of the data, and especially those for the upper few

Isotopes, Inc.

inches of soil, are usable.

Acknowledgments

We wish to acknowledge here, as we did in DASA-1300, that during the planning and accomplishment of the sampling phase of this soil program assistance was given us by numerous individuals who were not directly associated with the project. With regard to the sampling in Kansas we especially wish to express out gratitude to A. P. Nelson, Soil Conservationist, Salina, Kansas, who gave us invaluable aid in the selection of suitable sampling sites, and to Soil Conservation Service employees H. Penner, J. Rockers and D. Rott who accompanied us to the sampling sites and prepared descriptions of the soil profiles.

We also wish to thank again those who discussed with us the aims of this work and the procedures to be followed in accomplishing it. These included Dr. J. C. F. Tedrow of Rutgers University, G. A. Quackenbush, K. P. Wilson, S. L. Tinsley and M. Bolline of the Soil Conservation Service and Dr. L. T. Alexander of the U. S. Department of Agriculture at Beltsville, Maryland.

We also wish again to express our gratitude to Dr. R. G. Menzel of the Agricultural Research Service at Beltsville who provided a generous supply of pre-1945 soil to be used in "blank" samples.

Description of Kansas Soil Samples

Descriptions of all of the soil samples collected in Kansas during 1960 and analyzed radiochemically are given in Table 20. These descriptions contain all of the data on the physical, chemical and mineralogical characteristics of the samples which are available to us. The sampling sites are marked on the map of Eastern Kansas which is shown in Figure 71.

Table 20. Descriptions of Kansas Soil Samples

Soil Sample Number 27

Soil Type: Shellabarger sandy loam.

Location: 150 feet East and 40 feet South of the Northwest corner of Section 22-T25S-R7W, Reno County, Kansas.

Date of Sampling: September 26, 1960

Physiographic Position: Upland.

Climate: Subhumid (27" annual rainfall).

Drainage: Well drained, permeability moderate.

Vegetation: Native grass.

Described by: James J. Rockers, Soil Scientist, Soil Conservation Service.

Soil Profile Description

Horizon	Depth	Description
A_1	0-11"	Dark gray brown (10YR4/2d) very dark gray brown (10YR3/2m); sandy loam; weak granular; soft when dry, very friable when moist; numerous roots; pH 5.6; grades to A_3.
A_3	11-17"	Dark gray brown (10YR4/2d) very dark gray brown (10YR3/2m); sandy loam; moderate, medium granular; soft when dry, very friable when moist; numerous roots; pH 6.0; grades within about 3" to B_2.
B_2	17-29"	Brown (10YR4/3d) dark brown (10YR3/3m); heavy sandy loam; moderate medium granular and weak subangular blocky; slightly hard when dry, friable when moist; pH 6.3; grades within about 5" to C.
C	29-45"	Reddish yellow (7.5YR6/6d) brown (7.5YR5/4m); sandy loam; massive, soft when dry, very friable when moist; pH 6.5.

Remarks: The pH determination was made with a Hellige kit. Color is expressed in terms of Munsell's color notations.

Table 20. (Cont'd)

Soil Sample Number 28

Soil Type: Pratt loamy sand.

Location: 1970 feet west and 2600 feet north of the Southeast corner of Section 33-T22S-R5W, Reno County, Kansas.

Date of Sampling: September 26, 1960

Physiographic Position: Upland, eolian sand on undulating topography.

Climate: Subhumid (27" annual rainfall, approx.).

Drainage: Low runoff, well drained internally.

Vegetation: Tall native grass, Bluestem, Indian and Switch.

Described by: James J. Rockers, Soil Scientist, Soil Conservation Service.

Soil Profile Description

Horizon	Depth	Description
A_1	0-7"	Dark gray brown (10YR4/2d) very dark brown (10YR2/2m); loamy sand; weak fine granular; soft when dry, very friable when moist; numerous roots; pH 6.0; grades within about 2" to A_3.
A_3	7-12"	Brown (10YR5/3d) dark brown (10YR3/3m); loamy sand; moderate fine granular; soft when dry, very friable when moist; numerous roots; pH 6.0; grades within about 3" to B_2.
B_2	12-24"	Light yellowish brown (10YR6/4d) dark yellowish brown (10YR4/4m); heavy loamy sand; moderate fine granular; slightly hard when dry, friable when moist; numerous roots; pH 6.0; grades within about 4" to C.
C	24-40"	Pale brown (10YR6/3d) yellowish brown (10YR5/4m); loamy sand; single grain, loose when dry or moist; numerous roots; pH 5.5.
C	40-52"	Same as horizon above, except moist color is light yellowish brown (10YR6/4).

Remarks: The pH determination was made with a Hellige kit. Color is expressed in terms of Munsell's color notations.

Table 20. (Cont'd)

Soil Sample Number 29

Soil Type: Bethany silt loam (undisturbed).

Location: 1330 feet south and 660 feet west of the Northeast corner of Section 8-T22S-R4W, Reno County, Kansas.

Date of Sampling: September 27, 1960

Physiographic Position: Upland (elevation approximately 1700 feet).

Climate: Subhumid (27" annual rainfall, approx.).

Drainage: Well drained, permeability is moderately slow.

Vegetation: Native Blue-grama and Buffalo grass.

Described by: James J. Rockers, Soil Scientist, Soil Conservation Service.

Soil Profile Description

Horizon	Depth	Description
A_1	0-12"	Dark brown (10YR3/3d) very dark brown (10YR2/2m) silt loam; moderate medium granular; slightly hard when dry, very friable when moist; many fine grass roots; pH5.8; grades within 2" to A_3.
A_3	12-18"	Dark brown (10YR4/3d) (10YR3/3m) light silty clay loam; strong medium granular; hard when dry, friable when moist, fine roots are common; pH 6.0 grades within about 2" to B_{21}.
B_{21}	18-37"	Dark gray brown (10YR4/2d) very dark gray brown (10YR3/2m) silty clay; weak medium sub-angular blocky with slickensides of ten centimeters in diameter; extremely hard when dry, very firm when moist; few roots; pH 6.5; grades within about 5" to B_{22}.
B_{22}	37-45"	Gray brown (2.5Y5/2d) olive brown (2.5Y4/4m) silty clay loam; weak medium granular to massive; very hard when dry, firm when moist; mildly calcareous with scattered calcareous concretion some 5mm in diameter.

Remarks: A Hellige-Truog soil reaction tester was used to determine pH.
Soil colors determined by use of Munsell's Color Chart.

Table 20. (Cont'd)

Soil Sample Number 30

Soil Type: Bethany silt loam (cultivated).

Location: 1400 feet south and 600 feet west of the Northeast corner of Section 8-T22S-R4W, Reno County, Kansas.

Date of Sampling: September 27, 1960

Physiographic Position: Upland (1700 feet elevation, approx.).

Climate: Subhumid (27" annual rainfall).

Drainage: Well drained, permeability is moderately slow.

Vegetation: Cultivated; currently in wheat.

Described by: James J. Rockers, Soil Scientist, Soil Conservation Service.

Soil Profile Description

Horizon	Depth	Description
A_1	0-11"	Dark brown (10YR3/3d) very dark brown (10YR2/2m) silt loam; weak fine granular; slightly hard when dry, friable when moist; upper 8" disturbed by cultivation, lower 3" somewhat compacted; pH 5.7; grades within about 2" to A_3.
A_3	11-19"	Dark brown (10YR3/3d) very dark gray brown (10YR3/2m) light silty clay loam; strong medium granular; slightly hard dry, friable when moist; some dead roots & some worm casts; pH 6.0; grades within about 4" to B_{21}.
B_{21}	19-39"	Brown (10YR4/3d) dark brown (10YR3/3m) silty clay loam; moderate medium subangular blocky and blocky with slickensides; very hard when dry, very firm when moist; thin continous clay films; few fine roots; pH 6.5; grades within about 4" to B_{22}.
B_{22}	39-45"	Gray brown (10YR5/2d) dark gray brown (10YR4/2m) silty clay loam; weak to moderate, medium subangular blocky; hard when dry; firm when moist; weakly calcareous with scattered calcareous concretion some 3-5 mm in diameter.

Remarks: The pH was determined with a Hellige kit.
Color is expressed in terms of the Munsell's notation of color.

Table 20. (Cont'd)

Soil Sample Number 32

Soil Type: Irwin silt clay loam.

Location: 700 feet north and 70 feet west of E 1/4 corner Section 25-T-23S-R4E map 6-3, Butler County, Kansas.

Date of Sampling: September 27, 1960

Physiographic Position: Gently sloping, undulating, convex erosion upland, about 1.5% gradient.

Climate: Annual precipitation about 31".

Drainage: Runoff moderate, permeability slow.

Vegetation: Big Bluestem, little Bluestem, Switchgrass, tall Dropseed, Heath aster, Perennial ragweed. Used as native pasture.

Soil Profile Description

Horizon	Depth	Description
A_o	0-1/2"	Gray (10YR5/1 dry; 10YR3/1.5 moist) silt loam mulch consisting of decayed grass and particles of soils; slightly platy showing some compaction; boundary smooth and abrupt.
A_1	1/2-8"	Very dark gray (10YR3/1.5 moist) light silty clay loam; moderate medium granular; slightly hard; friable; many roots; boundary abrupt and smooth.
AB	8-9"	Very dark gray (10YR3/1.5 moist) heavy silty clay loam; moderate medium granular structure with slight graying on ped surfaces; slightly hard; friable; many roots; boundary abrupt and smooth.
B_{21}	9-23"	Very dark brown (10YR2/2 moist) silty clay; moderate medium and fine irregular angular blocky structure with peds adhering to one another; interior of peds are (10YR3/2 moist); roots are concentrated on ped surfaces very hard; very firm; clay films distinct and continuous; several slickensides noted at 21" depth; boundary smooth and gradual.
B_{22}	23-35"	Very dark grayish brown (10YR3/2 moist) silty clay loam; structure somewhat weaker than above horizon,

Table 20. Soil Sample Number 32 (Cont'd)

Horizon	Depth	Description
		otherwise very similar; few lime concretions at 32"; boundary smooth and gradual.
B_3	35-38"	Dark brown (10YR4/3 moist) silty clay; other characteristics same as above; boundary clear and smooth.
C_1	38-50"	Dark reddish brown (6YR3/2 moist) light silty clay; weak blocky structure; few patchy clay films; hard and firm; this horizon thought to be a truncated paleasal; boundary smooth and gradual.
C_2	50-68"	Dark reddish brown (5YR3/4 moist) silty clay; massive in place; mottled with dark red, grays and yellows; few shale chips in lower part.
Dr	68" +	Greenish clay shales of a waxy character with some lime disseminations.

Table 20. (Cont'd)

Soil Sample Number 34

Soil Type: Summit clay loam.

Location: 1700 feet west and 700 feet south of the northeast corner of Section 8-T30S-R24E, or about 120 feet north of the south edge of meadow and midway between the two drains, Crawford County, Kansas.

Date of Sampling: October 3, 1960

Physiographic Position: Gently rolling upland between two small drains about 75 yards apart.

Drainage: Surface well drained. Slow permeability.

Vegetation: Native bluestem meadow.

Soil Profile Description

Horizon	Depth	Description
A_{11}	0-1/4"	Very dark gray (10YR3/1 dry, 2/1 moist) light clay loam; compact fine or very fine platy; friable when moist, firm when dry, capped with a 1/16" layer of decayed vegetation and some tiny moss growth; pH 6.1; abrupt boundary to A_{12}.
A_{12}	1/4-4"	Very dark gray (10YR3/1 dry, 2/1 moist) clay loam; moderate medium granular; friable when moist; firm when dry; horizon held together by profuse root growth; pH 6.0; grades to A_{13}.
A_{13}	4-15"	Very dark gray (10YR3/1 dry, 2/1 moist) clay loam; moderate medium and coarse blocky with many peds crushing to moderate medium granular; firm when moist; hard when dry, occassional worm casts; a few very fine shot concretions; on occassional small chert fragment; considerable root growth; pH 6.2; grades to B_1.
B_1	15-20"	Dark grayish brown (2.5Y4/2 dry, 3/2 moist) silty clay; moderate medium irregular blocky; very fine when moist; very hard when dry; many small shot concretions usually coated with dark reddish brown; pH 6.3; grades to B_2.
B_2	20-28"	Dark grayish brown (2.5Y4/2 dry, 3/2 moist clay; weak blocky; extremely firm when moist; extremely hard when dry; several Fe-Mn shot concretions; 10% mottled with

Table 20. Soil Sample Number 34 (Cont'd)

Horizon	Depth	Description
		common fine distinct reddish brown mottles; pH 6.5; diffuse boundary to.C.
C	28-43" +	Dark grayish brown (2.5Y4/2 dry, 3/2 moist) clay; weak blocky to massive; extremely firm when moist; extremely hard when dry; 20% mottled with common medium distinct reddish brown and reddish yellow mottles; some black shot concretions; a few small chert fragements; an occassional small limestone fragment that reacts to 10% HCl; pH 7.1.
Remarks:		pH taken in the field with a Hellige-Truog soil reaction tester. Colors according to Munsell's color chart.

Table 20. (Cont'd)

Soil Sample Number 36

Soil Type: Cherokee silt loam.

Location: 400 feet north and 50 feet east of southwest corner of Section 11-T31S-R22E, Crawford County, Kansas.

Date of Sampling: October 3, 1960

Physiographic Position: Nearly level to flat uplands.

Drainage: Surface drainage fair to poor. Internal drainage very slow.

Vegetation: Native bluestem meadow.

Soil Profile Description

Horizon	Depth	Description
A_{11}	0-1"	Light brownish gray (10YR6/2 dry, 4/1 moist) silt loam; weak platy appearance may be due to the profuse root growth holding the horizon together; friable when moist; firm when dry; pH 6.5; clear boundary to A_{12}.
A_{12}	1-7"	Light gray (10YR7/2 dry, 4/1 moist) silt loam; weak blocky in place crushing easily to very fine granular; a few fine faint yellowish brown mottles; pH 5.2; diffuse transition to A_2.
A_2	7-14"	Nearly white (10YR7.5/1 dry, 5/1 moist) silt loam; weak structure in place but crushes to a powdery very fine granular; friable when moist; many tiny pin point like pores; pH 5.0; abrupt transition to B_{21}.
B_{21}	14-27"	Very dark gray (10YR4/1 dry, 3/1 moist) clay; moderate medium and coarse irregular blocky; extremely firm when moist; clay skins very evident; very dense and compact; 5% - 10% mottled with fine faint yellowish brown mottles; pH 5.1, grades to B_{22}.
B_{22}	27-37"	Grayish brown (10YR5/2 dry, 3/1.5 moist) clay; massive to very weak blocky; extremely firm when moist; a few fine faint yellowish brown mottles; a few very small shot concretions; occassional black staining between peds; pH 5.5; grades to B_3.

Table 20. Soil Sample Number 36 (Cont'd)

Horizon	Depth	Description
B_3	37-42" +	Grayish brown (10YR5/2 dry, 4/2 moist) and light gray (10YR7/2 dry, 6/2 moist) silt clay; massive; very firm when moist (but relatively more friable than the two horizons immediately above); some black Fe-Mn staining; common coarse distinct yellowish brown mottles;pH 5.5.
Remarks:		pH taken in the field using the Hellige-Truog soil reaction tester. Color determined with the Munsell's color chart.

Table 20. (Cont'd)

Soil Sample Number 37

Soil Type: Bates loam.

Location: 520 feet west and 60 feet south of the northeast corner of Section 31-T28S-R23E, Crawford County, Kansas.

Date of Sampling: September 30, 1960

Physiographic Position: Gently rolling upland. 2% convex slope to the south.

Drainage: Well drained, moderate permeability.

Vegetation: Native bluestem meadow.

Soil Profile Description

Horizon	Depth	Description
A_{11}	0-1"	Dark grayish brown (10YR4/2 dry, 2/2 moist) loam; weak structure in place but crushes to fine granular; friable when moist; slightly hard when dry; profuse roots tend to mat horizon together; pH 6.5; clear boundary to A_{12}.
A_{12}	1-4"	Dark grayish brown (10YR4/2 dry, 2/2 moist) loam; weak structure in place crushes to moderate fine granular; friable when moist; slightly hard when dry; does not have matted appearance of horizon above but appears more compacted than horizon below; pH 6.0; grades to A_{13}.
A_{13}	4-14"	Dark grayish brown (10YR 4/2 dry, 2/2 moist) loam; weak blocky crushing to moderate fine and medium granular; friable when moist slightly hard when dry; pH 6.0 grades to B.
B	14-22"	Dark brown (7.5YR4/3 dry, 3/2 moist) clay loam; weak blocky to moderate medium granular; friable when moist; hard when dry, contains some sandy fragments which are mottled or stained with reddish brown; pH 6.0; grades to C.
C	22-29"	Brown (7.5YR5/4 dry, 3/4 moist) light clay loam; massive or very weakly granular; firm when moist; hard when dry; many brownish yellow and yellowish brown fragmented sandy shales and/or sandstones; some black staining between shale layers; pH 5.8; rests on D_r.

Table 20. Soil Sample Number 37 (Cont'd)

Horizon	Depth	Description
Dr	29-31" +	Yellowish brown layered compacted sandstones and sandy shales; pH 5.8.
Remarks:		pH determined in the field with a Hellige-Truog soil reaction tester. Color determined with the Munsell's color chart.

Table 20. (Cont'd)

Soil Sample Number 38

Soil Type: Labette clay loam.

Location: 1640 feet south and 84 feet west of the northeast corner of Section 6-T31S-R24E, Crawford County, Kansas

Date of Sampling: September 30, 1960

Physiographic Position: Gently rolling upland. 2% slope to the north-northwest.

Drainage: Well drained, moderately slow permeability.

Vegetation: Native Bluestem meadows.

Soil Profile Description

Horizon	Depth	Description
A_{11}	0-1"	Dark grayish brown (10YR4/2 dry, 2/2 moist) clay loam; either weakly platy or somewhat compacted but will crush rather easily to a fine granular; slightly hard when dry; friable when moist; many fine roots present: pH 6.0
A_{12}	1-7"	Dark brown (7.5YR4/2 dry, 2/2 moist) clay loam; weak to moderate medium granular; slightly hard when dry; friable when moist; pH 5.5; grades to A_3.
A_3	7-12"	Dark brown (7.5YR 3/2 dry, 2/2 moist) silty clay loam; moderate to strong medium granular; hard when dry; firm when moist; a few fine faint yellowish brown mottles; a few small weathered chert fragments and corals; pH 6.1; grades to B_1.
B_1	12-15"	Dark reddish brown (5YR3/3 dry, 2/3 moist) silty clay; strong medium granular; hard when dry; firm when moist; a few small black Fe-Mn shot concretions; also a few small chert fragments; pH 6.0; grades to B_{21}.
B_{21}	15-27"	Dark reddish brown (5YR3/4 dry, 2/4 moist) heavy silty clay; weak blocky to moderate medium granular; hard when dry; firm when moist; several black Fe-Mn concretions about 1/8" in diameter; pH 6.0; grades to B_{22}.

Table 20. Soil Samples Number 38 (Cont'd)

Horizon	Depth	Description
B_{22}	27-36"	Very dark grayish brown (10YR3/2 dry, 2/2 moist) clay; moderate medium irregular blocky; estremely hard when dry; extremely firm when moist; 10% - 20% mottled with reddish yellow; some small chert fragments and occassional larger ones which will not react to 10%; some dark staining between peds; pH 7.8; rests on D_r.
Dr	36" +	Limestone bedrock.
Remarks:		pH was taken in the filed using the Hellige-Troug soil reaction tester. Color determined with the Munsell's color chart.

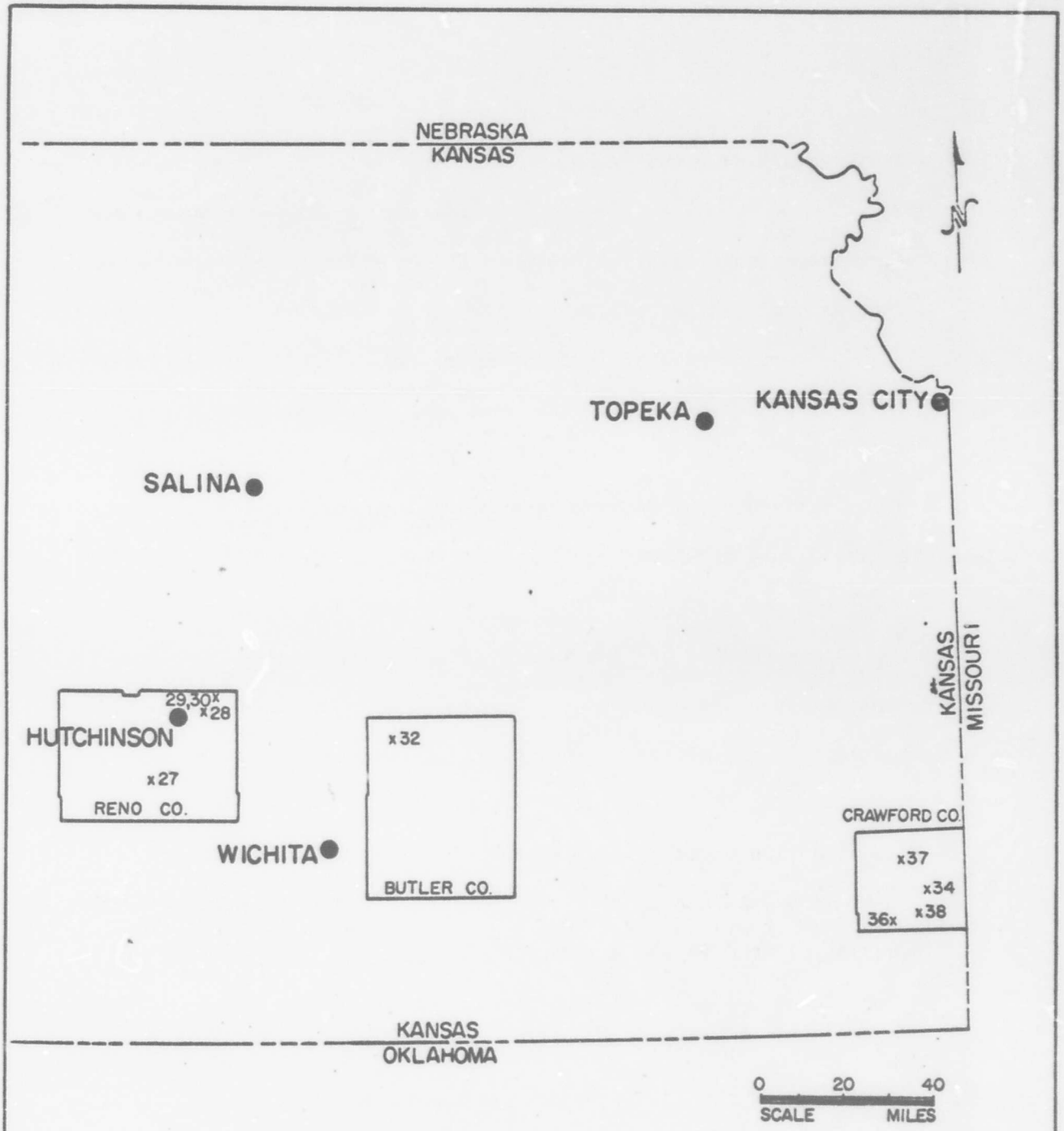

FIGURE 71 · LOCATION MAP OF EASTERN KANSAS SHOWING SOIL SAMPLING SITES

Isotopes, Inc.

The Radiochemical Procedures

The "pretreatment" to which the samples were subjected before being analyzed radiochemically was described in DASA-1300. This included the extrusion of the samples from the corers, their drying, pulverizing and blending.

A 100 mg. aliquot of each soil sample was analyzed for ruthenium-106. A second 100 mg. aliquot was analyzed sequentially for strontium-90, cesium-137 and cerium-144. Aliquots of the dried soil were also measured for cesium-137 using gamma spectrometry. The radiochemical and radiometric procedures employed were discussed in DASA-1300. However, because some changes have been made in the radiochemical procedures used on the Kansas soil samples, the revised procedures are given here.

The Separation and Determination of Ruthenium-106 and Rhodium-106 in Soils

1. Weigh 100 grams of prepared soil in a 250 ml beaker, add 30 mg of Ru carrier, mix thoroughly and dry in an oven for 2-3 hours at 110°C.
2. Melt 100 grams of NaOH pellets in a 500 ml nickel crucible and rotate the crucible to coat the walls with melt extending to within 1-1/2 inches from the top.
3. Transfer the dry soil sample to the crucible and clean the beaker with 150 grams of NaOH pellets. After thoroughly mixing the NaOH into the soil, cover the mixture with 50 grams of NaOH.
4. Place the crucible on a tripod and heat with the aid of four Fisher burners. When the mixture begins to melt, stir with a glass rod. (Caution: some frothing will occur but can be controlled by stirring and regulating the heat.)
5. After the frothing has stopped add 50 grams of Na_2O_2 in a series of

small portions while stirring with a glass rod.

6. Place the crucible in a furnace at 550°C and raise the temperature to 650°C over a period of one hour.
7. Remove the crucible from the furnace and sprinkle approximately 25 grams of Na_2O_2 on the crucible walls. Rotate the crucible to coat its walls with molten flux and again place in the furnace.
8. Raise the temperature to 700°C and heat the sample for 10 minutes. (Crucible should be cherry red in color.)
9. After the crucible has cooled to room temperature, cover the mouth of the crucible with a paper towel and tap the sides gently with a hammer to loosen the cake.
10. Invert the crucible in a 3 liter beaker and add 500 ml of H_2O. Remove the crucible, rinse the exterior with H_2O and wash the interior with H_2O. Combine the rinses and washes in the 3 liter beaker and heat for 1 hour to destroy all the Na_2O_2.
11. Cool the beaker in a water bath and add concentrated HCl, with continuous stirring, until white lumps of $Al(OH)_3$ appear. Cool in a water bath and add concentrated HCl until a yellow mass is obtained. At this point, add enough concentrated HCl to make the solution approximately 3N.
12. Add 50 ml of 48% HBr and digest on a hot plate for 2 hours with mechanical stirring. Replace any H_2O lost due to evaporation.
13. Filter the solution through a 24 cm Buchner funnel while still warm (approximately 50°C) using No. 41 H Whatman filter paper. Wash the SiO_2 precipitate twice with 100 ml portions of warm 3N HCL.

14. Disconnect the vacuum line, add 100 ml of warm H_2O to the precipitate, slurry with a stirring rod and apply vacuum. Again disconnect the vacuum line, add 100 ml of warm 3N HCl to the precipitate, slurry with a stirring rod and apply vacuum. Repeat alternate H_2O and 3N HCl washings until the precipitate is decolorized. Combine washings and the original filtrate.
15. Evaporate the solution until 1/2 inch of solution is covering the salts which have formed. Dissolve the salts in a minimum of hot H_2O. (Volume should not exceed 3 liters.)
16. Heat the solution to boiling. Add 0.2 grams of Thioacetamide for every 30 ml of solution. (Note 1.) Digest on a hot plate for 15 minutes, cool to approximately 50°C and filter the RuS_2 on a 9 cm Buchner funnel using No. 42 Whatman filter paper. Wash the precipitate with 100 ml of H_2O and discard the filtrate.
17. Transfer the precipitate and filter paper into a 500 ml distilling flask. Using a rubber policeman and H_2O, wash all the remaining RuS_2 from the walls of the funnel into the distilling flask (Note 2).
18. Add 30 ml of concentrated H_2SO_4 and cool the flask in an ice bath. (Add H_2SO_4 slowly to avoid charring of the filter paper.) Using a Bunsen burner heat the solution in the flask to completely mascerate the filter paper.
19. Cool the flask to room temperature and add 10 ml of saturated $NaBrO_3$ through an addition funnel. Heat the flask gently (with stirring) for 10 minutes and collect the volatile RuO_4 into two traps, each containing 30 ml of concentrated HCl. Cool the distilling flask, repeat the addition of 10 ml of saturated $NaBrO_3$, and distill for 10 minutes three more times.

20. After the last $NaBrO_3$ addition, distill until the liquid in the flask is clear.
21. Transfer the HCl-Ru distillate to a 250 ml Erlenmeyer flask and wash the traps with H_2O and 1N HCl. Combine the washing with the distillate and evaporate the solution to 50 ml (Hood: Br_2 evolved).
22. Cool and add powdered magnesium in small portions, swirling the flask between each addition until the reduction to the ruthenium metal is complete as indicated by a colorless solution.
23. After reduction is complete, transfer to a 40 ml centrifuge tube by portions centrifuge and discard the supernate.
24. Wash the ruthenium metal with 10 ml of 6N HCl followed by two washings with 10 ml of H_2O; slurry with H_2O and filter onto a previously washed and weighed Whatman No. 42 filter disk.
25. Wash the precipitate with 10 ml of H_2O followed by three 5 ml portions of acetone; dry in an oven for 15 minutes at 110°C, cool in a dessicator, weigh and record the chemical yield of ruthenium metal.

Note 1. Caution should be taken with the addition of Thioacetamide. Add only small portions at a time and stir continuously after each addition to retard the foaming which occurs.

Note 2. Volume should not exceed 50 ml.

Ruthenium-106 Counting Procedure

The Ru^{106} samples are counted in a low level beta counter. The samples are counted both without an absorber and with an aluminum absorber of 171.08 mg/cm^2 thickness. If the ratio between the non-absorber and absorber counts agrees with the previously determined standard absorber ratio within the prescribed counting statistics, the sample is accepted as radiochemically pure.

Appropriate counter efficiencies are applied to convert the count rate to disintegrations per minute.

The Sequential Separation of Strontium-90, Cesium-137 and Cerium-144 in Soils

1. To a 100 gram aliquot of a dry soil sample contained in a 250 ml beaker, add 1 ml of strontium carrier (20 mg Sr/ml), 1 ml of cesium carrier (20 mg Cs/ml) and 1 ml of cerium carrier (20 mgCe/ml) stirring in each carrier separately. Mix thoroughly and dry in an oven at 110°C for 2-3 hours.
2. Add 150 grams of NaOH pellets to the dry soil sample and mix thoroughly.
3. Melt 100 grams of NaOH pellets in a 500 ml nickel crucible and rotate the crucible to coat the walls with melt as high as 1 1/2 inches from the top.
4. Cool the nickel crucible, transfer the soil-NaOH mixture to the crucible and cover the soil mixture with 75 grams of NaOH pellets. Clean the beaker with 25 grams of NaOH and transfer to the crucible.
5. Place the crucible on a tripod and heat with four Meeker Burners. When the mixture begins to melt, stir with a glass rod. (Caution: some frothing may occur, but it can be controlled by stirring and heating.)
6. When the frothing has diminished, stir in 50 grams of Na_2O_2. Heat in a muffle furnace at 650°C for 1/2 hour. Remove the crucible from the furnace, add 25 grams of Na_2O_2 and heat in the furnace at 700°C for 1 hour.
7. Cool the crucible to room temperature and remove the cake by gently tapping the sides and bottom of the crucible with a hammer.

8. Transfer the cake to a 3 liter beaker and add enough water to cover the melt. Add water to 1/2 inch from the top of the nickel crucible, place the crucible on a hot plate, put a watch glass on top and heat until strong refluxing is evident. Combine the wash with the cake in the 3 liter beaker.
9. Heat the mixture until the large particles are broken. Then heat for 1 hour with mechanical stirring to remove all traces of Na_2O_2.
10. Cool, add enough concentrated HCl to bring the mixture to pH 13 and add 100 ml of saturated Na_2CO_3. Heat the solution for 1 hour on a hot plate with mechanical stirring.
11. Cool the mixture to room temperature and vacuum filter through a glass fiber filter paper contained in a 15 cm Buchner funnel. Wash the precipitate with warm H_2O to remove salts and reserve the filtrate for the cesium-137 purification procedure.
12. Transfer the precipitate and filter paper containing the strontium and cerium fractions to a 1 liter beaker. Wash the Buchner funnel with concentrated HCl until all of the precipitate is removed. Combine the wash and the precipitate.
13. Add to the wash and precipitate 500 ml of concentrated HCl and heat the solution until the filter paper has been mascerated.
14. Add 3 grams of NaI and heat with mechanical stirring for two hours. Cool the solution to room temperature and filter through a Whatman No. 541 filter paper contained in a Buchner funnel. Wash the residue with warm 6M HCl until colorless. Discard the residue.
15. Evaporate the filtrate and wash solution to approximately 300 ml and add enough 12 M NaOH to bring the solution to pH 14. Add 100 ml of

saturated Na_2CO_3, digest on a hot plate for 10 minutes and filter the solution through a Buchner funnel containing a 15 cm glass fiber filter paper. Wash the precipitate with 2N NaOH and filter to complete dryness. Discard the filtrate.

16. Transfer the precipitate and filter paper to a 1 liter beaker and add 150 ml of concentrated HNO_3. Wash the Buchner funnel with concentrated HNO_3 and add the wash to the 1 liter beaker.
17. Boil the mixture on a hot plate until the filter paper is completely macerated. Filter the solution through a Buchner funnel containing a 9 cm glass fiber filter paper (Note 1) and wash the precipitate with 100 ml of warm H_2O. Discard the precipitate.
18. Transfer the filtrate to a clean 1 liter beaker and evaporate to about 25 ml (Note 2). Cool and filter the mixture through a Buchner funnel containing a 9 cm asbestos filter pad. Wash the precipitate with 9 N HNO_3 and discard the precipitate.
19. Transfer the filtrate to a 250 ml beaker, boil to about 10 ml and add 2 grams of $NaBrO_3$.
20. Filter the mixture through a Buchner funnel containing a 9 cm asbestos pad and wash the precipitate with 9 N HNO_3.
21. Repeat steps (19) and (20) until no more MnO_2 is precipitated. Discard the precipitate after each treatment.
22. Take the solution to pH 9.0 with NH_4OH and add 100 ml of saturated Na_2CO_3. Heat on a hot plate for 10 minutes and filter through a Whatman No. 52 filter paper contained in a Buchner funnel. Transfer the precipitate to a 600 ml beaker, dissolve it in 200 ml of concentrated HCl and wash the funnel with concentrated HCl.

23. Transfer the solution to a 1 liter separatory funnel and wash the beaker with concentrated HCl. Add the washings to the separatory funnel.
24. Add 200 ml of alcohol free iso-propyl ether and shake for two minutes. If the aqueous (lower) phase is not colorless, add more concentrated HCl and shake until the aqueous phase is colorless. Allow the phases to separate and draw off the aqueous phase into a 1 liter beaker. (Note 3).
25. Evaporate the solution to about 50 ml, cool in an ice bath and add enough concentrated NH_4OH to bring the solution to pH 10. Filter through a Buchner funnel containing a 9 cm Whatman No. 52 filter paper.
26. Transfer the precipitate to a 1 liter beaker, dissolve in concentrated HCl and wash the Buchner funnel with HCl. Repeat step 25. Reserve the precipitate for the Ce-144 purification procedure as described in DASA-1300, Volume 5, pg. 244 (1961).
27. Transfer the filtrate to a 1 liter beaker and reserve the solution for the Sr-90 purification procedure as described in DASA-1300, Volume 5, pg. 230 (1961).

Note 1. A small portion of meta-titanic acid will precipitate during filtration.

Note 2. Meta-titanic acid will precipitate during evaporation.

Note 3. The ether fraction is reserved and purified for further use by distillation (boiling point $67.5^{o}C$).

Cesium-137 Purification Procedure

a) Add concentrated HCl to the clear filtrate from step 11 of the sequential separation until the solution is 6N HCl.

b) Cool to room temperature and filter onto a 24 cm Buchner funnel containing Whatman No. 41 H filter paper. Wash the SiO_2 alternately with 100 ml portions of hot 6 N HCl and hot water until the silica is decolorized. Combine the washings and filtrate. Discard the SiO_2 precipitate.

c) Evaporate the filtrate and washings until 1/2 inch of solution is covering the salts. Dissolve the salts in a minimum of hot H_2O (volume should not exceed 3 liters). Add, with stirring, 0.75 grams of $NiSO_4$ and 1 gram of $K_4Fe(CN)_6 \cdot 3H_2O$ and mechanically stir for 1 hour. Let the precipitate settle overnight.

d) Decant or siphon off the clear supernate and centrifuge the precipitate in portions. Discard the supernates.

e) Transfer the precipitate from step (d) into a #3 Coors porcelain crucible and dry the precipitate thoroughly under a heat lamp.

f) Ash the precipitate for 3 hours at 450°C in a muffle furnace.

g) Add 10 ml of 6 N HCl to the residue in the crucible. Use a rubber policeman to remove the precipitate from the walls of the crucible. Transfer the mixture to a 40 ml centrifuge tube and wash the crucible with 6 N HCl to remove any additional residue. Transfer the washes to the original mixture. Heat in a hot water bath for 10 minutes.

h) Cool, centrifuge and decant the supernate into a clean 100 ml beaker. Wash the precipitate twice with 10 ml portions of 6 N HCl and combine washes with the original supernate. Discard the precipitate.

i) Add 5 ml of 0.13M silico tungstic acid for every 30 ml of solution and 3 drops of aerosol solution, and heat the solution to a rolling boil for a half hour.

j) Cool, centrifuge in portions and discard the supernate. Wash the precipitate twice with 10 ml portions of 6 N HCl and discard the washes (Note 1).

k) Dissolve the cesium silico tungstate precipitate in 3 ml of 6 M NaOH, add 20 ml of 6 N HCl and digest the precipitate in a hot water bath for 30 minutes. Cool, centrifuge and transfer the supernate to a 100 ml beaker. Wash the precipitate twice with 5 ml portions of 6 N HCl and combine the washes with the original supernate. Discard the precipitate.

l) Add 3 drops of meta-cresol purple indicator to the supernate and neutralize with 50% NaOH. Transfer the solution to a 125 ml separatory funnel containing 10 ml of "citrate buffer solution" (1M $Na_3 C_6 H_5 O_7$, 0.5 M HNO_3).

m) Add 25 ml of 0.05 M sodium tetraphenyl boron-amyl acetate solution to the funnel, shake for 30 seconds and allow to stand for 3 minutes (Note 2).

n) Withdraw the aqueous (lower) phase and collect in another 125 ml separatory funnel. Extract again with 15 ml of 0.05 M sodium tetraphenyl boron-amyl acetate solution.

o) Withdraw and discard the aqueous phase. Combine the two portions of the organic phase in a separatory funnel.

p) Strip the cesium from the organic phase by extracting twice with two 10 ml portions of 3 M HCl. Combine the strips in a clean 100 ml beaker and heat on a hot plate for 30 minutes to distill off all traces of the amyl acetate.

q) Remove the solution from the hot plate; add 3 drops of meta-cresol

purple indicator and neutralize with 6 M NaOH. Add 2 ml of 10% chloroplatinic acid very slowly, via a pipette. Stir vigorously during the addition and allow to stand for 30 minutes.

r) Centrifuge and discard the supernate. Add 5 ml of H_2O and filter the precipitate onto a previously washed and weighed Whatman No. 42 filter disk without applying suction (Note 3). Wash the precipitate with two 5 ml portions of anhydrous "anhydrol" applying suction each time. Oven dry at 110°C for 15 minutes and cool in a desiccator. Weigh as the cesium chloroplatinate for chemical yield and mount on a brass planchet for beta counting.

Note 1. The cesium precipitate should be completely white in color after the two washes.

Note 2. An insoluble precipitate, cesium tetraphenyl boron, will form at the bottom of the amyl acetate layer, obscuring the interface. The aqueous phase may be readily separated by draining until the white precipitate just begins to appear in the bore of the stopcock.

Note 3. The Cs_2 Pt Cl_6 precipitate is a very fine powder and filtering without suction deposits the precipitates evenly on the surface of the filter disk with no tendency for seepage around the edge of the filtering column.

Cesium-137 Counting Procedure

The samples are counted in the low level beta counters. Radiochemical purity is ascertained by counting the sample without an absorber and with an aluminum absorber of 9.77 mg/cm^2 thickness. If the absorber ratio agrees with the theoretical absorber ratio (the latter previously determined by

counting absolute standards) the sample is accepted as radiochemically pure. Self-scattering self-absorption corrections are applied to convert to disintegrations per minute.

Isotopes, Inc.

Quality Control

The quality of the radiochemical analyses of Kansas soils performed during Project Star Dust may be judged on the basis of results from a series of blank samples analyzed with the soil samples and of results from analyses of duplicate aliquots of several samples.

Blank samples consisted of 25 gram portions of pre-1945 soil and were analyzed with the Kansas soil samples using the same reagents and procedures. These samples should contain no fission products, so any activity found in them must be attributed to contamination picked up during the analyses. In so far as possible the section of the laboratory in which the soil analyses were being performed was isolated from the remainder of the laboratory in which atmospheric filter samples, containing high activities of fission products, were being analyzed. New glassware and fresh reagents were set aside for use in the soil analyses. Nevertheless the blank samples analyzed with the Kansas soil samples displayed significant activities of each of the nuclides analyzed.

The results for the blank samples analyzed with the Kansas soil samples are summarized in Table 21. Typical values for blank samples analyzed with the New Jersey soil samples during Project HASP were: less than 1 dpm of strontium-90, ruthenium-106 and cesium-137 and about 2 dpm of cerium-144. The greater contamination experienced during the analysis of the Kansas samples must be attributed to the much higher levels of activity present in other types of samples in the laboratory in 1962 and 1963 compared to 1960 and 1961 when the New Jersey soil samples were analyzed.

The frequencies of occurence of nuclide activities within a series of concentration ranges in both the soil samples and the blank samples are shown in Figures 72 to 75. For ruthenium-106, cesium-137 and cerium-144 the

activities found in the blank samples fall in the same concentration range as do the activities of more than half of the soil samples. For strontium-90 the activities of about 55 percent of the soil samples fall above the concentration range which contains the blank samples. If the data for the blank samples are truly indicative of the levels of contamination to which all samples were subject, we can use very few, if any, of the ruthenium-106 or cerium-144 data with confidence. The activities of cesium-137 in about 25 percent of the soil samples and of strontium-90 in about 40 percent of the soil samples were about 10 times as high as the highest activities found in the blank samples. Perhaps, then, the possible contamination of these higher activity samples can be assumed to be negligible, in the absence of evidence to the contrary. Unfortunately even the strontium-90 and cesium-137 activities of most of the samples lie within the concentration range in which contamination may constitute much or most of the activity. In general, the samples which contain high activities of strontium-90 and cesium-137 were taken from the upper few inches of the cores, and the samples which contain the lower activities were taken from the lower sections of the cores.

The results of measurements of duplicate samples are presented in Table 22. Where poor duplication of activities was obtained, contamination of one or both of the samples can be blamed. Those samples which contained activities well above those found in blank samples showed reasonably good agreement between duplicate analyses.

Isotopes, Inc.

Table 21. Results for Blank Samples Analyzed with Kansas Soil Samples

Sample	Nuclide Activities (dpm/sample corr. to 1 Jul 1960)			
	Sr^{90}	Ru^{106}	Cs^{137}	Ce^{144}
1	-	-	12.0 ± 9.1%	-
2	6.25 ± 12.0%	66.0 ± 4.28%	16.8 ± 5.3%	113 ± 6.9%
3	-	16.02 ± 17.4%	4.30 ± 18.1%	≤ 149
4	3.59 ± 65.2%	30.17 ± 18.6%	6.78 ± 9.6%	87.4 ± 37.9%
5	-	81.10 ± 9.0%	18.3 ± 7.0%	351 ± 9.1%
6	4.06 ± 20.2%	103.4 ± 7.0%	13.5 ± 8.3%	-
7	4.29 ± 29.0%	52.1 ± 10.2%	8.98 ± 11.8%	267 ± 16.3%
8	≤ 1.75	79.8 ± 9.6%	6.77 ± 14.8%	273 ± 9.5%
9	-	48.5 ± 9.7%	-	-
10	4.11 ± 15.4%	10.6 ± 27.9%	5.91 ± 13.2%	321 ± 7.4%
11	-	38.7 ± 18.7%	5.74 ± 24.6%	271 ± 8.0%
12	-	174 ± 11.2%	6.71 ± 29.1%	302 ± 11.6%
13	-	144 ± 5.8%	-	298 ± 17.4%
Mean	4.0 ± 1.4	70 ± 50	9.6 ± 4.8	240 ± 90

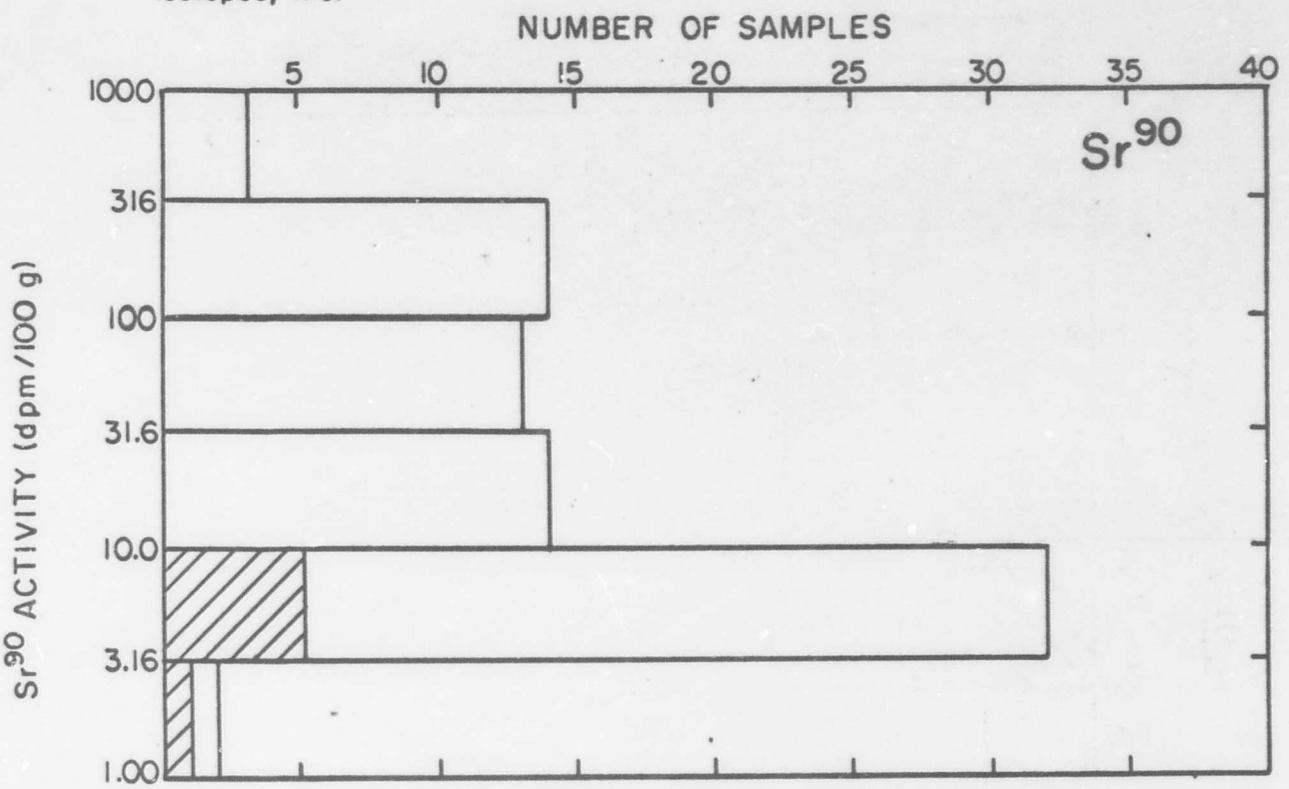

FIGURE 72 · FREQUENCY OF OCCURRENCE OF Sr-90 ACTIVITIES IN BLANK SAMPLES (cross hatched) AND IN SOIL SAMPLES

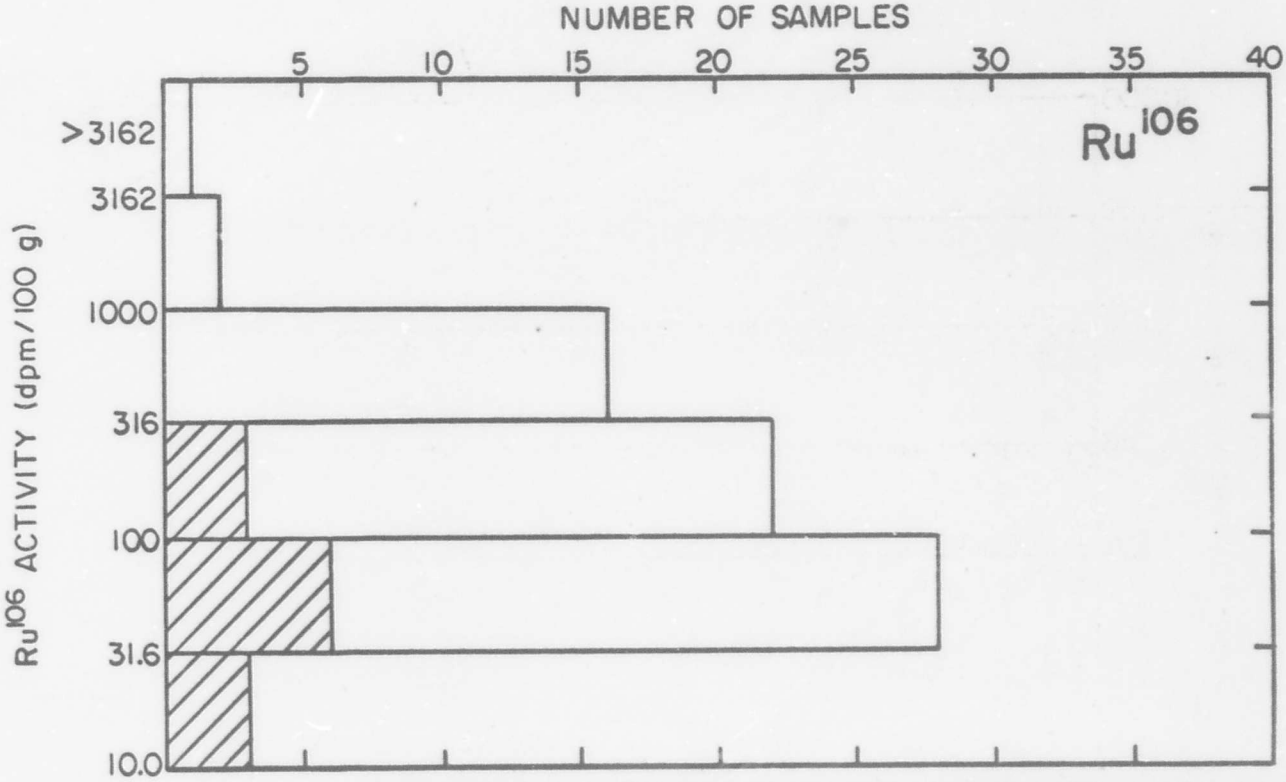

FIGURE 73 · FREQUENCY OF OCCURRENCE OF Ru-106 ACTIVITIES IN BLANK SAMPLES (cross hatched) AND IN SOIL SAMPLES

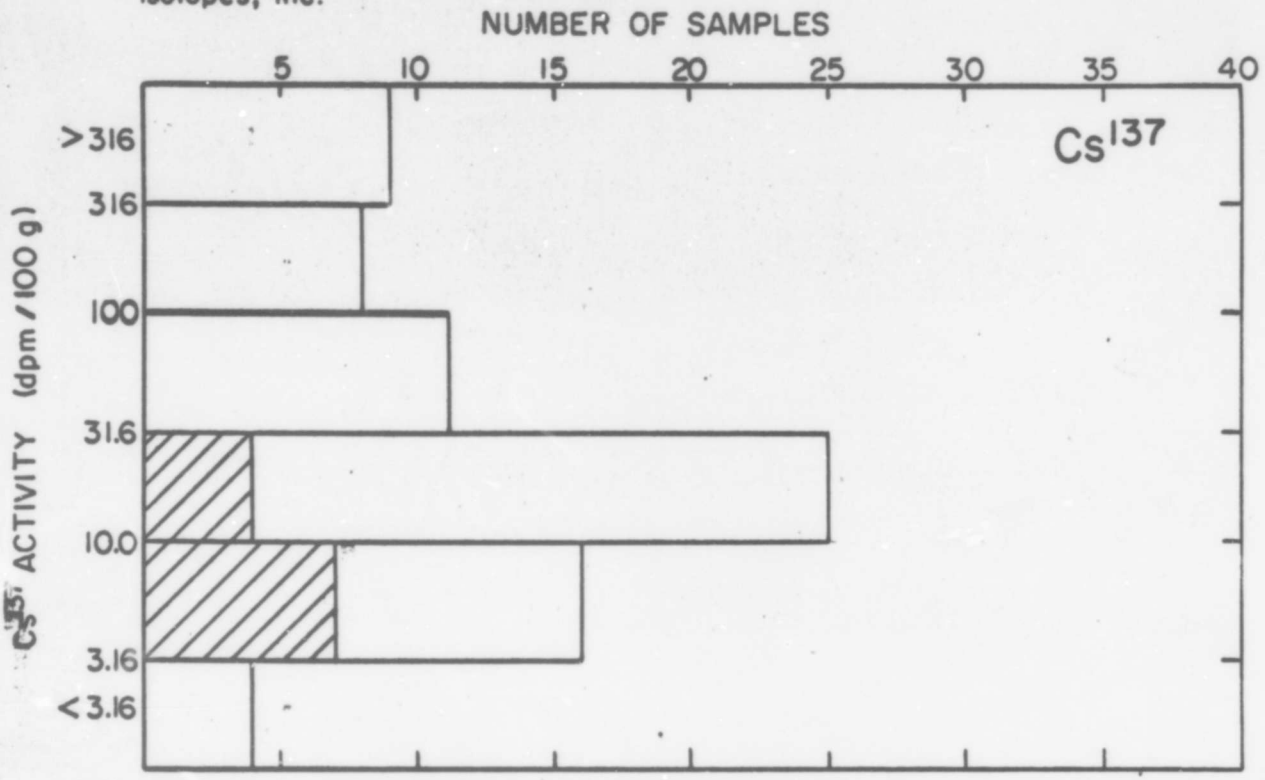

FIGURE 74 · FREQUENCY OF OCCURRENCE OF Cs-137 ACTIVITIES IN BLANK SAMPLES (cross hatched) AND IN SOIL SAMPLES

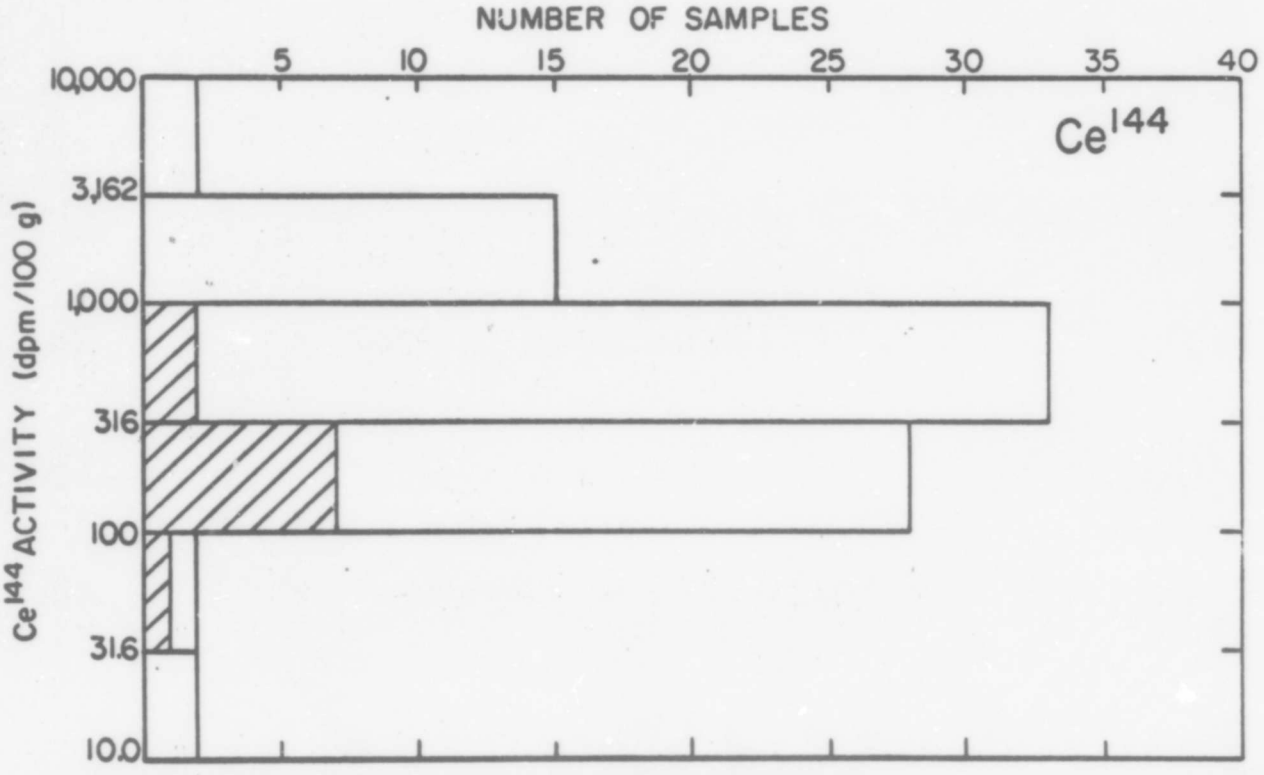

FIGURE 75 · FREQUENCY OF OCCURRENCE OF Ce-144 ACTIVITIES IN BLANK SAMPLES (cross hatched) AND IN SOIL SAMPLES

Isotopes, Inc.

Table 22. Results of Duplicate Analyses of Soil Samples

Sample Number	Individual Results (dpm/100g. of soil with % counting error)		Mean (with % standard deviation)
A. Analyses for strontium-90			
27-2	122 ± 1.6%	121 ± 1.5%	122. ± 0.82%
28-7	10.3 ± 5.5%	5.56 ± 11.8%	7.93 ± 42.2%
29-6	9.16 ± 11.9%	6.02 ± 9.1%	7.59 ± 29.2%
37-8	8.53 ± 8.5%	5.61 ± 7.3%	7.07 ± 29.1%
32-8	5.31 ± 22.0%	7.35 ± 14.2%	6.33 ± 17.2%
34-8	4.85 ± 13.6%	5.12 ± 10.5%	4.99 ± 3.83%
27-7	5.17 ± 15.7%	3.73 ± 17.3%	4.45 ± 22.9%
27-8	6.02 ± 18.2%	2.66 ± 20.5%	4.34 ± 54.6%
			Mean Standard Deviation = 25.0%
B. Analyses for ruthenium-106			
34-1	842 ± 2.6%	890 ± 2.8%	866. ± 7.18%
27-2	337 ± 2.6%	178 ± 8.3%	258 ± 43.4%
28-7	77.3 ± 18.5%	77.8 ± 6.3%	77.6 ± 0.47%
27-8	48.1 ± 12.4%	32.8 ± 10.0%	40.5 ± 25.4%
28-10	23.0 ± 26.5%	44.5 ± 23.7%	33.8 ± 45.0%
29-8	32.4 ± 17.1%	27.7 ± 12.9%	30.1 ± 11.1%
28-9	28.8 ± 15.4%	27.5 ± 13.8%	28.2 ± 3.27%
			Mean Standard Deviation = 19.4%
C. Analyses for cesium-137			
34-1	766 ± 1.0%	828 ± 0.8%	797. ± 5.49%
27-2	226 ± 1.6%	228 ± 1.4%	227. ± 0.62%
36-6	18.7 ± 7.3%	19.6 ± 5.6%	19.2 ± 3.24%
27-7	12.1 ± 11.0%	23.1 ± 10.8%	17.6 ± 44.2%
29-7	11.6 ± 8.7%	10.7 ± 14.0%	11.2 ± 5.72%
			Mean Standard Deviation = 11.9%

Table 22. (Cont'd)

Sample Number	Individual Results (dpm/100g. of soil with % counting error)		Mean (with % standard deviation)
D. Analyses for cerium-144			
34-1	3090 ± 4.0%	3310 ± 3.8%	3200. ± 4.88%
27-2	1350 ± 3.5%	1510 ± 3.7%	1430. ± 7.90%
36-8	830 ± 3.1%	637 ± 15.0%	734. ± 18.5%
32-8	558 ± 7.6%	478 ± 8.2%	518. ± 10.9%
27-7	505 ± 5.1%	482 ± 5.6%	494. ± 3.30%
36-6	683 ± 3.8%	221 ± 10.7%	452. ± 72.3%
30-4	216 ± 7.9%	566 ± 4.4%	391 ± 63.4%
34-8	433 ± 8.0%	238 ± 12.8%	336. ± 41.1%
29-6	422 ± 11.2%	211 ± 9.1%	317. ± 47.0%
29-8	340 ± 6.6%	226 ± 6.5%	283. ± 28.5%
27-8	169 ± 10.6%	238 ± 6.6%	204. ± 24.3%
29-7	179 ± 19.5%	177 ± 8.8%	178. ± 0.79%
		Mean Standard Deviation =	26.9%

Results of Radiochemical Analyses

The results of the radiochemical analyses of samples taken from 9 soil cores collected in Eastern Kansas during 1960 are given in Table 23. All nuclide activities have been corrected for radioactive decay to 1 July 1960. The calculated percent counting error for the analysis is given with each newly reported activity. Some of the data for samples 28 and 29 are taken from DASA-1300, Volume 5, Part III, Chapter 3, Table 3.4. Counting errors are not included with these data.

Some samples were analyzed in duplicate. The results for both aliquots are given in Table 23. For all samples, of course, ruthenium-106 measurements were performed on different aliquots from those used for the measurements of the other nuclides. When certain nuclide fractions were lost and had to be reanalyzed, the reanalyses were often done in duplicate. As a result only one or two nuclides for some samples have duplicate analyses reported.

Aliquots from the upper two inches of some of the Kansas soil cores were analyzed for cesium-137 by means of gamma spectrometry. The technique used was described in DASA-1300, Volume 5, Part III, Chapter 3. The contributions of the thorium and uranium series and of potassium-40 were stripped from the total gamma spectra of the samples and the 0.66 Mev. peak of cesium-137 in the residual spectra was used for the measurement.

Results from the gamma spectrometric measurements are compared with the results from radiochemical measurements of the same samples in Table 24. The agreement between these results is excellent for two samples, fair for several others and poor for about half the samples. The chief source of error in the spectrometric analyses is the uncertainty involved in the subtractions

from the spectra of the contributions of the natural activities in the soil. Small errors in these subtractions produce large errors in the residual spectra. The potential error from this source far exceeds the errors to be expected in the radiochemical analyses. Thus, in the following discussion, we will use the radiochemical data rather than the gamma spectrometric measurements of cesium-137.

Table 23 Nuclide Concentrations in Kansas Soil Samples

Sample 27. Shellabarger Sandy Loam:

Sample Number	Layer (inches)	Dry Wt. (g.)	Density (g/cm^3)	Nuclide Concentrations (dpm/100g corr. to 1 Jul 1960) Sr^{90}	Ru^{106}	Cs^{137}	Ce^{144}
2 -1	0-0.5	139	0.34	200 ± 2.7%	954 ± 3.1%	766 ± 0.8%	6490 ± 2.3%
27-2	0.5-1	546	1.32	122 ± 1.6%	337 ± 2.6%	226 ± 1.6%	1510 ± 3.7%
				121 ± 1.5%	178 ± 8.3%	228 ± 1.4%	1350 ± 3.5%
27-3	1-2	1240	1.50	55.1 ± 2.4%	289 ±10.1%	16.8 ± 6.0%	577 ± 6.5%
27-4	2-3	1438	1.74	17.7 ± 5.8%	115 ± 5.4%	6.24 ±18.8%	326 ± 7.0%
27-5	3-4	1371	1.66	6.38 ±16.1%	90.2 ± 7.1%	4.29 ±14.9%	11.9 ±19.6%
27-6	4-6	2843	1.72	7.87 ± 6.9%	37.8 ± 8.1%	10.3 ±10.6%	295 ± 7.8%
27-7	6-9	4053	1.64	5.17 ±15.6%	54.6 ± 9.2%	12.1 ±11.0%	505 ± 5.6%
				3.73 ±17.3%		23.1 ±10.8%	482 ± 5.1%
27-8	9-12	4313	1.74	6.02 ±18.2%	48.1 ±12.4%	6.66 ±37.7%	238 ± 6.6%
				2.66 ±20.5%	32.8 ±10.0%		169 ±10.6%

Table 23 (Cont'd)

Sample 28. Pratt Loamy Sand:

Sample Number	Layer (inches)	Dry Wt. (g.)	Density (g/cm^3)	Nuclide Concentrations (dpm/100g. corr. to 1 Jul 1960)			
				Sr^{90}	Ru^{106}	Cs^{137}	Ce^{144}
28-1	0-0.5	162	0.39	244*	891*	5384*	2596*
28-2	0.5-1	461	1.12	200**	348*	90.4*	603*
28-3	1-2	985	1.19	204*	117*	34.3*	103*
28-4	2-3	1095	1.33	26.7*	43.8*	$\leq$3.6*	22.5*
28-5	3-4	1188	1.44	63.5*	27.1*	0**	143 $\pm$ 10.7%
28-6	4-6	2483	1.51	10.5 $\pm$ 8.0%	66.6 $\pm$ 18.1%	8.93 $\pm$ 12.6%	287 $\pm$ 6.3%
28-7	6-9	3613	1.46	10.3 $\pm$ 5.5%	77.3 $\pm$ 18.5%	-	179 $\pm$ 8.5%
				5.56 $\pm$ 11.8%	77.8 $\pm$ 6.3%		
28-8	9-12	3843	1.55	7.42 $\pm$ 11.9%	440 $\pm$ 3.4%	8.69 $\pm$ 7.6%	255 $\pm$ 6.0%
28-9	12-18	7653	1.55	3.63 $\pm$ 15.0%	28.8 $\pm$ 15.4%	5.89 $\pm$ 7.7%	171 $\pm$ 7.7%
					27.5 $\pm$ 13.8%		
28-10	18-24	7933	1.60	3.97 $\pm$ 10.0%	23.0 $\pm$ 26.5%	2.57 $\pm$ 27.5%	669 $\pm$ 4.2%
					44.5 $\pm$ 23.7%		

* Result originally reported in DASA-1300, Vol. 5, p. 264

** Result originally interpolated in DASA-1300

Table 23 (Cont'd)

Sample 29. Bethany Silt Loam (undisturbed):

Sample Number	Layer (inches)	Dry Wt. (g.)	Density (g/cm^3)	Nuclide Concentrations (dpm/100g. corr. to 1 Jul 1960)			
				Sr^{90}	Ru^{106}	Cs^{137}	Ce^{144}
29-1	0-0.5	179	0.43	181*	374*	801*	1782*
29-2	0.5-1	452	1.10	117*	271*	279*	550*
29-3	1-2	1154	1.40	52.5*	92.2*	55.6*	83.8*
29-4	2-3	1249	1.52	-	45.8*	$\leq$15.3*	47.2*
29-5	3-4	1156	1.40	19.7 $\pm$ 31.3%	121 $\pm$ 5.7%	27.7 $\pm$ 9.4%	246 $\pm$ 6.7%
29-6	4-6	2450	1.49	9.16 $\pm$ 11.9%	50.6 $\pm$ 11.8%	11.4 $\pm$ 16.0%	422 $\pm$ 11.2%
				6.02 $\pm$ 9.1%			211 $\pm$ 9.8%
29-7	6-9	3336	1.35	12.1 $\pm$ 15.0%	52.5 $\pm$ 15.1%	11.6 $\pm$ 8.7%	179 $\pm$ 8.8%
						10.7 $\pm$ 14.0%	177 $\pm$ 19.5%
29-8	9-12	2384	0.96	2.42 $\pm$ 17.8%	32.4 $\pm$ 17.1%	1.38 $\pm$ 31.1%	340 $\pm$ 6.5%
					27.7 $\pm$ 12.9%		226 $\pm$ 6.6%

* Result originally reported in DASA-1300, Vol. 5, p. 265

Table 23 (Cont'd)

Sample 30. Bethany Silt Loam (cultivated):

Sample Number	Layer (inches)	Dry Wt. (g.)	Density (g/cm^3)	Nuclide Concentrations (dpm/100g. corr. to 1 Jul 1960)			
				Sr^{90}	Ru^{106}	Cs^{137}	Ce^{144}
30-1	0-2	1885	1.14	33.2 ± 6.0%	772 ± 3.2%	67.8 ± 2.0%	2360 ± 5.2%
30-2	2-4	2225	1.38	25.3 ± 4.6%	202 ± 6.3%	35.6 ± 11.6%	429 ± 7.9%
30-3	4-6	2338	1.42	34.3 ± 3.8%	66.3 ± 8.7%	62.1 ± 2.9%	282 ± 5.4%
30-4	6-9	3316	1.34	17.2 ± 6.8%	54.3 ± 8.7%	18.6 ± 7.5%	566 ± 4.4%
							216 ± 7.9%
30-5	9-12	3281	1.33	4.31 ± 17.7%	96.8 ± 8.0%	22.8 ± 3.1%	404 ± 6.8%

Table 23 (Cont'd)

Sample 32. Irwin Silt Clay Loam:

Sample Number	Layer (inches)	Dry Wt. (g.)	Density (g/cm^3)	Nuclide Concentrations (dpm/100g. corr. to 1 Jul 1960)			
				Sr^{90}	Ru^{106}	Cs^{137}	Ce^{144}
32-1	0-0.5	145	0.35	322 ± 1.0%	1180 ± 2.4%	515 ± 1.5%	2090 ± 9.5%
32-2	0.5-1	381	0.92	75.8 ± 2.6%	404 ± 5.6%	238 ± 1.4%	1050 ± 7.9%
32-3	1-2	884	1.07	132 ± 1.6%	180 ± 6.3%	227 ± 1.7%	1370 ± 7.0%
32-4	2-3	963	1.17	40.7 ± 4.1%	225 ± 5.5%	≤ 19.5	543 ± 5.2%
32-5	3-4	911	1.10	10.1 ± 13.4%	187 ± 5.6%	22.7 ± 4.8%	248 ± 9.8%
32-6	4-6	2303	1.40	3.57 ± 16.2%	28.7 ± 8.9%	12.6 ± 11.6%	550 ± 8.0%
32-7	6-9	3203	1.30	7.45 ± 9.6%	31.5 ± 9.7%	10.5 ± 7.3%	401 ± 4.5%
32-8	9-12	3065	1.24	5.31 ± 22.0%	60.0 ± 20.2%	11.4 ± 16.9%	558 ± 7.6%
				7.35 ± 14.2%			478 ± 8.2%

Table 23 (Cont'd)

Sample 34. Summit Clay Loam:

Sample Number	Layer (inches)	Dry Wt. (g.)	Density (g/cm^3)	Nuclide Concentrations (dpm/100g. corr. to 1 Jul 1960)			
				Sr^{90}	Ru^{106}	Cs^{137}	Ce^{144}
34-1	0-0.5	258	0.63	222 ± 1.8%	890 ± 2.8%	766 ± 1.0%	3090 ± 4.0%
				350 ± 1.7%	842 ± 2.6%	828 ± 0.8%	3310 ± 3.8%
34-2	0.5-1	411	1.00	153 ± 1.0%	683 ± 2.2%	87.5 ± 3.1%	884 ± 9.1%
34-3	1-2	918	1.11	53.9 ± 1.7%	122 ± 5.9%	44.3 ± 2.8%	655 ± 7.9%
34-4	2-3	1022	1.24	21.7 ± 5.2%	107 ± 11.7%	22.1 ± 8.3%	320 ± 8.6%
34-5	3-4	1025	1.24	7.49 ± 11.3%	94.0 ± 5.9%	22.3 ± 5.6%	181 ± 17.4%
34-6	4-6	2140	1.30	5.28 ± 12.6%	74.1 ± 7.5%	10.5 ± 13.5%	210 ± 8.2%
34-7	6-9	3218	1.30	6.39 ± 8.6%	14.4 ± 14.3%	8.21 ± 9.1%	231 ± 9.5%
34-8	9-12	3292	1.33	4.85 ± 13.6%	116 ± 4.2%	4.39 ± 27.8%	238 ± 12.8%
				5.12 ± 10.5%			433 ± 8.0%

Table 23 (Cont'd)

Sample 36. Cherokee Silt Loam:

Sample Number	Layer (inches)	Dry Wt. (g.)	Density (g/cm^3)	Nuclide Concentrations (dpm/100g. corr. to 1 Jul 1960)			
				Sr^{90}	Ru^{106}	Cs^{137}	Ce^{144}
36-1	0-0.5	173	0.42	241 ± 2.3%	499 ± 8.9%	594 ± 1.1%	2340 ± 6.2%
36-2	0.5-1	382	0.93	-	-	-	-
36-3	1-2	1060	1.29	67.4 ± 4.0%	252 ± 4.6%	60.7 ± 3.3%	384 ± 7.4%
36-4	2-3	1170	1.42	22.3 ± 4.4%	110 ± 10.8%	15.2 ± 16.2%	767 ± 7.6%
36-5	3-4	1097	1.33	11.6 ± 5.6%	512 ± 2.8%	8.06 ± 8.82%	298 ± 8.5%
36-6	4-6	2198	1.33	7.48 ± 10.4%	75.3 ± 12.3%	18.7 ± 7.3%	221 ± 10.7%
						19.6 ± 5.7%	683 ± 3.8%
36-7	6-9	3253	1.32	4.99 ± 9.9%	38.8 ± 21.7%	14.3 ± 8.2%	228 ± 9.3%
36-8	9-12	3178	1.29	5.60 ± 14.8%	31.8 ± 9.6%	4.45 ± 11.0%	637 ± 15.0%
							830 ± 3.1%

Table 23 (Cont'd)

Sample 37. Bates Silt Loam:

Sample Number	Layer (inches)	Dry Wt. (g.)	Density (g/cm^3)	Nuclide Concentrations (dpm/100g. corr. to 1 Jul 1960)			
				Sr^{90}	Ru^{106}	Cs^{137}	Ce^{144}
37-1	0-0.5	161	0.39	539 ± 3.0%	1690 ± 3.0%	1480 ± 1.1%	7440 ± 10.8%
37-2	0.5-1	414	1.00	208 ± 1.7%	146 ± 8.7%	271 ± 1.3%	1660 ± 4.5%
37-3	1-2	1170	1.42	97.7 ± 1.7%	516 ± 5.9%	170 ± 1.7%	1650 ± 8.1%
37-4	2-3	1159	1.41	19.9 ± 5.3%	207 ± 5.6%	44.6 ± 3.1%	491 ± 5.6%
37-5	3-4	1103	1.34	9.33 ± 10.3%	20400 ± 1.8%	9.06 ± 10.3%	297 ± 7.5%
37-6	4-6	2225	1.35	7.70 ± 8.9%	68.8 ± 7.4%	8.15 ± 11.1%	168 ± 7.8%
37-7	6-9	3543	1.43	3.20 ± 12.6%	79.1 ± 18.1%	7.38 ± 7.4%	741 ± 4.5%
37-8	9-12	3008	1.22	8.53 ± 8.5%	116 ± 9.9%	8.72 ± 10.8%	265 ± 6.1%
				5.61 ± 7.3%			

Table 23 (Cont'd)

Sample 38. Labette Clay Loam:

Sample Number	Layer (inches)	Dry Wt. (g.)	Density (g/cm^3)	Nuclide Concentrations (dpm/100g. corr.to 1 Jul 1960)			
				Sr^{90}	Ru^{106}	Cs^{137}	Ce^{144}
38-1	0-0.5	114	0.28	211 ± 2.3%	844 ± 3.6%	499 ± 1.7%	3020 ± 12.4%
38-2	0.5-1	336	0.82	99.7 ± 2.0%	387 ± 4.1%	128 ± 2.5%	660 ± 6.3%
38-3	1-2	557	0.68	65.8 ± 3.1%	293 ± 20.0%	72.2 ± 2.3%	779 ± 14.8%
38-4	2-3	1298	1.58	35.4 ± 4.7%	215 ± 6.9%	12.5 ± 12.6%	1020 ± 8.4%
38-5	3-4	1002	1.22	12.2 ± 10.4%	72.9 ± 16.1%	14.9 ± 13.5%	833 ± 6.7%
38-6	4-6	1703	1.03	3.94 ± 13.0%	139 ± 10.0%	11.7 ± 17.0%	454 ± 7.3%
38-7	6-9	3292	1.33	3.59 ± 10.1%	126 ± 8.2%	-	570 ± 7.3%
38-8	9-12	4881	1.98	4.87 ± 12.7%	54.1 ± 9.6%	16.0 ± 7.5%	288 ± 4.8%

Isotopes, Inc.

Table 24. Cesium-137 Concentrations in Kansas Soil Samples Determined Radiochemically and by Gamma Spectrometry

Sample Number	Cs^{137} Concentration (dpm/100g. corr. to 1 Jul 1960) Radiochemical	γ Spectrometry	Mean
27-1	766 ± 0.	A. 913 ± 3.2%	861 ± 32%
		B. 996 ± 3.7%	
27-2	A. 228 ± 1.4%	289 ± 2.2%	259 ± 17%
	B. 227 ± 1.6%		
30-1	67.8 ± 2.0%	28.4 ± 4.3%	48 ± 58%
30-2	35.6 ± 11.6%	28.8 ± 3.8%	33 ± 17%
32-1	515 ± 1.5%	931 ± 2.8%	723 ± 41%
32-2	238 ± 1.4%	234 ± 2.6%	236 ± 1.2%
32-3	227 ± 1.7%	55.2 ± 2.6%	141 ± 87%
34-1	A. 766 ± 1.0%	947 ± 2.2%	872 ± 12%
	B. 828 ± 0.8%		
34-2	87.5 ± 3.1%	209 ± 2.6%	149 ± 57%
34-3	44.3 ± 2.8%	28.2 ± 4.3%	36 ± 31%
36-1	594 ± 1.1%	595 ± 2.4%	595 ± 0.2%
36-3	60.7 ± 3.3%	43.6 ± 3.6%	52 ± 23%
37-1	1480 ± 1.1%	1770 ± 1.8%	1630 ± 13%
37-2	271 ± 1.3%	490 ± 1.2%	381 ± 41%
37-3	170 ± 1.7%	60.3 ± 2.5%	115 ± 68%
38-1	499 ± 1.7%	370 ± 1.5%	435 ± 21%
38-2	128 ± 2.5%	210 ± 3.1%	169 ± 34%
38-3	72.2 ± 2.3%	60.1 ± 2.4%	66.2 ± 13%

Discussion of Analytical Results

The soils discussed in this report were developed in a subhumid climate with a mean annual precipitation of approximately 27 inches. The bedrock from which the soils were derived varied from green clay shale to limestone. Due to the weathering processes in this climate, however, most of the soils show an acidic reaction when tested by a Hellige- Truog soil reaction tester. The measured pH values ranged from 5.0 to 7.8, but values about 7 were found only in a few subsoils derived from limestone.

Unfortunately we have no data on the mineral content, organic content or ion-exchange capacity of any of the soils or soil horizons sampled and analyzed in this program. Moreover our information on drainage at the sampling sites and on permeability of the soils is only qualitative. Each of these properties is capable of exerting an important influence on the distribution of fallout fission products in the soil. We hope to measure the ion-exchange capacities and organic material contents of at least some of these samples, and to discuss the results in a future report. Here, however, our discussion will have to be limited for the most part to a few hypotheses regarding the possible causes of the observed distributions of activity.

The cumulative deposit of strontium-90 and cesium-137 (in millicuries per square mile) in the 9 Kansas soils measured during this program are plotted as a function of depth in Figures 76 to 84. Similar plots for two New Jersey soils, the Marlton sandy loam and Lakewood sand, measured during Project HASP, are shown in Figures 85 and 86. Data for the Kansas soils may be compared with data for these New Jersey soils. The two New Jersey soils differ significantly from each other in the vertical distribution of their contained fission product activity.

In general, the curves in Figures 76 to 86 are convex upward as a result of preferential deposition of both fallout nuclides in the highest soil layers. The curves for the cultivated Bethany silt loam (Figure 79), however, show an almost linear increase in the cumulative deposit with depth for the first six inches. Doubtless this is mainly attributable to the repeated mixing of the soil during annual or semi-annual cultivation, but a similar distribution might also result from rapid percoloation through the disturbed soil by rainwater. The strontium-90 curve for the Lakewood sand (Figure 86) a very permeable soil, also shows a linear increase in cumulative deposit with depth for the first 4 inches. The Pratt loamy sand (Figure 78), which probably has the highest permeability of any of the Kansas soils studied, does not clearly show this linear relationship.

The total deposits of strontium-90 and cesium-137 in the upper 12 inches of the 9 Kansas soils are summarized in Table 25. The total deposits vary in size over a fairly wide range. For example, the Pratt loamy sand contains almost twice as much strontium-90 and more than twice as much cesium-137 as the average for the other eight samples. On the other hand the Labette clay loam contains only about 60 percent of the average deposit of the other samples.

The soil descriptions given in Table 20 provide clues to some of the causes of the variations in total deposition at the different soil sites. Thus the Pratt loamy sand is described as having low runoff and as being well drained internally. These characteristics, which would promote the movement through the soil of runoff from precipitation, are quite consistent with the relatively high concentration of fallout nuclides found in this soil. The Bates silt loam, which also contains higher than average concentrations, has

moderate permeability, while most of the other samples have low or moderately low permeability. On the other hand there is no clear reason why the total deposit in the Labette clay loam should be lower than that in the Bethany silt loam, the Irwin silt clay loam or the Summit clay loam. Perhaps if data on the ion-exchange capacities of these soils become available the variations in deposition can be explained.

When considering the data for the Kansas soil samples we cannot, of course, neglect to consider the possible effects of sample contamination. Some of the differences in nuclide distributions found may be the result of analytical error. Table 26 has been prepared to illustrate the possible contribution by contamination to the calculated deposits. We have assumed that, with a few exceptions, each sample was subjected during its analysis to contamination by 4.0 dpm of strontium-90 and 9.6 dpm of cesium-137, the mean values for the blank samples analyzed with the soils. The exceptions made involved the upper cuts of sample 28 (0 to 4 inches) and sample 29 (0 to 3 inches), which were analyzed during Project HASP, and those samples in which activities less than 4.0 dpm of strontium-90 and 9.6 dpm of cesium-137 were actually found. We have arbitrarily assumed 1.0 dpm of contamination of both nuclides in samples measured during Project HASP, and have attributed all activity to contamination for samples which contained lower activities than the average of the blanks. The "net deposits" listed in Table 26 should generally be more accurate than are the calculated deposits uncorrected for contamination, but since it is unlikely that contamination of the samples is uniform we cannot be certain whether the corrections actually improve all or only some of the results.

Isotopes, Inc.

The cumulative deposits of strontium-90 and cesium-137 in the soils collected in New Jersey during 1960 and analyzed during Project HASP have been calculated and are presented in Table 27. These data may be compared with those in Tables 25 and 26. Hardy et al. [46] have reported data on the strontium-90 deposit in soil samples collected at Manhattan, Kansas on 2 November 1960 and at New Brunswick, New Jersey on 12 September 1960 which we may also compare with the data in Tables 25 to 27. For Manhattan, Kansas they report 72.2 mc/mi^2, which is similar to the "corrected" deposits given in Table 26 for several of the Kansas soils measured by us. For New Brunswick, New Jersey they report 58.8 mc/mi^2, which is less than the deposits of all but one of the New Jersey soils measured during Project HASP and summarized in Table 27. Of course, the variations from one sampling site to another in both the New Jersey data and the Kansas data indicate that we cannot attach much significance to the agreement or lack of agreement between the results for the sampling sites at Manhattan and New Brunswick and the results obtained for the different sites sampled during Projects HASP and Star Dust.

It is interesting also to compare the relative distributions of strontium-90 and cesium-137 within each of the 9 Kansas soils which we have analyzed. We have used the total deposit of each of these nuclides within the upper twelve inches of each core sample as a reference datum. We have then calculated the fraction of the total deposit which lies above 0.5 inch, 1 inch, 2 inches, etc. in each core. The results are plotted in Figures 87 to 91. Similar plots of data for the Marlton sandy loam and the Lakewood sand are given in Figure 92.

Some of the soil samples, such as the Irwin silty clay loam and the Bates silt loam, show a close association of the strontium-90 and cesium-137 at all levels, but others, such as the Pratt loamy sand and Bethany silt loam show a separation of the nuclides. The differences in behavior between soils are doubtless caused mainly by differences in ion-exchange capacity, about which we as yet have no information. One can, however, see a similarity in nuclide distributions between the relatively permeable Pratt loamy sand and the very permeable Lakewood sand. Both show concentration of the cesium-137 in the upper inch of soil but fairly uniform distribution of the strontium-90 within the upper 4 inches of soil. Once can also explain the greater similarity in behavior between strontium-90 and cesium-137 in the cultivated than in the undisturbed Bethany silt loam, of course, for the cultivation of the soil would produce good mixing down almost to 8 inches depth.

If more data on the chemical, mineralogical and physical properties of the 9 Kansas soils described here can be obtained, we will endeavor to correlate these properties with the observed radionuclide distributions in a future report.

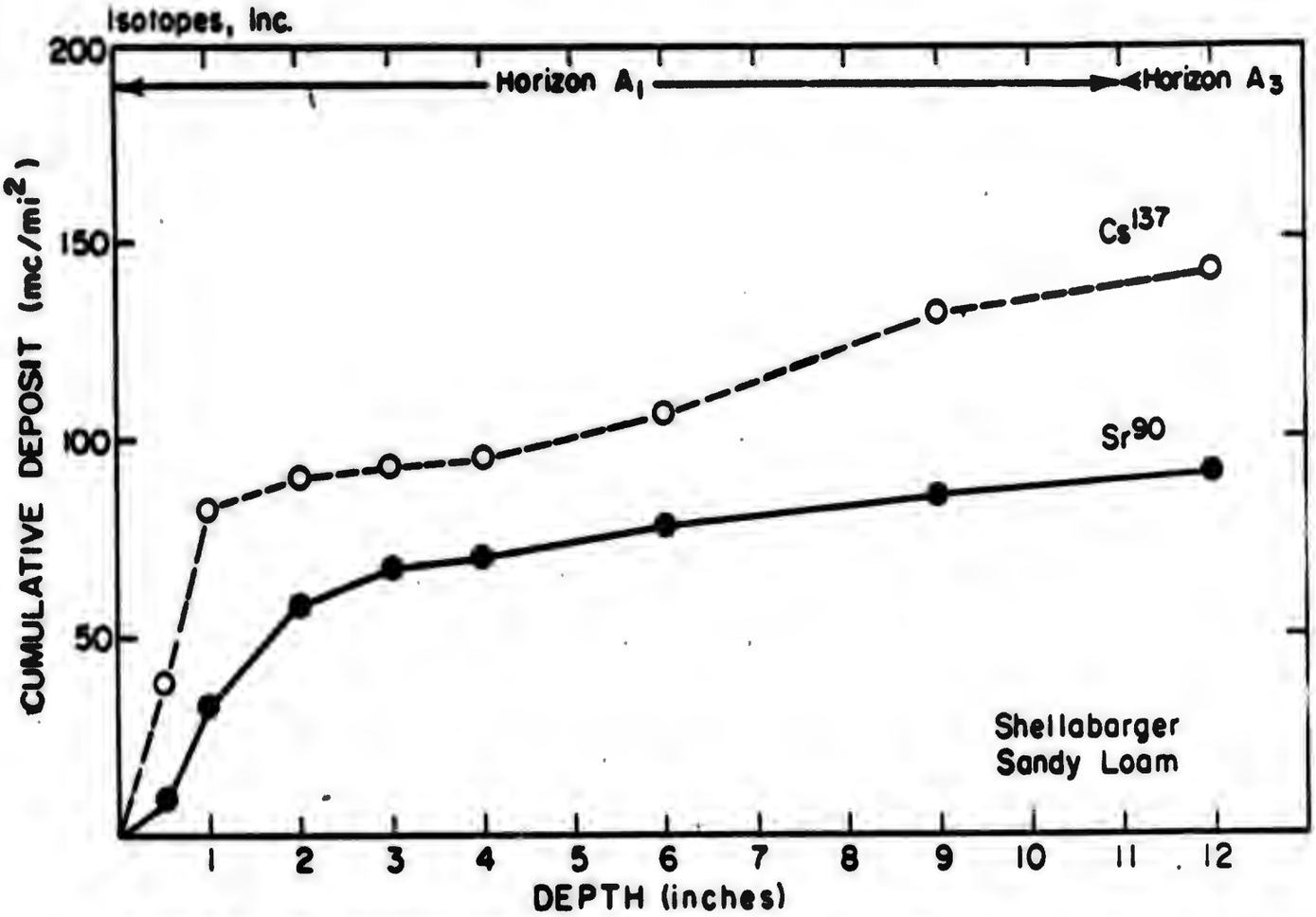

FIGURE 76 · DEPOSIT OF Sr-90 AND Cs-137 IN SAMPLE #27

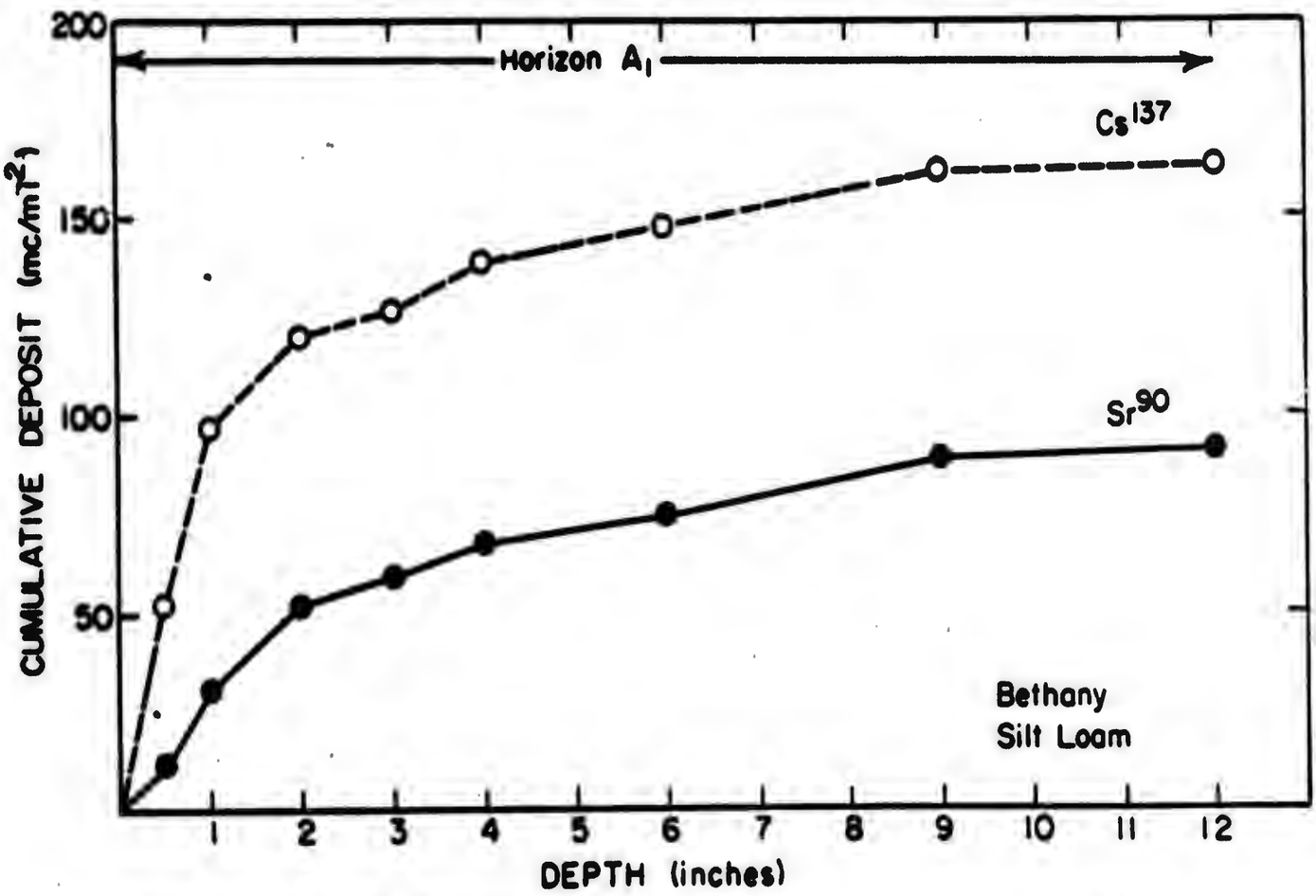

FIGURE 77 · DEPOSIT OF Sr-90 AND Cs-137 IN SAMPLE 29

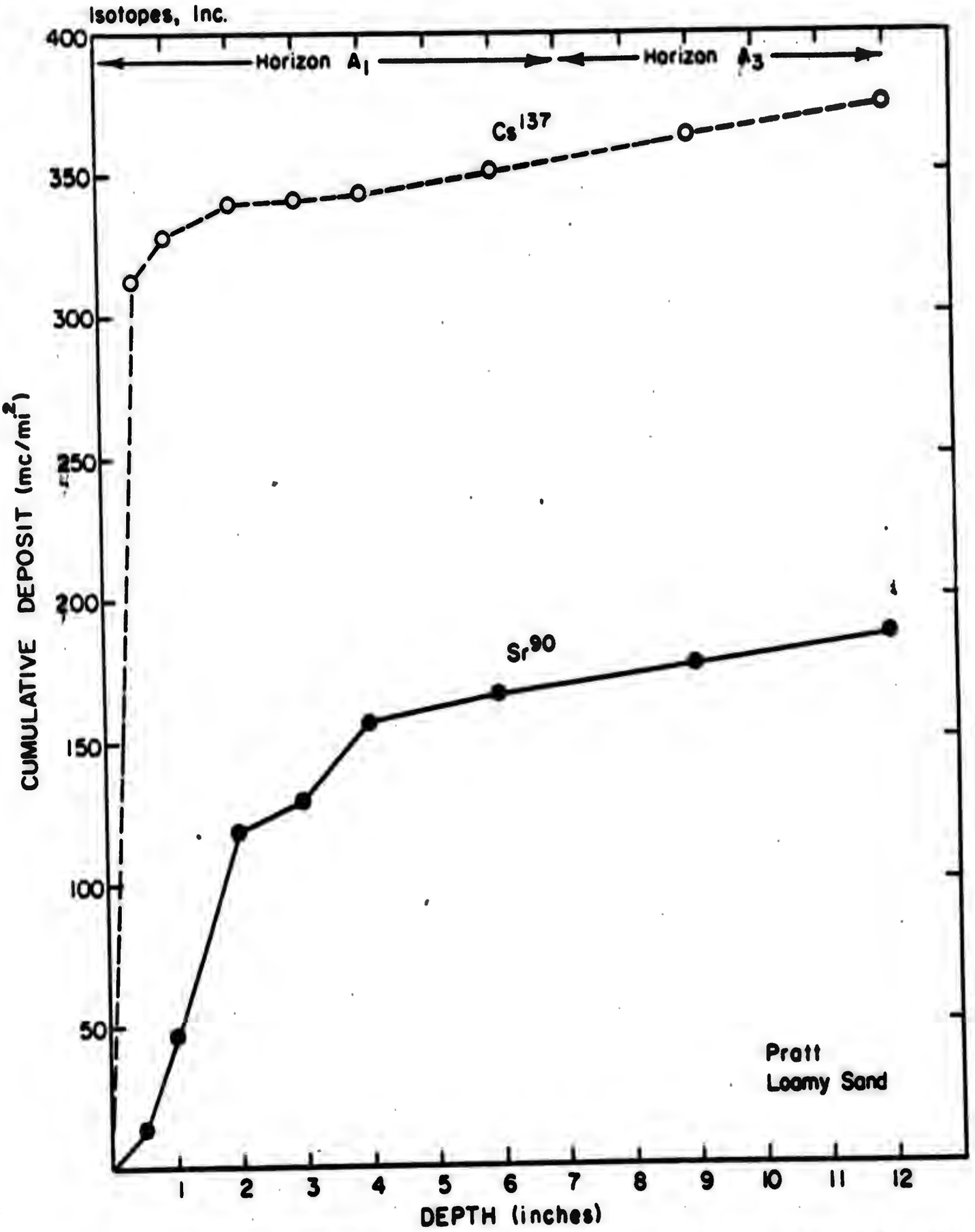

FIGURE 78· DEPOSIT OF Sr-90 AND Cs-137 IN SAMPLE 28

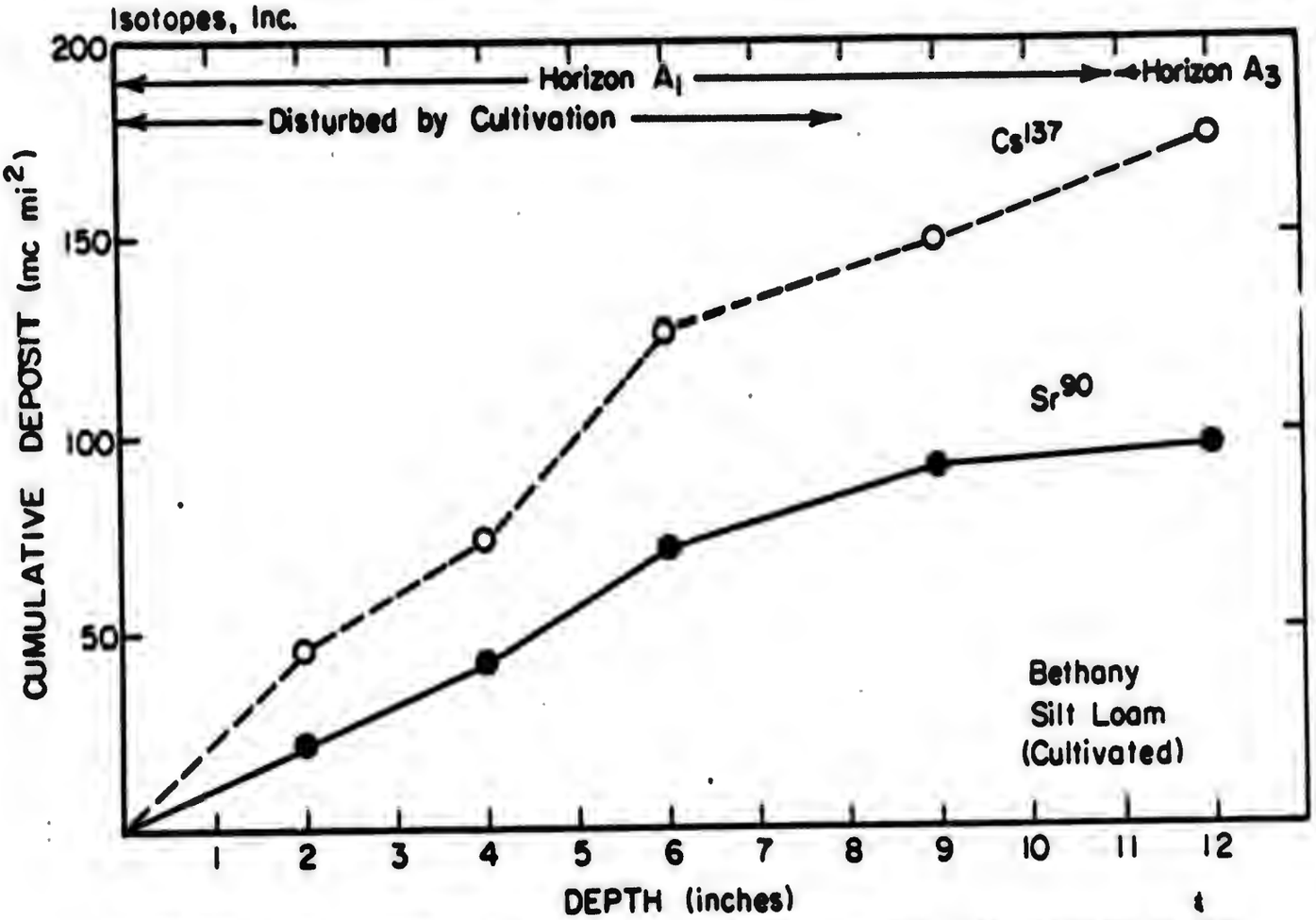

FIGURE 79· DEPOSIT OF Sr-90 AND Cs-137 IN SAMPLE 30

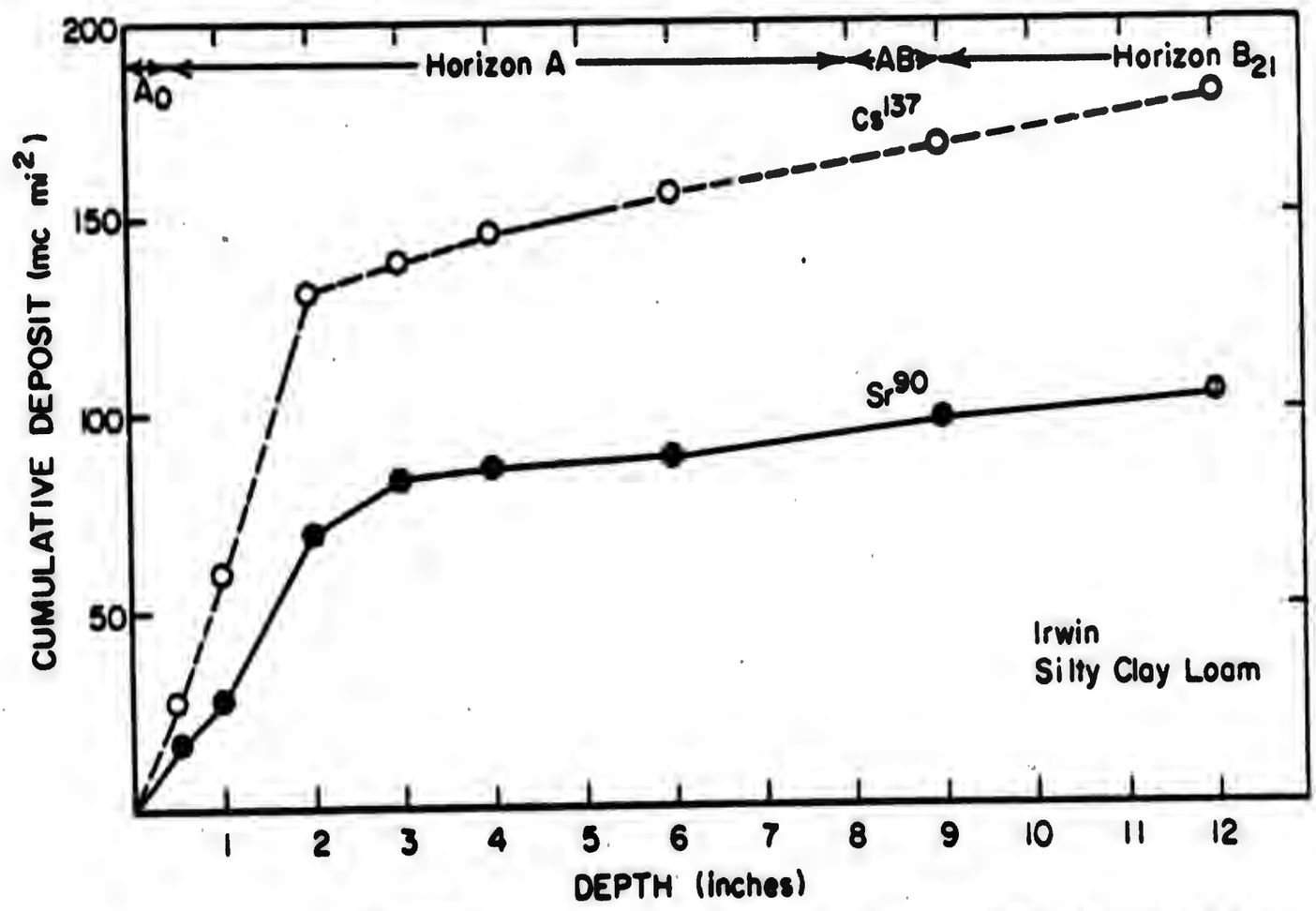

FIGURE 80· DEPOSIT OF Sr-90 AND Cs-137 IN SAMPLE 32

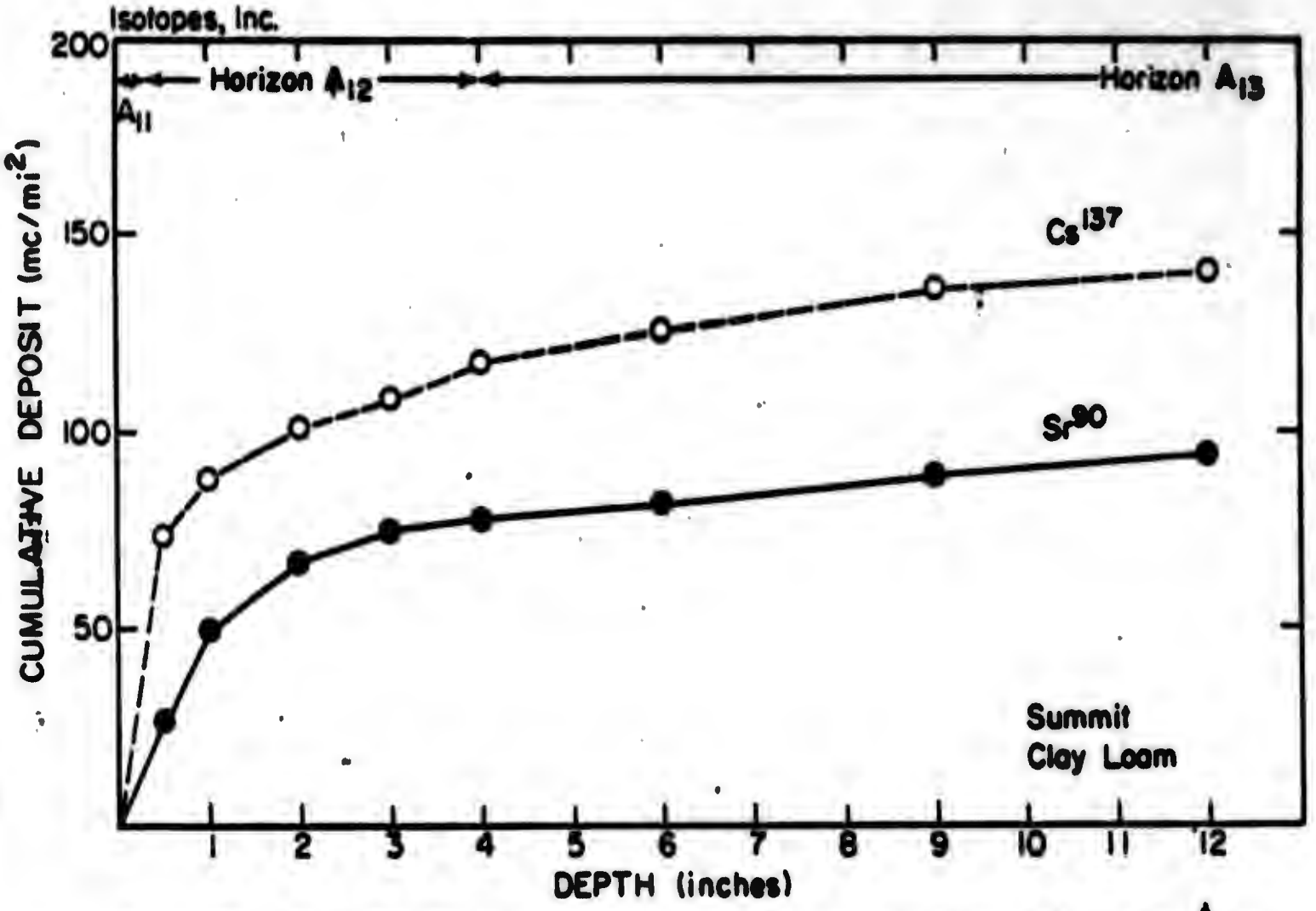

FIGURE 81 · DEPOSIT OF Sr-90 AND Cs-137 IN SAMPLE 34

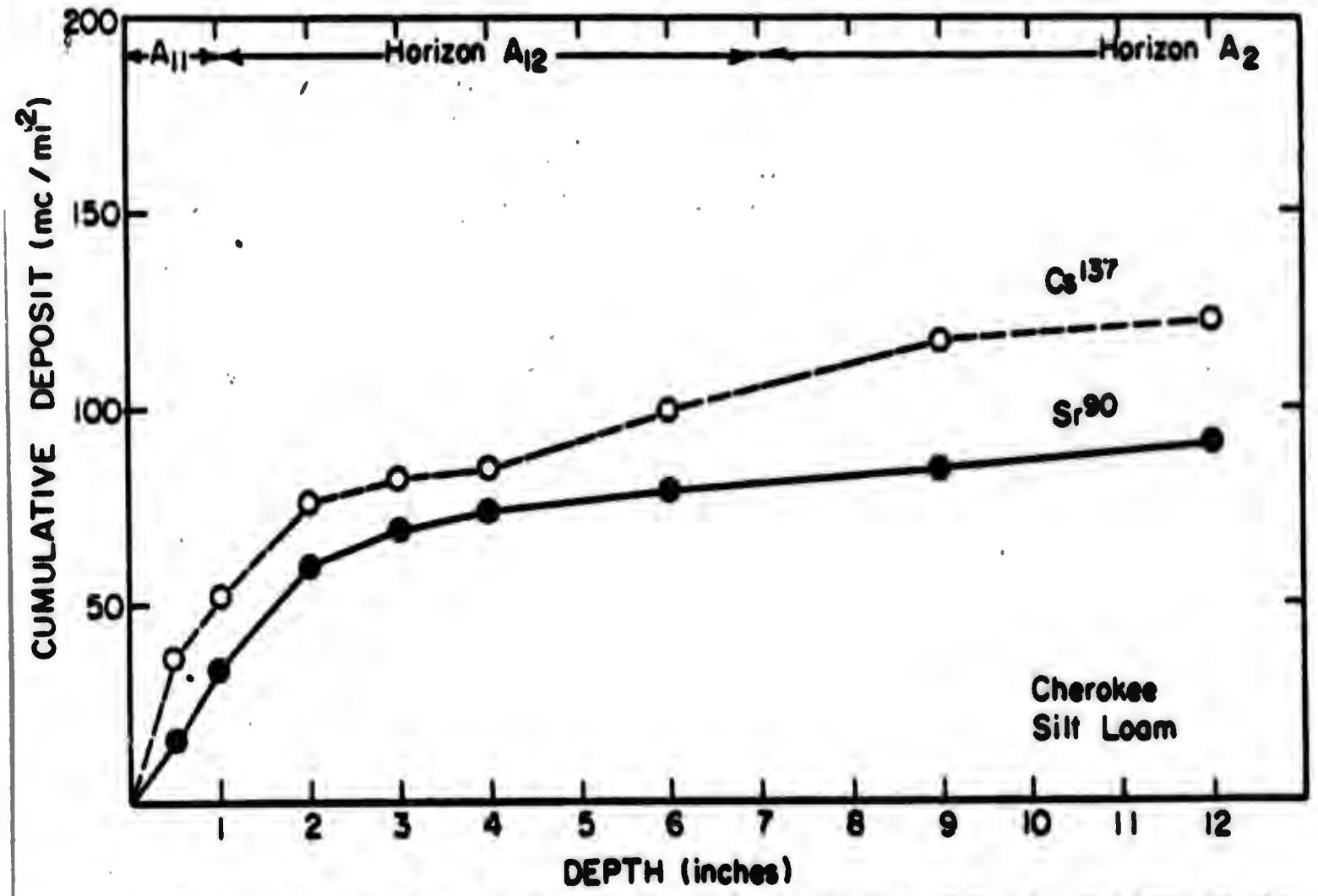

FIGURE 82 · DEPOSIT OF Sr·90 AND Cs-137 IN SAMPLE 36

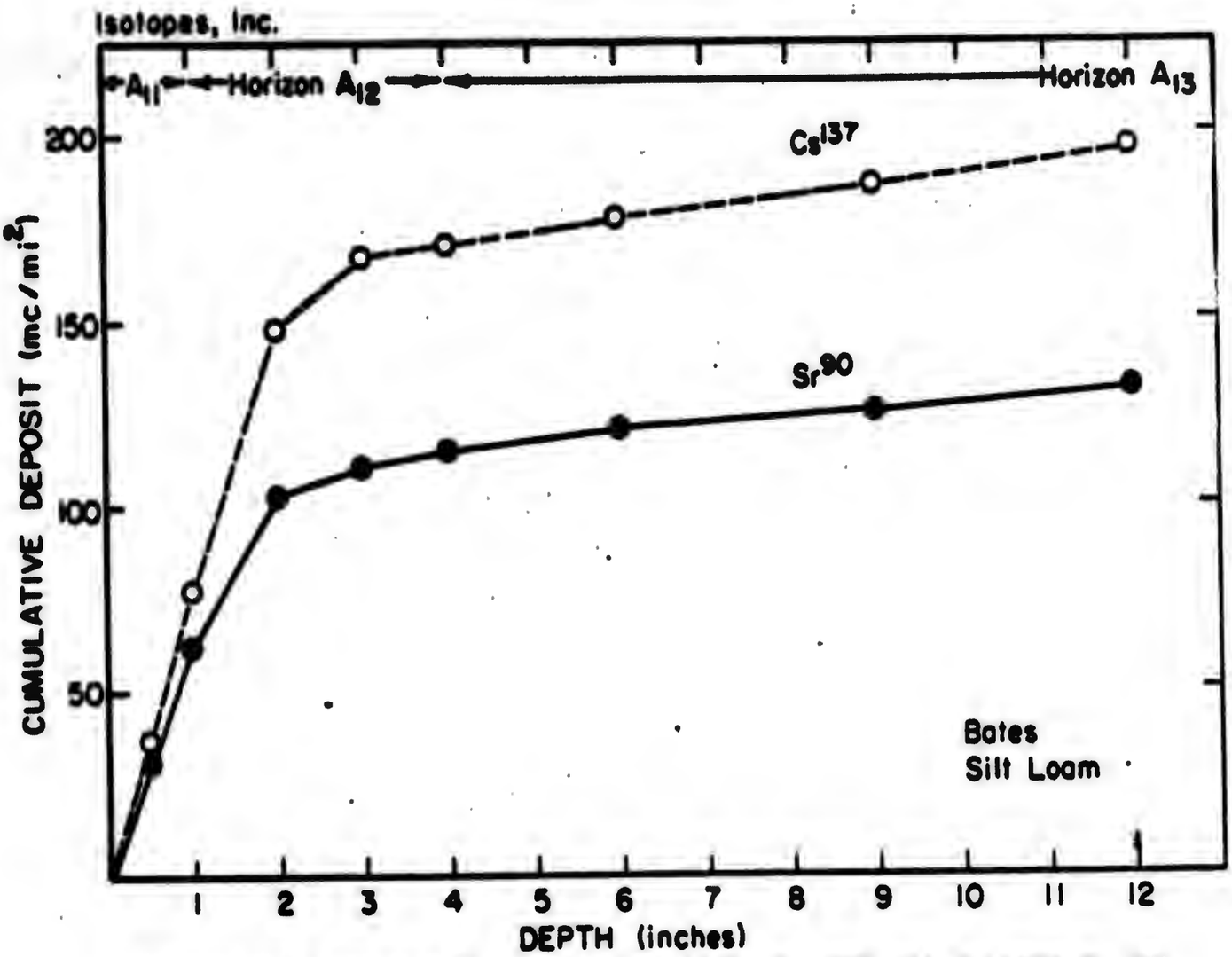

FIGURE 83 · DEPOSIT OF Sr-90 AND Cs-137 IN SAMPLE 37

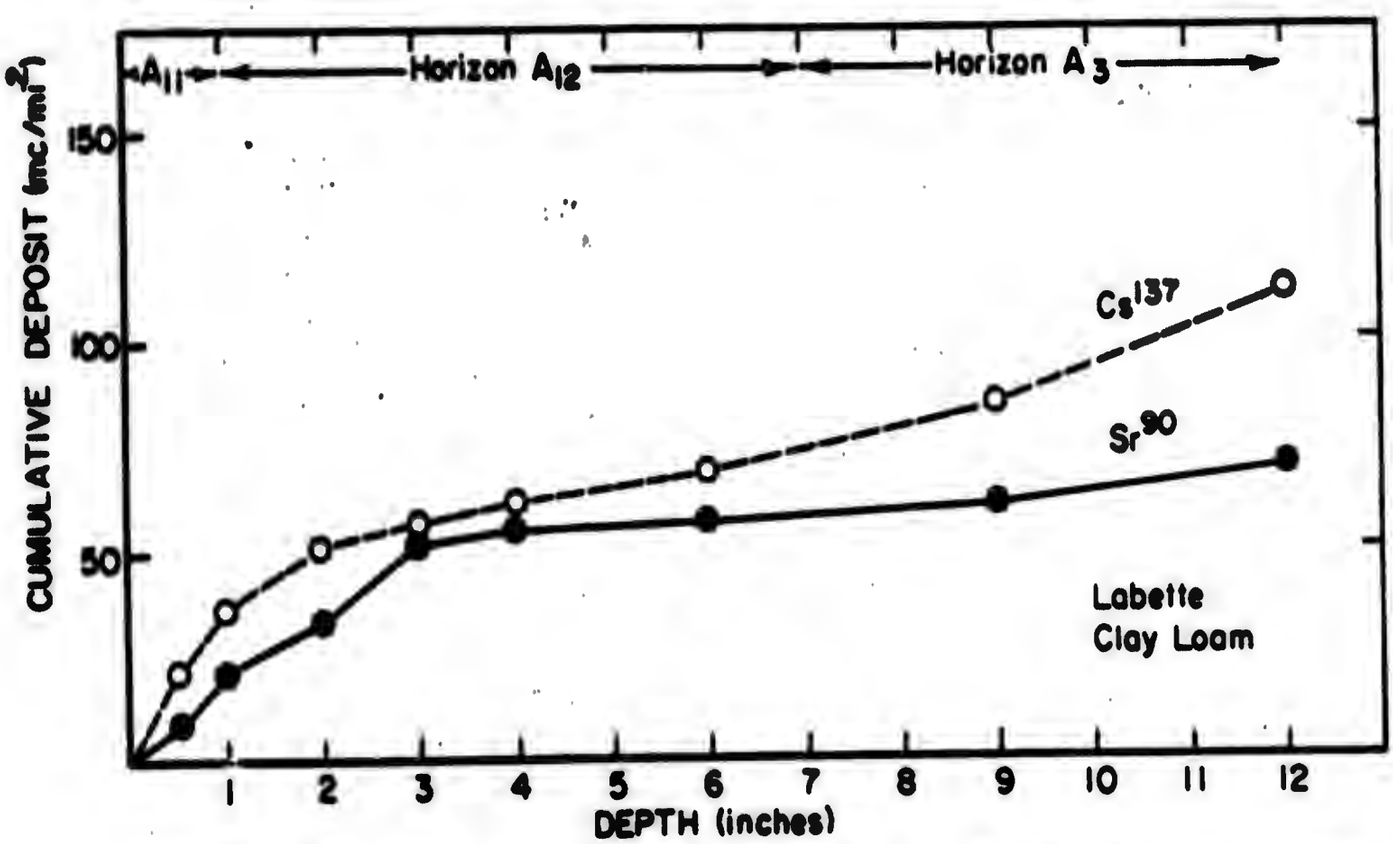

FIGURE 84 · DEPOSIT OF Sr-90 AND Cs-137 IN SAMPLE 38

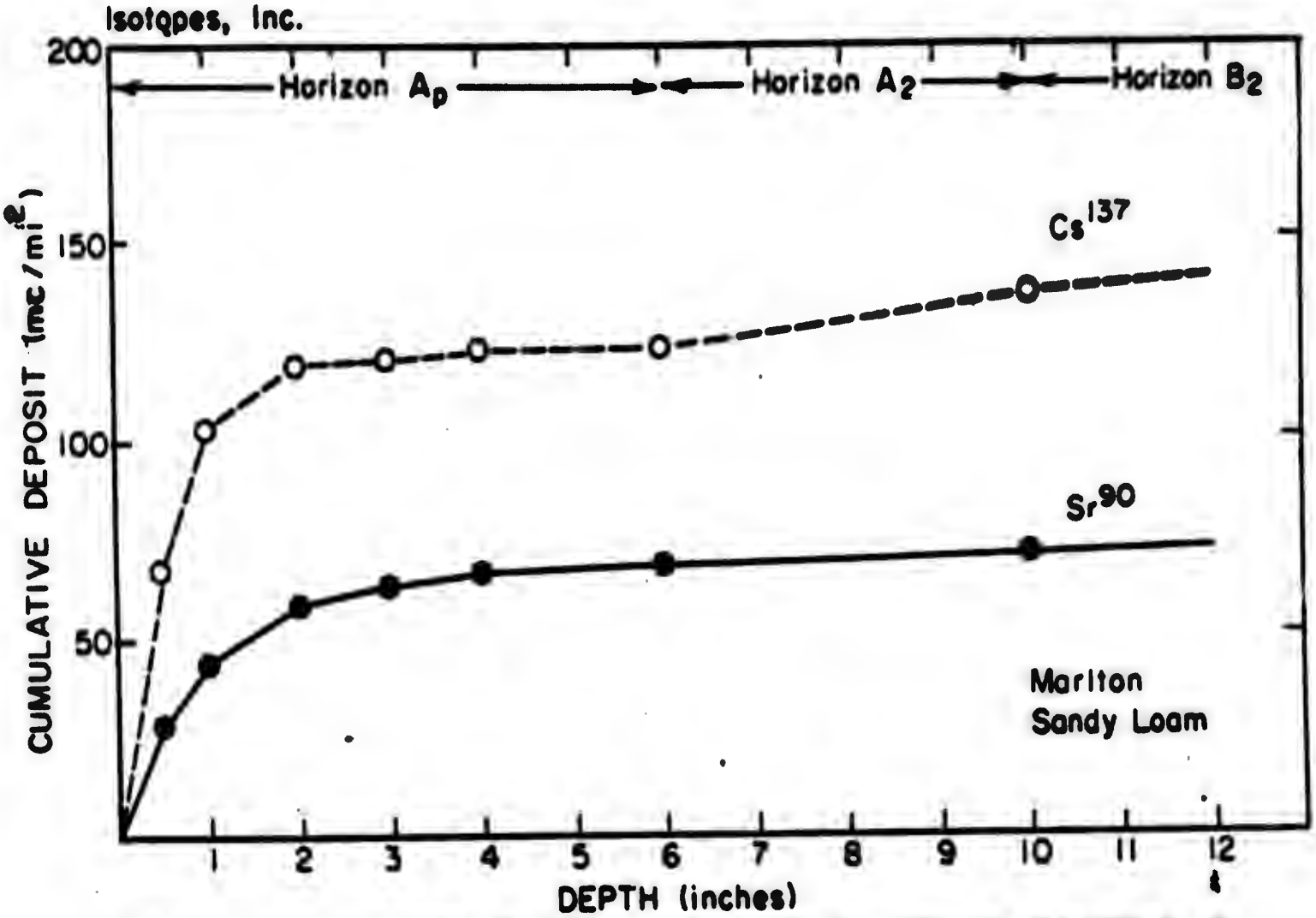

FIGURE 85 · DEPOSIT OF Sr-90 AND Cs-137 IN SAMPLE 8

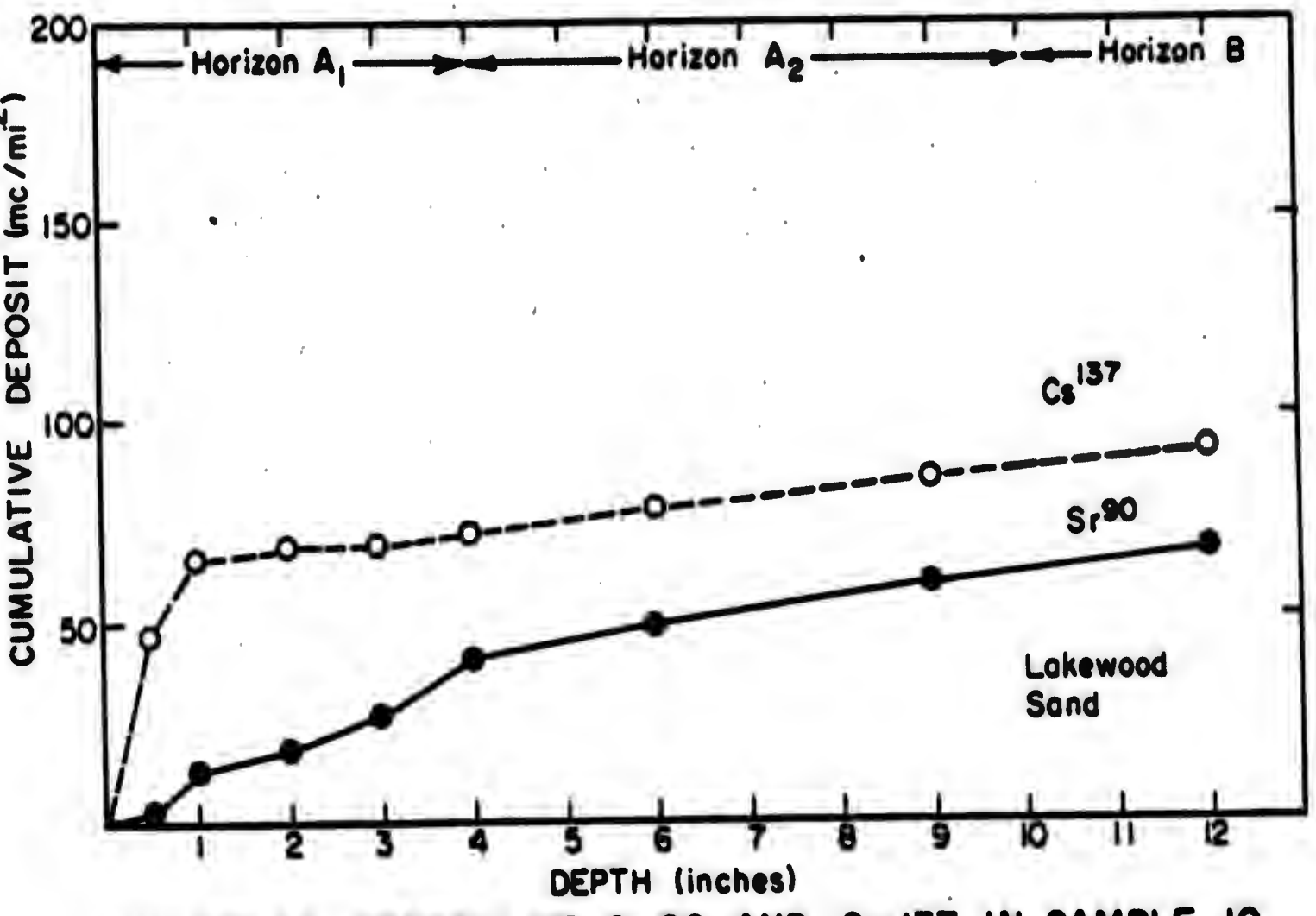

FIGURE 86 · DEPOSIT OF Sr-90 AND Cs-137 IN SAMPLE 10

Table 25 Cumulative Deposits of Strontium-90 and Cesium-137 in Kansas Soils on 1 July 1960* (In Upper 12 Inches of Soil)

Sample Number	Soil Type	Deposit (mc/mi^2) Sr^{90}	Deposit (mc/mi^2) Cs^{137}	Cs^{137}/Sr^{90}
27	Shellabarger Sandy Loam	91	140	1.54
28	Pratt Loamy Sand	186	373	2.00
29	Bethany Silt Loam	90	161	1.79
30	Bethany Silt Loam (cultivated)	96	174	1.81
32	Irwin Silty Clay Loam	104	179	1.72
34	Summit Clay Loam	94	139	1.48
36	Cherokee Silt Loam	90	120	1.33
37	Bates Silt Loam	132	195	1.48
38	Labette Clay Loam	69	111	1.61
	Mean	106±34	177±79	1.67

* Corrected for the interval between 1 July 1960 and collection date by means of precipitation data.

Table 26 Correction of the Calculated Deposits for Potential Sample Contamination*

Sample Number	Strontium-90 (mc/mi^2) Calculated Deposit	Potential Error	"Corrected" Deposit	Cesium-137 (mc/mi^2) Calculated Deposit	Potential Error	"Corrected" Deposit
27	91	23	68	140	46	94
28	186	16	170	373	33	340
29	90	14	76	161	26	135
30	96	19	77	174	46	128
32	104	17	87	179	41	138
34	94	18	76	139	35	104
36	90	18	72	120	37	83
37	132	20	112	195	40	155
38	69	19	50	111	46	65
Mean	106	18	88±35	177	39	138±81

Cs^{137}/Sr^{90} for mean "corrected" deposit = 1.57

* Assuming mean contamination of 4.0 dpm Sr^{90} and 9.6 dpm Cs^{137} in each sample

Table 27 Cumulative Deposits of Strontium-90 and Cesium-137 in New Jersey Soils on 1 July 1960* (In Upper 12 Inches of Soil)

Sample Number	Soil Type	Deposit (mc/mi^2) Sr^{90}	Cs^{137}	Cs^{137}/Sr^{90}
4	Collington Sandy Loam	75	160	2.13
5	Collington Sandy Loam (Cultivated)	88	132	1.50
7	Rutledge Fine Sandy Loam	82	193	2.35
8	Marlton Sandy Loam	72	141	1.96
10	Lakewood Sand	66	91	1.38
11	Leon Sand	84	221	2.63
13	Keyport Sandy Loam	48	-	-
17	Woodstown Sandy Loam	66	127	1.92
18	Bucks Silt Loam	76	225	2.96
19	Croton Silt Loam	96	153	1.59
20	Washington Loam	82	104	1.27
	Mean Sr^{90} Deposit	76±13	-	-
	Mean (omitting sample 13)	79±10	155±46	1.96

* Corrected for the interval between 1 July 1960 and collection date by means of precipitation data.

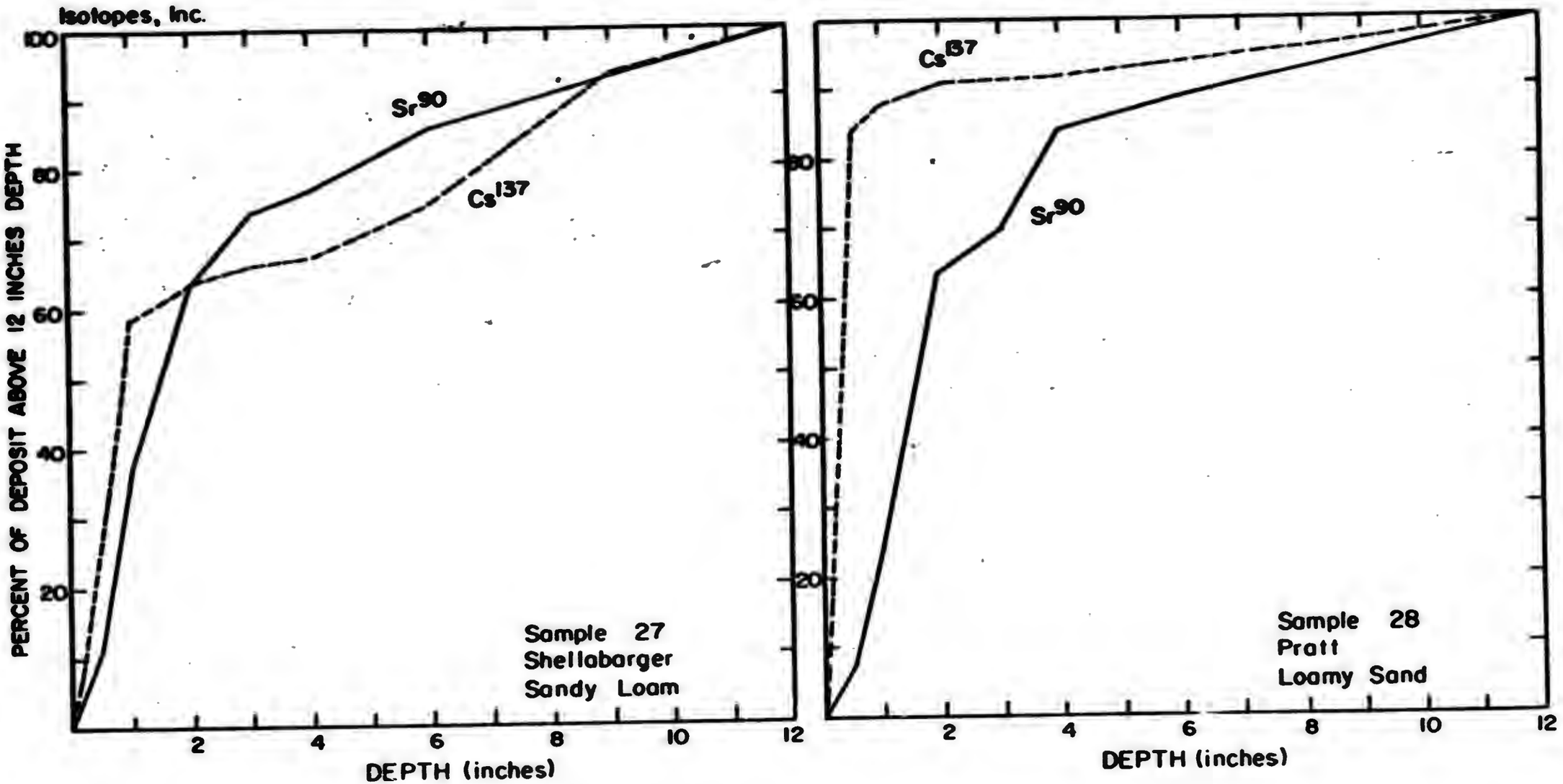

FIGURE 87· RELATIVE DEPTH PENETRATION OF Sr-90 AND Cs-137 IN SAMPLES 27 AND 28

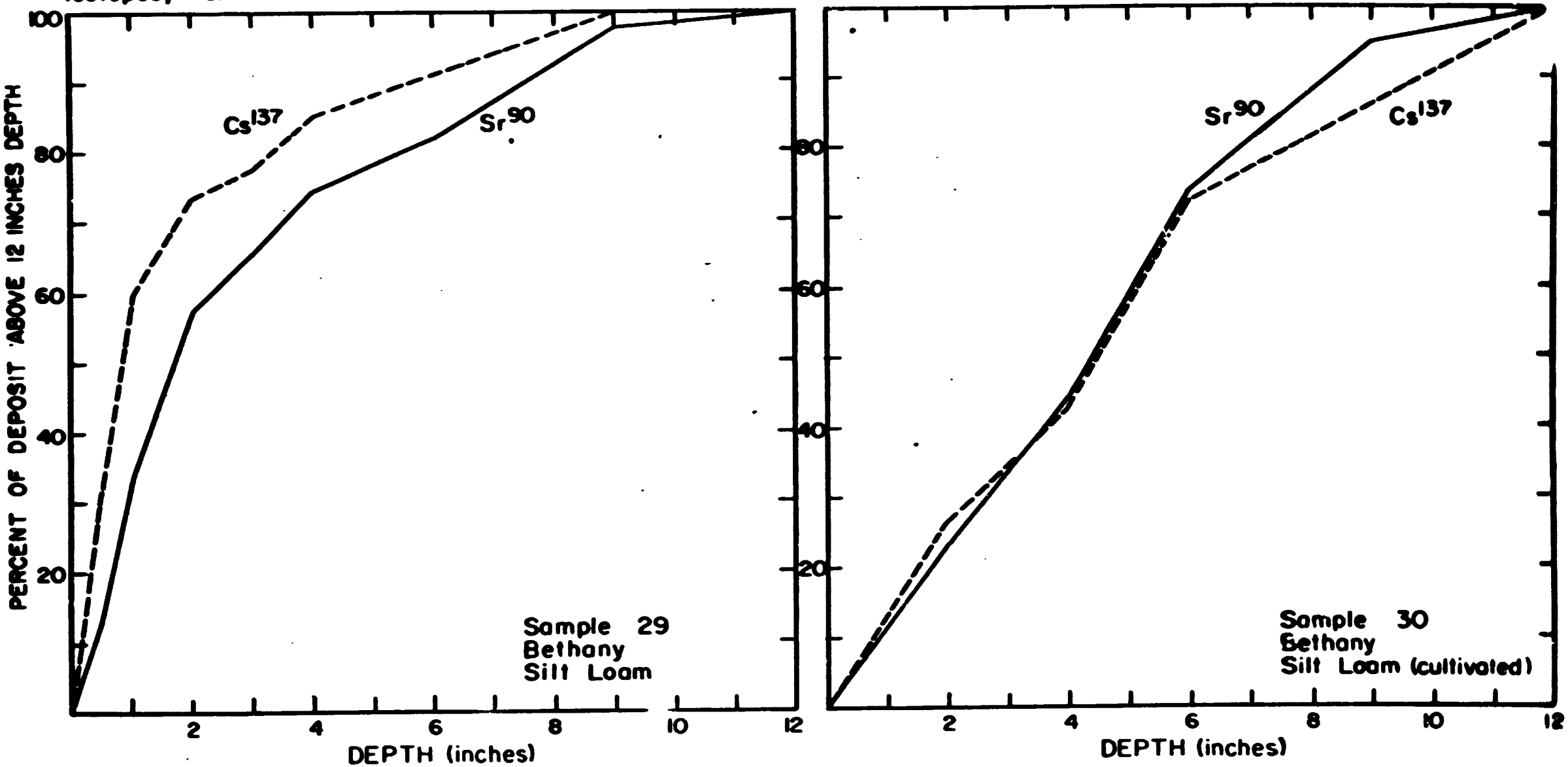

FIGURE 88 · RELATIVE DEPTH PENETRATION OF Sr-90 AND Cs-137 IN SAMPLE 29 AND 30

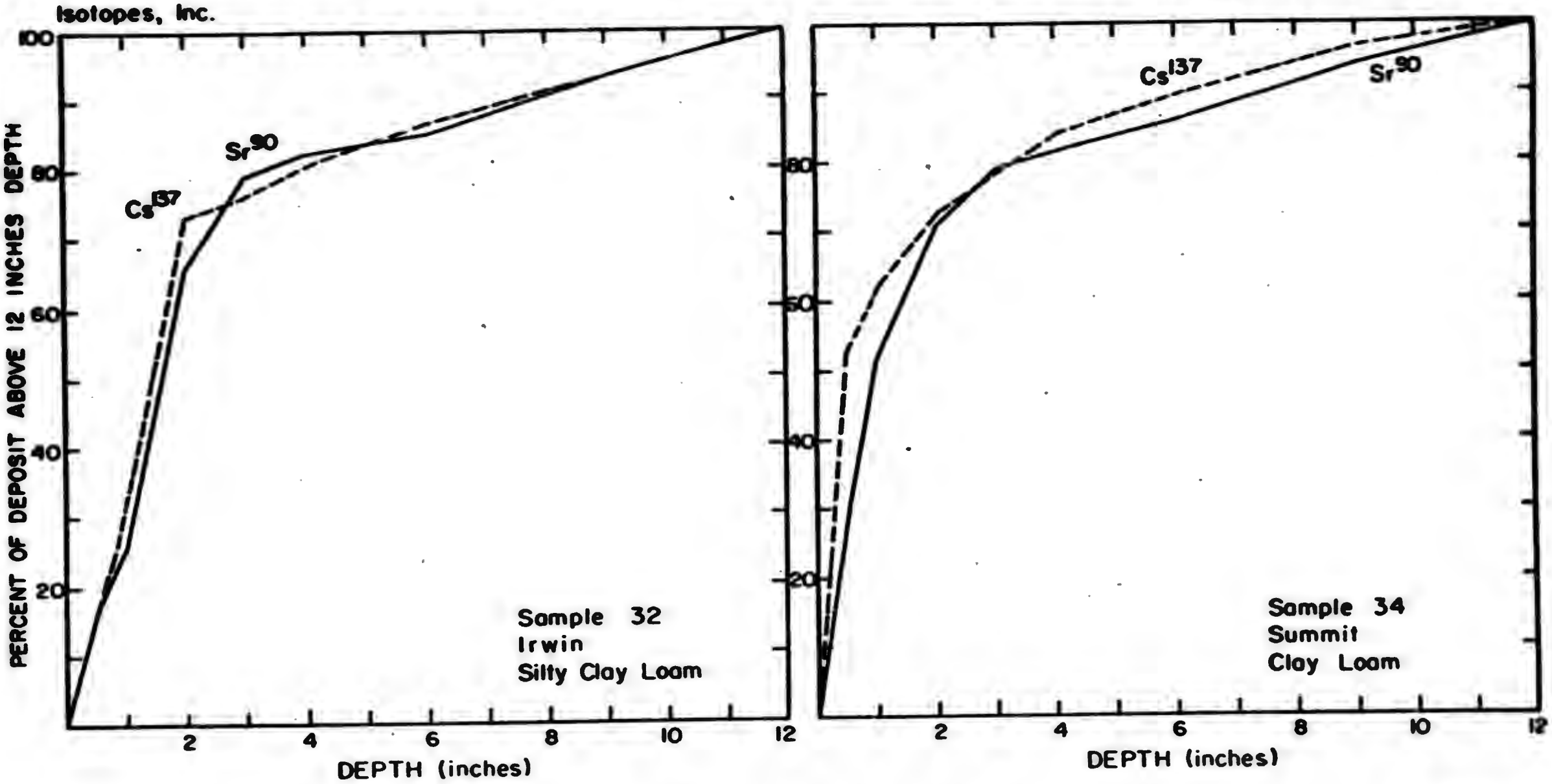

FIGURE 89 · RELATIVE DEPTH PENETRATION OF Sr-90 AND Cs-137 IN SAMPLES 32 AND 34

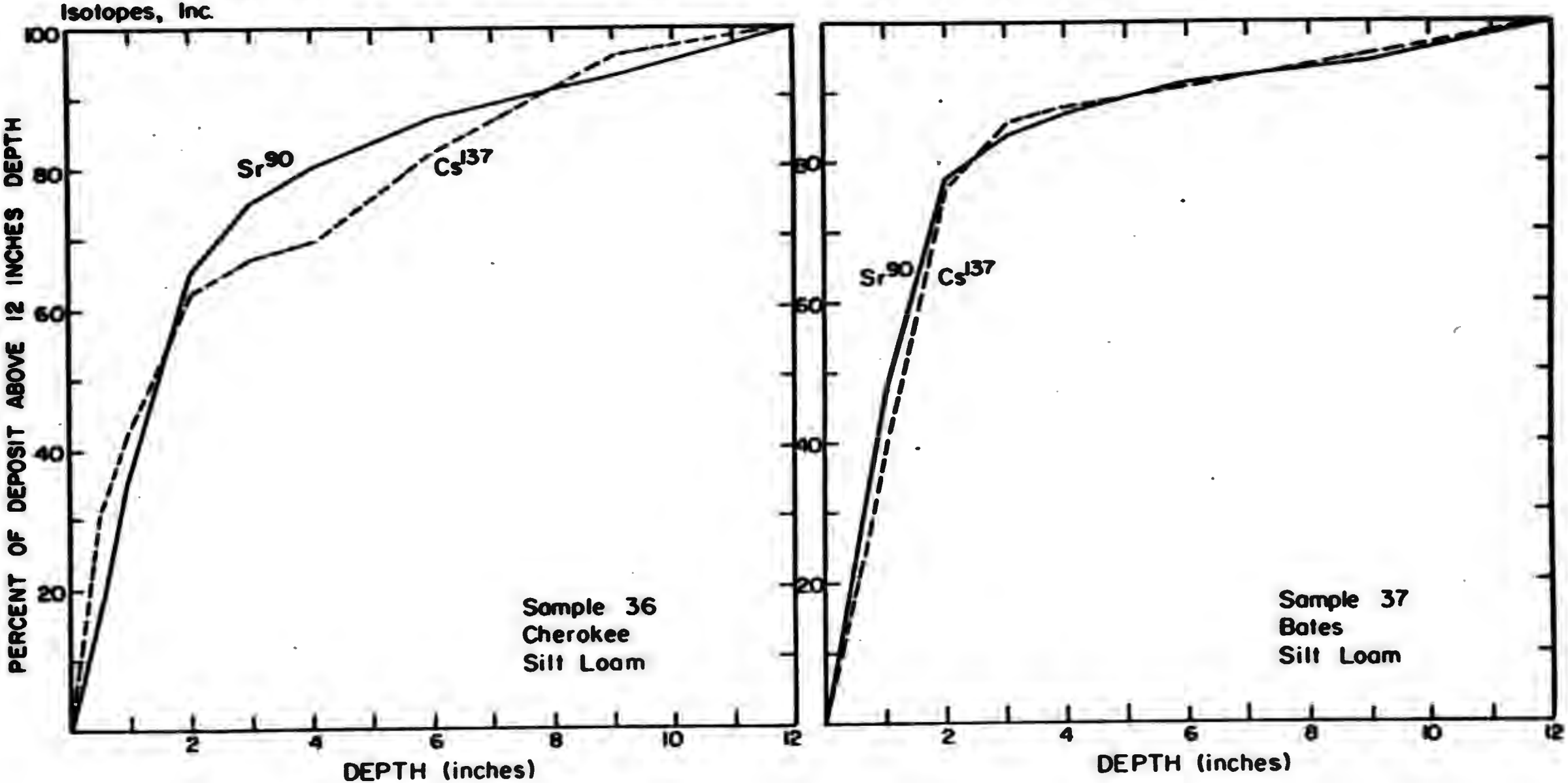

FIGURE 90· RELATIVE DEPTH PENETRATION OF Sr-90 AND Cs-137 IN SAMPLES 36 AND 37

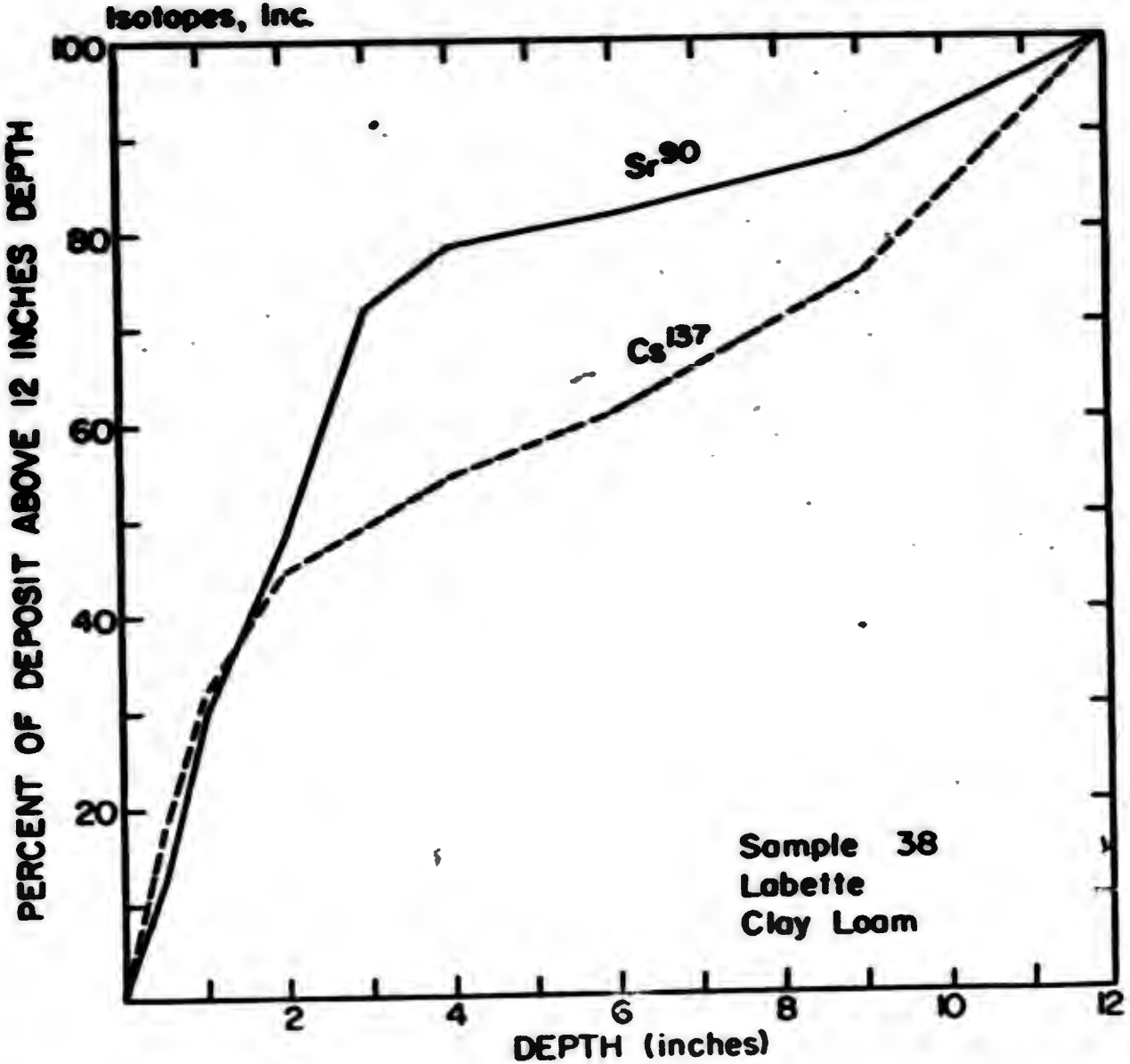

FIGURE 91 · RELATIVE DEPTH PENETRATION OF Sr-90 AND Cs-137 IN SAMPLE 38

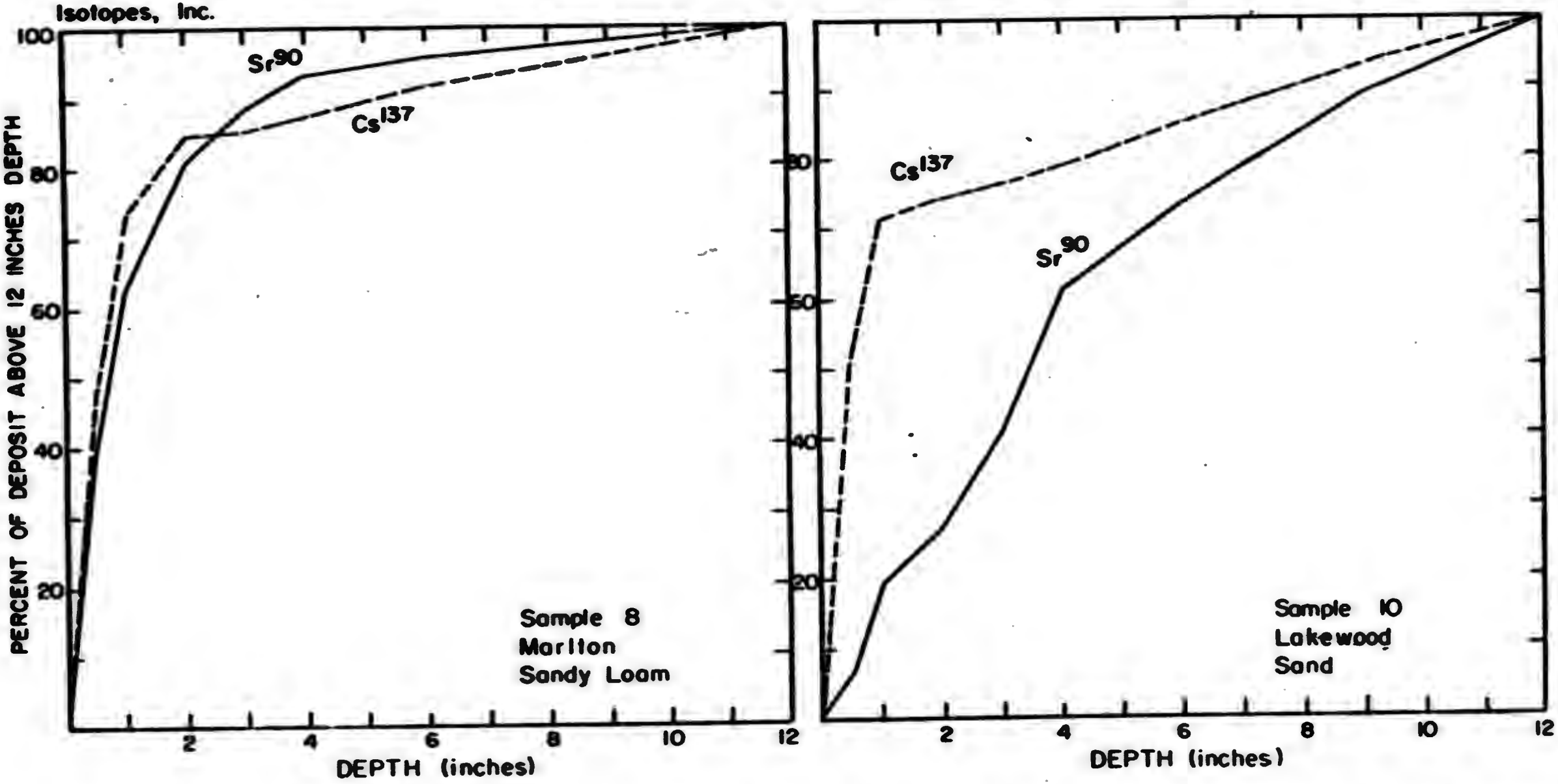

FIGURE 92· RELATIVE DEPTH PENETRATION OF Sr-90 AND Cs-137 IN SAMPLES 8 AND 10

CHAPTER 10. SUMMARY

The primary purpose of this report is to review the work which has been done on Project Star Dust during the past contract year. Techniques of sample collection and analysis and of data reduction in Project Star Dust which differ from those used in Project HASP are described. Results of measurements of stratospheric particulates, of filter samples of stratospheric radioactivity, of carbon-14 concentrations in ground level air and of fission products in kansas soils are discussed. Progress in the development of the Star Dust model of atmospheric circulation and exchange is reviewed.

The Star Dust Sampling Program

The Star Dust sampling program has been designed to provide repeated sampling of the stratosphere at a series of altitudes within a quasi-meridional corridor. WU-2 aircraft sample altitudes of 50, 55, 60, 65 and approximately 70 thousand feet between 70^{o}N and 50^{o}S latitude. RB-57 aircraft sample the lower stratosphere and collect some tropospheric samples. RB-52 aircraft fly monthly missions to the North Pole in the lower stratosphere. Intensive sampling in the vicinity of extrusions of stratospheric air into the troposphere was performed during the spring of 1963 as part of "Project Springfield".

The Stratospheric Aerosol

Samples of the stratospheric aerosol have been collected by direct flow impactors utilizing the improved "Mark III" sampling probe. The samples, collected on a thin carbon film, are studied by electron microscopy.

Although the probe samplers are air-tight, many samples show the effect of moisture on the hygroscopic ammonium sulfate particles of the aerosol, suggesting that these particles may exist to some extent in the stratosphere as moist solids or even as droplets.

The observed changes in particle concentration between 40 and 60 thousand feet are consistent with the vertical concentration profile reported by Junge et al[7]. Observed variations of nearly an order of magnitude in number concentrations for samples collected at various times at 60 thousand feet were found. These variations are consistent with the existence of the stratospheric aerosol in thin cloud-like laminae.

The observed form of the size distribution function of the aerosol in the range of radii between 0.1 and 1.0 micron is different than that found by Junge et al from the examination of particles collected by balloon-borne impactors. The average size distribution function for 14 samples closely approximates a log-normal distribution with a geometric mean radius of 0.275 micron and a geometric standard deviation of 1.37. The main region of disagreement with Junge et al is for radii $\leq$ 0.2 micron. The differences probably result from our exclusion from the particle counts of satellite particles which constitute the "halos" around "large" flat particles in samples affected by moisture.

Aitken nuclei, which have radii less than 0.1 micron, are not collected by the probe sampler used during Project Star Dust. It is possible that the actual distribution of particle sizes in the stratosphere may be bimodal, with peaks at radii of 0.3 micron (consisting of sulfate particles of stratospheric origin) and in the vicinity of 0.04 micron (consisting of Aitken nuclei).

The stratospheric origin of the sulfate particles is indicated by their chemical composition and by the location at 65 thousand feet of the maximum in their vertical concentration profile. The sulfate (and persulfate) of the particles presumably is produced by the photochemical oxidation of sulfur dioxide.

Calculations of the coagulation half-times of very small particles (with radii of 0.01 micron or less) suggest that nuclear debris should become attached primarily to Aitken nuclei. Smaller amounts should become attached to sulfate particles with radii greater than 0.3 micron, but virtually none should become attached to particles within the range 0.1 to 0.3 micron radius.

Radiochemical Analyses of Filter Samples

A number of the radiochemical and radiometric procedures used during Project Star Dust have been developed since the issuance of DASA-1300, in which the procedures used during Project HASP were described. Many of the new procedures were developed to analyze nuclides which were not measured during Project HASP, but others have replaced procedures which were used previously. Four sequential radiochemical separation procedures are in use. The first is designed to separate the fission products strontium-89, 90, yttrium-91, zirconium-95, molybdenum-99, barium-140 and cerium-141, 144. The second is used for samples to be analyzed for certain "tracer" nuclides and fission products: beryllium-7, strontium-89, 90, rhodium-102, cerium-141, 144, tungsten-181, 185, lead-210 and polonium-210. The third is designed to separate strontium-89, 90 and the neutron activation products manganese-54, iron-55, 59, cobalt-57, 58, 60, cadmium-109, 113m, 115m, antimony-124, 125 and thallium-204. The fourth is used for samples to be analyzed for the long-lived, potentially hazardous nuclides, strontium-90, cesium-137 and plutonium-239. New purification procedures have been developed for the analyses of beryllium-7, manganese-54, iron-55, 59, cobalt-57, 58, 60, molybdenum-99, cadmium-109, 113m, 115m, antimony-124, 125, iodine-131, cerium-141, 144, thallium-204 and lead-210.

Isotopes, Inc.

The versatility of the radiometric assay group working on Project Star Dust has been increased by the addition of improved equipment for measuring beta, gamma and x-ray emitters. Several low-level, thin window, geiger mode, gas flow detectors with background of approximately 0.5 counts per minute are now in use for beta counting. Total beta activities and a number of strontium samples are measured on two automatic sample changers which use proportional mode, gas flow detectors. Gamma measurements are performed on three multi-channel pulse height analyzers, using a 3 inch by 3 inch cylindrical NaI (Tl) crystal, a 2.5 inch by 1.75 inch well-type NaI (Tl) crystal or a 0.020 inch by 1.25 inch "thin" NaI (Tl) crystal (which is employed to detect weak gamma or x-radiation). An internal gas flow proportional counter is used to measure the 6.4 kev x-rays of iron-55.

Stratospheric Nuclear Debris

By mid-1961 only low concentrations of nuclear debris remained in the stratosphere of both the Northern and Southern Hemispheres, but the 1961 Soviet test series resulted in high concentrations of nuclear debris in the stratosphere of the Northern Hemisphere during the last third of 1961 and the first third of 1962. Debris injected into the equatorial stratosphere by United States tests during the second-third of 1962 spread toward both poles. Very high concentrations of debris were found in the stratosphere of the Northern Hemisphere during the last third of 1962 and the first two-thirds of 1963 as a result of the 1962 Soviet test series.

Measurements of barium-140 have been used to trace the movement of fresh debris during 1961-1963. The presence of an organized circulation in the vicinity of the tropopause gap is suggested by the observation that

at 30°N fresh debris moving poleward from an equatorial injection is most likely to be encountered at about 50 thousand feet, but fresh debris moving equatorward from a polar injection is most likely to be encountered at 60 thousand feet or higher.

There are limitations on the usefulness of fission product activity ratios, such as Mo^{99}/Zr^{95}, Mo^{99}/Ba^{140} and I^{131}/Ba^{140}, for determining the age of fresh debris. Nevertheless, it has been possible through their use to identify debris in Star Dust filter samples which originated in specific tests during the 1961 and 1962 Soviet test series and during the 1962 United States test series.

While the 1961 Soviet test series and the 1962 United States test series resulted in large increases in the stratospheric concentrations of strontium-90, concentrations of unprecedented size were found within the northern polar stratosphere following the 1962 Soviet tests. Concentrations exceeding 1800 disintegrations of strontium-90 per minute per 1000 cubic feet of air (STP) were still common at 65 thousand feet in the northern polar stratosphere after mid-1963.

Observations of strontium-90 from the 1961 Soviet test series seemed to confirm that debris injected into the stratosphere by Soviet weapons of megaton yield stabilizes, for the most part, at altitudes below 60 thousand feet, and that as it moves equatorward it increases in altitude. These observations also suggest that while debris injected at high latitudes may be spread laterally quite rapidly within the polar stratosphere, its transport through the tropical stratosphere is rather slow.

Isotopes, Inc.

It would appear that during the last two months of 1962 and the first four months of 1963 the stratospheric strontium-90 concentrations, outside of the equatorial region, were at least ten times as high in the Northern Hemisphere as in the Southern Hemisphere. We would assume that the excess strontium-90 concentrations in the Northern Hemisphere, compared to the Southern, represent debris produced by the 1961 and 1962 Soviet tests.

The distributions of strontium-90 in the Star Dust sampling corridor during several intervals between June 1961 and April 1963 have been used to calculate stratospheric burdens of strontium-90. The calculated burden in the Northern Hemisphere was 0.37 megacurie during June to September 1961 (with almost half attributable to the 1958 rocket shots), 1.6 megacuries during January to April 1962 (with 1.2 megacuries attributable to the 1961 Soviet test series), 2.5 megacuries during May to August 1962 (with 1.0 megacurie attributable to the 1962 United States test series), 2.2 megacuries during September to October 1962, 5.6 megacuries during November to December 1962, and 6.7 megacuries during January to April 1963. The calculated burden in the Southern Hemisphere was 0.47 megacurie during October to December 1961 (with 0.19 megacurie attributed to the 1958 rocket shots), 0.4 megacurie during January to April 1962, 1.0 megacurie during September to October 1962, 0.8 megacurie during November to December 1962, and 0.7 megacurie during January to April 1963. The total stratospheric burden rose from about 0.9 megacurie in June to September 1961, to 2.0 megacurie in January to April 1962, to 7.4 megacuries in January to April 1963.

The most significant observation resulting from measurements of rhodium-102 in HASP and Star Dust samples has been that this debris from

a high altitude injection at low latitudes first entered the lower stratosphere at high latitudes in both hemispheres, apparently during the winter season, and subsequently moved equatorward in the lower stratosphere.

A number of products of neutron activation, including manganese-54, iron-55, cobalt-57, antimony-124 and thallium-204, measured in Star Dust samples collected before September 1962, had a common origin in one or more events during the 1961 Soviet test series. Some events during the 1962 Soviet test series injected additional activation products (especially manganese-54 and iron-55) into the lower northern polar stratosphere. Additional antimony-124 was produced during the December 1962 Soviet tests, apparently on 23 or 24 December. By early 1963 there were significant differences between the stratospheric distributions in the Northern Hemisphere of antimony-124, which was found in high concentration only at altitudes of 55 thousand feet and higher, and manganese-54 and iron-55, which were fairly uniformly distributed with altitude between 40 thousand and 65 thousand feet. The stratospheric burden of manganese-54, corrected for decay to 15 October 1961, increased from 36 megacuries during May to August 1962 to 63 megacuries during January to April 1963.

Stratospheric Natural Activity

The stratospheric distributions of the cosmic ray product beryllium-7 from October 1959 to June 1960 and June 1960 to September 1961 were generally similar to the theoretical distribution in a stagnant atmosphere. Observed differences from the theoretical could be attributed to meridional eddy diffusion and to exchange of air between the stratosphere and troposphere. Artificial beryllium-7, attributable to the 1961 Soviet tests, was found in the northern polar stratosphere during January to

April 1962. During May to August 1962 artificial beryllium-7, attributable to the 1962 United States tests, was found in the tropical stratosphere. High concentrations of artificial beryllium-7 were present throughout the stratosphere of the Northern Hemisphere during January to March 1963 as a result of the 1962 Soviet tests.

Measurements of lead-210 and polonium-210 in samples collected in the Southern Hemisphere during October 1961 to April 1962 indicate that the concentration of natural lead-210 in both the tropical and polar stratosphere is about 0.3 dpm/1000 SCF, and that lead-210 and polonium-210 are in radioactive equilibrium in the stratosphere but not in the troposphere. Measurements of samples collected in the Northern Hemisphere during June to September 1961 suggest that the highest concentrations of lead-210 and polonium-210 occur in the 10 thousand feet thick layer which is immediately above the tropopause layer, and that concentrations are lower in the higher stratosphere.

The Star Dust Model

By incorporating a tropopause, a tropopause gap and a tropospheric sink in the form of a rainout mechanism, the basic numerical model of atmospheric mixing and transfer has been extended from the simple diffusion model, first studied, to a diffusion-rainout model. The tropopause is effected by the assignment of a larger (4 to 5 times) vertical exchange coefficient to the tropopause than to the stratosphere. For most of the experiments, the value of the meridional exchange coefficient is the same for both the troposphere and the stratosphere. The orders of magnitude of the vertical and meridional exchange coefficients are 10^4 cm ^{2}/sec and 10^9 cm ^{2}/sec., respectively. The tropopause gap is effected by

the assignment of relatively larger values to both exchange coefficients in a limited area between the tropical and polar tropopauses. The rainout mechanism is modeled by the periodic, f ıctional removal of debris at particular levels which represent realistic cloud levels. The fraction of removal is proportional to the mean annual rainfall of the appropriate latitude belt.

An initial series of experiments has been carried out wherein the magnitudes of the exchange coefficients and the period, levels and proportion of removal factor in the rainout mechanism have been varied in the attempt to determine the relative effects of the parameters on the distribution of the debris. No one set of initial conditions in the series of experiments has satisfactorily reproduced all of the features of the observed atmospheric distribution and deposit of tungsten-185.

A study of the results of four particular experiments provides some useful insight into the development of the model.

(a) The similarity in the mathematical form of the curves of time rate removal of total injection for the four models and that of the observed data indicates that the rainout mechanism being used is fairly realistic. These curves also indicate a sensitive, one to one, direct relationship between the removal mechanism and the magnitude of the vertical exchange coefficients in the experiment.

(b) A comparison of the curves of latitudinal distribution of deposit for various latitude belts in the Northern Hemisphere for observed data and for one of the models shows a similarity indicating that the observed latidudinal distribution of rainout can be reproduced. This distribution also is very sensitive to the magnitude of the vertical exchange coefficient.

(c) The time-dependent decrease of central concentration varies from one model to the other and all rates are slower than the observed rate. There are indications that the observed rate can be reproduced by an increase in the rate of rainout and by a greater latitudinal variation of the meridional exchange coefficient.

(d) A value of 1.5×10^{9} cm ^{2}/sec for the meridional exchange coefficient at the equator can successfully reproduce the observed latitudinal variation in concentration ratios.

(e) Reproduction of the observed poleward decrease in the height of the level of maximum concentration is dependent upon the distribution of the values of the vertical and meridional exchange coefficients and upon the removal mechanism. Reproduction can be accomplished for only the early stages of operation of the models. Beyond these early stages, the level of maximum concentration rises. As yet, adjustments in the vertical exchange coefficient in the stratosphere have failed to improve the results.

Further development of the model consists of incorporating the effects of particle terminal velocity and of the advection of debris by an organized meridional circulation.

Experiments including particle terminal velocities developed negative concentrations at the top of the model. To eliminate these negative concentrations, it was necessary to replace the centered finite difference scheme of solution by a simple upstream difference scheme. Further experiments showed that the rainout is quite sensitive to particle terminal velocities and that the use of the level of maximum concentration at the source was counteracted by particle terminal velocity.

Experiments including meridional circulation terms encountered the same development of negative concentrations in addition to a local distribution of the concentration field. Use of an upstream difference scheme managed to eliminate the negative concentrations, but was unable to conserve the mass of the diffusing material. Hence, the equation of continuity was incorporated into the model and was used to develop mutually consistent fields of vertical and meridional wind speeds. Using a centered finite difference scheme, mass was conserved but positive concentrations were not ensured. Experiments with a tropical source and using meridional circulations in which the flow is poleward in the lower stratosphere; upward at high latitudes; equatorward in the higher stratosphere and downward in the low latitudes have reproduced the observed poleward decrease in height of the level of maximum concentration and have maintained this height variation even with a strong mid-tropospheric sink.

The objective of further development of the model is to make it capable of reproducing the observed distributions of both polar and near-equatorial injections.

Carbon-14 in Ground Level Air

Measurements of carbon-14 in carbon dioxide from ground level in northern New Jersey have shown that a pronounced increase occurred in the carbon-14 concentration beginning in April 1963, doubtless representing carbon-14 injected into the stratosphere by the 1961 and 1962 nuclear weapons tests. A concentration of 191 per cent of the natural carbon-14 activity was reached in early August 1963.

Fission Products in Kansas Soils

The vertical distributions of strontium-90 and cesium-137 have been measured in 9 Kansas soils collected during 1960. An attempt to measure rhodium-102 and cerium-144 in these soils was unsuccessful.

The total deposition of strontium-90 indicated by the results for the upper 12 inches of soil varied from 50 mc/mi^2 for the Labette clay loam to 170 mc/mi^2 for the Pratt loamy sand (with the data corrected for possible contamination during analysis). The mean value for 9 soils was 88 $\pm$ 35 mc/mi^2. The total deposition of cesium-137 varied from 65 mc/mi^2 for the Labettte clay loam to 340 mc/mi^2 for the Pratt loamy sand. The mean value for 9 soils was 138 $\pm$ 81 mc/mi^2.

Some soils, such as the Irwin silty clay loam, show a close association of the strontium-90 and cesium-137 at all levels in the upper 12 inches of soil. Others, such as the Pratt loamy sand, show a separation of the nuclides. (The cesium-137 concentrated in the upper inch of the Pratt loamy sand, but the strontium-90 is fairly uniformly distributed within the upper 4 inches.)

REFERENCES

1. J. P. Friend, H. W. Feely, P. W. Krey, J. Spar and A. Walton, "The High Altitude Sampling Program", U. S. Dept. of Defense report DASA-1300 (1961)

2. M. I. Kalkstein, "High Altitude Studies Using Nuclear Tracers", a paper presented at the 13th General Assembly of the IUGG., Berkeley(1963)

3. J. P. Friend and H. W. Feely, "Second Quarterly Report on Project Star Dust", U.S. Dept. of Defense report DASA-1302 (1961)

4. J. P. Friend and H. W. Feely, "Fifth Quarterly Report on Project Star Dust", U.S. Dept. of Defense report DASA-1305 (1962)

5. H. W. Feely and J. P. Friend, "Evidence on Stratospheric Circulation from Measurements of Radioactive Bomb Debris Injected Above 20 km.", a paper presented at the 13th General Assembly of the IUGG, Berkeley (1963)

6. W. E. Ranz and J. B. Wong, "Impaction of Dust and Smoke Particles on Surface and Body Collectors", Ind. Eng. Chem. 44, 1371 (1952)

7. C. E. Junge, C. W. Chagnon and J. E. Manson, "Stratospheric Aerosols", Journal of Meteorology 18, 81 (1961)

8. G. Newkirk, Jr. and J. A. Eddy, "Light Scattering by Particles in the Upper Atmosphere", Journal Atmos. Sci., 21, 35 (1964)

9. C. E. Junge, "Vertical Profiles of Condensation Nuclei in the Stratosphere", Journal of Meteorology, 18, 501 (1961)

10. C. E. Junge and J. E. Manson, "Stratospheric Aerosols Studies", Journal of Geophysical Research 66, 2163 (1961)

11. R. D. Cadle, "Rates of Chemical Reactions in the Subionospheric Atmosphere", Journal of Geophysical Research 68, 3977 (1963)

12. C. E. Junge, "Possible Explanations of the Stratospheric Aerosol Layer", a paper presented at the 13th General Assembly of the IUGG, Berkeley (1963)

13. C. E. Junge, "Air Chemistry and Radioactivity", Academic Press, Inc., New York (1963)

REFERENCES (continued)

14. J. E. Manson, "The Interaction Between Radioactive and Non-Radioactive Particles in the Stratosphere", Radioactive Fallout from Nuclear Weapons Tests, TID-7632 Book 1 (1961)

15. E. H. Turk, "Revised Radiochemical Iodine Analytical Procedure", ANL-5271 (1954)

16. E. M. Scadden, N. E. Ballou, "The Radiochemistry of Molybdenum", NAS-NS 3009 (1960)

17. L. E. Glendenin, K. F. Flynn, R. E. Buchanan, E. P. Steinberg, Analytical Chemistry, 27, 59 (1955)

18. G. M. Iddings, "Radiochemical Procedures in use at the University of Californina Radiation Laboratory", (Livermore), edited by Manfred Lindner, U.C.R.L.-4377: 7 (1954)

19. T.T. Schull, "Collected Radiochemical Procedures", U.S.A.E.C., LA-1566, 22 (1953)

20. L. C. Covington, J. M. Miles, Analytical Chemistry 28, 1728 (1956)

21. W. M. Gibson, "The Radiochemistry of Lead", NAS-NS 3040 (1961)

22. "Standard Procedure for Radiochemical Analyses on Naval Reactor Plants at Initial and Refueling Startups", WAPD-M (CDA)-212 (Revised), pp 12

23. F. L. Moore, W. D. Fairman, J. G. Ganchoff and J. G. Surak, Analytical Chemistry, 31, 1148 (1959)

24. N. F. Davis, C. E. Osborne, H. Nash, Analytical Chemistry, 30, 2035 (1958)

25. W. H. Burgus, "Collected Radiochemical Procedures", U.S.A.E.C. LA-1721 (Revised), Edited by J. Kleinberg, 66 (1954)

26. L. E. Glendenin, "Collected Radiochemical Procedures", U.S.A.E.C. LA-1721 (Revised), Edited by J. Kleinberg (1954)

27. Knolls Atomic Power Laboratory, Private Communication

28. R. J. Prestwood, "Collected Radiochemical Procedures", U.S.A.E.C. LA-1721 (Revised), Edited by J. Kleinberg (1954)

29. J. Harley, U.S.A.E.C. New York Operations Office, Private Communication

REFERENCES (continued)

30. N. A. Hallden, I. M. Fisenne, L. D. Y. Ong and J. H. Harley, "Radioactive Decay of Weapons Debris", U.S.A.E.C. report HASL-117, pp 194-199 (1961)

31. U.S. Weather Bureau "Announced Nuclear Detonations, 1945-1962", U.S.A.E.C. report HASL-142, pp 218-242 (1964)

32. L. Machta, personal communication

33. H. W. Feely, J. P. Friend, R. J. Lagomarsino and A. B. Caridi, "Stratospheric Fallout from the 1958 Rocket Shots Measured Using the Fission Product Ratio Ce^{144}/Sr^{90}", Science (in press)

34. H. W. Feely and J. Spar, "Tungsten-185 from Nuclear Bomb Tests as a Tracer for Stratospheric Meteorology", Nature, 188, pp 1062-1064 (1960)

35. L. P. Salter, "High Altitude Balloon Sampling Program", U.S.A.E.C. report HASL-140, pp 166-214 (1963)

36. U.S. Government, "Global Atmospheric Radioactivity, May-June 1961", U.S.A.E.C. report HASL-117, pp 225-229 (1961)

37. S. Katcoff, "Fission Product Yields from Neutron-Induced Fission", Nucleonics, 18 (11), pp 201-208 (1960)

38. M. I. Kalkstein, "Rhodium-102 High Altitude Tracer Experiment", Science 137, pp 645-652 (1962)

39. U. S. Government, "Global Atmospheric Radioactivity, May-June 1960 and November 1960", U.S.A.E.C. report HASL-115, pp 177-183 (1961)

40. D. Lal and B. Peters, "Cosmic Ray Produced Isotopes and Their Application to Problems in Geophysics", in "Progress in Cosmic Ray and Elementary Particle Physics", vol. 6, North-Holland Publishing Co., Amsterdam (1962)

41. J. F. Bleichrodt, "Increased Concentration of Beryllium-7 in the Stratosphere After the Nuclear Test Explosions During September-October 1961", Nature, 193, No. 4820, 1065-1066 (1962)

42. L. Machta and H. F. Lucas, "Radon in the Upper Atmosphere", Science, 135, 296-299 (1962)

REFERENCES (continued)

43. W. M. Burton and N. G. Stewart, "Use of Long-Lived Natural Radioactivity as an Atmospheric Tracer", Nature, 186, 584-589 (1960)

44. Rama and M. Honda, "Natural Radioactivity in the Atmosphere", Journal of Geophysical Research, 66, 3227-3231 (1961)

45. W. Jacobi and K. Andre, "The Vertical Distribution of Radon 222, Radon 220 and Their Decay Products in the Atmosphere", Journal of Geophysical Research, 68, 3799-3814 (1963)

46. E. P. Hardy, Jr., R. J. List, L. Machta, L. T. Alexander, J. S. Allen and M. W. Meyer, "Strontium-90 on the Earth's Surface II, Summary and Interpretation of a World-Wide Soil Sampling Program: 1960-1961 Results", U.S.A.E.C. report TID-17090, November 1962

BLANK PAGE